

GEORG MAIER

SMOOTH MINIMUM ARC PATHS

CONTOUR APPROXIMATION WITH
SMOOTH ARC SPLINES

EINGEREICHT ZUR ERLANGUNG DES DOKTORGRADES DER NATURWISSENSCHAFTEN
AN DER FAKULTÄT FÜR INFORMATIK UND MATHEMATIK DER UNIVERSITÄT PASSAU

IM MÄRZ 2010

Abstract

Let P be a simple polygon with interior I and two disjoint edges designated as the start and the destination. A smooth arc path is a sequence of circular arcs and line segments joined smoothly and staying inside the closure of I . We elucidate the construction of a *smooth minimum arc path*, i.e. a start-destination smooth arc path with the minimal possible number of segments. Although this problem is well-known, it hasn't been solved yet. We present a mathematical characterization of possible solutions that enables a constructive approach leading to an $O(n^2)$ algorithm, where n denotes the number of vertices. However, in many practical applications our algorithm is even sub-quadratic. In fact, our approach is more general since we do not restrict ourselves to polygons but to a broader class of bounding curves, namely piecewise restricted analytic curves. We were able to show our constructive characterization of solutions for this class of curves as well.

Zusammenfassung

Sei P ein einfaches Polygon mit Innengebiet I und zwei als Start und Ziel ausgezeichneten, disjunkten Kanten. Unter einem *smooth arc path* verstehen wir eine Folge von Kreisbögen und Strecken-Segmenten, die glatt zusammengesetzt sind und im Abschluss von I verlaufen. Wir interessieren uns für die Konstruktion eines *smooth minimum arc path*, d.h. für einen glatten Start-Ziel Pfad mit minimaler Anzahl an Segmenten. Obwohl das Problem seit längerem bekannt ist, konnte es bisher nicht gelöst werden. Wir präsentieren eine mathematische Charakterisierung möglicher Lösungen, die ein konstruktives Verfahren ermöglicht. Dieses Verfahren lässt sich schließlich als Algorithmus mit quadratischer Laufzeit (abhängig von der Anzahl der Ecken n von P) implementieren. In vielen praktischen Tests konnten wir jedoch eine subquadratische Laufzeit feststellen.

Tatsächlich ist unser Ansatz sehr viel allgemeiner. Wir lassen nicht nur Polygone als begrenzende Kurve, sondern eine weitaus breitere Klasse von Kurventypen zu, nämlich stückweise analytisch fortsetzbare Kurven. Für diese Kurventypen gelang es ebenso unsere konstruktive Beschreibung der Lösungen zu beweisen.

Acknowledgments

First of all, I would like to thank my academic advisor Prof. Dr. K. Donner. It was him who called my attention to the connections between concepts from classical Approximation Theory and Computational Geometry with applications in Computer Aided Design and Computer Vision. He kindly gave me the opportunity to do my doctorate at his department. I thank him for his guidance, belief and patience and for thoroughly examining my work in the run-up.

Secondly, Prof. Dr. G. Pisinger deserves special thanks for all he did for me. He never hesitated to answer my questions or offer a comforting word. His feedback and all the intellectually challenging discussions we had have considerably improved this work.

The Research Scholarship Program of the ‘Elite Network of Bavaria’, based on the Bavarian Elite Aid Act (BayEFG), provided me with financial support during the last two years. Apart from financial benefits, I was able to attend an interdisciplinary and personal development excellence program. Thank you very much! I also want to thank the ‘Universität Bayern e.V’, which distributed the scholarship program.

Furthermore, my appreciation goes to Dr. E. Fuchs (CEO FORWISS, Institute for Software Systems in Technical Applications). Due to his exceptional commitment I had the opportunity to take part in some ambitious and very interesting research projects.

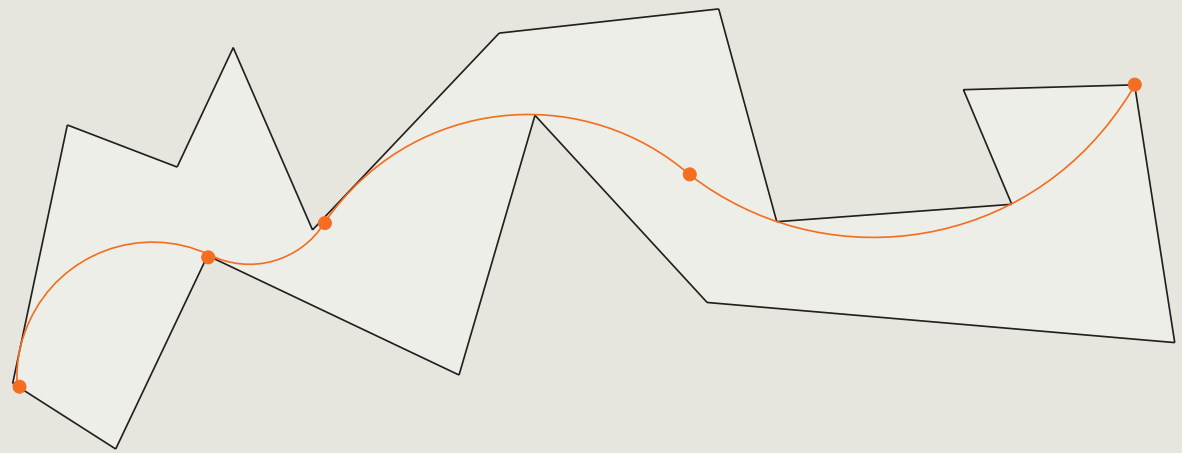
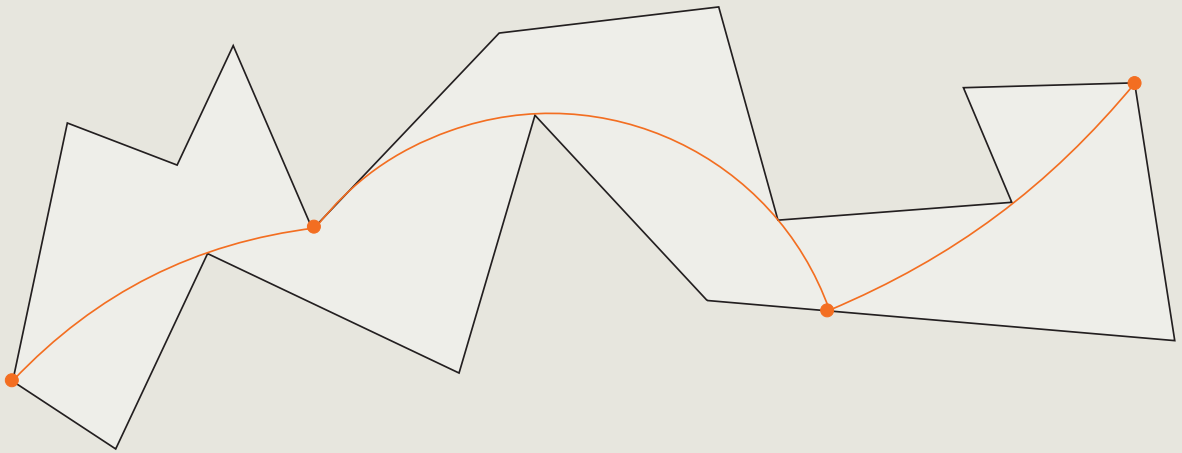
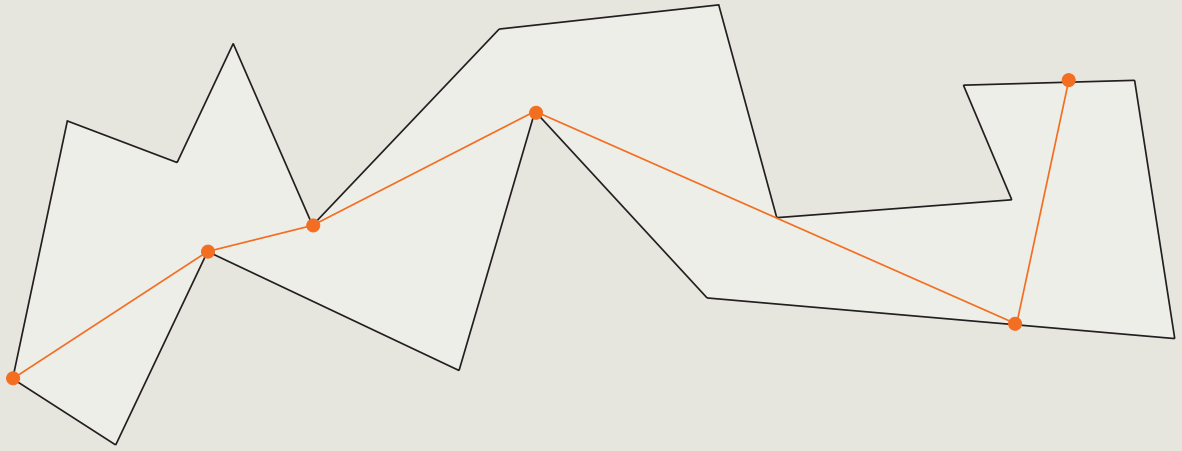
Also, I would like to thank Prof. Dr. S. Graf for taking the role of the second advisor. Special thanks go to M. Kuhnies, Dr. A. Zimmermann, M. Berberich, A. Schindler, Prof. Dr. T. Kaiser and P. Barth for the numerous helpful discussions and their support. With regard to proof-reading I would like to express my gratitude to M. Böhm (language) and Dr. E. Fuchs (content).

Most importantly, however, I wish to thank my family and friends. Without their support I would never have come this far. They never doubted that I would succeed and supported me wherever they could. Their optimism and encouragement helped me through difficult times in which my self-doubt would have driven me to resignation.

CONTENTS

Preface		iii
1 Introduction		1
1.1 Motivation		2
1.2 Visibility in Computational Geometry		6
1.3 Related Work on Arc Splines		10
1.4 Aim of this Work and Main Results		11
1.5 Outline of this Thesis		12
2 Basic Definitions and Notation		15
2.1 Conics and Circles		16
2.2 Set-Valued Analysis and Approximation Theory		21
2.3 Hausdorff Metric and Local Hausdorff Topology		23
2.4 Planar Curves		26
2.5 Arc Splines and their Properties		32
3 Mathematical Modeling and Results		45
3.1 Tolerance Channels		47
3.2 Alternating Sequences		60
3.3 Feasible Direction Sets		76
3.4 Characterization of the Visibility Set $V_K(\sigma)$		83
3.5 Continuity Properties of $T_K(\sigma, -)$		94

3.6	Characterization of the n -Visibility Set $V_K^n(\sigma)$	102
3.7	(Smooth) Minimum Arc Paths	122
3.8	Summary and Outlook	127
4	The Algorithmic Approach	135
4.1	Greedy Proceeding and Alternating Sequences	137
4.2	Circular Visibility Diagrams (CVD)	147
4.3	Circular Visibility of an Edge	153
4.4	Circular Visibility of an Arc	158
4.5	Continuation Channels and CVDs	162
4.6	Minimum Arc Paths and CVDs	167
4.7	Summary and Experimental Results	170
5	Applications	175
5.1	Edge Contours and Forms of Representation	177
5.2	Design of Suitable Channels	181
5.3	Shape Recognition	185
5.4	Reverse Engineering	188
5.5	Curve Approximation	195
6	Résumé and Further Work	199
6.1	Overview and Main Results	199
6.2	Possible Future Work and Open Problems	201
	References	203
	List of Symbols	211
	List of Figures	218
	List of Tables	219
	List of Algorithms	221
	Index	223



1

INTRODUCTION

In this preliminary chapter we motivate our work by giving an example of practical use in Reverse Engineering. The way in which an algorithm for computing a smooth arc path can be used for automatically generating CAD models from a quasi planar working piece is, however, only briefly outlined. Exact definitions and propositions are given in the following chapters. A more detailed presentation and some more examples of applications can be found in Chapter 5.

In the second section we discuss some well-established results of visibility tasks in Computational Geometry. We then give a short overview of visibility in the classical sense and variations existing on this subject, and we classify the challenge of computing a (smooth) minimum arc path within the field of visibility problems.

As minimum arc paths are included in the class of arc splines, we discuss known approaches to approximating points and curves by arc splines in Section 1.3.

Section 1.4 summarizes the main aims and results, whereas in the fifth section we give a short outline of this thesis.

*‘Dimidium facti, qui coepit, habet.
Once you’ve started, you’re halfway there.’*

(Horace, Roman lyric poet)

1.1 Motivation

The border of an object which can be seen in a camera image is called *contour*. The appropriate description of the contours of a quasi-planar object is an essential step when generating CAD¹-layouts automatically. It plays a crucial role in quality assurance purposes and vision metrology. Though the automatic generation of CAD models represents a standard problem in *Reverse Engineering*², a satisfying solution hasn't been found yet. We pursue a mathematical modeling that is in step with recent practice and yields an efficient algorithmic implementation.

Optical sensors generally sample objects only discretely. Therefore, the border of a captured object can simply be extracted as a finite list of pixel coordinates (cf. Section 5.1). By connecting adjacent points with each other, we get a simple polygonal curve, a so-called *contour point list*. For instance, a circular bore hole would yield a polygon with thousands of vertices. Obviously, this does not provide an adequate description and is computationally expensive so that it is improper for further software processing.

In fact, a representation of the contour by a (smooth) planar curve approximating the extracted points is desirable.

1.1.1 Problems in Sensor Sampling

Optical sensors can only provide a finite subset of such a curve. Since the corresponding coordinates are digitized, i.e. rounded, they are additionally subjected to errors. Every sampling is a physical measuring process, which means that the values have only finite accuracy. Consequently, the requirement that the curve has to run through all original points of the contour point list doesn't make much sense. However, the distance to these points should not be too big. The curve should therefore approximate them as well as possible. This requirement is met by accepting a maximum distance depending on the various positions.³

¹Computer-Aided Design (CAD) is the use of computer technology to aid in the design and particularly the drafting of a part or product.

²Reverse Engineering is a process, which involves measuring an object and then reconstructing it as a CAD model.

³A more detailed presentation can be found in Chapter 5.

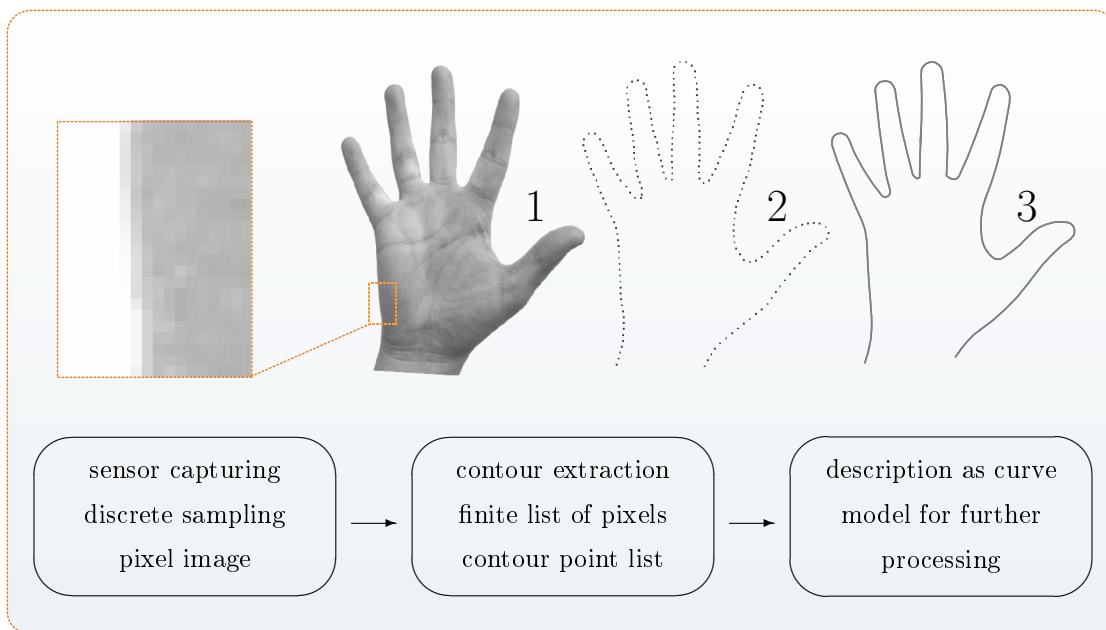


Figure 1: The particular steps from a real object to a CAD drawing.

1.1.2 Choice of the Curve Model

We are interested in a curve that not only approximates the extracted points up to unavoidable tolerance errors but also describes them effectively, i.e. with minimal complexity. Such a characterization allows coping with tasks in industrial quality control, like contactless measurement and shape recognition, more efficiently (see Chapter 5). As already indicated, polygons are not suited as a curve model, in this case. One approach in modeling contours is their description as *(circular) arc splines*, i.e. curves composed of circular arcs and line segments. Above all, smoothness at the breakpoints is required in order to enable a realistic modeling.¹ Since they are determined by only a few parameters and satisfy important invariance criteria, like invariance with respect to rotations, scalings and translations (cf. Section 2.5), they can be applied well to measurement tasks. A promising solution would be a smooth arc spline approximating the contour with respect to a given tolerance.

¹An exact definition can be found in Section 2.5.

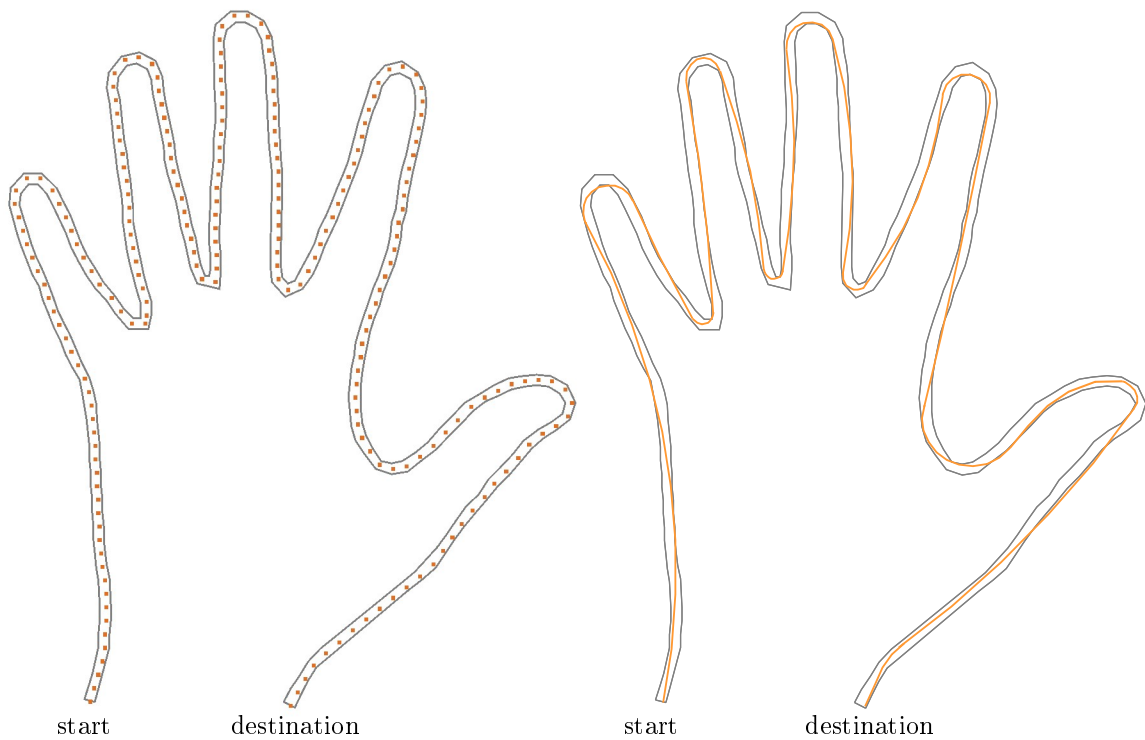


Figure 2: Start-destination channel including contour points (left) and smooth minimum arc path (right).

1.1.3 Competing Optimization Criteria

This approach turns the approximation problem outlined above into a multi-objective optimization: Obviously, the approximation error diminishes if the number of line and arc segments increases. The more exactly the contour points are approximated the more segments are needed. Hence the proposed method minimizes the number of segments while keeping a given tolerance that possibly can vary locally.

1.1.4 Start-Destination Channel

Our approach controls the approximation error by only focusing on solutions staying inside a so-called *start-destination channel*. Typically, such a channel is given by a simple polygon or an arc spline (cf. Figure 2). In addition, a source and a destination segment are fixed. Any smooth arc spline staying inside the start-destination channel and connecting the source and destination segments with a minimum number of segments solves the problem. As has already been mentioned, we call such a spline *smooth minimum arc path*.

1.1.5 Constructive Solution

The existence of a solution is quite easy to prove. However, practical implementation requires concrete and constructive approaches. For this purpose, a mathematical characterization of solutions by *alternating sequences* and *feasible direction sets* is supplied. Alternating sequences are families of points on the bounding curve of the channel that are alternately touched from the left and from the right as indicated in Figure 2 on the right. It is shown, how these theoretical results lead to the development of efficient algorithms.

1.2 Visibility in Computational Geometry

Visibility and intersection problems are among the most fundamental topics in *Computational Geometry*¹. The problems of shortest paths and visibility inside simple polygons have been extensively studied in the last three decades (cf. [41]).

As a part of our short overview² of visibility problems, we now present the following situation: Let P be a simple polygon with interior I . By \bar{I} we denote its closure.

One of the fundamental visibility problems is the computation of a point-visibility polygon, which means the subset of \bar{I} that is visible from a point $p \in \bar{I}$, i.e. the set of all points $x \in \bar{I}$ s.t. there exists a line segment $l \subset \bar{I}$ connecting p and x (cf. Figure 3 top left). Such line segments are called *visibility line segments*. Joe and Simpson developed in [2] a linear-time algorithm for constructing a point-visibility polygon inside a simple polygon.

Another fundamental visibility problem is the computation of an edge-visibility polygon (cf. Figure 3 bottom left). Introduced by Avis and Toussaint (cf. [10]), edge visibility is divided into three categories, complete, strong and weak:

Let e be an edge of P and let us denote the line segment running from x to $y \neq x$ by $l(x, y)$. A subset $M \subset \bar{I}$ is

- i) *completely visible from e* if for all $x \in M$ and for all $y \in e$ the line segment $l(x, y)$ is a visibility line segment.
- ii) *strongly visible from e* if there exists a point $y \in e$ s.t. for all $x \in M$ the line segment $l(x, y)$ is a visibility line segment.
- iii) *(weakly) visible from e* if for all $x \in M$ there exists a $y \in e$ s.t. the line segment $l(x, y)$ is a visibility line segment.

Whether a polygon is completely or strongly visible to a given edge can be answered by the *kernel algorithm* developed by Lee and Preparata (cf. [53]), and whether a polygon is weakly visible from an edge can be solved in linear time (cf. [10]). Guibas et al. show in [44] that an edge-visibility polygon inside a triangulated simple polygon can be constructed in linear time.

¹Computational Geometry is a discipline of Computer Science which is concerned with efficient algorithms and representations for geometric computation.

²This overview mainly follows [10], [23] and [39].

Among other variations on this subject, *circular visibility* was introduced by Agarwal and Sharir (see [4]). Whereas linear visibility is established by straight lines, circular visibility is established by circular arcs. Considering line segments as arcs with infinite radius, visibility can be extended by considering circularity. A point x is *circularly visible from a point* $p \in \bar{I}$ if there exists a circular arc running from p to x without leaving the polygon P (cf. Figure 3 top right). Such an oriented circular arc (clockwise or counterclockwise) is called *visibility arc*.

Besides being a natural extension of linear visibility, circular visibility is well suited to model physical systems like trajectories of electrically charged particles in a uniform magnetic field (cf. [39]).

Chou and Woo gave in [23] a method to compute the circular visibility inside a simple polygon in linear time. A so-called *Circular Visibility Diagram (CVD)* represents these sets of circular arcs by their centers in a planar partition. In [22] Chou et al. have shown how to determine the circular visibility of a given edge by using CVDs (cf. Figure 3 bottom right). The *general ray tracing problem*, i.e. computing the first intersection of a circular ray starting from an arbitrary point, has been solved by Agarwal and Sharir (cf. [3]). The first intersection can be computed in $O(\log^4 n)$ time with $O(n \log^3 n)$ preprocessing, where n is the number of vertices of the polygon.

Other possible variations involve generalizing the concept of a rectilinear polygon to the concept of a *splinegon* that is introduced by Dobkin and Souvaine (cf. [29]). A splinegon is a simple closed curve whose trace consists of ‘curved edges’, where every curved edge is contained in the boundary of its convex hull. In fact, a splinegon is a polygon bounded by algebraic curves which is implicitly given as the solution to a polynomial equation in two variables.

López and Ramos (see [39]) gave linear time algorithms for computing the weak visibility polygon of an arc inside a triangulated splinegon. They have also developed a linear time algorithm for computing the circular, elliptic, parabolic and hyperbolic visibility polygon of a point inside a simple polygon.

Similarly to visibility, other problems have been treated in literature: There are various criteria for optimizing the path between a source and a destination. For instance, a *minimum link path* minimizes the number of turns (see Figure 4 top), whereas the *shortest path* minimizes the length of the path (cf. [44]). Since this is related to the

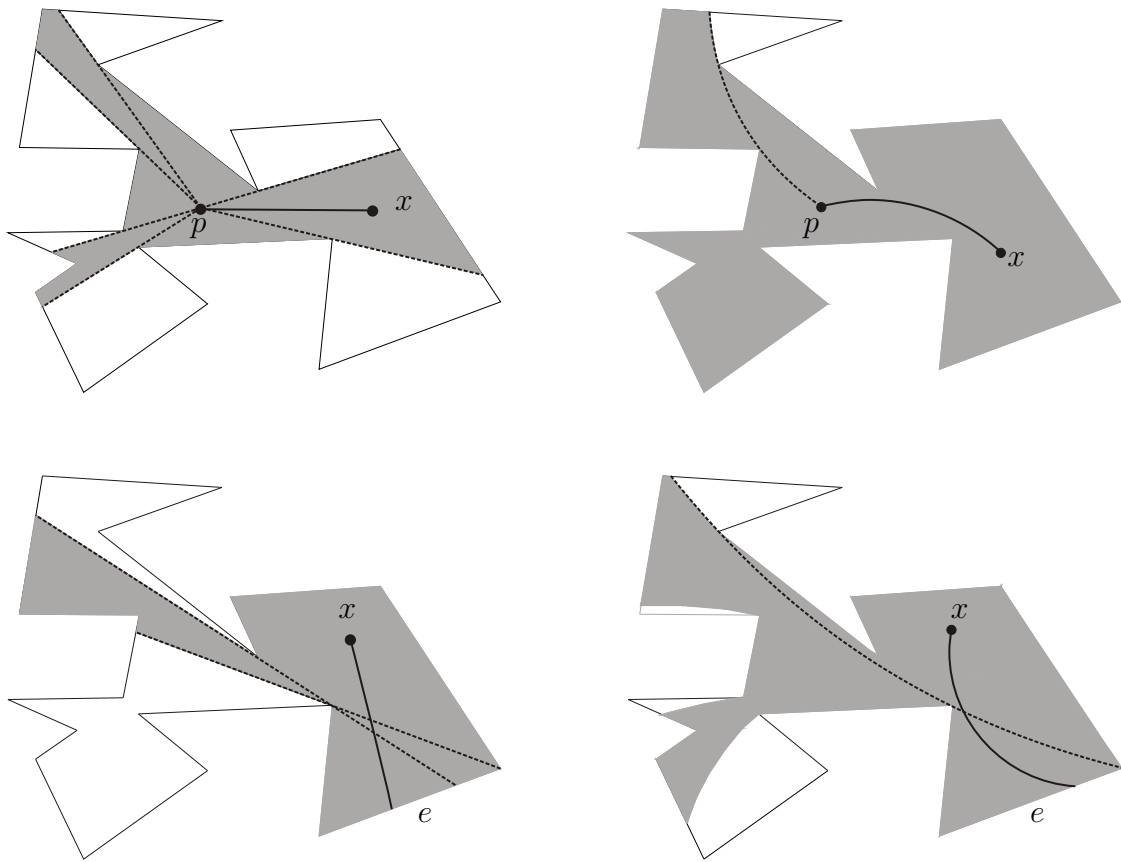


Figure 3: Various types of visibility polygons (shaded portions). Top: Linear and circular visibility with respect to a point p . Bottom: Linear and circular visibility with respect to an edge e . There are also some visibility arcs / line segments of x depicted.

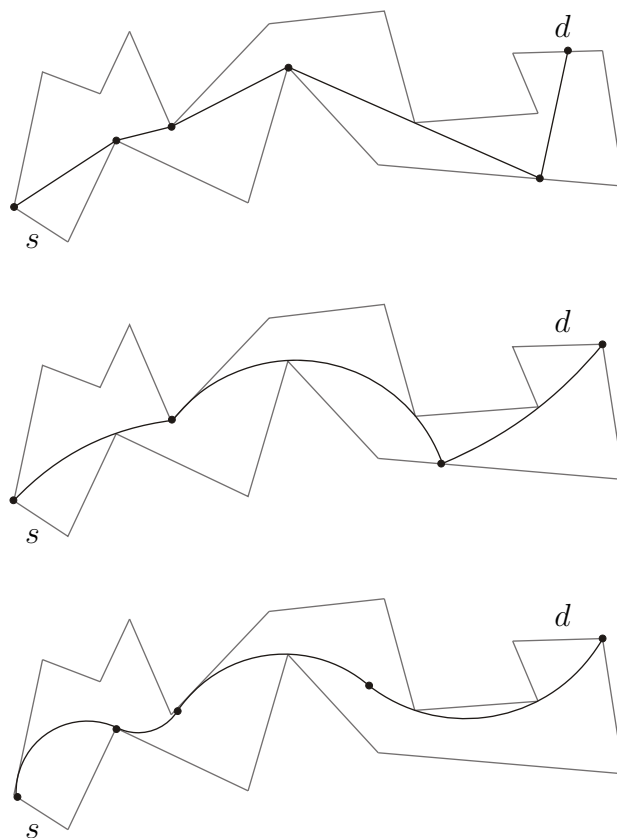


Figure 4: A minimum link path (5 segments), minimum arc path (3 segments) and a smooth minimum arc (4 segments) path within the same polygon and source edge s and destination edge d .

visibility problem, many papers provide efficient algorithms for computing the minimum link path inside a polygon. (e.g. [73, 74, 6, 9, 7]).

Several papers dealing with the computation of convex and simple paths of bounded curvatures between two points s and t and two directions of travel exist (cf. [15, 1]). However, none of the papers discusses the challenge of computing a (smooth) minimum arc path, a path from a given source edge to a given destination edge composed of circular arcs with a minimum number of segments (see Figure 4 middle and bottom). Particularly, such challenges have not been studied in any other context but within a boundary given by a polygon or splinegon.

It is well known that computing a minimum link path can be done iteratively but when generating a smooth minimum arc path, it is not clear at all where to put the break-points. However, the mathematical results of Chapter 3 enable an iterative approach.

1.3 Related Work on Arc Splines

The interest for arc splines is not strictly limited to the field of Computational Geometry. Their use is equally relevant to approximation tasks and applications in Geometric Modeling ([82, 21]), Computer Graphics ([68, 21]), Computer Vision ([68]) and Robot Path Planning ([82]). Because of their invariance with respect to translations, rotations and scalings and their easy offset computation, they are especially appropriate for the automatic generation of CAD data from measuring point sequences as well as tasks in Reverse Engineering (cf. Section 1.1 and Section 5.4) and target-performance comparisons of planar geometries like laminations, panes of glass and planks of shelves. As in computer-aided manufacturing environments tool paths are usually composed of line segments and circular arcs, arc splines play a very important role in many further applications such as Computerized Numerical Control (CNC) machinery (e.g. [21, 84, 85, 86]). We will present some examples of these applications in Chapter 5.

Research on arc splines has been very active in the last decades (e.g. [58, 59, 60, 70, 84, 82, 81, 33]). Two classical references to arc splines are [72] and a book of Nutbourne and Martin ([61]). Research covers both continuous arc splines (e.g. [54, 55, 33]) and smooth arc splines¹. Currently, the superior properties of smooth arc splines over continuous ones are being emphasized. Hence recent research on arc splines has focused on smooth arc splines (e.g. [65, 64, 82, 21, 85, 33]).

In particular, curves composed of *biarcs*, which are smooth curve segments consisting of two circular arcs, have been used in a large number of algorithms for approximation or interpolation of given point (and possibly tangent) data. For instance, Meek and Walton have discussed biarcs in a number of publications (e.g. [58, 59, 60]). Drysdale et al. [33] have presented an algorithm for approximating polygonal curves by continuous arc splines and curves composed by biarcs respectively with a minimum number of segments. However, all approaches currently known suffer from (unnecessary) restrictions to feasible arcs and biarcs. Mostly, they have to start and end at original points, and in case of biarcs the tangent directions at the starting and end point are usually determined by the original points as well. Hence the breakpoints of the approximating arc spline must be original points, which is very restrictive.

¹Smooth arc splines are curves composed of circular arcs and line segments having a continuously differentiable parametrization. An exact definition can be found in Chapter 2.

1.4 Aim of this Work and Main Results

Our goal is to develop an efficient algorithm that computes a smooth minimum arc path inside an arbitrary *start-destination channel*. A start-destination channel is defined by a piecewise restricted analytic Jordan curve with two designated circular arcs or line segments denoted as start and destination.

As seen in Section 1.2, a priori it is not clear where to put the breakpoints when computing a smooth minimum arc path, which is different when computing a minimum link path. Nevertheless, we give a mathematical characterization of possible solutions based on *feasible direction sets* and *alternating sequences* which enable a constructive and iterative approach. Thus, we can develop a *greedy algorithm*¹ solving the problem. This approach is substantially expandable even to cyclic channels.

When improving the efficiency of our algorithmic approach, we focus on start-destination channels given by a simple polygon P . Denoting the interior of P by I , we have already seen that the subset of \bar{I} which is circularly visible from a point in \bar{I} can be determined by computing its Circular Visibility Diagram (CVD) in $O(n)$ -time, where n is the number of the vertices of P . Therefore, our algorithm uses CVDs iteratively to construct a smooth minimum arc path, which leads to an $O(kn)$ -time algorithm where k is the number of CVDs computed. In the worst case k equals n , but in many practical applications k is considerably smaller than n .

In particular, arc paths are arc splines. Hence computing a smooth minimum arc path inside a suitable start-destination channel enables a new and efficient approach to approximating two dimensional point data and curves by (smooth) arc splines. In contrast to the existing approaches (c.f Section 1.3), we can guarantee a minimum number of segments without any restrictions to the breakpoints. By the width of the channel we can flexibly and locally control the maximum tolerance error. Therefore, our results make a considerable contribution to quite a lot of applications in all the research fields mentioned in the previous sections.

Based on mathematical foundations, this thesis is thus a bridging of Nonlinear Approximation and Computational Geometry with applications in Computer Vision, Graphics and Computer Aided Design in mind.

¹A greedy algorithm is an algorithm that follows the strategy for making the locally optimal choice at each stage (cf. [24]).

1.5 Outline of this Thesis

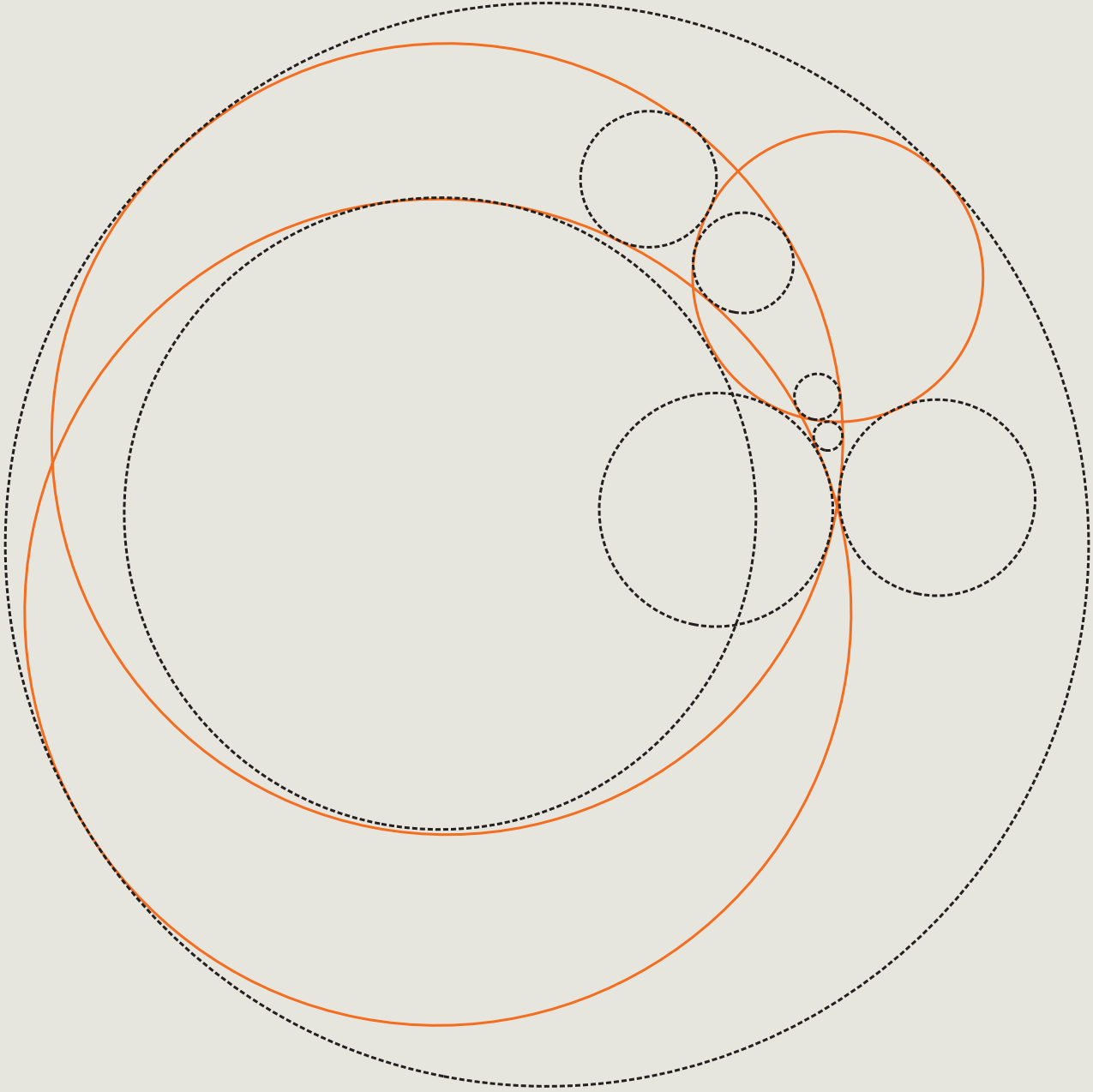
After having seen a short introduction to one motivating application in Reverse Engineering, some introductory comments on *visibility* in Computational Geometry, a summary of well-known methods in approximation with arc splines and an overview of the main results, the remaining part of the thesis consists of three main parts:

The mathematical part starts with fundamentals concerning conics, approximation theory, Hausdorff metric, planar curves and circular arc splines, which are discussed in Chapter 2. This chapter mainly serves to present well-established results and familiarize the reader with our notation.

In Chapter 3 we elucidate a mathematical modeling of the problem sketched in Chapter 1. We introduce various forms of circular visibility and characterize smooth minimum arc paths within so-called tolerance channels.

The second part includes our algorithmic approach in which algorithms for computing circular n -visibility and (smooth) minimum arc paths are outlined. Especially, the case of tolerance channels given by polygons, is thoroughly discussed.

In Chapter 5, the third main part, we sketch some applications of (smooth) minimum arc paths for tasks in Reverse Engineering, Shape Recognition and Curve Approximation. Finally, in Chapter 6 we give an overall résumé of this thesis and have a look at potential further work.



2

BASIC DEFINITIONS AND NOTATION

In this preliminary chapter we fix some notation and state well-established results. However, we only focus on notions and results which are needed in the main part. We mostly keep away from far-reaching generalizations of definitions and terms but confine ourselves to introducing useful language in a relatively short manner. Readers who are familiar with all those basics may skip this chapter and merely refer to it for the main notations. In the first section of this chapter we introduce conics and circles and establish some of their properties. Before introducing some notions and properties of the Hausdorff metric and its expansion, the local Hausdorff topology, we present some well-known results of Set-Valued Analysis and Approximation Theory. In the fourth section the theory of planar curves is introduced to finally enable a definition of arc splines. This definition and some properties of arc splines are worked out in the fifth section.

Since we sometimes use notation which might appear uncommon, we want to refer to page 211 ff., where you can find an exhaustive list of the symbols we'll subsequently use.

*'Everyone knows what a curve is,
until he has studied enough mathematics
to become confused through the countless number
of possible exceptions.'*

(Felix Klein, German mathematician)

2.1 Conics and Circles

The theory of conics is well-established (cf. [14]). Therefore, we only give a short introduction to familiarize the reader with our notation.

For $n, m \in \mathbb{N}$ let $\mathcal{P}_n(\mathbb{R}^m, \mathbb{R})$ denote the vector space of the real valued polynomial functions on \mathbb{R}^m of degree at most n . A set $C \subset \mathbb{R}^m$ is called *quadric* if there exists a polynomial $p \in \mathcal{P}_2(\mathbb{R}^m, \mathbb{R}) \setminus \{0\}$ whose zero set is C , i.e. $C = p^{-1}(\{0\})$. Since the zero set doesn't change when multiplying p with a non-zero real number, every projective point $x \in S := \mathbb{P}(\mathcal{P}_2(\mathbb{R}^m, \mathbb{R}))$ corresponds to a quadric C_x . Let us denote the projective equivalence class of the polynomial p by \hat{p} . However, it should be noted that the mapping $\Phi : S \rightarrow \mathfrak{Q}$, $\Phi(x) = C_x$ is not bijective, where \mathfrak{Q} denotes the set of all quadrics. For instance, the two polynomials $p(x, y) = x^2 + 1$ and $q(x, y) = 1$ have empty zero sets but their equivalence classes \hat{p} and \hat{q} are obviously distinct. In the case $m = 2$, quadrics are also called *conics*.

2.1.1 Remark. The polynomials $p_0, \dots, p_5 \in \mathcal{P}_2(\mathbb{R}^2, \mathbb{R})$ defined by $p_0(x, y) := x^2$, $p_1(x, y) := xy$, $p_2(x, y) := y^2$, $p_3(x, y) := x$, $p_4(x, y) := y$ and $p_5(x, y) := 1$ for $(x, y) \in \mathbb{R}^2$, form an \mathbb{R} -basis of $\mathcal{P}_2(\mathbb{R}^2, \mathbb{R})$.

A special type of conics are (*generalized*) *circles*, consisting of points, lines, circles and the empty set. Since this thesis deals with arc splines, we focus on this subset.

2.1.2 Remark. Generalized circles appear, as is well-known, as zero set of polynomials $p = \sum_{i=0}^3 \alpha_i q_i \in \mathcal{P}_2(\mathbb{R}^2, \mathbb{R}) \setminus \{0\}$ with coefficients α_i with at least one $\alpha_i \neq 0$, where $q_0(x, y) = p_0(x, y) + p_2(x, y) = x^2 + y^2$, $q_1(x, y) = p_3(x, y) = x$, $q_2(x, y) = p_4(x, y) = y$ and $q_3(x, y) = p_5(x, y) = 1$, with p_0, \dots, p_5 as in Remark 2.1.1. The corresponding vector subspace $\mathcal{P}_{\text{circ}} := \text{span}(q_0, q_1, q_2, q_3)$ has dimension four.

2.1.3 Remark. The more common definition of a circle is $C = \{x \in \mathbb{R}^2 \mid \|x - c\| = r\}$ with *center* $c \in \mathbb{R}^2$ and *radius* $r > 0$ and a line is given in the form $l := a + \mathbb{R}v$ for some $a \in \mathbb{R}^2$ and $v \in \mathbb{S}^1$, where \mathbb{S}^1 denotes the unit sphere of \mathbb{R}^2 and $\|\cdot\|$ the euclidean norm.

2.1.4 Lemma. The zero set $C = C_{\hat{p}}$ given by a polynomial $p = \sum_{i=0}^3 \alpha_i q_i$ is

- i) a line $\Leftrightarrow \alpha_0 = 0$, but $\alpha_i \neq 0$ for some $i \in \{1, 2\}$,
- ii) a circle $\Leftrightarrow \alpha_0 \neq 0$ and $\alpha_1 + \alpha_2 > 4\alpha_0\alpha_3$,
- iii) the whole plane $\mathbb{R}^2 \Leftrightarrow \alpha_i = 0$ for all $i = 0, 1, 2, 3$,

Proof. E.g. [66], 5.2. □

2.1.5 Lemma. *Given three points $x_1, x_2, x_3 \in \mathbb{R}^2$, there exists at least one generalized circle containing them. If these three points are pairwise distinct, the generalized circle is unique. Similarly, given two points $x_1, x_2 \in \mathbb{R}^2$ and a vector $e \in \mathbb{S}^1$, there exists at least one polynomial $p \in \mathcal{P}_{\text{circ}}$ satisfying $p(x_1) = p(x_2) = 0$ and $\langle e | \nabla p(x_1) \rangle = 0$, where $\nabla p(x_1)$ denotes the gradient p at x_1 . All such polynomials p yield the same projective equivalence class \hat{p} if $x_1 \neq x_2$.*

Addendum: *Four arbitrary distinct points $x_0, x_1, x_2, x_3 \in \mathbb{R}^2$ are on a generalized circle if and only if*

$$\det \begin{pmatrix} q_0(x_0) & \cdots & q_3(x_0) \\ \vdots & & \vdots \\ q_0(x_3) & \cdots & q_3(x_3) \end{pmatrix} = 0,$$

with q_0, \dots, q_3 from Remark 2.1.2.

Proof. A polynomial $p \in \mathcal{P}_{\text{circ}}$ with $p(x_i) = 0$ for all $i = 1, 2, 3$ is in demand. But x_1, x_2, x_3 are roots of p if and only if the coefficients $\alpha_0, \alpha_1, \alpha_2, \alpha_3 \in \mathbb{R}$ with $p = \sum_{i=0}^3 \alpha_i q_i$ satisfy the linear system of equations

$$\begin{pmatrix} q_0(x_1) & \cdots & q_3(x_1) \\ q_0(x_2) & \cdots & q_3(x_2) \\ q_0(x_3) & \cdots & q_3(x_3) \end{pmatrix} \begin{pmatrix} \alpha_0 \\ \alpha_1 \\ \alpha_2 \\ \alpha_3 \end{pmatrix} = 0$$

and at least one coefficient does not vanish. The system matrix has maximal rank 3. Therefore, the solution space is at least one-dimensional, i.e. the system has non-trivial solutions.

In the second case we have a desired polynomial $p = \sum_{i=0}^3 \alpha_i q_i$ if and only if

$$\begin{pmatrix} q_0(x_1) & \cdots & q_3(x_1) \\ q_0(x_2) & \cdots & q_3(x_2) \\ \langle e | \nabla q_0(x_1) \rangle & \cdots & \langle e | \nabla q_3(x_1) \rangle \end{pmatrix} \begin{pmatrix} \alpha_0 \\ \vdots \\ \alpha_3 \end{pmatrix} = 0$$

which can be simplified to

$$\begin{pmatrix} \langle x_1 | e_1 \rangle^2 + \langle x_1 | e_2 \rangle^2 & \langle x_1 | e_1 \rangle & \langle x_1 | e_2 \rangle & 1 \\ \langle x_2 | e_1 \rangle^2 + \langle x_2 | e_2 \rangle^2 & \langle x_2 | e_1 \rangle & \langle x_2 | e_2 \rangle & 1 \\ 2 \langle e | x_1 \rangle & \langle e | e_1 \rangle & \langle e | e_2 \rangle & 0 \end{pmatrix} \begin{pmatrix} \alpha_0 \\ \vdots \\ \alpha_3 \end{pmatrix} = 0$$

when setting $e_1 := (1, 0)^T$ and $e_2 := (0, 1)^T$. Again, the solution space is non-trivial. If x_1 and x_2 are distinct, the system matrix has rank 3 due to $e \neq 0$. Therefore, the solution space has dimension 1 and the coefficients $\alpha_0, \dots, \alpha_3$ solving the system are unique up to scale. Four pairwise distinct points $x_0, x_1, x_2, x_3 \in \mathbb{R}^2$ are on a generalized circle if and only if there exists a non-trivial coefficient vector $(\alpha_0, \dots, \alpha_3) \in \mathbb{R}^4$ with $\sum_{i=0}^3 \alpha_i q_i(x_j) = 0$ for $j = 0, \dots, 3$. But this is equivalent to the existence of a non-trivial solution of the following homogeneous linear system of equations:

$$\begin{pmatrix} q_0(x_0) & \cdots & q_3(x_0) \\ \vdots & & \vdots \\ q_0(x_3) & \cdots & q_3(x_3) \end{pmatrix} \begin{pmatrix} \alpha_0 \\ \vdots \\ \alpha_3 \end{pmatrix} = 0.$$

In turn, this is obviously equivalent to

$$\det \begin{pmatrix} q_0(x_0) & \cdots & q_3(x_0) \\ \vdots & & \vdots \\ q_0(x_3) & \cdots & q_3(x_3) \end{pmatrix} = 0,$$

which proves the addendum. □

These results lead to the following definition:

2.1.6 Definition. For three pairwise distinct points $x_1, x_2, x_3 \in \mathbb{R}^2$ let $C(x_1, x_2, x_3)$ denote the uniquely determined generalized circle containing them. By abuse of notation we also denote the circle containing x_1 and x_2 and having tangent direction $v \in \mathbb{S}^1$ in x_2 by $C(x_1, x_2 | v)$.

2.1.7 Definition. A non-empty connected and compact set $A \subset \mathbb{R}^2$ is called (**generalized**) **arc** if it is a subset of a circle or a line.

We now give a brief and rather historical excursus to mathematical results concerning circles and lines, which partly follows [78]. The so-called *Apollonius' Problem* concerns the following: Given three objects, each of which may be a point, line or circle, draw a circle that is tangent to each. There are a total of ten cases. Euclid solved the two cases involving three points and three lines in his *Elements*, and the others (with the exception of the three circle problem), appeared in the *Tangencies of Apollonius* which was, however, lost. The general problem is, in principle, solvable by straightedge and compass alone.

The three-circle problem was solved by Viète (cf. [16]), and the solutions are called *Apollonius circles*. There are eight total solutions. A solution is obtained by solving the three simultaneous quadratic equations

$$(x - x_1)^2 + (y - y_1)^2 - (r \pm r_1)^2 = 0 \quad (1)$$

$$(x - x_2)^2 + (y - y_2)^2 - (r \pm r_2)^2 = 0 \quad (2)$$

$$(x - x_3)^2 + (y - y_3)^2 - (r \pm r_3)^2 = 0 \quad (3)$$

in the three unknowns x , y , r for the eight triplets of signs (cf. [25]). Expanding the equations gives

$$(x^2 + y^2 - r^2) - 2xx_i - 2yy_i \pm 2rr_i + (x_i^2 + y_i^2 - r_i^2) = 0$$

for $i = 1, 2, 3$. Since the first term is the same for each equation, taking (2) – (1) and (3) – (1) gives

$$ax + by + cr = d$$

$$a'x + b'y + c'r = d',$$

where $a = 2(x_1 - x_2)$, $b = 2(y_1 - y_2)$, $c = 2(\pm r_1 \pm r_2)$, $d = (x_1^2 + y_1^2 - r_1^2) - (x_2^2 + y_2^2 - r_2^2)$ and similarly for a', b', c' and d' (where ‘ $_2$ ’ is replaced by ‘ $_3$ ’). Solving these two simultaneous linear equations, plugging back into the quadratic equation (1) and using the quadratic formula, we can calculate a solution. Figure 5 depicts an exemplary situation.

2.1.8 Remark. Using the abbreviations P - point, L - line and C - circle, which are taken from [45], we list the ten different constellations of input data and give the maximum number of different solution in Table 2.1 (cf. [69]):

Table 2.1: The different constellations of the Apollonius’ Problem

type	PPP	LLL	PPL	PLL	PCL	CLL	CPP	CCP	CCL	CCC
nr. of sol.	1	4	2	2	4	8	2	4	8	8

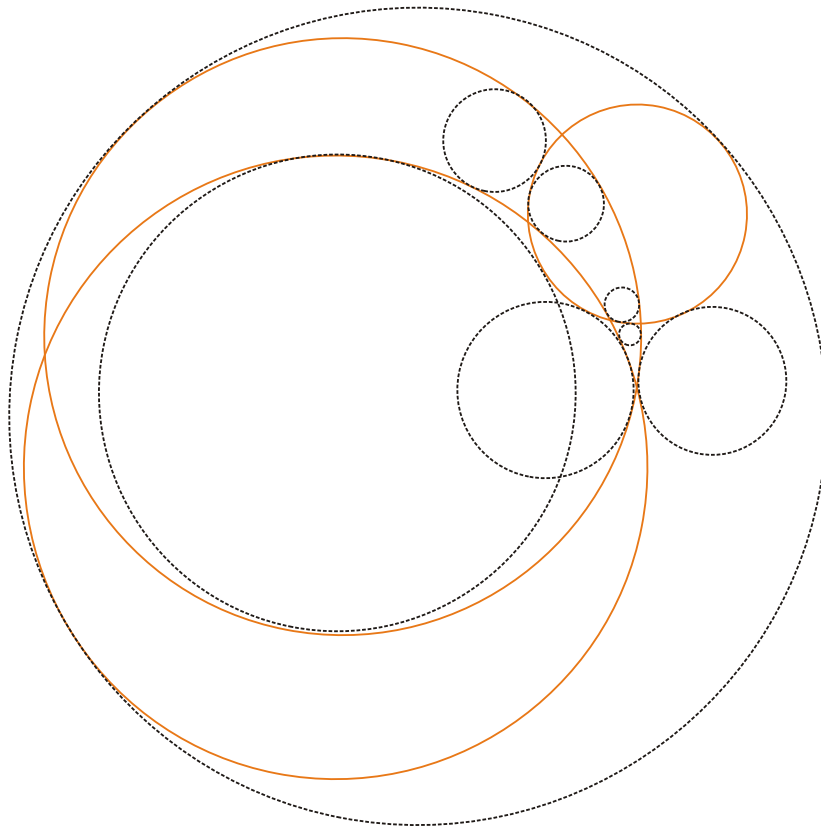


Figure 5: Example of the three-circle problem. The given circles are depicted solid, orange and the eight possible solutions are the dashed, black circles.

2.2 Set-Valued Analysis and Approximation Theory

Since generalized arcs and circles are subsets of \mathbb{R}^2 , i.e. an element of the power set $\mathfrak{P}(\mathbb{R}^2)$, we deal in this section with set-valued maps and sequences of sets. We introduce the terms of lower and upper semi-continuous mappings in case of compact valued maps. In addition we want to present the notion of cones, especially tangent cones, and state some important properties.

For the remaining part of this section let X and Y be metric spaces and $F : X \rightarrow \mathfrak{P}(Y)$ a **set-valued mapping** with $F(x)$ compact for all $x \in X$, and our notion follows [8], [43] and [30]. We set $\text{Dom}(F) := \{x \in X \mid F(x) \neq \emptyset\}$, and $B_\varepsilon(x) := \{y \in X \mid d_X(x, y) < \varepsilon\}$ for an arbitrary point $x \in X$ and $\varepsilon > 0$, where d_X is the metric on X . For a subset $M \subset X$ we define:

$$B_\varepsilon(M) := \bigcup_{x \in M} B_\varepsilon(x).$$

2.2.1 Definition. F is said to be **upper semi-continuous at** $x \in X$ if

$$\forall \varepsilon > 0 \exists \delta > 0 \forall x' \in B_\delta(x) : F(x') \subset B_\varepsilon(F(x)).$$

The mapping F is called **upper semi-continuous** if F is upper semi-continuous at every $x \in X$.

2.2.2 Definition. F is said to be **lower semi-continuous at** $x \in X$ if for any $y \in F(x)$ and any sequence $(x_n)_{n \in \mathbb{N}}$ converging to x , there exists a sequence of elements $y_n \in F(x_n)$ converging to y . The mapping F is called **lower semi-continuous** if F is lower semi-continuous at every $x \in X$.

2.2.3 Definition. F is said to be **continuous (at** $x \in X)$ if F is upper and lower semi-continuous (at $x \in X$).

A topological formulation can be found in Section 2.3. We will use both of them. It is easy to see that $\text{Dom}(F)$ is closed if F is continuous.

2.2.4 Example. The set-valued map¹ $F_1 : \mathbb{R} \rightarrow \mathfrak{P}(\mathbb{R}^2)$ defined by

$$F_1(x) := \begin{cases} [-1, 1] & , x \neq 0 \\ \{0\} & , x = 0 \end{cases}$$

¹This example is taken from [8], p.41.

is lower but not upper semi-continuous at 0, whereas the map $F_2 : \mathbb{R} \rightarrow \mathfrak{P}(\mathbb{R}^2)$,

$$F_2(x) := \begin{cases} \{0\} & , x \neq 0 \\ [-1, 1] & , x = 0 \end{cases}$$

is upper but not lower semi-continuous at 0.

2.2.5 Lemma. *If X is locally compact and if for every compact subset K of X the set $\{(x, y) \in K \times Y \mid y \in F(x)\}$ is compact, then F is upper semi-continuous.*

Proof. See [8], Prop. 1.4.12. □

Now we focus on another useful concept, the concept of cones.

2.2.6 Definition. *Let E be a real vector space. A subset A of E is called a **cone** if $\lambda x \in A$ for all $x \in A$ and $\lambda > 0$.*

Let $(A_i)_{i \in I}$ be a family of cones in E . It is clear that the empty set, $\bigcap_{i \in I} A_i$ and $\bigcup_{i \in I} A_i$ are also cones. The closure \overline{A} of a cone A is also a cone and $0 \in \overline{A}$ if E is normed and $A \neq \emptyset$. If $0 \notin A$, the cone generated by $A \cap \mathbb{S}^1$ equals A , i.e.

$$\{\lambda x \mid \lambda > 0, x \in A \cap \mathbb{S}^1\} =]0, \infty[\cdot (A \cap \mathbb{S}^1) = A.$$

2.2.7 Definition. *Let $n \in \mathbb{N}$, $M \subset \mathbb{R}^n$ and $a \in \overline{M}$. The cone*

$$T_M(a) := \bigcap_{\varepsilon > 0}]0, \infty[\cdot \overline{(B_\varepsilon(0) \cap (M - a))}$$

*is called **tangent cone to M at a** .*

2.2.8 Definition. *Given two non-empty metric spaces (X, d_X) and (Y, d_Y) and a mapping $f : X \rightarrow Y$, we define the **graph of f** as follows:*

$$\text{graph}(f) := \{(x, f(x)) \mid x \in X\} \subset X \times Y.$$

Tangent cones characterize local tangent directions to M , even if an approach via classical differentiation concepts is not possible. The following Lemma gives a connection to the theory of differentiation.

2.2.9 Lemma. *Let $m, n \in \mathbb{N}$, U be an open subset of \mathbb{R}^m and $f : U \rightarrow \mathbb{R}^n$ be differentiable at $u \in U$. Using the abbreviation $a := (u, f(u))$ we obtain: $T_{\text{graph}f}(a) = \text{graph}(Df(u))$, where D denotes the differential operator.*

Proof. See [31]. □

2.3 Hausdorff Metric and Local Hausdorff Topology

We now sketch some theoretical background and mathematical foundations concerning set-valued mappings and set limits. We want to present this within a comfortable topological framework which is not so common. The definitions and results are mainly based on set limits as seen in the previous section (cf. [8]). Thus, this chapter deals with a general topological foundation of some basic concepts of set-valued analysis. The following treatise is mainly based on [30].

The notion of set limits, as introduced in [8] and [51], can be formulated in the setting of topological spaces. In fact, we end up with a metrizable topological space if the underlying locally compact space is σ -compact and metrizable. Let us first briefly sketch some topological technicalities.

2.3.1 Definition. *Let (X, d) be a metric space.*

1) *For non-empty sets $A, B \subset X$ we define the distance*

$$\text{dist}(A, B) := \inf_{x \in A} \inf_{y \in B} d(x, y).$$

*We set $\text{dist}(A, B) := \infty$ if A or B is empty. If A is a singleton $\{x\}$ we use the notation $\text{dist}(x, B)$ instead of $\text{dist}(\{x\}, B)$. In case of $X = \mathbb{R}^n$ endowed with the euclidean norm dist is also called the **euclidean distance**.*

2) *Let $\mathfrak{K}(X)$ denote the system of all non-empty, compact subsets of X and $\mathfrak{C}(X)$ the system of all closed subsets of X .*

3) *We endow $\mathfrak{K}(X)$ with the **Hausdorff metric***

$$\mathfrak{h}(A, B) := \max\left\{\sup_{x \in A} \text{dist}(x, B), \sup_{x \in B} \text{dist}(x, A)\right\}.$$

If X is complete, the metric space $(\mathfrak{K}(X), \mathfrak{h})$ is complete as well (cf. [47]).

If (X, d) is a locally compact metric space possessing a sequence of compact subsets covering X (σ -compactness), a sequence $(K_n)_{n \in \mathbb{N}}$ of compact subsets of X exists s.t. K_n is contained in the interior K_{n+1}° of K_{n+1} for every $n \in \mathbb{N}$ and $\bigcup_{n \in \mathbb{N}} K_n^\circ = X$. If X is compact, $K_n = X$ for sufficiently large natural numbers n is implied. An increasing covering sequence $(K_n)_{n \in \mathbb{N}}$ of this type is called an *exhaustive sequence* in X . For every $n \in \mathbb{N}$

$$d_n(A, B) = \max\left\{\sup_{x \in A} \text{dist}(x, B \cup \overline{X \setminus K_n}), \sup_{x \in B} \text{dist}(x, A \cup \overline{X \setminus K_n})\right\}$$

is a pseudometric on $\mathfrak{C}(X) \setminus \{\emptyset\}$. The sequence $(d_n)_{n \in \mathbb{N}}$ defines a locally compact topology on $\mathfrak{C}(X) \setminus \{\emptyset\}$ (see [30], Section 7). Endowing $\mathfrak{C}(X)$ with the topology of Alexandrov's one point compactification of $\mathfrak{C}(X) \setminus \{\emptyset\}$ (thus identifying \emptyset with the point at infinity) $\{U_n \mid n \in \mathbb{N}\}$ is a fundamental system of neighborhoods of \emptyset in $\mathfrak{C}(X)$, where $U_n := \{A \in \mathfrak{C}(X) \mid A \cap K_n = \emptyset\}$ for every $n \in \mathbb{N}$ (cf. [30], Proposition 7.2).

2.3.2 Definition. *The topology introduced above will be called the **local Hausdorff topology** (abbreviated **LH-topology**) on $\mathfrak{C}(X)$ throughout this thesis.*

The pseudometrics d_n are sometimes clumsy to work with. Setting

$$\tau_n(A, B) = \max \left\{ \sup_{x \in A \cap K_n} \text{dist}(x, B), \sup_{x \in B \cap K_n} \text{dist}(x, A) \right\}$$

and $V_{n,\varepsilon}(A) := \{B \in \mathfrak{C}(X) \setminus \{\emptyset\} \mid \tau_n(A, B) \leq \varepsilon\}$ for $A \in \mathfrak{C}(X) \setminus \{\emptyset\}$, it is shown in [30] that $\{V_{n,\varepsilon}(A) \mid n \in \mathbb{N}, \varepsilon > 0\}$ is a fundamental system of neighborhoods of A with respect to the LH-topology (see [30], Prop. 7.1).

The LH-topology is metrizable as the defining family of pseudo-metrics is countable. To check topological properties via convergence it is therefore sufficient to use sequences in this case.

In order to simplify the notations, we assume that all locally compact spaces mentioned are σ -compact and metrizable!

The notion of semi-continuity is also used for set-valued maps as we have seen in the section before. We here give a topological definition. It is not hard to prove that both definitions yield the same.

2.3.3 Definition. *Let (X, d_X) and (Y, d_Y) be metric spaces, where (Y, d_Y) is locally compact. For every system S of closed subsets in Y let*

$$S_- := \{A \in \mathfrak{C}(Y) \mid \exists C \in S : A \subset C\}$$

*denote the system of all closed subsets of some set C of S . With this notation a function $f : X \rightarrow \mathfrak{C}(Y)$ is called **upper semi-continuous** at a point $x \in E$ if for every neighborhood U of the set $f(x)$ there is $\delta > 0$ s.t. $f(v) \in U_-$, whenever $v \in X$ satisfies $d_X(x, v) < \delta$. The mapping f is **upper semi-continuous** if it is upper semi-continuous at every point of X .*

2.3.4 Proposition. *If B is a subset of X , the distance function $\mathfrak{C}(X) \rightarrow [0, +\infty]$, $A \mapsto \text{dist}(A, B)$ is upper semi-continuous in the LH-topology. It is continuous if B is compact.*

Proof. See [30], Proposition 2.2. □

2.3.5 Theorem. *Let A be a metric space, $n \in \mathbb{N}$ and let X be an open subset of \mathbb{R}^m with $m \geq n$. Furthermore, let $f : A \times X \rightarrow \mathbb{R}^n$ be continuous s.t. the partial maps $f_a(x) = f(a, x)$ are differentiable at every $x \in f_a^{-1}(\{0\})$ for every $a \in A$. If the total differentials $Df_a(x)$ are surjective for every $x \in f_a^{-1}(\{0\})$ and all $a \in A$, the mapping $A \rightarrow \mathfrak{C}(X)$, $a \mapsto f_a^{-1}(\{0\})$ is LH-continuous.*

Proof. Follows immediately from [30], Theorem 3.13. □

2.3.6 Remark. Since we have $\mathfrak{K}(Y) \subset \mathfrak{B}(Y)$ for any metric space Y , a set-valued mapping $F : X \rightarrow \mathfrak{K}(Y)$ is continuous with respect to the Hausdorff metric if and only if F is upper and lower semi-continuous in the sense of Definition 2.2.1 and 2.2.2.

2.3.7 Remark. If θ is a metric on $\mathfrak{C}(X)$ induced by the LH-topology, $(\mathfrak{K}(X), \theta|_{\mathfrak{K}(X)})$ is a metric space as well. However, in general, the LH-topology and the topology induced by \mathfrak{h} are not equal. For instance, the sequence $(A_n)_{n \in \mathbb{N}}$ with $A_n := [-n, n]$ converges to \mathbb{R} with respect to the LH-topology, but it is not a Cauchy-sequence with respect to the Hausdorff metric. If a mapping $F : X \rightarrow \mathfrak{K}(Y)$ is continuous with respect to the Hausdorff metric, it is also continuous with respect to the LH-topology, i.e. the LH-topology is coarser than the topology given by the Hausdorff metric. (cf. [30]) Nevertheless, if X is compact, we have $\mathfrak{K}(X) = \mathfrak{C}(X) \setminus \{\emptyset\}$ and the LH-topology as well as the Hausdorff metric induce the same topology on $\mathfrak{K}(X)$.

2.4 Planar Curves

Let us recall in a few pages some elementary notions of the geometry of planar curves, which we want to use in the following. All definitions are given in the plane. Most of them can be generalized in higher dimensions, but we keep a two-dimensional point of view, which is sufficient for our issues. Proofs of the presented results and the evidence that the terms we will introduce are well-defined, can be found in [28], [38] or [27].

2.4.1 Definition. A mapping $f : [a, b] \rightarrow \mathbb{R}^n$ with $n \in \mathbb{N} \setminus \{0\}$ is called \mathcal{C}^1 if an $\varepsilon > 0$ exists s.t. $g :]a - \varepsilon, b + \varepsilon[\rightarrow X$ is continuously differentiable and $g|_{[a,b]} = f$. f is said to be **piecewise \mathcal{C}^1** if there exists a subdivision $a =: t_0 < t_1 < \dots < t_{n+1} := b$ s.t. $f|_{[t_k, t_{k+1}]}$ is a \mathcal{C}^1 -mapping for all $0 \leq k \leq n$. In the same way (piecewise) \mathcal{C}^m , $m > 1$ mappings $f : [a, b] \rightarrow \mathbb{R}^n$ can be defined.

2.4.2 Definition. We call $w : [a, b] \rightarrow \mathbb{R}^2$ a **parametrized curve** or **parametrization** if it is piecewise \mathcal{C}^1 .

Note that mostly in literature parametrized curves are understood as continuous or \mathcal{C}^∞ mappings. But we want to focus on piecewise \mathcal{C}^1 mappings. Since we are not interested in the parametrization w itself but only in the image $w([a, b])$ and its orientation, we use an equivalence relation. For this purpose, the following definition is useful:

2.4.3 Definition. A **change of parameters** is a continuous mapping $\phi : [a, b] \rightarrow [c, d]$, which is piecewise \mathcal{C}^1 , surjective and satisfies $\phi'(s) > 0$ aside from finitely many points.

It can be shown that every change of parameters is a strictly monotonically increasing homeomorphism and the composition $w \circ \phi : [a, b] \rightarrow \mathbb{R}^2$ is a piecewise \mathcal{C}^1 parametrization if w is piecewise \mathcal{C}^1 .

Now we are able to introduce an equivalence relation on the set of all parameterizations.

2.4.4 Definition. Two parametrized curves $w_1 : [a, b] \rightarrow \mathbb{R}^2$ and $w_2 : [c, d] \rightarrow \mathbb{R}^2$ are called **equivalent** if there exists a change of parameters $\phi : [a, b] \rightarrow [c, d]$ with $w_1 = w_2 \circ \phi$. The corresponding equivalence classes are called **oriented paths** or **oriented curves**.

For the sake of brevity we often simply write *path* and *curve* instead of oriented path and oriented curve. Let us denote the set of all oriented paths by $\mathcal{W}(\mathbb{R}^2)$.

If ω is a path, the images $w_1([a, b])$ and $w_2([c, d])$ are equal for every two parameterizations $w_1 : [a, b] \rightarrow \mathbb{R}^2$ and $w_2 : [c, d] \rightarrow \mathbb{R}^2$ in ω .

2.4.5 Definition. *This image set is called **trace of** ω and is denoted by $\text{tr}(\omega)$. Likewise, we have $w_1(a) = w_2(c)$ and $w_1(b) = w_2(d)$. Hence we can speak of the **starting point** $S(\omega)$ and the **endpoint** $E(\omega)$ of ω . If $S(\omega) = E(\omega)$, ω is said to be **closed** or a **loop**. Paths ω possessing an injective parametrization are said to be **simple**. A closed curve is called **Jordan curve**¹ if it has a parametrization $w : [a, b] \rightarrow \mathbb{R}^2$ whose restriction $w|_{[a, b[}$ is injective.*

For any two paths ω_1 and ω_2 with $E(\omega_1) = S(\omega_2)$ there exists a path ω , s.t. for every two parameterizations $w_1 : [0, 1] \rightarrow \mathbb{R}^2$ of ω_1 and $w_2 : [1, 2] \rightarrow \mathbb{R}^2$ of ω_2 the parametric curve $w : [0, 2] \rightarrow \mathbb{R}^2$ with $w|_{[0, 1]} = w_1$ and $w|_{[1, 2]} = w_2$ is a parametrization of ω .

2.4.6 Definition. *In the situation above ω is also called **juxtaposition of** ω_1 and ω_2 .*

Obviously, the juxtaposition yields an associative composition. We use the more uncommon notation $\omega_1 \cdots \omega_n$ for the juxtaposition of the curves $\omega_1, \dots, \omega_n$.

2.4.7 Definition. *For an arbitrary path ω the **inverse path** ω^{-1} of ω is defined as follows: Choosing any representative $w : [a, b] \rightarrow \mathbb{R}^2$ of ω , ω^{-1} is the equivalence class of $w^* : [a, b] \rightarrow \mathbb{R}^2$ with $w^*(t) = w(b + a - t)$.*

Clearly, we have $\text{tr}(\omega) = \text{tr}(\omega^{-1})$ and $(\omega^{-1})^{-1} = \omega$.

Identifying \mathbb{C} with \mathbb{R}^2 , we can define the *winding number* since we are only dealing with piecewise \mathcal{C}^1 mappings.

2.4.8 Definition. *Let ω be a Jordan curve and $a \in \mathbb{R}^2 \setminus \text{tr}(\omega)$. The number*

$$\mathfrak{w}(\omega, a) = \frac{1}{2\pi} \int_{\omega} \frac{dz}{z - a}.$$

*is then called the **winding number of** ω .*

2.4.9 Theorem (Jordan). *Let ω be a Jordan curve and $K := \text{tr}(\omega)$. Then the open set $\mathbb{R}^2 \setminus K$ has two connected components, a bounded one $I \subset \mathbb{R}^2 \setminus K$ and an unbounded one $E \subset \mathbb{R}^2 \setminus K$. For the boundaries of I and E we obtain $\partial I = \partial E = K$ and, additionally, we get $\forall x \in E \mathfrak{w}(\omega, x) = 0$ and $(\forall x \in I \mathfrak{w}(\omega, x) = 1 \text{ or } \forall x \in I \mathfrak{w}(\omega, x) = -1)$.*

¹In literature, a Jordan curve usually does not need to have a piecewise \mathcal{C}^1 but only a continuous parametrization.

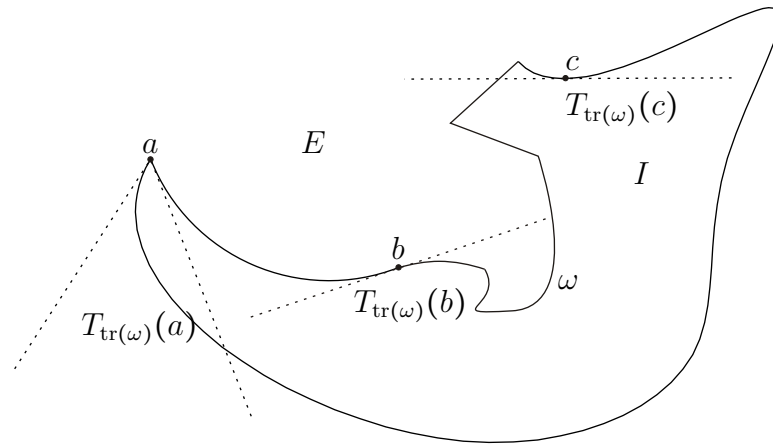


Figure 6: Illustration of Definitions 2.4.10 and 2.4.11. The points b and c are smooth points whereas a is a vertex. The dotted lines indicate the corresponding tangent cones.

Proof. cf.[27], Ch. IX, Ap. 4.2. □

2.4.10 Definition. In the situation of Theorem 2.4.9, I is called the **interior** of ω and E the **exterior** of ω . If $\mathbf{w}(\omega, x) = 1$ for all $x \in I$, ω is said to be **counterclockwise (CCW) oriented** and otherwise **clockwise (CW) oriented** (cf. Figure 6).

2.4.11 Definition. Let M be the trace of a curve. A point $a \in M$ is called **smooth** if $T_M(a)$ is a line, i.e. $T_M(a) = \mathbb{R} \cdot v$ for some $v \in \mathbb{S}^1$. Otherwise, a is said to be a **vertex**.

An example is illustrated in Figure 6.

2.4.12 Remark. Since we have restricted ourselves to piecewise \mathcal{C}^1 mappings, the number of vertices of a curve is obviously finite.

In order to be able to examine curves in a more detailed manner, we need the term *tangent vector*:

2.4.13 Definition. Let $w : [a, b] \rightarrow \mathbb{R}^2$ be a parametric curve that is \mathcal{C}^1 at $t \in [a, b]$. If the **tangent vector** $w'(t) \in \mathbb{R}^2$ does not vanish, we can consider the **tangent unit vector** $\frac{w'(t)}{\|w'(t)\|}$. Since this vector does not depend on the choice of the representative w of ω , we can set $\tau_\omega(x) := \frac{w'(t)}{\|w'(t)\|}$ and call it the **tangent unit vector of ω at $x := w(t)$** .

We are able to define a (strict) total order on the traces of simple paths, since we have built the equivalence classes order-preservingly.

2.4.14 Definition. *Let ω be a simple path. Then the [strict] total order \leq_ω [$<_\omega$] is given as follows:*

$$\forall x_1, x_2 \in \text{tr}(\omega) : x_1 \leq_\omega x_2 [x_1 <_\omega x_2] :\Leftrightarrow t_1 \leq t_2 [t_1 < t_2],$$

where $w : [a, b] \rightarrow \mathbb{R}^2$ is an arbitrary parametrization of ω and $t_i \in [a, b]$ are the unique parameters with $w(t_i) = x_i$, $i = 1, 2$.

In this situation we set additionally:

$$[x_1, x_2]_\omega := \{w(t) \in \text{tr}(\omega) \mid t \in [t_1, t_2]\}.$$

If there is no ambiguity, we simply write $[x_1, x_2]$.

We denote the curve that corresponds to the parametrization $w|_{[t_1, t_2]}$ by $\omega|_{[x_1, x_2]}$.

We also need to introduce the length of a curve, which is introduced in the following definition.

2.4.15 Definition. *Let ω be an oriented path.*

- 1) *Choosing an arbitrary parametrization $w : [a, b] \rightarrow \mathbb{R}^2$, the **length of ω** is defined as follows: $\text{len}(\omega) := \int_a^b \|w'(t)\| dt$.*
- 2) *If there exists a parametrization with $w'(t) \neq 0$ for all $t \in [a, b]$, we call ω **regular**.*

It is easy to show that these terms are really well-defined.

2.4.16 Definition. *Let ω be a regular curve. A parametrization $w \in \omega$ is called **arc length parametrization of ω** if $\|w'(t)\| = 1$ for all t . In this case we also call w **normal**.*

2.4.17 Lemma. *Every regular curve ω possesses an arc length parametrization.*

Proof. See e.g. [28] or [38]. □

2.4.18 Lemma. *Let $w : [a, b] \rightarrow \mathbb{R}^2$ be an arc length parametrization of a curve ω . Let w be piecewise \mathcal{C}^2 . Then we obtain $\langle w'(t) | w''(t) \rangle = 0$ for all $t \in [a, b]$ except for a finite number of points.*

Proof. Follows immediately from the equation $\langle w'(t) | w'(t) \rangle = 1$ and the chain rule. □

2.4.19 Definition. Let $w : [a, b] \rightarrow \mathbb{R}^2$ be an arc length parametrization of a curve ω that is \mathcal{C}^2 . Identifying \mathbb{C} with \mathbb{R}^2 and denoting the imaginary unit by i , there exists a function $\kappa : [a, b] \rightarrow \mathbb{R}$ s.t. $w''(t) = \kappa(t) \cdot i \cdot w'(t)$ which is called **curvature**. The **normal** is defined by $n(t) := i \cdot w'(t)$.

Let $x := w(t) \in \text{tr}(\omega)$ for some $t \in [a, b]$ with w \mathcal{C}^2 at t . In this case, we say that ω has **curvature** $\kappa(t)$ at x .

2.4.20 Remark. By definition $(w'(t), n(t))$ is an orthonormal base of \mathbb{R}^2 . We also speak of curvature and the normal in case of piecewise \mathcal{C}^2 curves, although these functions are only defined except for finitely many points.

2.4.21 Remark. Let ω be piecewise \mathcal{C}^2 and $w : [a, b] \rightarrow \mathbb{R}^2$ a parametrization of ω . For every smooth point $a \in \text{tr}(\omega)$ with non-vanishing curvature, there exist a neighborhood U of a and a linear mapping $l : \mathbb{R}^2 \rightarrow \mathbb{R}$ s.t. $l^{-1}(\{0\}) = T_{\text{tr}(\omega)}(a)$ and $l(x) \geq 0$ for all $x \in U \cap \text{tr}(\omega)$.

Next, we focus on another class of curves that has somewhat ‘nice’ properties. This class will be very useful for the mathematic modeling in Chapter 3.

2.4.22 Definition. An oriented curve ω is called **analytic** (\mathcal{C}^ω) if it has a parametrization $w : I \rightarrow \mathbb{R}^2, w(t) := (w_1(t), w_2(t))^T$ s.t. for every $t_0 \in I$ there are real coefficients a_n, b_n , and power series $\sum_{n=0}^{\infty} a_n(t-t_0)^n$ and $\sum_{n=0}^{\infty} b_n(t-t_0)^n$, which are convergent to w_1 and w_2 respectively in a neighborhood of t_0 .

If ω has a parametrization $w : [a, b] \rightarrow \mathbb{R}^2$ with an analytic extension $\tilde{w} :]a-\varepsilon, b+\varepsilon[\rightarrow \mathbb{R}^2$, i.e. $\tilde{w}|_{[a,b]} = w$, for some $\varepsilon > 0$, the curve ω is said to be **restricted analytic** (\mathcal{R}^ω).

2.4.23 Definition. The juxtaposition $\omega := \omega_1 \cdots \omega_n$ of finitely many restricted analytic curves is called **piecewise restricted analytic** or **piecewise \mathcal{R}^ω** .

We need some important properties of regions bounded by piecewise restricted analytic curves in order to enable a well-arranged formulation of our mathematical modeling in Chapter 3.

2.4.24 Proposition. *Let ω be a piecewise \mathcal{R}^ω Jordan curve with interior I . For every $x, y \in \bar{I}$ there exists a piecewise \mathcal{R}^ω curve γ of finite length starting at x and ending in y with $\text{tr}(\gamma) \cap \text{tr}(\omega) \subset \{x, y\}$ and $\text{tr}(\gamma) \subset \bar{I}$.*

Proof. By the Curve Selection Lemma ([76], Corollary 1.5) and by [75], p. 192 there are restricted analytic functions w_1 and w_2 with $w_1(0) = x$, $w_2(0) = y$ and $w_1(t), w_2(t) \in I$ for all $t > 0$. Then Theorem 6.10 in [13] yields the existence of a curve of finite length joining $w_1(1)$ and $w_2(1)$ in I and therefore of one joining x and y with the desired properties. \square

2.4.25 Proposition. *Let γ_1 and γ_2 be two piecewise \mathcal{R}^ω curves. Then there exist a finite set E , a set J and a $n \in \mathbb{N}$ s.t. $\text{tr}(\gamma_1) \cap \text{tr}(\gamma_2) = E \cup J$ and J is homeomorphic to n intervals in \mathbb{R} .*

Proof. The set $\text{tr}(\gamma_1) \cap \text{tr}(\gamma_2)$ is a bounded semi-analytic set¹. By [75], p. 192 and [13], Corollary 2.7, every bounded semi-analytic set has finitely many components which are points or homeomorphic to an interval, thus concluding the proof. \square

¹A definition can be found in [13, 75].

2.5 Arc Splines and their Properties

Now we are able to give an exact definition of circular arc splines:

2.5.1 Definition. A path $\gamma \in \mathcal{W}(\mathbb{R}^2)$ is called (*circular*) **arc spline** if

- i) γ is a simple curve or a Jordan curve and
- ii) there exists a finite family $(A_i)_{1 \leq i \leq n}$ of generalized arcs with $\text{tr}(\gamma) = \bigcup_{i=1}^n A_i$.

Such sequences $(A_i)_{1 \leq i \leq n}$ are called **defining sequences** of γ . The minimal possible number $n \in \mathbb{N}$ s.t. there exists a defining sequence $(A_i)_{1 \leq i \leq n}$ is called **segment number** of γ . We use the abbreviation $|\gamma| := n$. Arc splines γ with $|\gamma| = 1$ are also called (*oriented*) **arcs**.

2.5.2 Proposition. Let γ be an arc spline with $|\gamma| = n$. Then every defining sequence $(A_i)_{1 \leq i \leq n}$ of γ satisfies: $\text{card}(A_i \cap A_j) \leq 1$ for all $i \neq j$.

Proof. Follows immediately from Lemma 2.1.5 and the minimality of n . \square

Therefore, there always exists a unique representation $\gamma = \gamma_1 \cdots \gamma_n$ with oriented arcs γ_i . Throughout this thesis we simply write $\gamma = \gamma_1 \cdots \gamma_n$ for an arc spline with $|\gamma| = n$ and do not explicitly mention that the unique representation introduced above is meant.

2.5.3 Definition. Let $\gamma = \gamma_1 \cdots \gamma_n$ be an arc spline with breakpoints $a_1 < \cdots < a_{n-1}$. If $\tau_{\gamma_i}(a_i) = \tau_{\gamma_{i+1}}(a_i)$ is satisfied for all $i = 1, \dots, n$, the arc γ is said to be **smooth**. Additionally, $\tau_{\gamma_n}(E(\gamma)) = \tau_{\gamma_1}(S(\gamma))$ is required if γ is closed, i.e. $S(\gamma) = E(\gamma)$. The direction $\tau_\gamma(E(\gamma)) \in \mathbb{S}^1$ is called the **exiting direction** of γ .

We denote the set of all smooth arc splines with segment number $n \in \mathbb{N}$ by \mathfrak{S}^n , and use the abbreviations: $\mathfrak{S} := \mathfrak{S}^1$ and $\mathfrak{S}^\infty := \bigcup_{n \in \mathbb{N}} \mathfrak{S}^n$.

Biarcs are smooth arc splines with two segments.

An illustration can be found in Figure 7.

2.5.4 Remark. Many authors refer to the smoothness condition in Definition 2.5.3 as \mathbf{G}^1 -continuity (e.g. [65]). It is clear that this is equivalent to requiring a regular \mathcal{C}^1 -parametrization.

2.5.5 Definition. We denote the corresponding generalized circle for an arbitrary oriented arc by $C(\gamma) \subset \mathbb{R}^2$.

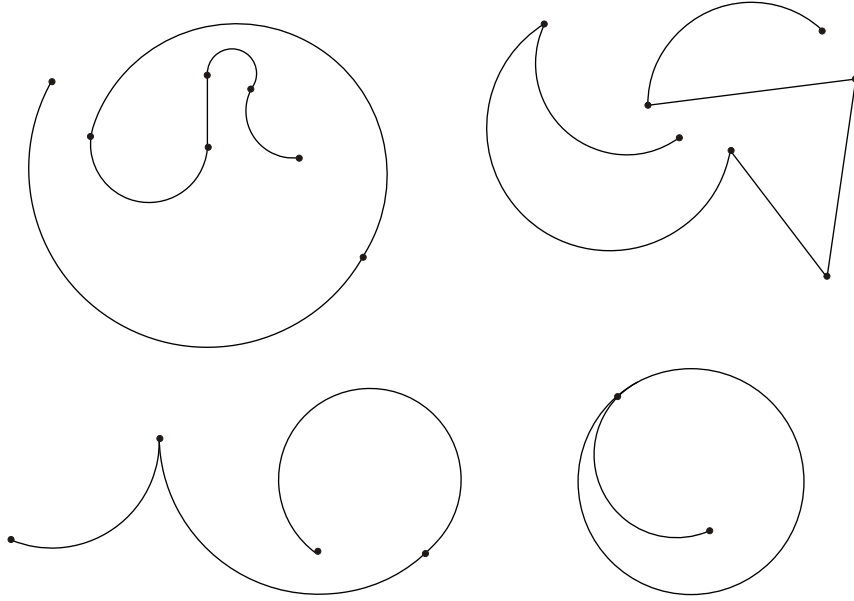


Figure 7: Illustration of Definition 2.5.1 and 2.5.3. Top left: Smooth arc spline with six segments. Top right: Arc spline with six segments that is not smooth. Bottom left: Non-smooth arc spline. Bottom right: No arc spline since the curve is not simple and not a Jordan curve.

2.5.6 Remark. Although a point is a generalized arc since it is a non-empty, connected and compact subset of a generalized circle, there is no oriented arc whose trace is a point.

2.5.7 Definition. The oriented arcs γ_i of an arc spline $\gamma_1 \cdots \gamma_n \in \mathfrak{S}^n$ are called *segments*.

In the same manner as arc splines we can define polygonal curves, which simply consist of line segments but not generalized arcs:

2.5.8 Definition. A curve $\omega \in \mathbb{R}$ is called *polygonal curve* if it can be represented by $\omega := \omega_1 \cdots \omega_n$ with *oriented line segments* ω_i , i.e. $\text{tr}(\omega_i)$ is a line segment. In this case we can refer to *segments* as well. A *polygon* is a polygonal Jordan curve.

In some cases, we will also need a parametric form of arc splines. Before we give a closed form of such a parametrization, we introduce some more notation:

2.5.9 Definition. Let $D := \left\{ (a, b, v) \in \mathbb{R}^2 \times \mathbb{R}^2 \times \mathbb{S}^1 \mid a \neq b, v \neq \frac{a-b}{\|a-b\|} \right\}$. Given an element $(a, b, v) \in D$, we denote the uniquely determined oriented arc starting at a and ending at b with exiting direction v by $\gamma_{a,b,v}$.

2.5.10 Definition. For any complex number $z \in \mathbb{C} \setminus \{0\}$ the **argument** is set to:

$$\arg(z) := \begin{cases} \frac{\pi}{2} - \arctan\left(\frac{\Re(z)}{\Im(z)}\right) & , \Im(z) > 0 \\ 0 & , \Im(z) = 0, \Re(z) > 0 \\ \pi & , \Im(z) = 0, \Re(z) < 0 \\ -\frac{\pi}{2} - \arctan\left(\frac{\Re(z)}{\Im(z)}\right) & , \Im(z) < 0 \end{cases} ,$$

where $\Re(z)$ and $\Im(z)$ denote the real and the imaginary part of z .

The function is continuous on $\mathbb{C} \setminus]-\infty, 0]$ and we have $z = |z| \cdot e^{i \arg(z)}$ for all $z \in \mathbb{C} \setminus \{0\}$ (cf. [37]). Let $a, b \in \mathbb{R}^2$ be two distinct points and $v \in \mathbb{S}^1$ with $v \neq -\frac{b-a}{\|b-a\|}$. Identifying $\mathbb{R}^2 \cong \mathbb{C}$ and setting

$$\sigma := \det(b-a, v) \text{ and } \tau := \langle v | b-a \rangle ,$$

we can give a parametrization of $\gamma_{a,b,v}$ in a closed form: It can be shown that $r := -\frac{\|b-a\|^2}{2\sigma}$ and $c := b + r \cdot iv$ are the corresponding radius and center of $\gamma_{a,b,v}$ if $\gamma_{a,b,v}$ is not a line segment.

2.5.11 Definition. With the notion introduced above, we can define the **opening angle**.

For any $(a, b, v) \in D$ satisfying $v \neq \frac{b-a}{\|b-a\|}$ we set:

$$\kappa(a, b, v) := \begin{cases} \operatorname{sgn}(\sigma) \cdot \kappa_0(a, b, v) & , \tau > 0 \\ \operatorname{sgn}(\sigma) \cdot \pi & , \tau = 0 \\ \operatorname{sgn}(\sigma) \cdot |2\pi - \kappa_0(a, b, v)| & , \tau < 0 \end{cases}$$

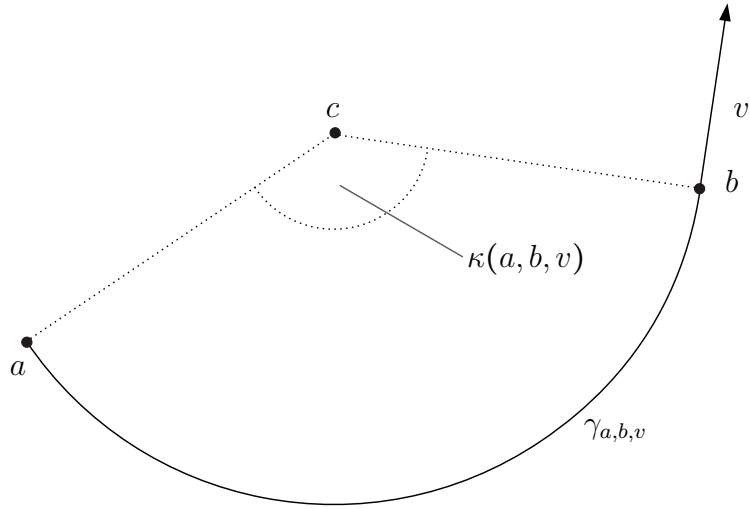
where $\kappa_0(a, b, v) := |\arg(b-c) - \arg(a-c)|$ with c defined above, and introduce the mapping

$$f : D \times [0, 1] \rightarrow \mathbb{R}^2, \quad f((a, b, v), t) := \begin{cases} a + (b-a) \frac{e^{i\kappa(a,b,v)t} - 1}{e^{i\kappa(a,b,v)} - 1} & , v \neq \frac{b-a}{\|b-a\|} \\ a + (b-a) \cdot t & , v = \frac{b-a}{\|b-a\|} \end{cases}$$

2.5.12 Remark. It is easy to verify that the mapping $f_{a,b,v} : [0, 1] \rightarrow \mathbb{R}^2, t \mapsto f((a, b, v), t)$ is a parametrization of the circular arc $\gamma_{a,b,v}$. Figure 8 shows an illustration of such an arc.

2.5.13 Remark. It is not hard to prove that $\kappa(a, b, v) \in]-2\pi, 2\pi[$. If $v = \frac{b-a}{\|b-a\|}$, we parametrize the line segment between a and b . Otherwise, we have $\kappa(a, b, v) \neq 0$ and

$$f(a, b, v, t) = \frac{b-a}{e^{i\kappa(a,b,v)} - 1} \cdot e^{i\kappa(a,b,v)t} + a - \frac{b-a}{e^{i\kappa(a,b,v)} - 1}$$

Figure 8: Visualization of the arc $\gamma_{a,b,v}$.

for all $t \in [0, 1]$. We can also compute the center and the radius in other terms:

$$c = a - \frac{b-a}{e^{i\kappa(a,b,v)} - 1} \quad \text{and} \quad r = \left| \frac{b-a}{e^{i\kappa(a,b,v)} - 1} \right|.$$

Note that for every radius $r > \frac{1}{2}|b-a|$ there exist four different circular arcs with radius r from a to b (see Figure 9).

2.5.14 Lemma. *The mapping $f : D \times [0, 1] \rightarrow \mathbb{R}^2$ in Definition 2.5.11 is continuous.*

Proof. Extending κ to the domain D when setting $\kappa(a, b, \frac{b-a}{\|b-a\|}) := 0$, we first show that $\kappa : D \rightarrow]-2\pi, 2\pi[$ is continuous. Since $\kappa_0(a, b, v) = |2\pi - \kappa_0(a, b, v)| = \pi$ for $\tau = 0$, it remains to show that κ is continuous at $v_{a,b} := \frac{b-a}{\|b-a\|}$. In this case, we have

$$\lim_{\substack{v \rightarrow v_{a,b} \\ v \in \mathbb{S}^1 \setminus \{v_{a,b}\}}} \kappa_0(a, b, v) = 0$$

and $\tau > 0$. Therefore, κ is continuous at $v_{a,b}$. Setting $\Delta := \{(a, b) \in \mathbb{R}^2 \mid a = b\}$, the mapping

$$g : ((\mathbb{R}^2 \times \mathbb{R}^2) \setminus \Delta) \times]-2\pi, 2\pi[\times [0, 1] \rightarrow \mathbb{R}^2, \quad g((a, b, \rho), t) := \begin{cases} a + (b-a) \frac{e^{i\rho t} - 1}{e^{i\rho} - 1} & , \rho \neq 0 \\ a + (b-a) \cdot t & , \rho = 0 \end{cases}$$

is also continuous since we obtain by L'Hospital's rule:

$$\lim_{\rho \rightarrow 0} a + (b-a) \frac{e^{i\rho t} - 1}{e^{i\rho} - 1} = a + \lim_{\rho \rightarrow 0} (b-a) \frac{e^{i\rho t} - 1}{e^{i\rho} - 1} = a + \lim_{\rho \rightarrow 0} (b-a) \frac{e^{i\rho t} i t}{e^{i\rho} i} = a + (b-a)t.$$

Therefore, $f = g \circ \kappa$ is continuous as well. \square

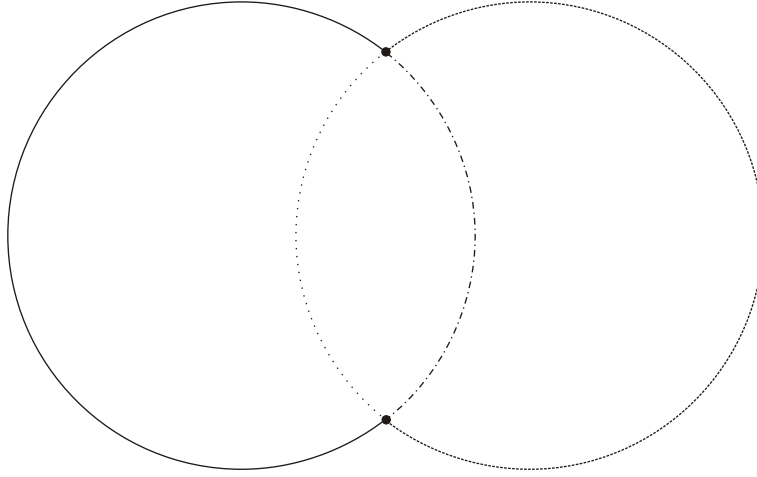


Figure 9: Illustration of all circular arcs from a to b with the same radius.

2.5.15 Definition. For any $(a, b, v) \in D$ and $\xi \in \mathbb{R}^2$ we define

$$A_{a,b,v}(\xi) := \begin{pmatrix} a_1^2 + a_2^2 & a_1 & a_2 & 1 \\ b_1^2 + b_2^2 & b_1 & b_2 & 1 \\ 2(b_1 v_1 + b_2 v_2) & v_1 & v_2 & 0 \\ \xi_1^2 + \xi_2^2 & \xi_1 & \xi_2 & 1 \end{pmatrix} \in \mathbb{R}^{4 \times 4}.$$

Furthermore, we define the mapping

$$h : D \times \mathbb{R}^2 \rightarrow \mathbb{R}, \quad h((a, b, v), \xi) := \det(A_{a,b,v}(\xi))$$

and for fixed $(a, b, v) \in D$

$$h_{a,b,v} : \mathbb{R}^2 \rightarrow \mathbb{R}, \quad h_{a,b,v}(\xi) := h((a, b, v), \xi).$$

Using the notation of Remark 2.1.2, we obtain

$$A_{a,b,v}(\xi) = \begin{pmatrix} q_0(a) & \cdots & q_3(a) \\ q_0(b) & \cdots & q_3(b) \\ \langle v | q_0(b) \rangle & \cdots & \langle v | q_3(b) \rangle \\ q_0(\xi) & \cdots & q_3(\xi) \end{pmatrix}.$$

2.5.16 Definition. The mapping $A : D \rightarrow \mathfrak{K}(\mathbb{R}^2)$, $A(a, b, v) := \text{tr}(\gamma_{a,b,v})$ assigns the trace of the oriented arc $\gamma_{a,b,v}$ to every triple (a, b, v) . The mapping that yields the corresponding generalized circles can be defined as follows:

$$C : D \rightarrow \mathfrak{K}(\mathbb{R}^2), \quad C(a, b, v) := h_{a,b,v}^{-1}(\{0\}),$$

where $h_{a,b,v}$ is defined in Definition 2.5.15.

2.5.17 Lemma. *The mapping C defined in Definition 2.5.16 is continuous with respect to the LH-Topology.*

Proof. Obviously, $h : D \times \mathbb{R}^2 \rightarrow \mathbb{R}$ is continuous. Let $(a, b, v) \in D$ and $\xi \in h_{a,b,v}^{-1}(\{0\})$. Then $h_{a,b,v}$ is differentiable at ξ and it is not hard to prove that $Dh_{a,b,v}(\xi)$ is surjective. Using Theorem 2.3.5 completes the proof. A more detailed proof can be found in [30]. \square

2.5.18 Lemma. *The mapping A defined in Definition 2.5.16 is continuous with respect to the Hausdorff metric.*

Proof. We have $\text{tr}(\gamma_{a,b,v}) = f(a, b, v, [0, 1])$, where f is the mapping defined in 2.5.11. Let $\varepsilon > 0$, $\theta_0 \in D$ and $\rho > 0$ s.t. $K := \{\theta \in \mathbb{R}^2 \times \mathbb{R}^2 \times \mathbb{S}^1 \mid \|\theta - \theta_0\| \leq \rho\} \subset D$. By Lemma 2.5.14, f is continuous. Since $K \times [0, 1]$ is compact, f is uniformly continuous on $K \times [0, 1]$. Thus, there exists a $\delta > 0$ s.t. for all $\xi, \eta \in K \times [0, 1]$ the implication

$$\|\xi - \eta\| < \delta \Rightarrow \|f(\xi) - f(\eta)\| < \varepsilon$$

holds. Then, for any $\phi_0 \in D$ with $\|\phi_0 - \theta_0\| < \min(\rho, \delta)$ and for all $t \in [0, 1]$, we have $\|f(\xi, t) - f(\eta, t)\| < \varepsilon$. Therefore, we obtain

$$\sup_{x \in f(\theta_0, [0, 1])} \text{dist}(x, f(\phi_0, [0, 1])) < \varepsilon \quad \text{and} \quad \sup_{x \in f(\phi_0, [0, 1])} \text{dist}(x, f(\theta_0, [0, 1])) < \varepsilon,$$

which means $\mathfrak{h}(f(\theta_0, [0, 1]), f(\phi_0, [0, 1])) = \mathfrak{h}(A(\theta_0), A(\phi_0)) < \varepsilon$. Hence A is continuous. \square

2.5.19 Lemma. *If $C_{\hat{p}}$ is a generalized circle given by a polynomial p and*

$$D_0 := \{(a, b, v) \in D \mid 1 \leq \text{card}(C(a, b, v) \cap C_{\hat{p}}) \leq 2\},$$

then the mapping

$$D_0 \rightarrow \mathfrak{C}(\mathbb{R}^2), (a, b, v) \mapsto g_{a,b,v}^{-1}(\{0\})$$

is LH-continuous, where g is defined as follows:

$$g : D_0 \times \mathbb{R}^2 \rightarrow \mathbb{R}^2, g((a, b, v), \xi) := \begin{pmatrix} h((a, b, v), \xi) \\ p(\xi) \end{pmatrix}.$$

Proof. Clearly, g is continuous and $g_{a,b,v}$ is differentiable for all $(a, b, v) \in D_0$. Similar to the proof of Lemma 2.5.17, we can show the continuity of the mapping defined above by using Theorem 2.3.5. \square

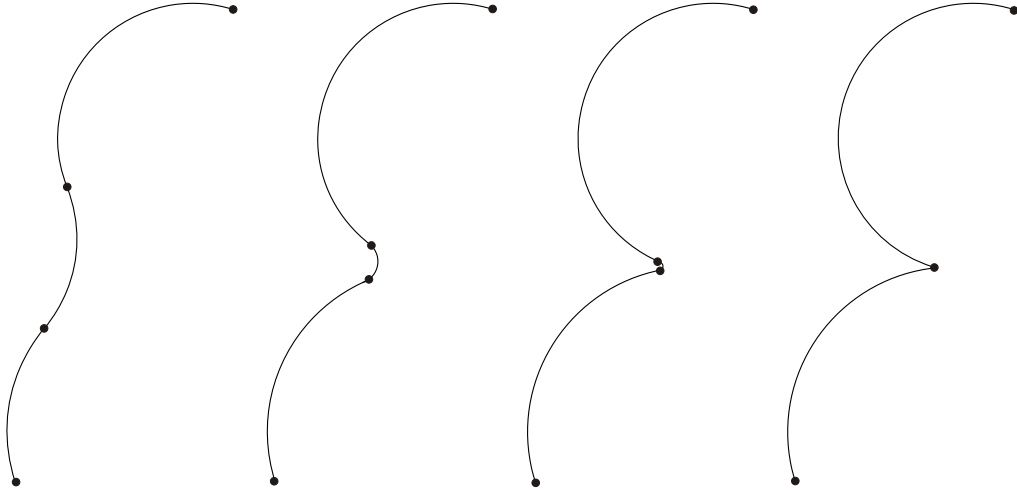


Figure 10: Convergent sequence $(A_n)_{n \in \mathbb{N}}$ in $\overline{\text{tr}(\mathfrak{S}^3)}$ with $A_n := \text{tr}(\gamma_1^{(n)} \gamma_2^{(n)} \gamma_3^{(n)})$. On the right the limit set of the sequence is indicated. While every A_n is the trace of a smooth arc spline, the limit is the trace of a non-smooth arc spline where the second segment collapsed to a point.

Next, we concern ourselves to the set of arc splines with more than one segment and work out important properties.

2.5.20 Definition. Let $n \in \mathbb{N} \setminus \{0\}$. For every subset \mathfrak{M} of \mathfrak{S}^n the set

$$\text{tr}(\mathfrak{M}) := \{\text{tr}(\gamma) \in \mathfrak{K}(\mathbb{R}^2) \mid \gamma \in \mathfrak{M}\}$$

is called the **trace of \mathfrak{M}** .

2.5.21 Remark. Attention: The set $\text{tr}(\mathfrak{S}^n)$ is **not** closed with respect to the Hausdorff-metric, as indicated in Figure 10.

In fact, it is not hard to show that $\overline{\text{tr}(\mathfrak{S}^\infty)}$ is the set of all compact, connected subsets of \mathbb{R}^2 that are a finite union of generalized arcs. These sets are also called *arc conglomerates*.

2.5.22 Definition. Let γ be an arbitrary arc spline. The set $V(\gamma)$ of all non-smooth points of γ is called the **vertex set of γ** . Denoting the set of all (not necessarily smooth) arc splines by \mathfrak{T} , we set for all $n \in \mathbb{N} \setminus \{0\}$:

$$\overline{\mathfrak{S}^n} := \{\gamma \in \mathfrak{T} \mid |\gamma| + \text{card}(V(\gamma)) \leq n\}.$$

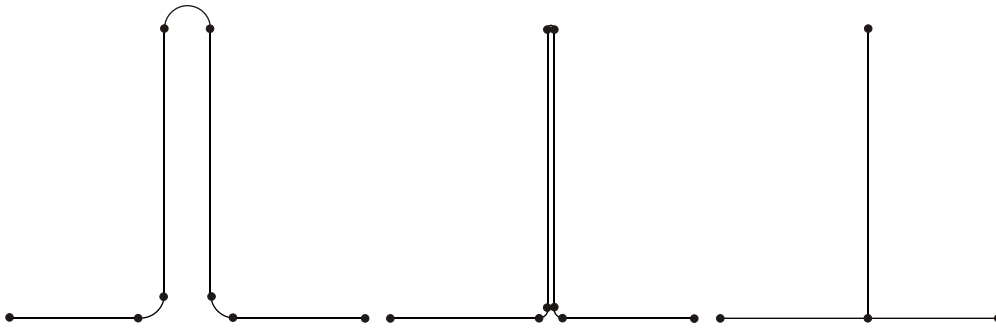


Figure 11: Convergent sequence in $\overline{\text{tr}(\mathfrak{S}^7)}$ whose limit point is not the trace of an arc spline.

Note that we didn't endow \mathfrak{S}^n with any topology. Thus, $\overline{\mathfrak{S}^n}$ does **not** mean the closure of \mathfrak{S}^n with respect to a topology on \mathfrak{T} . Moreover, we can state the following properties:

2.5.23 Remark. Obviously, we have $\mathfrak{S} = \overline{\mathfrak{S}}$ and it is not hard to see the set inclusion $\mathfrak{S}^n \not\subseteq \overline{\mathfrak{S}^n}$ for all $n > 1$. As indicated in Figure 11, there are sequences in $\overline{\text{tr}(\mathfrak{S}^n)}$ converging to an arc conglomerate which cannot be represented as an arc spline, and therefore we have $\text{tr}(\overline{\mathfrak{S}^n}) \not\subseteq \overline{\text{tr}(\mathfrak{S}^n)}$.

However, since every $\gamma \in \overline{\mathfrak{S}^n}$ is an arc spline, we can always choose the uniquely determined, minimal representation $\gamma = \gamma_1 \cdots \gamma_m$ with $m = |\gamma| \leq n - \text{card}(V(\gamma))$.

2.5.24 Remark. The following propositions are easy to see (proofs can be found in [57], Theorem 1-2-2):

- i) Suppose that $(A_n)_{n \in \mathbb{N}}$ is a sequence in $\mathfrak{K}(\mathbb{R}^2)$ converging to $A \in \mathfrak{K}(\mathbb{R}^2)$ with respect to the Hausdorff metric. Then for every $a \in A$ there exists a sequence of points $(a_n)_{n \in \mathbb{N}}$ with $a_n \in A_n$ convergent to a .
- ii) Let $n \in \mathbb{N}$. For every $i \in \{1, \dots, n\}$ let $(A_{i,m})_{m \in \mathbb{N}}$ be a convergent sequence in $\mathfrak{K}(\mathbb{R}^2)$. Setting $A_i := \lim_{m \rightarrow \infty} A_{i,m}$ for $i = 1, \dots, n$, we obtain: $\lim_{m \rightarrow \infty} \bigcup_{i=1}^n A_{i,m} = \bigcup_{i=1}^n A_i$

With these propositions we are able to show the following lemma, which can also be found in [57] (Corollary on page 22).

2.5.25 Lemma. *The set \mathfrak{Z} of all non-empty, compact and connected subsets of \mathbb{R}^2 is a closed subset of $\mathfrak{K}(\mathbb{R}^2)$ with respect to the Hausdorff metric.*

Proof. Let $(Z_n)_{n \in \mathbb{N}}$ be a sequence in \mathfrak{Z} that converges to an arbitrary $Z \in \mathfrak{K}(\mathbb{R}^2)$. Then we have to show that Z is connected. For this purpose, we suppose to the contrary $Z \notin \mathfrak{Z}$.

Clearly, there exists a connected and compact set $L \subset \mathbb{R}^2$ with $Z \subset L^\circ$ and therefore a bound $N \in \mathbb{N}$ s.t. Z_n is included in L for all $n \geq N$. Since Z is not connected, we can choose two disjoint open sets U_1 and U_2 with $U_1 \cap Z \neq \emptyset \neq U_2 \cap Z$ covering Z . Then the set $L \setminus (U_1 \cup U_2)$ is not empty and compact. Furthermore, there exists a number $M \in \mathbb{N}$ s.t. $Z_n \subset U_1 \cup U_2$ for all $n \geq M$. Otherwise, we could choose a subsequence $(Z_{n_i})_{i \in \mathbb{N}}$ with $Z_{n_i} \cap (L \setminus (U_1 \cup U_2)) \neq \emptyset$ and hence $Z \cap (L \setminus (U_1 \cup U_2)) \neq \emptyset$, which would be a contradiction to $Z \subset U_1 \cup U_2$. Altogether, we obtain for a sufficiently large $n \in \mathbb{N}$: $U_1 \cap Z_n \neq \emptyset \neq U_2 \cap Z_n$ since $U_1 \cap Z \neq \emptyset \neq U_2 \cap Z$. But this contradicts the fact that Z_n is connected and proves the claim. \square

2.5.26 Lemma. *The set of all generalized arcs in \mathbb{R}^2 is a closed subset of $\mathfrak{A}(\mathbb{R}^2)$.*

Proof. Let $(S_n)_{n \in \mathbb{N}}$ be a sequence of generalized arcs which is convergent to $S \in \mathfrak{A}(\mathbb{R}^2)$. By Lemma 2.5.25, we have $S \in \mathfrak{J}$ since $\overline{\text{tr}(\mathfrak{S})}$ is a subset of \mathfrak{J} . It is therefore sufficient to show that S is the subset of a generalized circle. W.l.o.g. we can suppose S not to be a singleton. Since S is connected, it contains an infinite number of points. We will now show that every quadruple of distinct points $(a^{(0)}, a^{(1)}, a^{(2)}, a^{(3)})$ on S lies on a generalized circle. Since $(S_n)_{n \in \mathbb{N}}$ converges to S with respect to the Hausdorff metric, we have sequences $(a_n^{(i)})_{n \in \mathbb{N}}$ of points $a_n^{(i)} \in S_n$ convergent to $a^{(i)}$ for all $i \in \{0, 1, 2, 3\}$. Due to the fact that all arcs S_n have corresponding circles C_n containing them, we obtain by Lemma 2.1.5:

$$\det \begin{pmatrix} q_0(a_n^{(0)}) & q_1(a_n^{(0)}) & q_2(a_n^{(0)}) & 1 \\ q_0(a_n^{(1)}) & q_1(a_n^{(1)}) & q_2(a_n^{(1)}) & 1 \\ q_0(a_n^{(2)}) & q_1(a_n^{(2)}) & q_2(a_n^{(2)}) & 1 \\ q_0(a_n^{(3)}) & q_1(a_n^{(3)}) & q_2(a_n^{(3)}) & 1 \end{pmatrix} = 0$$

with $q_0(\xi_1, \xi_2) = \xi_1^2 + \xi_2^2$, $q_1(\xi_1, \xi_2) = \xi$ and $q_2(\xi_1, \xi_2) = \xi_2$. Since the determinant mapping is continuous regarding the matrix entries, we have

$$\det \begin{pmatrix} q_0(a^{(0)}) & q_1(a^{(0)}) & q_2(a^{(0)}) & 1 \\ q_0(a^{(1)}) & q_1(a^{(1)}) & q_2(a^{(1)}) & 1 \\ q_0(a^{(2)}) & q_1(a^{(2)}) & q_2(a^{(2)}) & 1 \\ q_0(a^{(3)}) & q_1(a^{(3)}) & q_2(a^{(3)}) & 1 \end{pmatrix} = \lim_{n \rightarrow \infty} \det \begin{pmatrix} q_0(a_n^{(0)}) & q_1(a_n^{(0)}) & q_2(a_n^{(0)}) & 1 \\ q_0(a_n^{(1)}) & q_1(a_n^{(1)}) & q_2(a_n^{(1)}) & 1 \\ q_0(a_n^{(2)}) & q_1(a_n^{(2)}) & q_2(a_n^{(2)}) & 1 \\ q_0(a_n^{(3)}) & q_1(a_n^{(3)}) & q_2(a_n^{(3)}) & 1 \end{pmatrix} = 0.$$

Hence the points $a^{(0)}, a^{(1)}, a^{(2)}, a^{(3)}$ lie on a generalized circle C , and S is contained in C . Let now $x \neq a_i$ for all $i = 0, 1, 2$ be an arbitrary point of S . Then there exists a

generalized circle C_2 including x_1, a_0, a_1 and a_2 . But by Lemma 2.1.5, we obtain $C = C_2$. Since $x \in S$ was chosen arbitrarily, this proves the assertion. \square

From that we can easily deduce:

2.5.27 Corollary. *The set of all generalized arcs in \mathbb{R}^2 is equal to $\overline{\text{tr}(\mathfrak{S})}$, and we have the equation of sets $\overline{\mathfrak{S}^2} = \mathfrak{S} \cup \mathfrak{S}^2$.*

As already indicated in Chapter 1, arc splines satisfy important invariance criteria, namely:

2.5.28 Proposition. *Circular arc splines are invariant with respect to rotations, scalings and translations, i.e. $\lambda e^{i\phi} \cdot \text{tr}(\gamma) + t$ is the trace of a (smooth) arc spline for any (smooth) arc spline $\gamma \in \mathfrak{S}^n$, rotation angle $\phi \in [0, 2\pi]$, scalar $\lambda > 0$ and translation vector $t \in \mathbb{R}^2 \cong \mathbb{C}$.*

Proof. W.l.o.g. we can assume $\gamma \in \mathfrak{S}$ with starting point a , end point b and exiting direction $v \in \mathbb{S}^1$. Then γ can be parametrized by

$$g_{a,b,v}(t) := a + (b - a) \frac{e^{i\kappa(a,b,v)t} - 1}{e^{i\kappa(a,b,v)} - 1}.$$

Setting $A(x) := \lambda e^{i\phi} \cdot x + t$, it can be easily verified that

$$A(g_{a,b,v}(t)) = A(a) + (A(b) - A(a)) \frac{e^{i\kappa(A(a),A(b),A(v))t} - 1}{e^{i\kappa(A(a),A(b),A(v))} - 1}$$

and $\kappa(a, b, v) = \kappa(A(a), A(b), A(v))$. Hence we have $A(g_{a,b,v}(t)) = g_{A(a),A(b),A(v)}(t)$, which concludes the proof. \square

We now present further properties of arc splines without proof since they are well-known. Nevertheless, they are particularly important for our applications outlined in Chapter 5.

2.5.29 Definition. *Let $M \subset \mathbb{R}^2$ be compact and $\varepsilon > 0$. The ε -**offset** of M is defined as follows: $M_\varepsilon := \{a \in \mathbb{R}^2 \mid \text{dist}(a, M) = \varepsilon\}$. If ω is a curve with regular parametrization $w : [0, 1] \rightarrow \mathbb{R}^2$ and normal $n(t)$, the ε -**parallel curve** of ω is the curve given by $w_\varepsilon(t) := w(t) + \varepsilon n(t)$.*

2.5.30 Remark. For sufficiently small $\varepsilon > 0$ the ε -offset of the trace of an arc spline is the trace of an arc spline as well. Likewise, the ε -parallel curve of an arc spline is an arc spline.

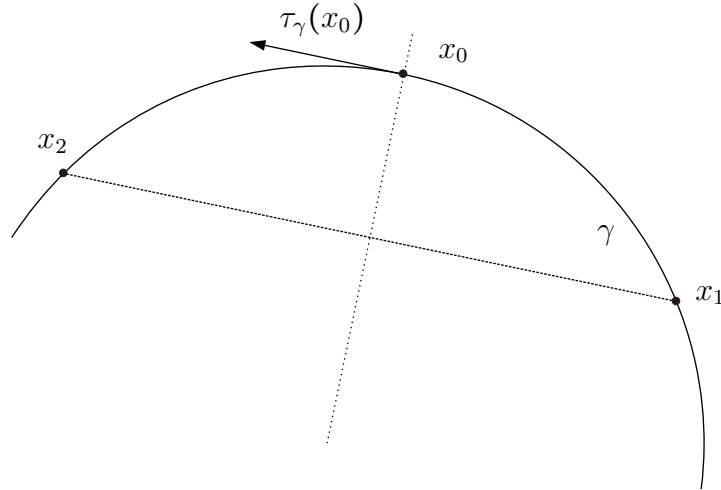


Figure 12: Visualization of Proposition 2.5.33.

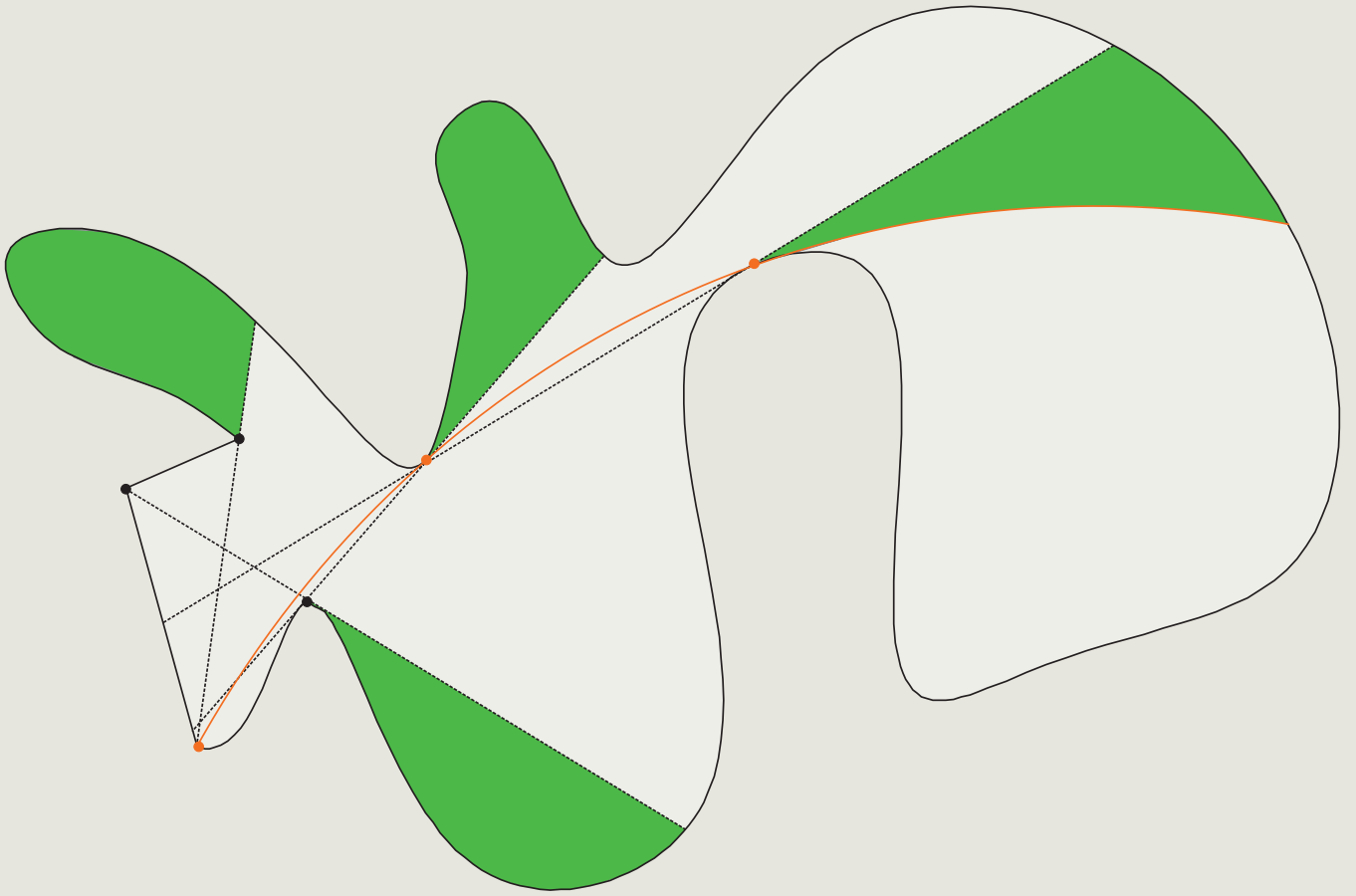
The claims above are satisfied for all $\varepsilon < \min\{r_1, \dots, r_n\}$, where r_i denotes the radius of the segment γ_i corresponding to the considered arc spline $\gamma = \gamma_1 \cdots \gamma_n \in \mathfrak{T}$, where the radius of a line segment is set to ‘ ∞ ’.

2.5.31 Proposition. *The curvature of an oriented arc is $\pm 1/r$ when r denotes the radius of the corresponding circle or vanishes if its trace is a line segment. A regular curve is an arc spline if and only if its curvature is a step function.*

2.5.32 Definition. *Since the curvature of an oriented arc $\gamma \in \mathfrak{S}$ is a constant function, we can identify it with its value and denote it by $\kappa(\gamma) \in \mathbb{R}$.*

The following proposition is easy to see as well:

2.5.33 Proposition. *Let γ be an oriented arc with arc length parametrization $w : I \rightarrow \mathbb{R}^2$ and $t_1, t_2 \in I$ with $t_1 < t_2$. Setting $t_0 := \frac{t_2 - t_1}{2} \in I$ and $x_i := w(t_i)$ for $i \in \{0, 1, 2\}$, we obtain: $\tau_\gamma(x_0) = w'(t_0) = \frac{x_2 - x_1}{\|x_2 - x_1\|}$ (cf. Figure 12).*



3

MATHEMATICAL MODELING AND RESULTS

One method of modeling the application outlined in Chapter 1 is given in this chapter. Additionally, we give some useful terms and definitions and specify solutions mathematically in order to enable an efficient algorithmic approach. For this purpose, we stick to practice as closely as required.

In general, we characterize the set of points that can be reached by a (smooth) circular arc spline with n segments ($n \in \mathbb{N} \setminus \{0\}$) starting from a given generalized arc or point $tr(s)$ and staying inside a so called *tolerance channel*. This set is called the circular n -visibility set. We introduce this term in Section 3.1 and show that common boundaries like polygons (example in Figure 13) and arc splines used in classical visibility problems are just examples of this abstract term.

In order to give an efficient mathematical characterization of the circular n -visibility sets, *alternating sequences* (Section 3.2) and *feasible direction sets* (Section 3.3) are defined and various properties are examined. With the aid of these two notions, we specify the set of all circularly visible points inside a tolerance channel (Section 3.4).

*‘As far as the laws of mathematics refer to reality,
they are not certain; and as far as they are certain,
they do not refer to reality.’*

(Albert Einstein, German physicist)

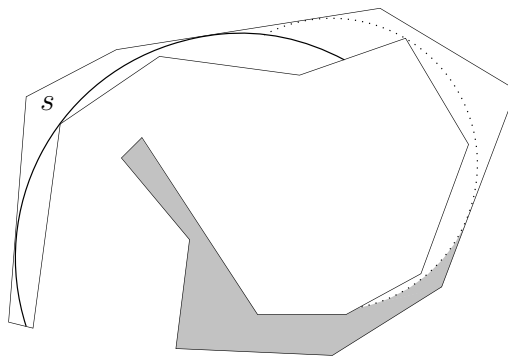


Figure 13: Simple polygon K , a circular arc s (solid curve). The shaded portion of $\overline{I_K}$ is not circularly visible from s .

The general approach is to investigate the set of visibility arcs for a fixed end point and exiting direction first. In a subsequent step we examine how this set acts when the exiting directions and then consequently also the endpoints are varied. For this characterization we use the terminology of alternating sequences.

Feasible direction sets of a point a are those sets built by all exiting directions corresponding to visibility arcs ending in a . Since they feature certain continuity properties, which is shown in Section 3.5, we are able to give an equivalent condition (Section 3.6) for an oriented arc smoothly joined to a visibility arc. The characterization of the set of all n -visible points follows by induction. The abstract formulation of tolerance channels affords using the results of Section 3.4 for the examination of the n -visibility sets.

In Section 3.7, we work out characterizations of (smooth) minimum arc paths. We present an approach for the computation of a solution based on alternating sequences. Since we can again proceed inductively, this leads to a constructive, iterative procedure, which will result in a greedy algorithm (cf. Chapter 4).

In the last section (3.8) we briefly summarize the main results and draw a comparison to the well-studied linear visibility and minimum link paths. In addition, we give an outlook to ‘cyclic’ tolerance channels and ‘(smooth) cyclic minimum arc paths’.

3.1 Tolerance Channels

In literature minimum link paths (e.g.[73]) and visibility problems ([9, 7, 23, 22, 4]) are treated within the scope of polygons and splinegons (cf. [39]). In order to formulate the problem we are interested in, we introduce a new term which is more general and abstract, including polygons, arc splines and splinegons. *Tolerance Channels* enable a well-arranged presentation of our results and a unified approach to all the visibility problems presented in Chapter 1 within a more general scope. The abstract formulation is especially useful to describe the set of points inside the channel that can be reached by a smooth arc spline with more than one segment starting from a designated generalized arc. It seems quite intuitive that a tolerance channel should consist of

- a simply connected region bounded by a ‘well-behaving’ Jordan curve,
- a starting segment given by an oriented arc or point the visibility arcs have to start from.

We have already seen an example in Figure 13. Another one is depicted in Figure 14. Before we address ourselves to defining *tolerance channels*, we introduce the term *channel*, which is just used as an auxiliary notion to define further refinements.

3.1.1 Definition. *A pair (K, s) consisting of*

- i) *a compact set $K \subset \mathbb{R}^2$ that is the trace of a piecewise \mathcal{R}^ω Jordan curve with interior I_K and exterior E_K ,*
- ii) *a path s whose trace is a generalized arc included in $\overline{I_K}$ with $S(s), E(s) \in K$ and $(T_{\overline{I_K}}(x))^\circ \neq \emptyset$ for all $x \in \text{tr}(s)$, where $T_{\overline{I_K}}(x)$ denotes the tangent cone to $\overline{I_K}$ at x ,* is called a **channel**. *In this case, we denote the uniquely determined path which is CCW oriented and starts at $S(s)$ with $K = \text{tr}(\omega_K)$ by ω_K .*

The requirement that the interior of $T_{\overline{I_K}}(x)$ is not empty for all $x \in \text{tr}(s)$ means that we have a positive ‘angle’ at all points of $\text{tr}(s)$ and therefore there exists an oriented arc starting from s into $\overline{I_K}$.

We want to use the concept of tolerance channels for examining both the 1-visibility and the n -visibility for any $n > 1$. We will show that this can be done by iteratively investigating special types of *tolerance channels*. However, these tolerance channels require more complicated *starting conditions* of their feasible arcs. In general, it is not

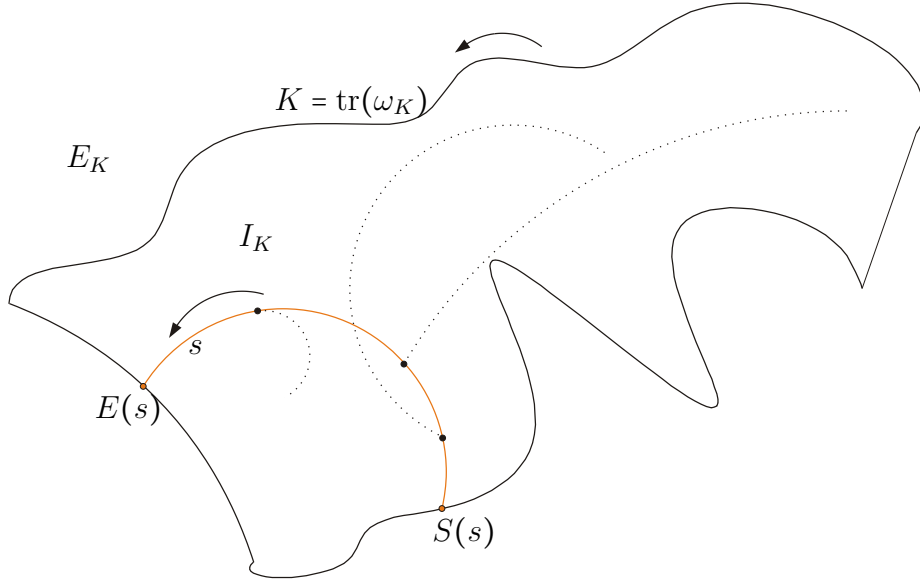


Figure 14: Illustration of a channel (K, s) .

enough to just start from $\text{tr}(s)$. We will see that it can be reasonable to reject the feasibility of an arc although it has its starting point on $\text{tr}(s)$ and stays inside $\overline{I_K}$.

For this purpose, we additionally take a set-valued mapping $\sigma : F \rightarrow \mathfrak{K}(\text{tr}(s))$ with a non-empty subset F of $\mathbb{R}^2 \times \mathbb{S}^1$ into account. The mapping σ models restrictions on the feasible starting points. In fact, σ assigns the set of all feasible starting points of the corresponding visibility arcs to every potential end point and exiting direction. For an arbitrary fixed endpoint a and exiting direction $v \in \mathbb{S}^1$ the corresponding visibility arcs are uniquely determined by their starting points $x \in \sigma(a, v)$.

We want to focus on set-valued maps σ which assure some sort of maximality of their definition sets and have ‘nice’ properties:

3.1.2 Definition. *Let s be a path of a generalized arc $\text{tr}(s)$ and let $F \neq \emptyset$ be a subset of $G := \{(a, v) \in (\mathbb{R}^2 \setminus \text{tr}(s)) \times \mathbb{S}^1 \mid \exists x \in \text{tr}(s) : (x, a, v) \in D\}$ with D from Definition 2.5.9. A mapping $\sigma : F \rightarrow \mathfrak{K}(\text{tr}(s))$ is called **restriction map (of s)** if the following is satisfied:*

- i) The set $F \subset G$ is closed with respect to the relative topology on G .*
- ii) σ is continuous with respect to the Hausdorff metric.*
- iii) If $(a, v) \in F$ and $x \in \sigma(a, v)$, then $(x, a, v) \in D$ and for all $b \in \text{tr}(\gamma_{x,a,v}) \setminus \text{tr}(s)$ there exists a direction $w \in \mathbb{S}^1$ with $(b, w) \in F$.*

iv) $\sigma(a, v)$ has at most two connected components for every $(a, v) \in F$.

In general, we cannot extend F to $\mathbb{R}^2 \times \mathbb{S}^1$ since otherwise σ might have the value of the empty set and would be not well-defined. Before we introduce more useful and important notation, in Definitions 3.1.3, 3.1.4 and 3.1.5 we give some examples of restriction maps that will play an important role when examining the circular visibility sets.

3.1.3 Definition. *Let s be a path whose trace is a generalized arc. For any pair $(a, v) \in \mathbb{R}^2 \times \mathbb{S}^1$ we set*

$$\sigma(a, v) := \{x \in \text{tr}(s) \mid \exists \gamma \in \mathfrak{G} : S(\gamma) = x, E(\gamma) = a, \tau_\gamma(a) = v, \text{card}(\text{tr}(s) \cap \text{tr}(\gamma)) = 1\}$$

and $F := \{(a, v) \in \mathbb{R}^2 \times \mathbb{S}^1 \mid \sigma(a, v) \neq \emptyset\}$, and call the mapping

$$\sigma : F \rightarrow \mathfrak{K}(\text{tr}(s)), (a, v) \mapsto \sigma(a, v)$$

starting restriction. If $\text{tr}(s)$ is a point, σ is said to be **degenerate**.

An example is depicted in Figure 15 on the left.

It is not hard to prove that the mapping defined above is well-defined and satisfies the requirements of a restriction map: E.g. the continuity can be easily deduced from Lemma 2.5.19 and Remark 2.3.7, and property *i)* can be seen as follows: Clearly, F is a subset of G , and for every sequence $(a_n, v_n)_{n \in \mathbb{N}}$ in F converging to some $(a, v) \in G$, one can choose a convergent sequence $(x_n)_{n \in \mathbb{N}}$ in $\text{tr}(s)$ with $x_n \in \sigma(a_n, v_n)$ for all $n \in \mathbb{N}$. Then the corresponding limit point x is included in $\text{tr}(s)$ and hence we get $x \in \sigma(a, v)$, as there exists an arc starting at x and ending in a with exiting direction v . Therefore, $(a, v) \in F$ and it follows that F is closed in G . Property *iii)* and *iv)* are easy to see.

Obviously, this sort of restriction map is needed in the very first step when computing the circular visibility with respect to s . The intersection $\text{tr}(s) \cap \text{tr}(\gamma)$ is required to be a singleton and seems unnatural, but this way we can guarantee for every $(a, v) \in F$ and $x, y \in \sigma(a, v)$:

$$C(\gamma_{x,a,v}) = C(\gamma_{y,a,v}) \Leftrightarrow x = y.$$

The other special types of restriction maps we introduce will be important for the characterization of the sets containing the points that can be reached by arc splines with more than one segment. As already mentioned, we will see that we can proceed iteratively. In Section 3.6 we show that oriented arcs satisfying the following starting

condition given by σ can be joined smoothly to a visibility spline starting from the primary starting segment. The properties which these different types of restriction maps have in common are sufficient to prove all the results needed for exploiting the n -circular visibility sets for every $n \in \mathbb{N} \setminus \{0\}$. Hence we introduce this further type although, at the moment, it is not yet clear why using the word 'continuation' is justified.

3.1.4 Definition. *Let s be an oriented arc. For any $(a, v) \in \mathbb{R}^2 \times \mathbb{S}^1$ we set*

$$\sigma(a, v) := \{x \in \text{tr}(s) \mid \exists \gamma \in \mathfrak{S} : S(\gamma) = x, E(\gamma) = a, \tau_\gamma(a) = v, \tau_\gamma(S(\gamma)) = \tau_s(S(\gamma))\}.$$

*Setting $F := \{(a, v) \in \mathbb{R}^2 \times \mathbb{S}^1 \mid \sigma(a, v) \neq \emptyset\}$, the mapping $\sigma : F \rightarrow \mathfrak{K}(\text{tr}(s))$ is called **degenerate unidirectional restriction**. An arc $\gamma \in \mathfrak{S}$ with $E(\gamma) = a$, $\tau_\gamma(a) = v$ and $S(\gamma) \in \sigma(a, v)$ for some $(a, v) \in F$ is said to satisfy the **degenerate continuation condition (DCC)** (cf. Figure 15 bottom right).*

Obviously, arcs satisfying the DCC can be smoothly joined to an arc γ with $C(\gamma) = C(s)$. However, there is a more general starting condition including the DCC that enables arcs to be joined smoothly (see Section 3.6). Hence it makes sense to use the word 'continuation'.

3.1.5 Definition. *Let s be an oriented arc. An arc $\gamma \in \mathfrak{S}$ is said to satisfy the **continuation condition (CC)** if either γ satisfies the DCC or $\text{tr}(\gamma) \cap \text{tr}(s) = \{x_1, x_2\}$ for some $x_1, x_2 \in \mathbb{R}^2$ and $x_1 <_s x_2$, $x_1 <_\gamma x_2$. For any $(a, v) \in \mathbb{R}^2 \times \mathbb{S}^1$ we set.*

$$\sigma(a, v) := \{x \in \text{tr}(s) \mid \exists \gamma \in \mathfrak{S} : S(\gamma) = x, E(\gamma) = a, \tau_\gamma(a) = v \text{ satisfying the CC}\}.$$

*and $F := \{(a, v) \in \mathbb{R}^2 \times \mathbb{S}^1 \mid \sigma(a, v) \neq \emptyset\}$. Then, we call the mapping $\sigma : F \rightarrow \mathfrak{K}(\text{tr}(s))$ **unidirectional restriction**.*

An exemplary situation is visualized in Figure 15, top right.

Again, it is not hard to prove that the mappings defined in Definitions 3.1.4 and 3.1.5 are restriction maps. The continuity of σ can be also deduced from Lemma 2.5.19, when possibly restricting the domain D_0 , and the properties *i*), *iii*) and *iv*) can be seen in the same manner as in case of a starting restriction.

It is important to demand the arcs satisfying the CC to have two intersections with $\text{tr}(s)$ compared to the starting restriction defined in Definition 3.1.3. I.e. for the starting point x of a feasible arc $\gamma \in \mathfrak{S}$ we obtain $x = \min \text{tr}(s) \cap \text{tr}(\gamma)$, where the minimum is taken with respect to $<_\gamma$.

In Figure 15 the different starting conditions given by various restriction mappings is illustrated.

3.1.6 Remark. In case of a degenerate starting / unidirectional restriction σ , the sets $\sigma(a, v)$ are singletons by definition. It is not hard to show that $\sigma(a, v)$ is connected for all $(a, v) \in F$ in case of a continuation restriction. The boundary points¹ x of $\sigma(a, v)$ in case of non-degenerate starting / unidirectional restrictions are the boundary points of $\text{tr}(s)$ or $x = S(\gamma)$ for some $\gamma \in \mathfrak{S}$ with $\tau_\gamma(x) = \pm\tau_s(x)$ (cf. Figure 15). Note that in case of a non-degenerate starting restriction, there might exist $(a, v) \in F$ s.t. $\sigma(a, v)$ has really two connected components. An example is given in Figure 16.

As an oriented arc is uniquely defined by its starting and end point and exiting direction, restriction maps restrict the set of all feasible oriented arcs ending in the same point and having the same exiting direction. Recalling the notation \mathfrak{S}^n of Definition 2.5.3, we can define the set of all arc splines which satisfy a starting restriction given by a restriction map $\sigma : F \rightarrow \mathfrak{K}(\text{tr}(s))$ depending on a starting segment s . We define the sets of arc splines that satisfy the starting restrictions given by a generalized arc s and a corresponding mapping σ . Note that these sets are at first independent on K for a channel (K, s) ; they only depend on s and σ respectively.

3.1.7 Definition. Let s be a path of a generalized arc $\text{tr}(s)$, and let $\sigma : F \rightarrow \mathfrak{K}(\text{tr}(s))$ be a restriction map. For each $(a, v) \in F$ we define the set of all oriented arcs ending in a with exiting direction v and satisfying the starting condition given by σ :

$$\mathfrak{S}^1(\sigma, a, v) := \mathfrak{S}(\sigma, a, v) := \{\gamma \in \mathfrak{S} \mid E(\gamma) = a, \tau_\gamma(a) = v, S(\gamma) \in \sigma(a, v)\}.$$

Accordingly, we set:

$$\mathfrak{S}^1(\sigma, a) := \mathfrak{S}(\sigma, a) := \bigcup_{v \in \mathbb{S}^1 \text{ with } (a, v) \in F} \mathfrak{S}(\sigma, a, v) \quad \text{and} \quad \mathfrak{S}^1(\sigma) := \mathfrak{S}(\sigma) := \bigcup_{(a, v) \in F} \mathfrak{S}(\sigma, a, v).$$

Let $n \in \mathbb{N} \setminus \{0\}$. Then, the set of all (smooth circular) arc splines with n segments ending in $a \in \mathbb{R}^2$ with exiting direction $v \in \mathbb{S}^1$ and satisfying the starting condition given by σ is set as follows:

$$\mathfrak{S}^n(\sigma, a, v) := \{\gamma := \gamma_1 \cdots \gamma_n \in \mathfrak{S}^n \mid E(\gamma) = a, \tau_\gamma(a) = v, \gamma_1 \in \mathfrak{S}(\sigma)\}.$$

Likewise, we can define the sets $\mathfrak{S}^n(\sigma, a)$ and $\mathfrak{S}^n(\sigma)$.

¹The boundary is built with respect to the relative topology on $C(s)$.

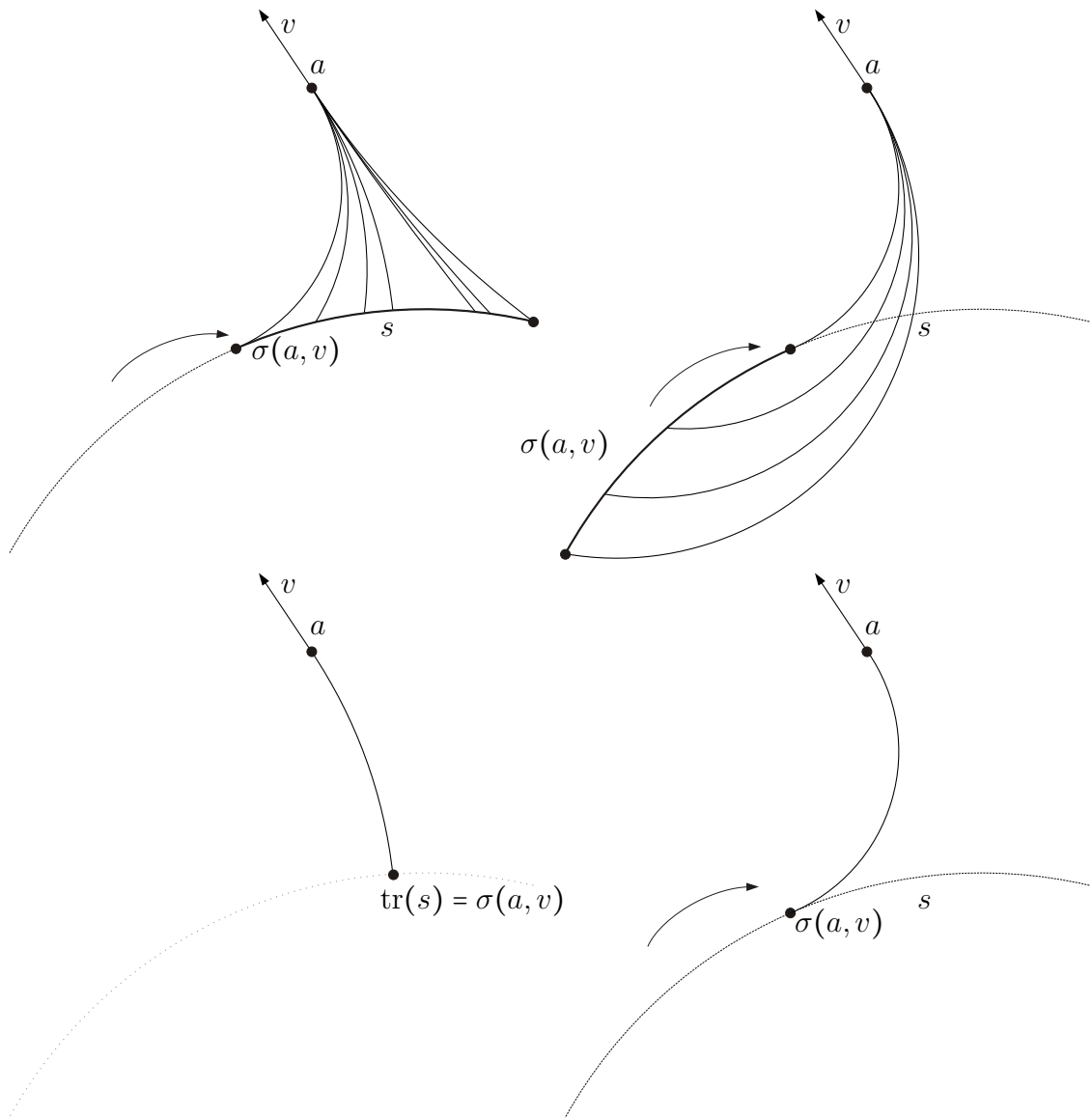


Figure 15: Illustration of restriction maps given by Definitions 3.1.3, 3.1.4 and 3.1.5 for an arbitrary $(a, v) \in F$. Top left: Starting restriction. Bottom left: Degenerate starting restriction. Top right: Unidirectional restriction. Bottom right: Degenerate unidirectional restriction

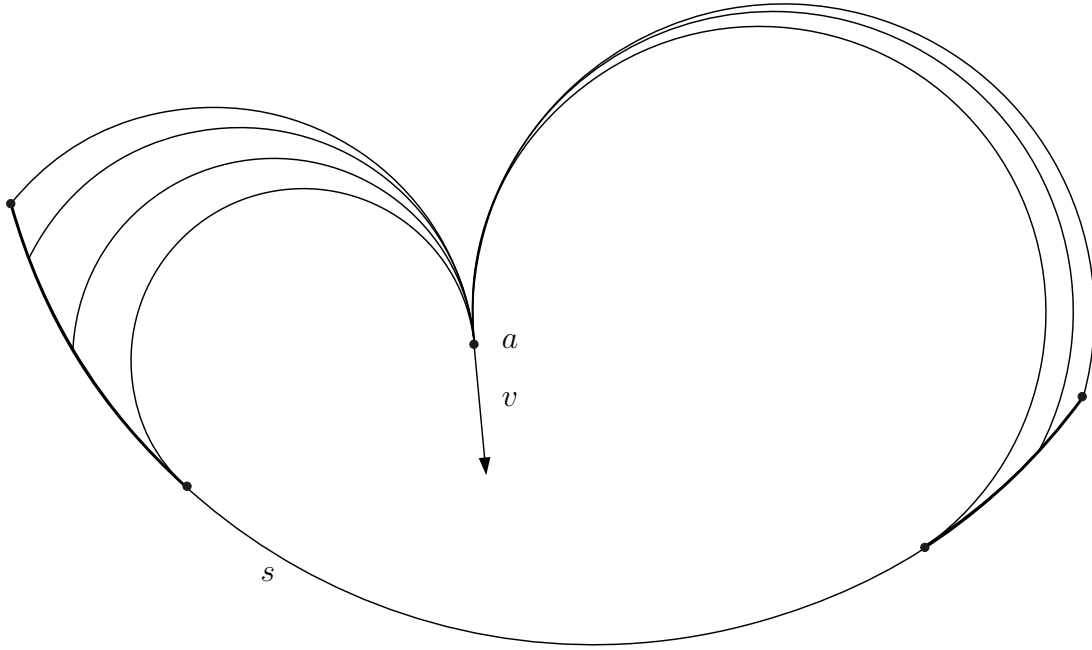


Figure 16: Example of $\sigma(a, v)$ having two connected components.

So far, we have seen that generalized arcs induce restrictions on those arc splines we are interested in by corresponding mappings σ . However, the channel itself restricts the set of feasible arc splines as well. Clearly, we only want to focus on those arc splines staying inside the channel, i.e. inside $\overline{I_K}$.

For every (K, s) we use the notations ω_K , I_K and E_K as defined in Definition 3.1.1. Then we can define the subsets of arcs contained in $\mathfrak{S}^n(\sigma)$ (cf. Definition 3.1.7) which additionally stay inside $\overline{I_K}$:

3.1.8 Definition. Let (K, s) be a channel and $\sigma : F \rightarrow \mathfrak{R}(\text{tr}(s))$ a restriction map. For every $n \geq 1$ we define subsets which only include the elements contained in $\overline{I_K}$:

- i) $\mathfrak{S}_K^n(\sigma, a, v) := \{\gamma \in \mathfrak{S}^n(\sigma, a, v) \mid \text{tr}(\gamma) \subset \overline{I_K}\}$,
- ii) $\mathfrak{S}_K^n(\sigma, a) := \{\gamma \in \mathfrak{S}^n(\sigma, a) \mid \text{tr}(\gamma) \subset \overline{I_K}\}$,
- iii) $\mathfrak{S}_K^n(\sigma) := \{\gamma \in \mathfrak{S}^n(\sigma) \mid \text{tr}(\gamma) \subset \overline{I_K}\}$.

The elements of $\mathfrak{S}_K^n(\sigma, a, v)$ are called **visibility splines (with segment number n) (with respect to (K, s, σ))**.

We use the abbreviations $\mathfrak{S}_K(\sigma) := \mathfrak{S}_K^1(\sigma)$, $\mathfrak{S}_K(\sigma, a) := \mathfrak{S}_K^1(\sigma, a)$ and $\mathfrak{S}_K(\sigma, a, v) := \mathfrak{S}_K^1(\sigma, a, v)$. A visibility spline consisting of one segment is simply called **visibility arc**.

When examining the points that can be reached by a smooth arc spline, we first focus on the set of points that are *circularly n -visible* with respect to the elements of $\overline{\mathfrak{S}^n}$ since $\text{tr}(\mathfrak{S}^n)$ is not closed as seen in Chapter 2. Working with these sets simplifies the complexity of notation considerably.

3.1.9 Definition. *Recalling Definition 2.5.22, we set for $(a, v) \in F$ and $n \in \mathbb{N} \setminus \{0\}$:*

$$\overline{\mathfrak{S}_K^n}(\sigma, a, v) := \left\{ \gamma \in \overline{\mathfrak{S}^n} \mid \exists A \in \overline{\text{tr}(\mathfrak{S}_K^n(\sigma, a, v))} \text{ with } \text{tr}(\gamma) = A, \tau_\gamma(a) = v \right\}.$$

Likewise, we define the sets $\overline{\mathfrak{S}_K^n}(\sigma, a)$ and $\overline{\mathfrak{S}_K^n}(\sigma)$.

*Then the set of all n -**(circularly) visible points (with respect to (K, s, σ))** is defined by*

$$V_K^n(\sigma) := \left\{ a \in \overline{I_K} \mid \overline{\mathfrak{S}_K^n}(\sigma, a) \neq \emptyset \right\} \cup \text{tr}(s).$$

*Instead of 1-visible we just say **(circularly) visible** and write: $V_K(\sigma) := V_K^1(\sigma)$.*

*We call the paths of $\overline{\mathfrak{S}_K^n}(\sigma)$ **generalized visibility splines**.*

Each $\gamma \in \overline{\mathfrak{S}_K^n}(\sigma, a, v)$ is an arc spline (not necessarily smooth) by definition and it is not hard to show that γ has the endpoint a . Hence $\overline{\mathfrak{S}_K^n}(\sigma, a, v)$ is well-defined.

Since the visibility splines and visibility sets depend on both a channel and a restriction map, the following definition is useful:

3.1.10 Definition. *A triple (K, s, σ) is called **tolerance channel** if (K, s) is a channel and $\sigma : F \rightarrow \mathfrak{R}(\text{tr}(s))$ is a restriction map for s .*

*If σ is a (degenerate) starting or a (degenerate) unidirectional restriction, we call (K, s, σ) a **(degenerate) starting channel** or **(degenerate) continuation channel** respectively. If σ is not degenerate, we also call (K, s, σ) **non-degenerate**.*

(Degenerate) continuation channels play an important role in examining the sets $V_K^n(\sigma)$ (cf. Section 3.6) and therefore in solving Problem 3.1.16. Before we establish some properties of tolerance channels, which we need to prove the subsequent claims, we give two examples.

3.1.11 Example. Let $\omega := \omega_1 \cdots \omega_n$ be a closed CCW oriented polygonal curve in minimal representation. We set $K := \text{tr}(\omega)$ and choose a generalized arc s with $\text{tr}(s) \subset \overline{I_K}$. Denoting the corresponding starting restriction of s by $\sigma : F \rightarrow \mathfrak{R}(\text{tr}(s))$ (cf. Definition 3.1.3), we obtain a starting channel (K, s, σ) and, in case of s being a point, a

degenerate starting channel. Both situations are visualized in Figure 17 (top left and bottom left).

In this example we obtain the circular visibility set which in literature is called *circular visibility of s* if $\text{tr}(s)$ is an edge of K , and *circular visibility of x* if $\text{tr}(s) =: \{x\}$ is a point.

3.1.12 Example. Assuming the situation described in Example 3.1.11 and replacing the restriction map σ by the (degenerate) unidirectional restriction of s (cf. Definition 3.1.4 and Definition 3.1.5), we get a (degenerate) continuation channel (K, s, σ) .

Example 3.1.12 is visualized in Figure 17 (top right, bottom right). The shaded portions shall indicate the set $\overline{I_K} \setminus V_K(\sigma)$ for the four different restriction maps.

Note that the boundary of the sets $V_K(\sigma)$ are given by visibility arcs which have points with K in common. These arcs ‘alternatively’ touch K from the ‘right’ and from the ‘left’ in a convenient manner. In the next section we will introduce the term *alternating sequence* in order to characterize these visibility arcs and $V_K(\sigma)$ by such alternating boundary points.

Another important property of tolerance channels is presented in the following lemma.

3.1.13 Lemma. *Let (K, s, σ) be a tolerance channel and $a \in \overline{I_K}$. Then, there exists an $\varepsilon > 0$ s.t. (\tilde{K}, s, σ) is a tolerance channel, where \tilde{K} is defined by $I_{\tilde{K}} = I_K \cup B_\varepsilon(a)$.*

Proof. Since ω_K is piecewise \mathcal{R}^ω , \tilde{K} is the trace of a piecewise \mathcal{R}^ω Jordan curve for sufficiently small $\varepsilon > 0$. □

We now examine further properties of tolerance channels:

3.1.14 Remark. Although $\mathfrak{S}_K(\sigma, a) = \overline{\mathfrak{S}_K(\sigma, a)}$ for all $a \in V_K(s) \setminus \text{tr}(s)$, there might be points inside $\overline{I_K}$ which can be reached by an arc spline $\gamma \in \overline{\mathfrak{S}_K^n(\sigma)}$, but there is no visibility spline with n segments ending in one of these points (cf. Figure 53 on page 120). Hence the set $\{a \in \overline{I_K} \mid \mathfrak{S}_K^n(\sigma, a) \neq \emptyset\}$ is not closed in general, as we will see later on. Consequently, the definition of $V_K^n(\sigma)$ is quite canonical.

As indicated in Chapter 1, we are looking for an arc spline starting at $\text{tr}(s)$ and ending in a certain destination. Therefore, we establish the following definition:

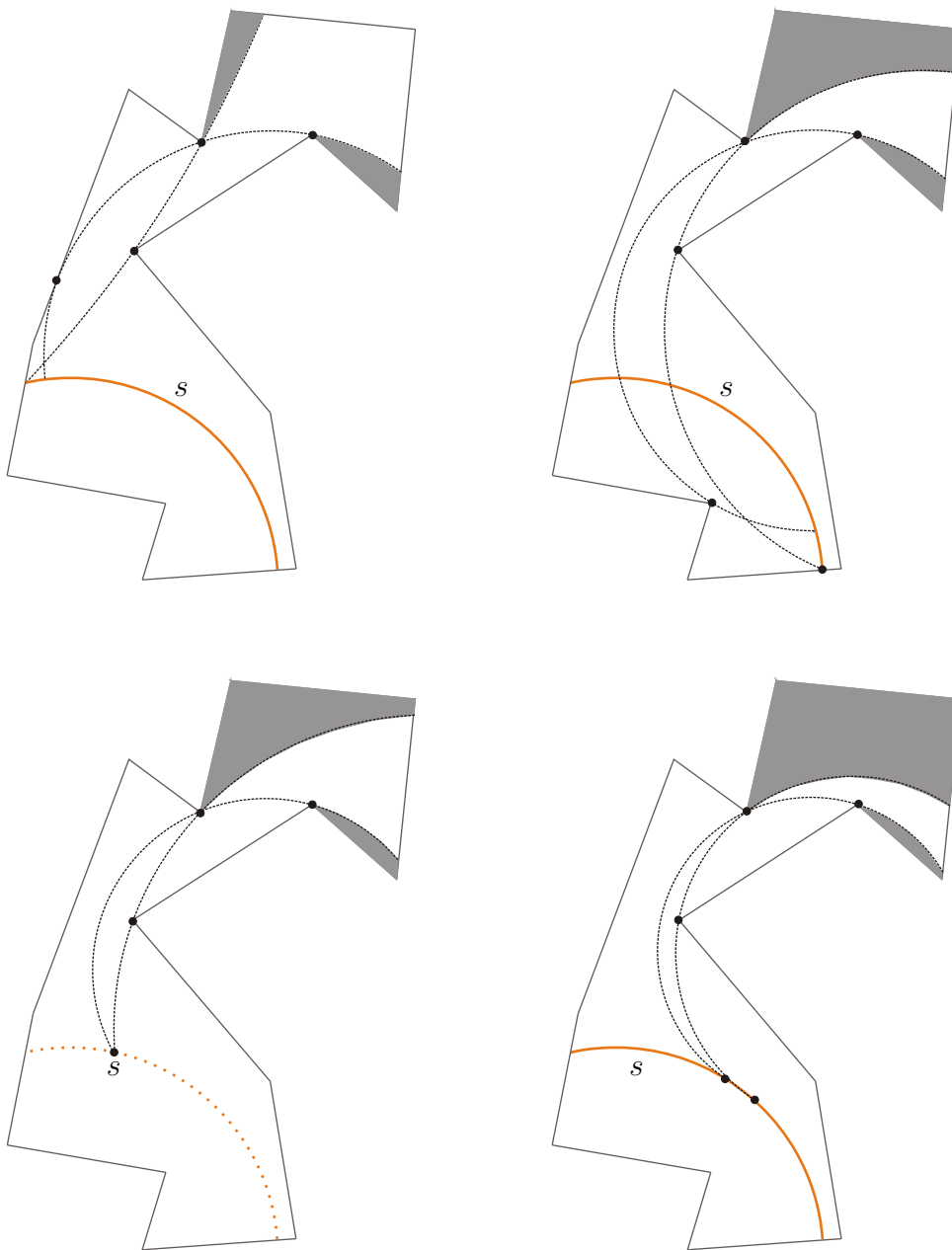


Figure 17: Illustration of (degenerate) starting /continuation channel given by a polygon and their corresponding visibility sets. Top left: Non-degenerate starting channel; top right: Non-degenerate continuation channel; bottom left: Degenerate starting channel; bottom right: Degenerate continuation channel.

3.1.15 Definition. A quadruple (K, s, σ, d) is called **start-destination channel** if (K, s, σ) is a tolerance channel with $\text{tr}(s) \subset K$ and d is a path of a generalized arc with

- i) $\text{tr}(d) \subset K$ and
- ii) $(T_{\overline{I_K}}(x))^\circ \neq \emptyset$ for all $x \in \text{tr}(d)$
- iii) $\text{tr}(d) \cap \text{tr}(s) = \emptyset$.

If K is a polygon and $\text{tr}(s)$ and $\text{tr}(d)$ are edges or vertices of K , we exactly have the situation given in the *minimum link problem*. However, we want to focus on the generalization to smooth arc splines and an arbitrary start-destination channel.

Setting $\mathfrak{S}_K^\infty(\sigma, d) := \{\gamma \in \mathfrak{S}_K^\infty(\sigma) \mid E(\gamma) \in \text{tr}(d)\}$ by abuse of notation, we can formulate the problem we are interested in, precisely:

3.1.16 Problem.

Let (K, s, σ, d) be an arbitrary start-destination channel.

Then we are searching for an arc spline $\gamma_0 \in \mathfrak{S}_K^\infty(\sigma, d)$ with

$$|\gamma_0| = \min \{|\gamma| \in \mathbb{N} \mid \gamma \in \mathfrak{S}_K^\infty(\sigma, d)\}.$$

We have already seen an exemplary situation in Figure 4 on page 9. In this formulation we consciously omitted the closure bar over $\mathfrak{S}_K^\infty(s, d)$, i.e. we are interested in a **smooth** arc spline satisfying the properties required above.

3.1.17 Remark. As already mentioned, according to the term *minimum link path* (cf. [6, 73, 74]), call an arc spline solving the problem formulated above **smooth minimum arc path (with respect to (K, s, σ, d))**.

Every start-destination channel possesses a smooth minimum arc path since we now show that $\mathfrak{S}_K^\infty(\sigma, d)$ is not empty.

3.1.18 Proposition. For every start-destination channel (K, s, σ, d) the set $\mathfrak{S}_K^\infty(\sigma, d)$ is not empty.

Proof. By Proposition 2.4.24 we can choose a curve γ of finite length starting at $\text{tr}(s)$ and ending in $\text{tr}(d)$ with $\text{tr}(\gamma) \subset \overline{I_K}$ and $K \cap \text{tr}(\gamma) \subset \text{tr}(s) \cup \text{tr}(d)$. Since the interior of $T_{\overline{I_K}}(x)$ is not empty for all $x \in \text{tr}(s) \cup \text{tr}(d)$ and $\text{dist}(\text{tr}(\gamma), K \setminus (U \cup V)) > 0$ for every open set U, V containing $\text{tr}(s)$ and $\text{tr}(d)$ respectively, we can approximate this curve by a smooth arc spline with a finite number of segments and staying in $\overline{I_K}$. \square

Thus, the minimum number defined above and therefore a minimum arc path always exists. Of course, we obtain the existence of a solution this way. However, practical implementation requires concrete and constructive approaches. For this purpose, a mathematical characterization of solutions is needed.

In order to solve the problem constructively we first examine the sets $V_K^n(\sigma)$ since it is a priori not clear at all where to set the breakpoints when constructing a smooth minimum arc path γ_0 . In any case, the destination segment d is n - but not $(n-1)$ -circularly visible for some $n \in \mathbb{N}$, i.e. the intersection $\text{tr}(d) \cap V_K^n(\sigma)$ is not empty, but $\text{tr}(d) \cap V_K^{n-1}(\sigma) = \emptyset$. Since it might happen that we only obtain a generalized visibility spline $\gamma_0 \in \overline{\mathfrak{S}}_K^\infty(\sigma, d)$, we give a strategy how to 'smooth' such a generalized visibility spline without losing the minimal possible number required in the problem formulation above, in Section 3.7.

For the remaining part of this chapter let (K, s, σ) be an arbitrary tolerance channel.

Finally, we examine some basic properties of the visibility set $V_K(\sigma)$, in this section.

3.1.19 Lemma. *$V_K(\sigma)$ is (path-)connected and compact.*

Proof. For any two points $a_1, a_2 \in V_K(\sigma)$ there exist paths $\gamma_i \in \mathfrak{S}_K(\sigma, a_i)$, $i = 1, 2$. Since $\text{tr}(\gamma_1)$, $\text{tr}(\gamma_2)$ and $\text{tr}(s)$ are subsets of $V_K(\sigma)$, there is a path ω in $V_K(\sigma)$ with $\text{tr}(\omega) \subset \text{tr}(\gamma_1) \cup \text{tr}(\gamma_2) \cup \text{tr}(s)$ connecting a_1 and a_2 .

Since $V_K(\sigma) \subset \overline{I}_K$ is bounded, it is sufficient to show that $V_K(\sigma)$ is closed. Let $(a_n)_{n \in \mathbb{N}}$ be a sequence in $V_K(\sigma)$ with limit point $a := \lim_{n \rightarrow \infty} a_n$, which is contained in \overline{I}_K since \overline{I}_K is compact. W.l.o.g we can assume $a_n, a \notin \text{tr}(s)$ for all $n \in \mathbb{N}$ (cf. Remark 3.1.14). Hence by definition there exists a visibility arc $\gamma_n \in \mathfrak{S}_K(\sigma, a_n)$ for each $n \in \mathbb{N}$. Setting $x_n := S(\gamma_n)$ and $v_n := \tau_\gamma(a_n)$, we obtain convergent subsequences $(x_{n_j})_{j \in \mathbb{N}}$ and $(v_{n_j})_{j \in \mathbb{N}}$ in \overline{I}_K and \mathbb{S}^1 respectively, with $x := \lim_{j \rightarrow \infty} x_{n_j}$ and $v := \lim_{j \rightarrow \infty} v_{n_j}$. As $\text{tr}(\gamma_n)$ is included in the compact set \overline{I}_K for all $n \in \mathbb{N}$ and $a \notin \text{tr}(s)$, we have $(a, v) \in G$ and therefore $(a, v) \in F$ (cf. Definition 3.1.2). By Lemma 2.5.26 and Lemma 2.5.18, we have $\lim_{j \rightarrow \infty} \text{tr}(\gamma_{x_{n_j}, a_{n_j}, v_{n_j}}) = \text{tr}(\gamma_{x, a, v}) \subset \overline{I}_K$. Since σ is continuous, we have $\lim_{j \rightarrow \infty} \sigma(a_{n_j}, v_{n_j}) = \sigma(a, v)$ and hence $x = S(\gamma_{x, a, v}) \in \sigma(a, v)$. Consequently, $\gamma_{x, a, v} \in \mathfrak{S}_K(\sigma)$ and therefore $a \in V_K(\sigma)$. \square

3.1.20 Definition. *If (K, s, σ, d) is a start-destination channel, the set $K \setminus (\text{tr}(s) \cup \text{tr}(d))$ has two connected components O_l and O_r . Then we define the compact subsets*

$$K_l := \overline{O_l} = \text{tr}(\omega_l) \text{ and } K_r := \overline{O_r} = \text{tr}(\omega_r)$$

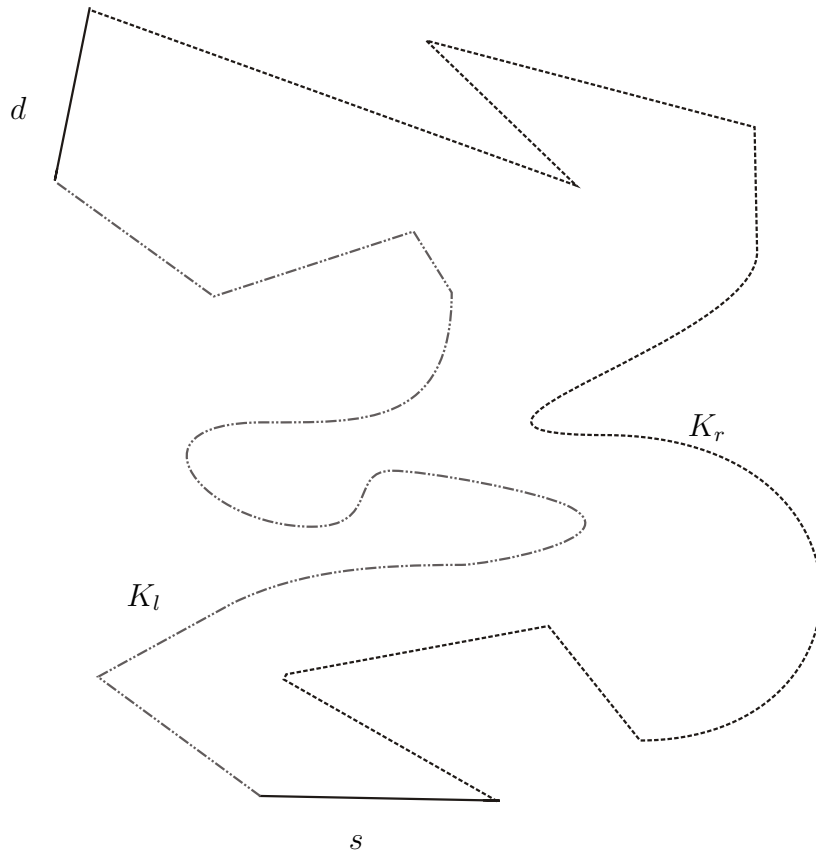


Figure 18: Left K_l and right bordering set K_r .

where ω_l and ω_r are paths starting in $\text{tr}(s)$ and ending in $\text{tr}(d)$ with $\omega_l = \omega_K^{-1} |_{[a_l, b_l]}$ and $\omega_r = \omega_K |_{[a_r, b_r]}$ for some points $a_l, a_r \in \text{tr}(s)$ and $b_l, b_r \in \text{tr}(d)$. Therefore, K_l is called the **left bordering set** and K_r the **right bordering set** (see Figure 18).

One can imagine the left and right channel as the subset of K which can be seen on the left or the right respectively ‘standing’ on $\text{tr}(s)$ and looking into the interior I_K .

3.2 Alternating Sequences

Motivated by classical *Chebyshev* approximation theory¹, we introduce a new and very useful term: *Alternating Sequences*. As we have seen in Lemma 2.1.5, circles and lines have finite interpolation properties. For example, a circle is uniquely determined by three distinct points, a line by two. Regarding this is therefore of great importance when reading the following sections. A physicist would say an arc has three ‘degrees of freedom’. Alternating sequences are used to characterize these ‘degrees of freedom’ defining a circular arc or a line segment.

In approximation theory *alternation sets* are treated in the field of function and spline spaces, where alternating sequences of +1 and -1 characterize certain solutions. Although we cannot transfer this concept directly, we use the main idea of alternately obtaining ‘oppositional terms’ like ‘left’ and ‘right’. Whenever a visibility arc of a tolerance channel is in an ‘extremal’ position, its ‘variability’ is restricted by *left* and *right restrictions*.

Before we can introduce the terms *alternating sequence* and *alternating number*, we need some notation and basic definitions: The starting point of this approximation calculus is the concept of *best approximation*. Although we could generalize this concept, for instance, to normed vector spaces, we, at this point, restrict ourselves to the real plane. For every subset M of \mathbb{R}^2 and $x \in \mathbb{R}^2$ we can consider the set

$$P_M(x) := \{u \in M \mid \|x - u\| = \text{dist}(x, M)\}$$

containing all *nearest points* to x from M . These elements are also said to be *best approximating points* (cf. [17]). Usually P_M is understood as set-valued mapping $P_M : \mathbb{R}^2 \rightarrow \mathfrak{P}(\mathbb{R}^2)$ and is called the *metric projection of \mathbb{R}^2 on M* .

In general, $P_M(x)$ is not a singleton, but setting $\mathcal{O}_M := \{x \in \mathbb{R}^2 \mid \text{card}(P_M(x)) = 1\}$, we have exactly one $u_x \in M$ with $P_M(x) = \{u_x\}$ for every $x \in \mathcal{O}_M$ and hence the mapping $\pi_M : \mathcal{O}_M \rightarrow \mathbb{R}^2$, $\pi_M(x) := u_x$ is well-defined. Figure 19 depicts an exemplary situation.

The idea of alternating sequences is based on alternately touching K from the left and the right. In this case, the terms ‘left’ and ‘right’ depend on the arc, so they have to be understood in a local, not a global sense. For this purpose, we introduce some useful

¹The term Chebyshev approximation problem is commonly used for the approximation problem for the space of real or complex valued function on a compact set endowed with the sup-norm (cf. [17]).

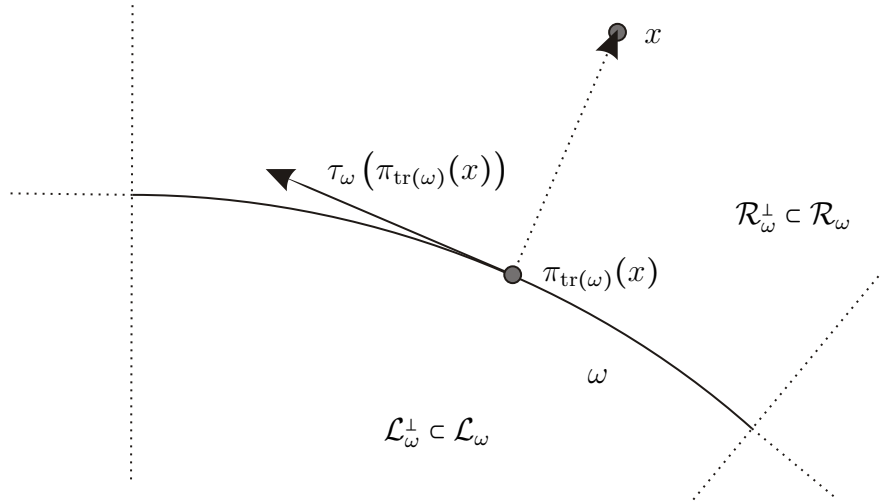


Figure 19: Illustration of Definition 3.2.1.

notions depending on the paths or arcs that shall supply such alternating sequences. The terms which are introduced are somewhat technical. Nevertheless, they will simplify further definitions and proofs.

3.2.1 Definition. Let ω be a smooth oriented curve in \mathbb{R}^2 . If we set $M := \text{tr}(\omega)$, we can define

i) $\mathcal{R}_\omega := \{x \in \mathbb{R}^2 \mid \det(x - y, \tau_\omega(y)) > 0 \text{ for all } y \in P_M(x)\}$ and analogously

ii) $\mathcal{L}_\omega := \{x \in \mathbb{R}^2 \mid \det(x - y, \tau_\omega(y)) < 0 \text{ for all } y \in P_M(x)\}$

where $\tau_\omega(x)$ denotes the tangent unit vector of ω in $x \in \text{tr}(\omega)$. We call \mathcal{R}_ω the **right region** and \mathcal{L}_ω the **left region of ω** . Furthermore, we define the subsets

i) $\mathcal{R}_\omega^\perp := \{x \in \mathcal{R}_\omega \mid \langle x - y, \tau_\omega(y) \rangle = 0 \text{ for all } y \in P_M(x)\}$ and

ii) $\mathcal{L}_\omega^\perp := \{x \in \mathcal{L}_\omega \mid \langle x - y, \tau_\omega(y) \rangle = 0 \text{ for all } y \in P_M(x)\}$.

Figure 19 illustrates the sets defined above.

For the remaining part of this section let (K, s, σ) be an arbitrary tolerance channel. Visibility arcs of (K, s, σ) starting at boundary points¹ of $\sigma_K(a, v)$ are ‘extremal’ in a certain way. Therefore, we define the following sets:

¹The boundary is built with respect to the relative topology on $\text{tr}(s)$.

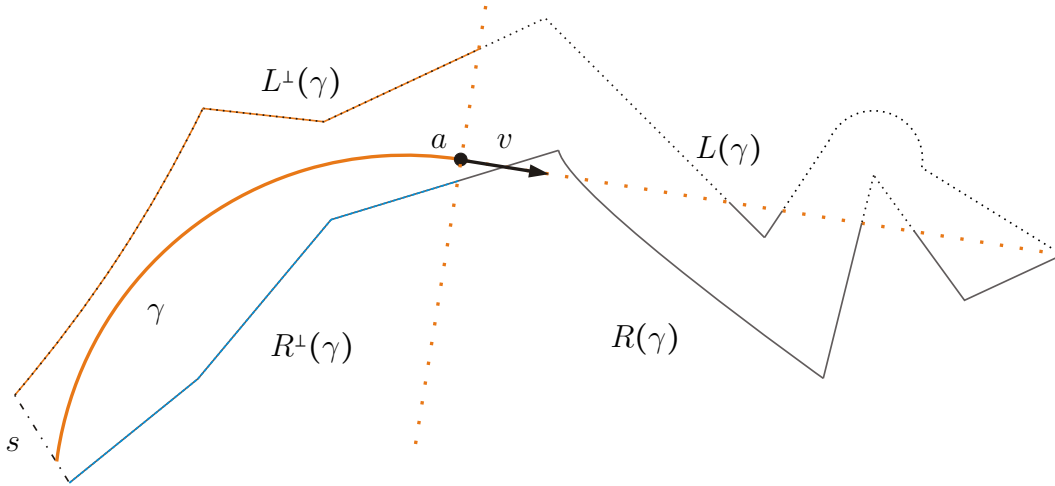


Figure 20: Illustration of Definition 3.2.3. Visibility arc $\gamma \in \mathfrak{S}_K(\sigma, a, v)$ for some $a \in V_K(\sigma)$ and $v \in \mathbb{S}^1$. $L(\gamma)$: Black dashed; $R(\gamma)$: solid grey; $L^\perp(\gamma)$: Orange part of $L(\gamma)$; $R^\perp(\gamma)$: Blue part of $R(\gamma)$.

3.2.2 Definition. Let s be an oriented arc and M a compact subset of $\text{tr}(s)$. Then we define the subsets

- i) $\text{Ext}^{\min}(M) := \{x \in M \mid x = \min C \text{ for some } C \in \mathfrak{Z}\}$ and
- ii) $\text{Ext}^{\max}(M) := \{x \in M \mid x = \max C \text{ for some } C \in \mathfrak{Z}\}$,

where \mathfrak{Z} denotes the set of connected components of M and \min, \max are taken with respect to ' \prec_s '. We call the elements of $\text{Ext}(M) := \text{Ext}^{\max}(M) \cup \text{Ext}^{\min}(M)$ the **extremal points** of M and $M^{\text{ri}} := M \setminus \text{Ext}(M)$ the **relative interior** of M (see Figure 21).

If M is a singleton, we have $M = \text{Ext}(M)$ and $M^{\text{ri}} = \emptyset$.

In order to define left and right restrictions, we introduce the subsets of K which are on the 'left' and on the 'right' of a visibility arc γ :

3.2.3 Definition. Let $a \in V_K(\sigma)$ and $\gamma \in \mathfrak{S}_K(\sigma, a)$. The subsets $\overline{\mathcal{L}_\gamma \cap (K \setminus \text{tr}(s)^{\text{ri}})}$ and $\overline{\mathcal{R}_\gamma \cap (K \setminus \text{tr}(s)^{\text{ri}})}$ of K are called **left** and **right contour with respect to** γ . We use the abbreviations $L(\gamma)$ and $R(\gamma)$ respectively, and in the same way we define: $L^\perp(\gamma) := \overline{\mathcal{L}_\gamma^\perp \cap (K \setminus \text{tr}(s)^{\text{ri}})}$ and $R^\perp(\gamma) := \overline{\mathcal{R}_\gamma^\perp \cap (K \setminus \text{tr}(s)^{\text{ri}})}$.

An illustration can be found in Figure 20.

Using the notions already introduced, we show: If two visibility arcs γ_1, γ_2 are feasible, i.e. $\gamma_1, \gamma_2 \in \mathfrak{S}_K(\sigma)$, the arcs 'between' them are feasible as well. In fact, this isn't an inclusion in the common sense, but nevertheless we call the following lemma the *Inclusion-Lemma*. However, first we need another term, which is important in order

to formalize what ‘between’ means. We want to be able to talk about left and right extremal points of sets $\sigma(a, v)$, and to introduce an order on these sets.

3.2.4 Definition. *Let $(a, v) \in F$ and $x_0 \in \text{Ext}(\sigma(a, v))$. We set*

$$\tilde{x}_0 := \max(\text{tr}(\gamma_{x_0, a, v}) \cap \text{tr}(s)) \text{ and } M := \{\max(\text{tr}(\gamma_{x, a, v}) \cap \text{tr}(s)) \mid x \in \sigma(a, v)\},$$

where \max is taken with respect to $<_{\gamma_{x, a, v}}$. Then x_0 is called a **left [right] extremal point of M with respect to (a, v)** if there exists a neighborhood U of \tilde{x}_0 s.t. for all $x \in T_M(\tilde{x}_0)$ and $y \in U \cap \text{tr}(\gamma_{x_0, a, v})$ the inequality $\det(x, y - \tilde{x}_0) \geq 0$ [≤ 0] holds.

A visualization can be found in Figure 21. If (K, s, σ) is a starting channel, we have $M = \sigma(a, v)$ and otherwise $\text{card}(\sigma(a, v) \cap M) = 1$.

3.2.5 Remark. If $(a, v) \in F$ and Z is an arbitrary connected component of $\sigma(a, v)$, then there exists exactly one left extremal point x_l and one right extremal point x_r of Z . We denote the canonical order on s which induces x_l to be the minimum and x_r to be the maximum of Z by $\preceq_{(a, v)}$.

Informally speaking, one can imagine the left and the right extremal point of a connected component Z of $\sigma(a, v)$ as the points which you can see on the left and on the right ‘standing’ on Z and looking towards the starting direction of the corresponding arcs ending in a with exiting direction v .

3.2.6 Convention. *Let x_1, x_2 be points of a connected component of $\sigma(a, v)$. Then we use the abbreviation $[x_1, x_2] := \{x \in \sigma(a, v) \mid x_1 \preceq_{(a, v)} x \preceq_{(a, v)} x_2\}$ instead of writing $[x_1, x_2]_{(a, v)}$. The sets $]x_1, x_2]$, $[x_1, x_2[$ and $]x_1, x_2[$ are defined analogously.*

Once we have introduced the order $<_{(a, v)}$, we can now state and prove the Inclusion-Lemma:

3.2.7 Lemma (Inclusion). *Let $(a, v) \in F$ and $\gamma_1, \gamma_2 \in \mathfrak{S}(\sigma, a, v)$ s.t. $T :=]S(\gamma_1), S(\gamma_2)[$ is a subset of $\sigma(a, v)$. For every $x \in T$ we get $\text{tr}(\gamma_{x, a, v}) \setminus \{a\} \subset \overline{\mathcal{R}_{\gamma_1}} \cap \overline{\mathcal{L}_{\gamma_2}}$.*

Proof. The path ω defined by $\omega := s \mid_{[S(\gamma_1), S(\gamma_2)]} \gamma_2 \gamma_1^{-1}$ is a loop in $\overline{I_K}$. Denoting the interior of ω by I_{12} , on the one hand, we obtain $\text{tr}(\gamma_{x, a, v}) \subset I_{12} \cup \{a\} \cup T$ for every $x \in T$ since $I_{12} \subset \overline{I_K}$ is simply connected. On the other hand, we have $\text{tr}(\gamma_{x, a, v}) \cap \text{tr}(\gamma_1) = \{a\} = \text{tr}(\gamma_{x, a, v}) \cap \text{tr}(\gamma_2)$ and $I_{12} \subset \overline{\mathcal{R}_{\gamma_1}} \cap \overline{\mathcal{L}_{\gamma_2}}$ since $\overline{\mathcal{R}_{\gamma_1}} \cup \overline{\mathcal{L}_{\gamma_2}} = \mathbb{R}^2$ and $\mathcal{R}_{\gamma_1}, \mathcal{L}_{\gamma_2}$ are disjoint for every oriented arc γ . Hence the assertion follows. \square

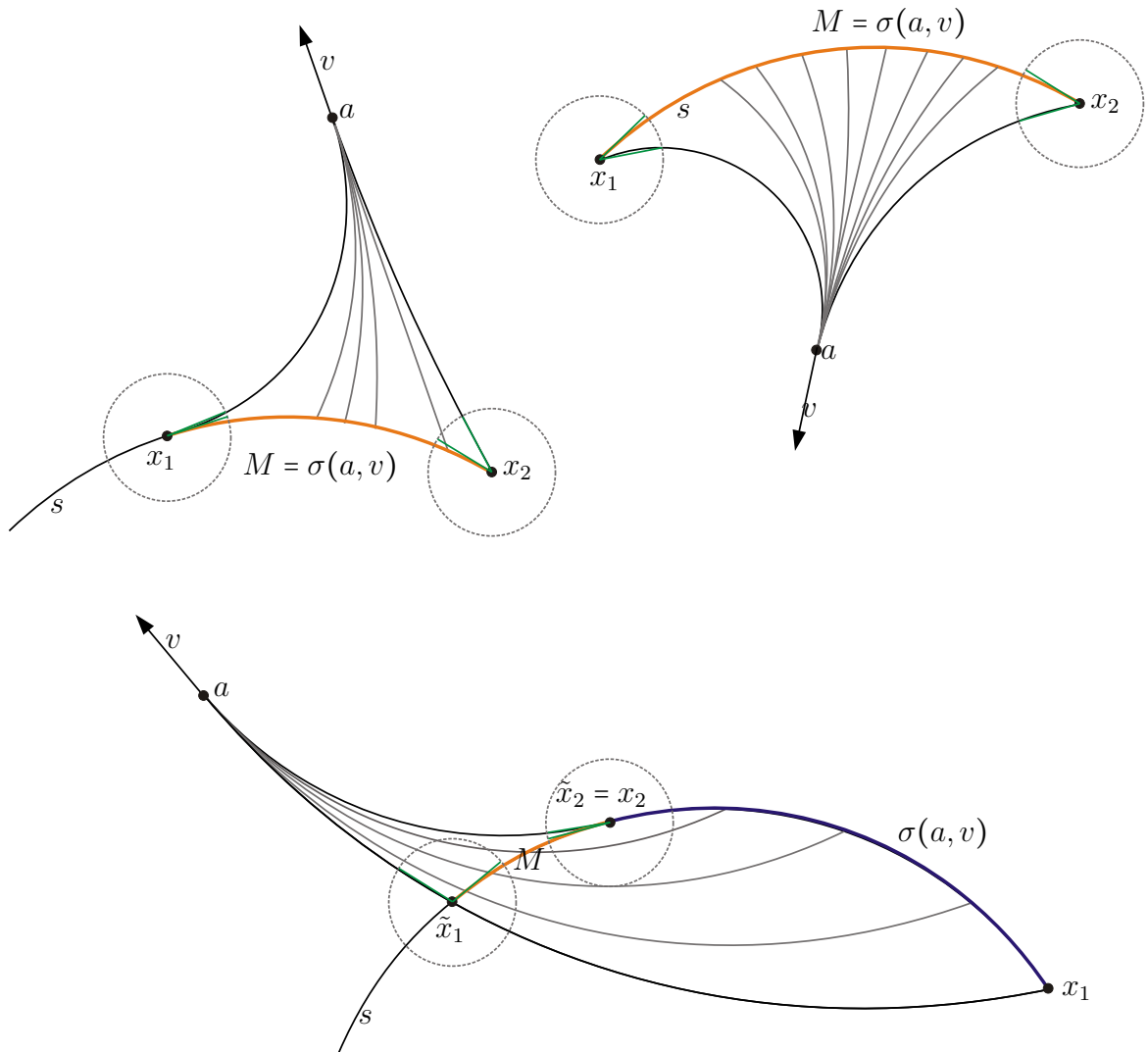


Figure 21: Extremal points of $\sigma(a, v) \subset \text{tr}(s)$. Top left: $\tilde{x}_1 = x_1$ left extremal, $\tilde{x}_2 = x_2$ right extremal; top right: $\tilde{x}_1 = x_1$ right extremal, $\tilde{x}_2 = x_2$ left extremal; bottom: x_1 left extremal, x_2 right extremal; The dashed circles indicate neighborhoods U and the green line segments indicate x and $y - \tilde{x}_0$ as in Definition 3.2.4

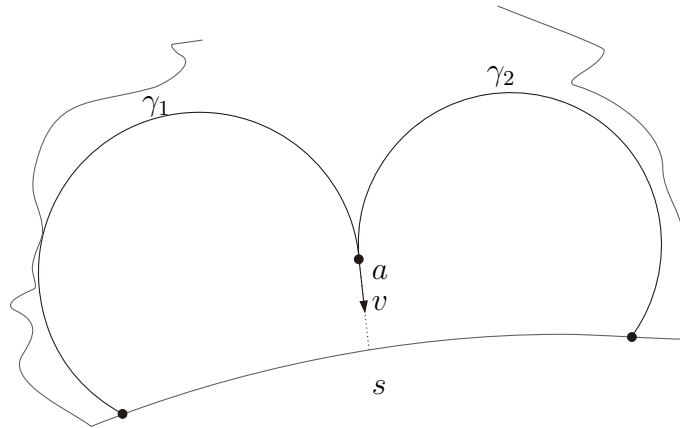


Figure 22: $L(\gamma_1) = K \neq \emptyset = L(\gamma_2)$ and $R(\gamma_1) = \emptyset \neq K = R(\gamma_2)$ with $\gamma_1, \gamma_2 \in \mathfrak{S}_K(\sigma, a, v)$.

While $\sigma(a, v)$ is the set of feasible starting points with respect to the starting condition given by σ and s , we introduce the subset of all starting points $x \in \sigma(a, v)$ whose corresponding arcs $\gamma_{x, a, v}$ stay in $\overline{I_K}$:

3.2.8 Definition. For any $(a, v) \in F$ with $\mathfrak{S}_K(\sigma, a, v) \neq \emptyset$ we define the set

$$\sigma_K(a, v) := \{S(\gamma) \in \sigma(a, v) \mid \gamma \in \mathfrak{S}_K(\sigma, a, v)\}.$$

3.2.9 Remark. Considering the situation of the definition above, we obtain by the Inclusion-Lemma 3.2.7: The left contour $L(\gamma)$ and right contour $R(\gamma)$ with respect to all $\gamma \in \mathfrak{S}_K(\sigma, a, v)$ are equal if $\sigma_K(a, v)$ is connected.

Note that, if $\sigma_K(a, v)$ has two connected components, arcs $\gamma_1, \gamma_2 \in \mathfrak{S}_K(\sigma, a, v)$ having distinct left or right contours might exist. In fact, $L(\gamma), L^\perp(\gamma)$ and $R(\gamma), R^\perp(\gamma)$ are compact, but they might be empty (see Figure 22).

3.2.10 Proposition. Let $(a, v) \in F$ with $\mathfrak{S}_K(\sigma, a, v) \neq \emptyset$. Then $\sigma_K(a, v)$ has at most two connected components.

Proof. By definition $\sigma_K(a, v)$ is a subset of $\sigma(a, v)$ and for every connected component C of $\sigma(a, v)$ the set $C \cap \sigma_K(a, v)$ is connected in $\text{tr}(s)$ by the Inclusion-Lemma 3.2.7. The fact that $\sigma(a, v)$ has at most two connected components (cf. Lemma 3.1.13) concludes the proof. \square

Now we are able to state the terms left/right restriction and the associated notions *alternating sequences* and *alternating numbers*.

3.2.11 Definition. Let $\gamma \in \mathfrak{S}_K(\sigma)$ and $M := \sigma(E(\gamma), \tau_\gamma(E(\gamma)))$. A point $a \in \text{tr}(\gamma)$ is called a **right restriction point (of γ)** if one of the following conditions are satisfied:

- i) $a \in R(\gamma)$ is neither the starting point nor the endpoint of γ ,
- ii) $a = E(\gamma) \in R(\gamma)$ and $-\tau_\gamma(a) \in T_K(a)$,
- iii) $a = S(\gamma)$ is a right but not a left extremal point of M and $a \notin L(\gamma)$ or
- iv) $a = S(\gamma)$ and $-\tau_\gamma(a) \in T_{R(\gamma)}(a)$.

We also say γ has a **right restriction** at a . **Left restriction points** can be defined analogously. A point $a \in \text{tr}(\gamma)$ is called **restriction point** if it is a left or right restriction point.

The terms left and right restriction point are well-defined. The cases i) and ii) are clear. In case of a right restriction at the starting point $a := S(\gamma)$, the cases iii) and iv) are consistent with one another. If $a := S(\gamma)$ is an extremal point of M but $a \notin \text{Ext}(\text{tr}(s))$, we have $a \notin L(\gamma) \cup R(\gamma)$ since $a \notin \overline{K \setminus \text{tr}(s)}$.

The various cases of right restrictions of a visibility arc γ with respect to a starting channel are depicted in Figure 24 and 25 and, in case of a continuation channel, in Figure 26. The first two pictures illustrate case i) and the third one case ii). Examples for right restrictions at the starting point $S(\gamma)$ can be seen in the second row of Figure 24. As $\sigma(a, v)$ is always a singleton for all $(a, v) \in F$ in case of a degenerate restriction map σ , the corresponding starting point would be a left and a right restriction point, but this case has been excepted from Definition 3.2.11 for good reasons as we will see later on. Moreover, we introduce a further term, *pseudo restrictions* to include this situation.

A similar situation might appear when considering a non-degenerate tolerance channel. There might be a pair $(a, v) \in F$ and $\gamma \in \mathfrak{S}_K(\sigma, a, v)$ s.t. all the other arcs $\gamma_{x, a, v}$ with $x \in \sigma(a, v) \setminus \{S(\gamma)\}$ start in the direction of E_K and not inside I_K (cf. Figure 23).

We now give a formal definition of the ideas indicated above:

3.2.12 Definition. Let $\gamma \in \mathfrak{S}_K(\sigma, a)$ for some $a \in V_K(\sigma)$ and $v := \tau_\gamma(a)$. The starting point $x_0 := S(\gamma)$ is called **pseudo restriction (of γ)** if

- i) $\text{card}(\sigma(a, v)) = 1$ or
- ii) for all $x \in \sigma(a, v) \setminus \{x_0\}$ and all neighborhoods U of x the intersection $U \cap \text{tr}(\gamma_{x, a, v}) \cap E_K$ is not empty.

We also say that γ has a **pseudo restriction** at x_0 .

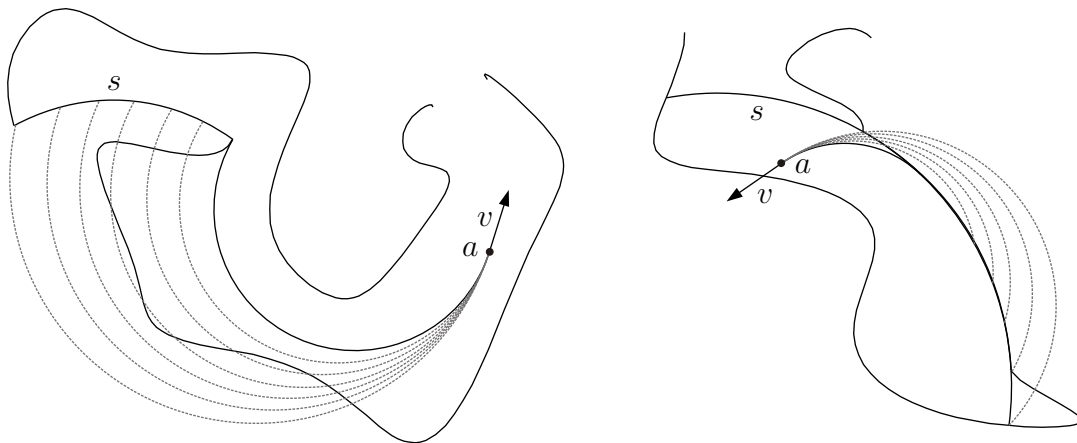


Figure 23: Pseudo restrictions x of $\gamma \in \mathfrak{S}_K(\sigma, a, v)$ within a starting channel (left) and continuation channel (right). The gray, dashed arcs start in the direction of E_K . Particularly, they are not contained in $\mathfrak{S}_K(\sigma, a, v)$.

Obviously, every visibility arc of a degenerate tolerance channel has a pseudo restriction at $S(\gamma)$, but pseudo restrictions might also appear in the case of non-degenerate tolerance channels as shown in Figure 23.

In literature (e.g. [23]) the term **support** is used in a similar manner as left and right restrictions but not in such a strict and general sense. Supports depend on the explicit structure of polygons as bounding channels and they are limited to starting channels. Furthermore, they do not supply notions like ‘support sequences’ and ‘support numbers’, which are essential for the calculus of circular visibility. The treatment of pseudo restrictions is missing, too. Hence the results of Chou et al. (cf. [22]) are not generally correct, as we will see later on.

3.2.13 Remark. Note that a point $a \in \text{tr}(\gamma)$ cannot simultaneously be a left and a right restriction point, but it could be a left / right restriction and a pseudo restriction point. In Figure 24 bottom right a is a right but not a left restriction point although a is a left extremal point of $\text{tr}(s)$ with respect to γ . Hence we have a pseudo restriction additionally. Assuming that (K, s, σ) is degenerate, every starting point of every visibility arc is a pseudo restriction point since $\sigma(a, v)$ is a singleton for all $(a, v) \in F$.

We now characterize the coherence of the sets $L^\perp(\gamma)$, $L(\gamma)$ [$R^\perp(\gamma)$, $R(\gamma)$] and the set of all left [right] restrictions of a visibility arc γ .

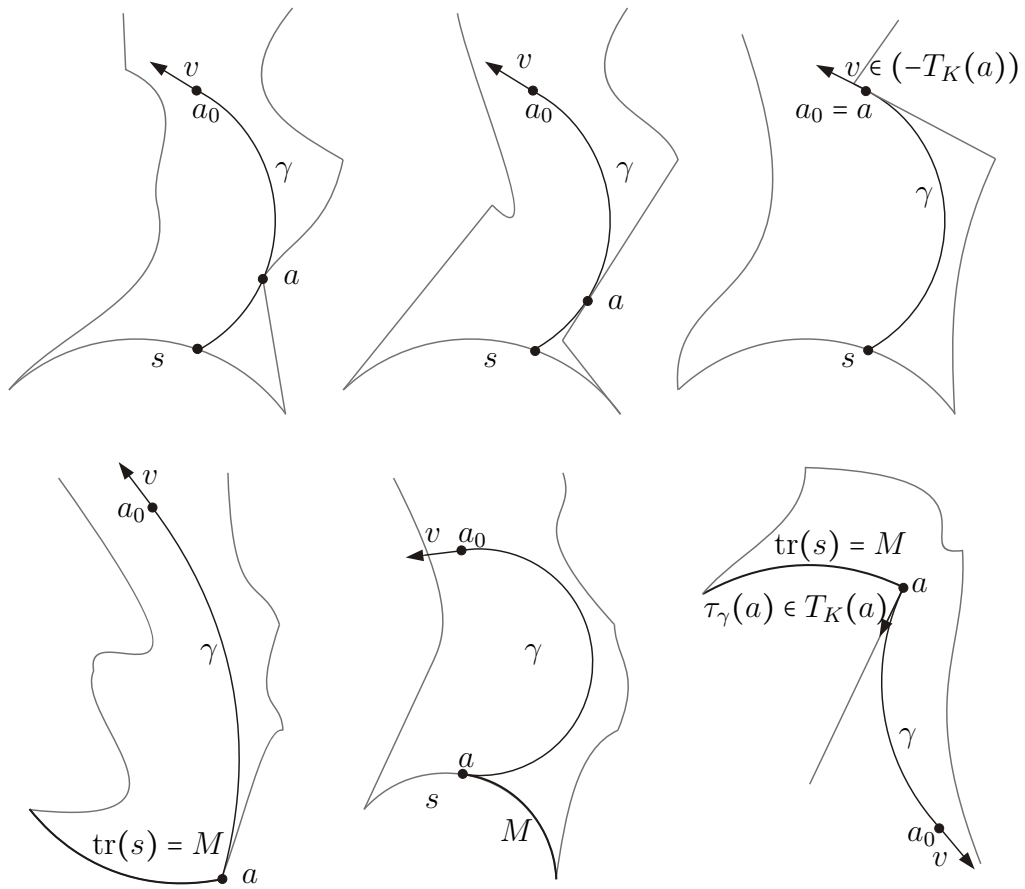


Figure 24: Illustration of Definition 3.2.11 in case of a starting channel. The various possibilities of right restrictions a of a visibility arc $\gamma \in \mathfrak{S}_K(\sigma, a_0, v)$ are depicted.

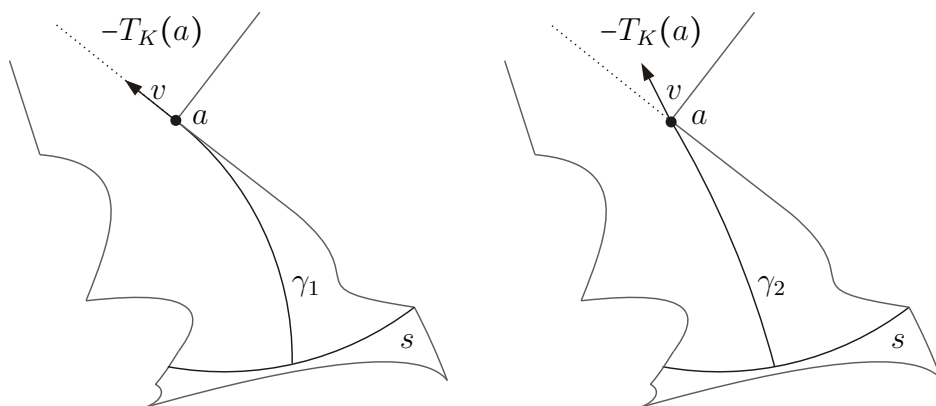


Figure 25: Right restrictions at the endpoint of a visibility arc. On the left we can see that $v \in (-T_K(a))$, whereas on the right γ doesn't touch K . Hence γ_1 has a right restriction in a but γ_2 not.

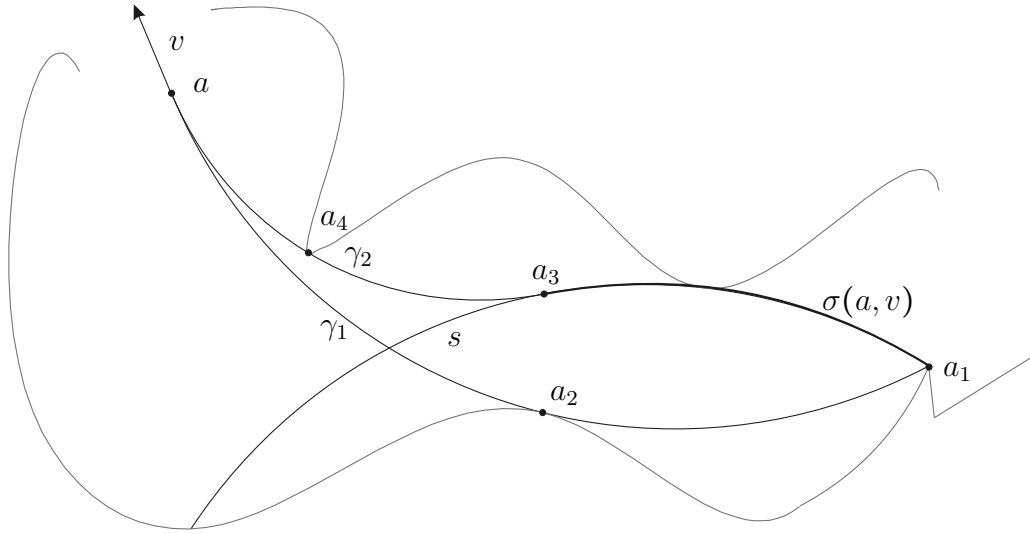


Figure 26: Illustration of Definition 3.2.11 in case of a continuation channel. Left restrictions a_1, a_2 and right restrictions a_3, a_4 . The point $a_1 = \min(\text{tr}(s))$ with respect to $\langle \cdot, s \rangle$, but it is a left and not a right extremal point of $\sigma(a, v)$.

3.2.14 Remark. Clearly, the intersection $\text{tr}(\gamma) \cap L^\perp(\gamma)$ is empty if and only if the set $\text{tr}(\gamma) \cap L(\gamma)$ is empty. If γ has no left restriction at $S(\gamma)$ and $E(\gamma) \notin K$, this is also equivalent to γ having no left restriction. Similar conditions hold for right restrictions, $R(\gamma)$ and $R^\perp(\gamma)$. Note that the requirement not to consider the endpoint of γ is crucial for the statement above (see Figure 25).

With the aid of left and right restrictions *alternating sequences* can be defined as follows:

3.2.15 Definition. Let $\gamma \in \mathfrak{S}_K(\sigma)$. A finite sequence of points $(a_i)_{1 \leq i \leq m}$ in $\text{tr}(\gamma) \cap K$ is called **alternating sequence (of γ)** if

- i) it is increasing with respect to \preceq_γ and
- ii) a_1 is a pseudo, right or left restriction point and a_i is a right or left restriction point of γ for all $2 \leq i \leq m$.

The set of all alternating sequences is denoted by $\mathfrak{A}(\gamma)$ and for every $(a_i)_{1 \leq i \leq m} \in \mathfrak{A}(\gamma)$ we can set the numbers

$$\sigma_i := \begin{cases} 1 & \text{if } a_i \text{ is a right restriction point,} \\ -1 & \text{if } a_i \text{ is a left restriction point,} \\ 0 & \text{if } a_i \text{ is a pseudo restriction point,} \end{cases} \quad \text{for } 1 \leq i \leq m \text{ and}$$

$$\varepsilon_i := \varepsilon(\sigma_i) := \begin{cases} 1 & \text{if } \sigma_i \sigma_{i+1} \leq 0, \\ 0 & \text{otherwise} \end{cases} \quad \text{for } 1 \leq i \leq m-1.$$

3.2.16 Definition. Hence the **alternating number of** $(a_i)_{1 \leq i \leq m}$ is set to

$$\mathcal{A}((a_i)_{1 \leq i \leq m}) := 1 + \sum_{i=1}^{m-1} \varepsilon_i \in \mathbb{N}.$$

We say $(a_i)_{1 \leq i \leq m}$ is **of length** k if $\mathcal{A}((a_i)_{1 \leq i \leq m}) = k$. Accordingly, we get the **alternating number of** γ :

$$\mathcal{A}(\gamma) := \max_{(a_i)_i \in \mathfrak{A}(\gamma)} \mathcal{A}((a_i)_i),$$

where $\mathcal{A}(\gamma)$ is set to 0 if $\mathfrak{A}(\gamma)$ is empty.

3.2.17 Remark. The number $\mathcal{A}(\gamma)$ is finite for all $\gamma \in \mathfrak{S}_K(\sigma)$: Since $L(\gamma)$, $R(\gamma)$ and $\text{tr}(\gamma)$ are traces of piecewise \mathcal{R}^ω curves, by Proposition 2.4.25 there exist finite sets E_L , E_R , sets J_L , J_R and integers $n_L, n_R \in \mathbb{N}$ s.t.

- i) $L(\gamma) \cap \text{tr}(\gamma) = E_L \cup J_L$ and $R(\gamma) \cap \text{tr}(\gamma) = E_R \cup J_R$ and
- ii) J_L (J_R) is homeomorphic to a disjoint union of n_L (n_R) intervals in \mathbb{R} .

Furthermore, $L(\gamma) \cap R(\gamma) \subset \text{tr}(s)$ and every left / right restriction point $a \in \gamma \setminus \text{tr}(s)$ is included in $L(\gamma)$ / $R(\gamma)$. Thus, we have

$$\mathcal{A}((a_i)_i) \leq \text{card}(E_L) + \text{card}(E_R) + n_L + n_R + 2$$

for every alternating sequence $(a_i)_i$ of γ and hence $\mathcal{A}(\gamma)$ is well-defined.

These ‘alternating conditions’ depend on local properties: Left restrictions might appear in K_r or vice versa (see Figure 28 on the right). They allow an efficient characterization of circular arcs describing the circular visibility set, but before we proceed with our theory, we’ll give an example to familiarize ourselves with alternating sequences and alternating numbers. Further illustrations can be found in Figure 28 and 29.

3.2.18 Example. Let (K, s, σ) be a non-degenerate starting channel and $\gamma \in \mathfrak{S}_K(\sigma)$. Considering the alternating sequence $(a_i)_{1 \leq i \leq 6}$, which is depicted in Figure 27, we have three left restriction points a_1, a_2, a_6 and three right restriction points a_3, a_4 and a_5 . Thus, we obtain $\varepsilon_1 = \varepsilon_3 = \varepsilon_4 = 0$, $\varepsilon_2 = \varepsilon_5 = 1$ and the alternating number of $(a_i)_{1 \leq i \leq 6}$ is $1 + \sum_{i=1}^5 \varepsilon_i = 3$. Since this sequence contains all left and right restriction points of γ , we have $\mathcal{A}(\gamma) = 3$.

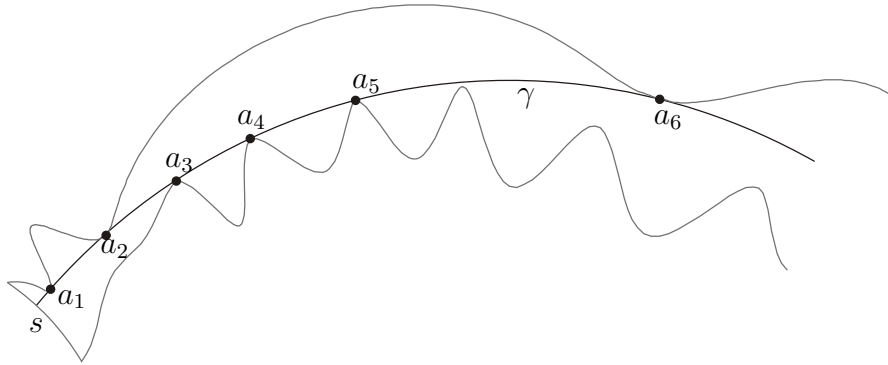


Figure 27: Example for the calculation of the alternating number of a visibility arc.

For an arbitrary visibility arc γ , we generally have a range of corresponding alternating sequences supplying the same alternating number or rather yielding the alternating number of γ . Due to this, the term introduced in the following definition is useful:

3.2.19 Definition. Let $\gamma \in \mathfrak{S}_K(\sigma)$. An alternating sequence (a_1, a_2) of length 2 is called **maximal with respect to a_2** if

$$a_1 = \max \{x \in \text{tr}(\gamma) \mid (x, a_2) \text{ is an alternating sequence of length 2}\}.$$

An alternating sequence (a_1, \dots, a_m) of length m ($m \geq 2$) is said to be **maximal with respect to a_m** if (a_{m-i}, a_{m-i+1}) is maximal with respect to a_{m-i+1} for all $i = 1, \dots, m-1$.

Examples are illustrated in Figure 28 and 29.

Before we can use alternating sequences to characterize the visibility set $V_K(\sigma)$, we need some preliminaries first. The following propositions are rather technical and are only used to prove the main results formulated subsequently.

3.2.20 Proposition. Let $a \in V_K(\sigma)$, $\gamma \in \mathfrak{S}_K(\sigma, a)$ with exiting direction $v \in \mathbb{S}^1$ and $L(\gamma) = \emptyset$. Then there exists a neighborhood U of $(S(\gamma), a, v)$ s.t. the set $L^\perp(\gamma_{x,b,w})$ is empty for all $(x, b, w) \in U$.

Proof. This can be easily deduced from Lemma 2.5.18. □

3.2.21 Proposition (Contour Inclusion). Let $a \in V_K(\sigma)$, $\gamma \in \mathfrak{S}_K(\sigma, a)$ with exiting direction $v \in \mathbb{S}^1$. Then there exist neighborhoods U of v in \mathbb{S}^1 and V of $S(\gamma)$ in $\text{tr}(s)$ s.t. the inclusions $L^\perp(\gamma_{x,a,w}) \subset L(\gamma)$ and $R^\perp(\gamma_{x,a,w}) \subset R(\gamma)$ hold for all $w \in U$ and all $x \in \text{tr}(s) \cap \sigma(a, w)$.

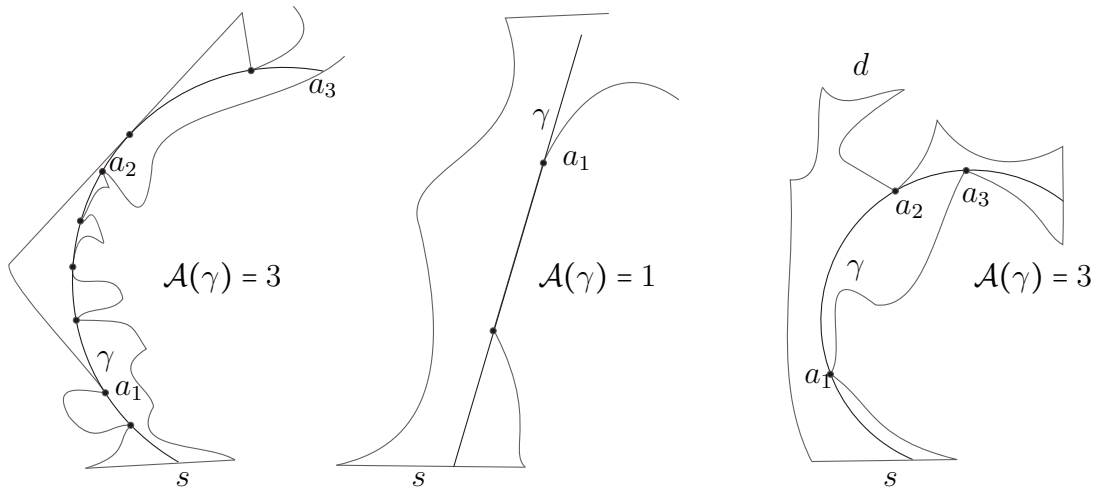


Figure 28: Illustration of alternating sequences. The arc on the left has four left and four right restrictions, but its alternating number is only three. In the middle we can see an arc having an infinite number of right restrictions, but $\mathcal{A}(\gamma) = 1$. The right picture points out that 'alternating conditions' depend on local properties. All depicted sequences $(a_i)_i$ are maximal with respect to its last point.

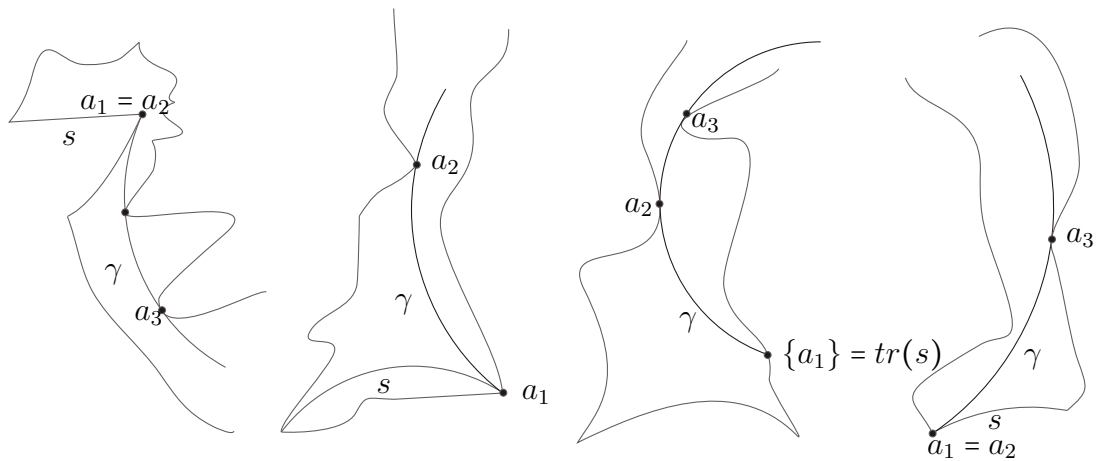


Figure 29: Illustration of alternating sequences II.

- 1) Non-degenerate starting channel; γ has a pseudo and a right restriction at $S(\gamma)$; $\mathcal{A}(\gamma) = 3$.
 - 2) Non-degenerate continuation channel, $\mathcal{A}(\gamma) = 2$.
 - 3) Degenerate starting channel; trivially γ has a pseudo restriction at $S(\gamma)$; $\mathcal{A}(\gamma) = 3$.
 - 4) Degenerate continuation channel; γ has a pseudo and a left restriction at $S(\gamma)$; $\mathcal{A}(\gamma) = 3$.
- All depicted sequences $(a_i)_i$ are maximal with respect to its last point.

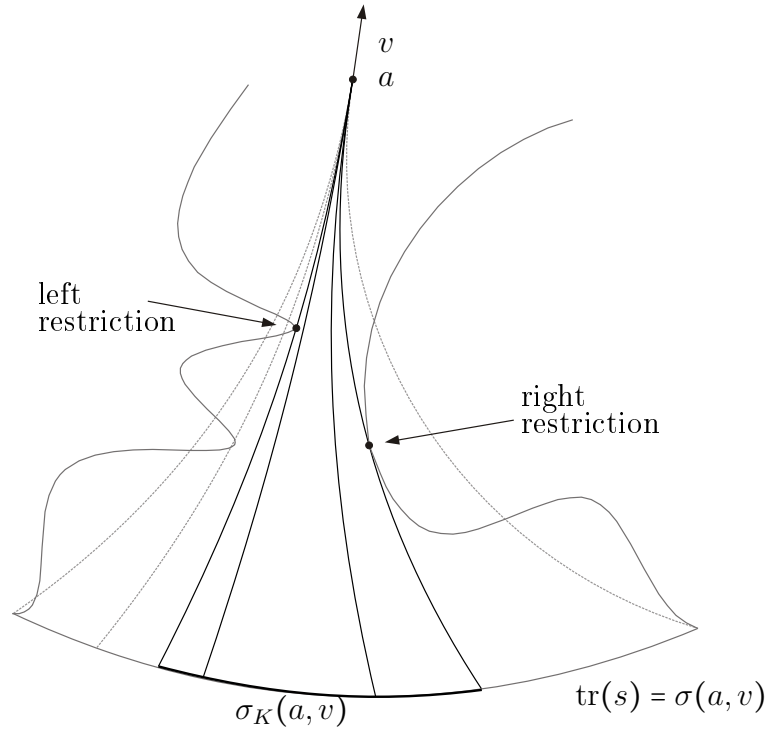


Figure 30: Restrictions given by K . In general we have $\sigma(a, v) \neq \sigma_K(a, v)$

Proof. Again, the proposition follows from Lemma 2.5.18. \square

We now develop further useful propositions that are also subsequently used to examine characterizations of the visibility set $V_K(\sigma)$.

Assuming a visibility spline $\gamma \in \mathfrak{S}_K(\sigma)$ with $a := E(\gamma)$ and $v := \tau_\gamma(a)$, we show the existence of a $\gamma_0 \in \mathfrak{S}_K(\sigma, a, v)$ with $\mathcal{A}(\gamma_0) \geq 1$. In case of a degenerate tolerance channel this is clear since $\mathfrak{S}_K(\sigma, a) = \{\gamma\}$ and $S(\gamma)$ is a pseudo restriction point. Otherwise, we even prove that there are always visibility arcs γ_l and γ_r having a left and right restriction respectively. The corresponding starting points are left and right extremal points of $\sigma_K(a, v)$. In general, the sets $\sigma(a, v)$ and $\sigma_K(a, v)$ are not equal. The next proposition characterizes the sets $\sigma_K(a, v)$. An illustration can be found in Figure 30.

3.2.22 Proposition. *Let γ_l and γ_r be two oriented arcs ending in $a \in V_K(\sigma)$ with exiting direction $v \in \mathbb{S}^1$ s.t. $[S(\gamma_l), S(\gamma_r)] \subset \sigma(a, v)$, $\text{tr}(\gamma_l) \notin \overline{I_K}$, $\text{tr}(\gamma_r) \in \overline{I_K}$ and $S(\gamma_r)$ is not a pseudo restriction of γ_r . Then there exists a visibility arc $\gamma_m \in \mathfrak{S}_K(\sigma, a, v)$ with $S(\gamma_l) \prec_{(a,v)} S(\gamma_m) \preceq_{(a,v)} S(\gamma_r)$ and $L(\gamma_m) \cap \text{tr}(\gamma_m) \neq \emptyset$.*

Proof. For any $x \in [S(\gamma_l), S(\gamma_r)] \subset \sigma(a, v)$ we have $L(\gamma_{x,a,v}) \subset L(\gamma_r)$. If $\text{tr}(\gamma_r)$ and $L(\gamma_r)$ are not disjoint, we can set $\gamma_m := \gamma_r$ and we are done. Otherwise, we have the non-empty

set $X := \{x \in [S(\gamma_l), S(\gamma_r)] \mid \text{dist}(\text{tr}(\gamma_{x,a,v}), L(\gamma_r)) > 0\}$. Obviously, X is bounded below with respect to ' $<_{(a,v)}$ ' and we can set $\gamma_m := \gamma_{x_0,a,v}$ with $x_0 := \inf(X) \in \sigma(a, v)$. Since $S(\gamma_r)$ is not a pseudo restriction, for all points $x \in [S(\gamma_l), S(\gamma_r)]$ there exists a neighborhood U s.t. $U \cap \text{tr}(\gamma_{x,a,v}) \cap E_K = \emptyset$. Then, due to continuity reasons, it is easy to show by means of the Inclusion-Lemma 3.2.7 that $\gamma_m \in \mathfrak{S}_K(\sigma, a, v)$ and $L(\gamma_r) \cap \text{tr}(\gamma_m)$ is not empty. This concludes the proof since every intersection point of $L(\gamma_r) \cap \text{tr}(\gamma_m)$ is trivially contained in $L(\gamma_m)$. \square

Changing the roles of 'left' and 'right', we obtain:

3.2.23 Proposition. *Let γ_l and γ_r be two oriented arcs ending in $a \in V_K(\sigma)$ with exiting direction $v \in \mathbb{S}^1$ s.t. $[S(\gamma_l), S(\gamma_r)] \subset \sigma(a, v)$, $\text{tr}(\gamma_l) \subset \overline{I_K}$, $\text{tr}(\gamma_r) \not\subset \overline{I_K}$ and $S(\gamma_l)$ is not a pseudo restriction of γ_l . Then there exists a visibility arc $\gamma_m \in \mathfrak{S}_K(\sigma, a, v)$ with $S(\gamma_l) \preceq_{(a,v)} S(\gamma_m) <_{(a,v)} S(\gamma_r)$ and $R(\gamma_m) \cap \text{tr}(\gamma_m) \neq \emptyset$.*

Proof. See Proposition 3.2.22. \square

3.2.24 Lemma. *Let $a \in V_K(\sigma)$, $v \in \mathbb{S}^1$ s.t. $\sigma_K(a, v) \neq \emptyset$ and $\sigma(a, v)$ contains no pseudo restriction point. Furthermore, let Z be an arbitrary connected component of $\sigma_K(a, v)$. Then there exist points x_l and x_r s.t. $[x_l, x_r] = Z$, where $\gamma_{x_l,a,v}$ has a left and $\gamma_{x_r,a,v}$ has a right restriction.*

Proof. We can choose a connected component $[x_1, x_2]$ of $\sigma(a, v)$ that includes Z . If $x_1 \in \sigma_K(a, v)$, we can set $x_l := x_1$. Otherwise, $\text{tr}(\gamma_{x_1,a,v})$ is not included in $\overline{I_K}$ and the situation of Proposition 3.2.22 is given. Hence the existence of a starting point $x_l \in [x_1, x_2]$ satisfying $\gamma_l := \gamma_{x_l,a,v} \in \mathfrak{S}_K(\sigma, a, v)$ and $\text{tr}(\gamma_l) \cap L(\gamma_l) \neq \emptyset$ follows. In any case, the arc γ_l has a left restriction. In the same way we get a point x_r with the desired properties. The Inclusion-Lemma 3.2.7 yields $Z = [x_l, x_r]$. \square

From this result we can easily deduce the following:

3.2.25 Corollary. *Let $(a, v) \in F$ with $\sigma_K(a, v) \neq \emptyset$. If $\sigma(a, v)$ contains no pseudo restriction point, we can choose visibility arcs $\gamma_l, \gamma_r \in \mathfrak{S}_K(\sigma, a, v)$ supplying a left or a right restriction respectively.*

Note that γ_l and γ_r are not necessarily distinct and we get:

3.2.26 Lemma. *Let $a_0 \in V_K(\sigma)$, $\gamma_0 \in \mathfrak{S}_K(\sigma, a_0)$ and $v_0 := \tau_{\gamma_0}(a_0) \in \mathbb{S}^1$. If γ_0 has no left [right] restriction there exists a neighborhood U of (a_0, v_0) in $\overline{I_K} \times \mathbb{S}^1$ s.t. for all $(a, v) \in U$ there exists a $\gamma \in \mathfrak{S}_K(\sigma, a, v)$ having no left [right] restriction.*

Proof. Setting $D := \overline{I_K} \times \mathbb{S}^1$, there exists an $\varepsilon_0 > 0$ and a neighborhood U of (a_0, v_0) in D s.t. for all $(a, v) \in U$ there exists a $x \in \sigma(a, v)$ with $\text{tr}(\gamma_{x,a,v}) \cap B_\varepsilon(a_0) \cap L(\gamma_0) \subset \{a_0\}$ for all $0 < \varepsilon < \varepsilon_0$ since γ_0 has no left restriction and therefore $\text{tr}(\gamma_0) \cap L(\gamma_0) \subset \{a\}$. Then $L(\gamma_0) \setminus B_\varepsilon(a_0)$ is compact and $\text{dist}(\text{tr}(\gamma_0), L(\gamma_0) \setminus B_\varepsilon(a_0)) > 0$. Because of the continuity properties of σ and the mapping $(x, a, v) \mapsto \text{tr}(\gamma_{x,a,v})$ and Proposition 3.2.21 after possible diminution of U , for all $(a, v) \in U$ we can choose $x \in \sigma(a, v)$ s.t. for all $0 < \varepsilon < \varepsilon_0$ we have

$$\text{dist}(\text{tr}(\gamma_{x,a,v}), L(\gamma_0) \setminus B_\varepsilon(a_0)) > 0$$

and $L^\perp(\gamma_{x,a,v}) \subset L(\gamma_0)$. Hence we have $\text{dist}(\text{tr}(\gamma_{x,a,v}), L^\perp(\gamma_{x,a,v})) > 0$ and the intersection $\text{tr}(\gamma_{x,a,v}) \cap B_\varepsilon(a_0) \cap L(\gamma_{x,a,v})$ is included in $\{a_0\}$.

If $\sigma(a, v)$ is a singleton, we are done. Otherwise, since $S(\gamma_0)$ is not a left extremal point of $\sigma(a_0, v_0)$ and σ is continuous, for sufficiently small U we can choose an element $x \in \sigma(a, v)$ which is no left extremal point of $\sigma(a, v)$. Altogether, we have found a neighborhood U s.t. for all $(a, v) \in U$ there exists an arc $\gamma \in \mathfrak{S}_K(\sigma, a, v)$ which has no left restriction. The argumentation works in a complete analogy if ‘left’ and ‘right’ is changed. \square

Visibility arcs γ having an alternating number of at least two separate $\overline{I_K}$ into at least two connected components. Thus, every arc passing through these components ‘cuts’ γ between each two alternating restriction points:

3.2.27 Lemma (Cutting). *Let $\gamma \in \mathfrak{S}_K(\sigma, a)$ for a circularly visible point $a \in V_K(\sigma)$. For every alternating sequence (a_1, a_2, \dots, a_m) of length $m \geq 2$ and $a_1 \neq S(\gamma), a_m \neq E(\gamma)$ we obtain: $\text{tr}(\gamma_2) \cap [a_i, a_{i+1}]_\gamma \neq \emptyset$ for all $\gamma_2 \in \mathfrak{S}_K(\sigma, a)$ and $i = 1, \dots, m-1$.*

Proof. Let $i \in \{1, \dots, m-1\}$. Then there exist two connected components Z_1 and Z_2 of $\overline{I_K} \setminus [a_i, a_{i+1}]_\gamma$ with $\text{tr}(s) \subset Z_1$ and $a \in Z_2$. Hence for $\gamma_2 \in \mathfrak{S}_K(\sigma, a)$ we obtain $S(\gamma_2) \in Z_1$ and $E(\gamma_2) \in Z_2$. Since $\text{tr}(\gamma_2)$ is connected, it is no subset of $Z_1 \cup Z_2$, and the set inclusion $\overline{\text{tr}(\gamma_2) \cap Z_1} \cup \overline{\text{tr}(\gamma_2) \cap Z_2} \subset [a_i, a_{i+1}]_\gamma$ concludes the proof. \square

3.3 Feasible Direction Sets

Let (K, s, σ) be an arbitrary tolerance channel. Generally, more than one circular arc ending in a point $a \in V_K(\sigma)$ is feasible. In this section we are interested in all the exiting directions $\tau_\gamma(a)$ of these visibility arcs γ since we later want to compose circular arcs smoothly. I.e. the ending direction of the predecessor segment has to equal the starting direction of the successor segment.

For this purpose, we first introduce the set of all feasible exiting directions of corresponding visibility arcs ending in the same circularly visible point:

3.3.1 Definition. For every $a \in V_K(\sigma) \setminus \text{tr}(s)$ the set

$$T_K(\sigma, a) := \{v \in \mathbb{S}^1 \mid \exists \gamma \in \mathfrak{S}_K(\sigma, a) \text{ s.t. } v = \tau_\gamma(a)\}$$

of all exiting directions of visibility arcs of a is called **feasible direction set of a** . We set $T_K(\sigma, a) := \emptyset$ for all $a \in \text{tr}(s)$.

An illustration can be found in Figure 31.

Note that $T_K(\sigma, a)$ is closely related to tangent cones of visibility arcs ending in a since

$$]0, \infty[\cdot T_K(\sigma, a) = \bigcup_{\gamma \in \mathfrak{S}_K(\sigma, a)} -T_{\text{tr}(\gamma)}(a).$$

Due to more convenient formulations in the sequel, we prefer the notation introduced in Definition 3.3.1.

3.3.2 Remark. The terms $T_K(\sigma, a)^\circ$ and $\partial T_K(\sigma, a)$ denote the interior and the boundary of $T_K(\sigma, a)$ with respect to the relative topology on \mathbb{S}^1 !

The properties of the feasible direction sets of the circularly visible points allow characterizing the sets $\mathfrak{S}_K(\sigma, a)$ efficiently. First we can show:

3.3.3 Proposition. For every $a \in V_K(\sigma) \setminus \text{tr}(s)$ the set $\text{tr}(\mathfrak{S}_K(\sigma, a))$ is closed with respect to the Hausdorff metric.

Proof. Let $(A_n)_{n \in \mathbb{N}}$ be a convergent sequence in $\text{tr}(\mathfrak{S}_K(\sigma, a))$ with $A := \lim_{n \rightarrow \infty} A_n$. By Lemma 2.5.26 A is a compact subset of $\overline{I_K}$ and is either a point or $A = \text{tr}(\gamma)$ for some $\gamma \in \mathfrak{S}$. It is clear that $a \in A$ and $\text{tr}(s) \cap A \neq \emptyset$ since $\text{tr}(s)$ is compact. Thus, A cannot be a point. Let γ_n be the visibility arc corresponding to A_n for every $n \in \mathbb{N}$ and $\gamma \in \mathfrak{S}$

with $\text{tr}(\gamma) = A$. The directions $\tau_{\gamma_n}(a)$ converge to $\tau_\gamma(a)$. Since σ is continuous and all A_n are bounded, we get $(a, \tau_\gamma(a)) \in G$ and hence $(a, \tau_\gamma(a)) \in F$ and $S(\gamma) \in \sigma(a, \tau_\gamma(a))$. Thus, $\gamma \in \mathfrak{S}_K(\sigma, a)$, i.e. $A \in \text{tr}(\mathfrak{S}_K(\sigma, a))$. \square

3.3.4 Lemma. *The feasible direction set $T_K(\sigma, a) \subset \mathbb{S}^1$ is compact for every $a \in V_K(\sigma)$.*

Proof. It is sufficient to consider a point $a \in V_K(\sigma) \setminus \text{tr}(s)$ since $T_K(\sigma, a) = \emptyset$ for all $a \in \text{tr}(s)$. According to Proposition 3.3.3, the trace set $\mathfrak{M} := \text{tr}(\mathfrak{S}_K(\sigma, a))$ is closed with respect to the Hausdorff metric. Let $E_a := \{(x, v) \in \text{tr}(s) \times \mathbb{S}^1 \mid (a, v) \in F, x \in \sigma(a, v)\}$ be the subset of all feasible pairs of starting points and exiting directions in a . Furthermore, the mapping $f_a : E_a \rightarrow \mathfrak{K}(\mathbb{R}^2)$, $(x, v) \mapsto \text{tr}(\gamma_{x,a,v})$ is continuous with respect to the product topology and by construction \mathfrak{M} is a subset of $f_a(E_a)$. Hence the pre-image $f_a^{-1}(\mathfrak{M})$ is closed in $E_a \subset \text{tr}(s) \times \mathbb{S}^1$ and thus compact since $\text{tr}(s) \times \mathbb{S}^1$ is compact. Consequently,

$$\pi_2(f_a^{-1}(\mathfrak{M})) = \bigcup_{(x,v) \in f_a^{-1}(\mathfrak{M})} \{v\} = \bigcup_{\gamma \in \mathfrak{S}_K(\sigma, a)} \{\tau_\gamma(a)\} = T_K(\sigma, a) \subset \mathbb{S}^1$$

is also compact since the canonical projection π_2 is continuous. \square

To examine further properties, we focus on special exiting directions, namely ‘extremal’ ones in the following way:

3.3.5 Definition. *Let $a \in V_K(\sigma)$ and $v \in T_K(\sigma, a)$.*

- i) We call v **left (right) extremal** in $T_K(\sigma, a)$ if there exists a neighborhood U of v in $T_K(\sigma, a)$ s.t. $\det(v, w) \leq 0$ ($\det(v, w) \geq 0$) for every $w \in U$.*
- ii) For neighborhoods U of $v \in \mathbb{S}^1$ we use the abbreviations $U^l := \{w \in U \mid \det(v, w) > 0\}$ and $U^r := \{w \in U \mid \det(v, w) < 0\}$.*
- iii) A visibility arc $\gamma \in \mathfrak{S}_K(\sigma, a)$ is called **left/right extremal** if $\tau_\gamma(a)$ is left/right extremal in $T_K(\sigma, a)$.*

3.3.6 Proposition. *$T_K(\sigma, a)$ is locally connected for every $a \in V_K(\sigma)$.*

Proof. By definition we have $T_K(\sigma, a) = \{v \in \mathbb{S}^1 \mid \exists \gamma \in \mathfrak{S}_K(\sigma, a) \text{ s.t. } v = \tau_\gamma(a)\}$ and ω_K is piecewise \mathcal{R}^ω . Assuming w.l.o.g. that $T_K(\sigma, a) \neq \mathbb{S}^1$, $T_K(\sigma, a)$ is semi-analytic set by [75, 76] (cf. proof of Proposition 2.4.25). Hence it is homeomorphic to a finite union of points and intervals in \mathbb{R} , which shows the assertion. \square

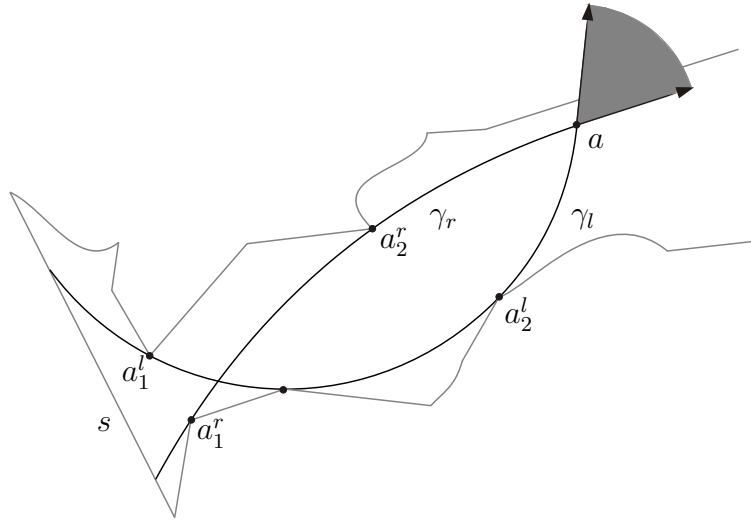


Figure 31: Extremal directions of a feasible direction set $T_K(\sigma, a)$. $T_K(\sigma, a)$ is displayed by the grey sector. The boundary of it consists of the left and right extremal direction. Corresponding visibility arcs γ_l, γ_r with associated alternating sequences (a_1^l, a_2^l) and (a_1^r, a_2^r) are depicted as well. These alternating sequences of length 2 satisfy the configuration given in Theorem 3.3.9.

Thus, the boundary points $\partial T_K(\sigma, a)$ are left or right extremal. For the sake of brevity we simply call them *extremal*. If we consider a left (right) extremal exiting direction v of $a \in V_K(\sigma)$, then no visibility arc $\gamma \in \mathfrak{S}_K(\sigma, a)$ with a direction $\tau_\gamma(a)$ that is to the left (right) of v in a suitable small neighborhood exists. The terms ‘left’ and ‘right’ are used in a local, not in a global sense.

We will merge the two concepts ‘alternating sequences’ and ‘feasible direction sets’ subsequently. In Section 3.2 we have seen that for fixed $a \in V_K(\sigma)$ and $v \in T_K(\sigma, a)$ one can always choose a visibility arc γ with $\mathcal{A}(\gamma) \geq 1$. We now show that we even get $\mathcal{A}(\gamma) \geq 2$ in case of an extremal direction $v \in T_K(\sigma, a)$. As already indicated, alternating sequences are used to characterize the three degrees of freedom that visibility arcs possess. Fixing two degrees and ‘driving one into an extremal position’, we obtain an alternating number of at least 1. If only the endpoint is fixed, we have two degrees of freedom that can be modified until they are in an extremal situation. Hence we obtain an alternating number $\mathcal{A}(\gamma) \geq 2$.

3.3.7 Remark. Let $a \in V_K(\sigma) \cap K$ and $v \in T_K(\sigma, a)$ with $-v \in T_K(a)$. Then a is a right [left] restriction point for every visibility arc $\gamma \in \mathfrak{S}_K(\sigma, a, v)$ if $a \in R(\gamma)$ [$L(\gamma)$]. Obviously, if a is a right [left] restriction point of γ , then v is left [right] extremal.

3.3.8 Proposition. *Let $a \in V_K(\sigma)$ and $v \in T_K(\sigma, a)$ be left [right] extremal. Then there exists a $\gamma \in \mathfrak{S}_K(\sigma, a, v)$ having a right [left] restriction.*

Proof. It is not hard to prove this proposition since the mapping $(a, b, v) \mapsto \text{tr}(\gamma_{a,b,v})$ is continuous and the function $A \mapsto \text{dist}(A, L(\gamma))$ is upper semi-continuous for every visibility arc γ (cf. Proposition 2.3.4). \square

3.3.9 Theorem (Extremal directions). *Let $a \in V_K(\sigma)$ and $v \in \partial T_K(\sigma, a)$. Then there exist a visibility arc $\gamma \in \mathfrak{S}_K(\sigma, a, v)$ and a corresponding alternating sequence (a_1, a_2) of length 2 s.t. a_2 is a right (left) restriction point if v is left (right) extremal. In particular, we have $\mathcal{A}(\gamma) \geq 2$.*

An illustration can be found in Figure 31.

Proof. Because of Proposition 3.3.8 we can assume $\text{card } \sigma(a, v) = \infty$. Let v be left extremal. By Corollary 3.2.25 there exists a visibility arc $\gamma \in \mathfrak{S}_K(\sigma, a, v)$ having a right restriction. Let X_r denote the set of all right restriction points of γ . Since X_r is compact and not empty, we can set $x_r := \max X_r$ with respect to \prec_γ . If $x_r = a$, we have $a \in K$ and $-v \in T_K(a)$. But in this case a is a right restriction point of every visibility arc of a with exiting direction v . Hence Corollary 3.2.25 allows choosing γ with an additional left restriction. Otherwise, we have $x_r \prec_\gamma a$ and hence there exists a point $b \in \text{tr}(\gamma)$ and $\varepsilon > 0$ s.t. $x_r \prec_\gamma b \prec_\gamma a$ and $B_\varepsilon(b) \subset I_K$. Let $\gamma_1 \in \mathfrak{S}_K(\sigma, b, \tau_\gamma(b))$ and $\gamma_2 := \gamma_{b,a,v}$ s.t. $\gamma = \gamma_1 \gamma_2$. If γ_1 additionally has a left restriction, we are done. Hence let us assume γ_1 not to have a left restriction for contradiction. Then neighborhoods U_1 of $\tau_{\gamma_1}(b)$ in \mathbb{S}^1 and V of $S(\gamma)$ in $\text{tr}(s)$ exist s.t. $V^l \subset \sigma(b, w)$ for all $w \in U_1^r$ and every visibility arc $\omega_1^{(w)} \in \mathfrak{S}_K(\sigma, b, w)$ defined by $(x, b, w) \in V^l \times \{b\} \times U_1^r$ has neither a left nor a right restriction.

Since γ_2 has no right restriction by construction, we can choose a neighborhood U_2 of v in \mathbb{S}^1 s.t. for every $\tilde{v} \in U_2^l$ the arc $\omega_2^{(\tilde{v})}$ defined by (b, a, \tilde{v}) has no right restriction and $\tau_{\omega_2^{(\tilde{v})}}(b) \in U_1^r$ since the mapping $w \mapsto \tau_{\omega_2^{(w)}}(b)$ is continuous.

Thus, we get

$$\forall w \in U_2^l \exists x \in V^l \exists \tilde{v} \in U_1^r \text{ s.t. } \gamma_w := \omega_1^{(\tilde{v})} \omega_2^{(w)} \in \mathfrak{S}(\sigma, a, w).$$

By construction, $S(\gamma_w) \in \sigma_K(a, w)$, i.e. $\gamma_w \in \mathfrak{S}_K(\sigma, a, w)$ (see Figure 32). Therefore, U_2^l is a subset of $T_K(\sigma, a)$. This contradicts v to be left extremal and proves the assertion.

The argumentation proceeds similarly if v is right extremal. \square

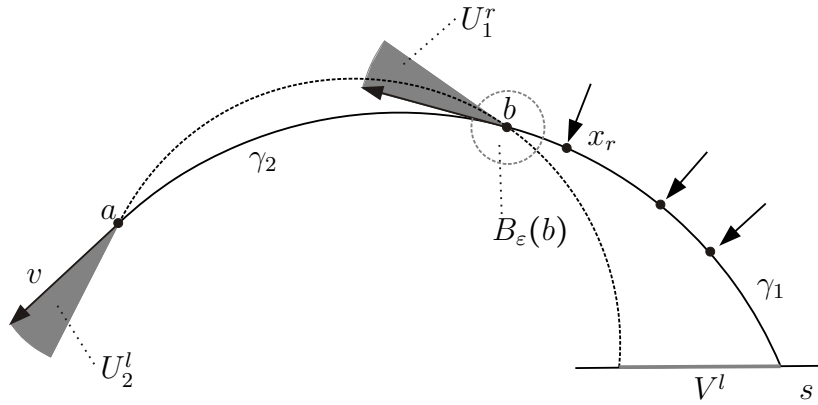


Figure 32: Illustration of the proof of Theorem 3.3.9. The solid arc is $\gamma = \gamma_1 \gamma_2$ and the dashed one γ_w for some $w \in U_2^l$ as defined in the proof. The arrows indicate the points of X_r .

3.3.10 Remark. Note that the converse of the claim in the Theorem above is not true in general. In Figure 33 we can see visibility arcs $\gamma_1, \gamma_2 \in \mathfrak{S}_K(\sigma, a, v)$ having alternating sequences $(a_1^{(i)}, a_2^{(i)})$ of length 2 of γ_i , $i = 1, 2$, but v is neither left nor right extremal. It is not hard to prove that this is equivalent to $T_K(\sigma, a) = \mathbb{S}^1$.

Furthermore, it is easy to see that $T_K(\sigma, a) = \mathbb{S}^1$ implies that a is **not** on the boundary of $V_K(\sigma)$. At least the following holds:

3.3.11 Lemma. *Let $a \in V_K(\sigma)$ and $v \in T_K(\sigma, a) \neq \mathbb{S}^1$ s.t. $\sigma_K(a, v)$ is connected. If a visibility arc $\gamma \in \mathfrak{S}_K(\sigma, a, v)$ has an alternating sequence (a_1, a_2) of length 2 with a left [right] restriction point a_2 , then v is right [left] extremal.*

Proof. It is sufficient to consider a visibility arc $\gamma \in \mathfrak{S}_K(\sigma, a, v)$ with an alternating sequence (a_1, a_2) of length 2, where a_2 is a right restriction point. Let us assume to the contrary that γ is not left extremal. Then for every neighborhood U of v there exists a direction $w \in U$ s.t. $w \in T_K(\sigma, a)$, $\det(v, w) > 0$ and $\sigma_K(a, w)$ is connected. Hence $\gamma_w|_{[x, a]} \in \overline{\mathcal{R}_\gamma}$ for some $\gamma_w \in \mathfrak{S}_K(\sigma, a, w)$ and $x \in \text{tr}(\gamma_2)$. On the one hand $\text{tr}(\gamma_2) \cap [a_2, a[$ is not empty whenever $\|v - w\|$ is sufficiently small since $\sigma(a, w)$ is connected. But on the other hand we have $[S(\gamma), a_2] \cap \text{tr}(\gamma_2) \neq \emptyset$. Consequently, $\text{card}(\text{tr}(\gamma) \cap \text{tr}(\gamma_2)) \geq 3$. Lemma 2.1.5 yields $\gamma = \gamma_2$, a contradiction. \square

The characterization of left and right extremal directions of the feasible direction sets by alternating sequences enables the examination of further properties of $T_K(\sigma, a)$:

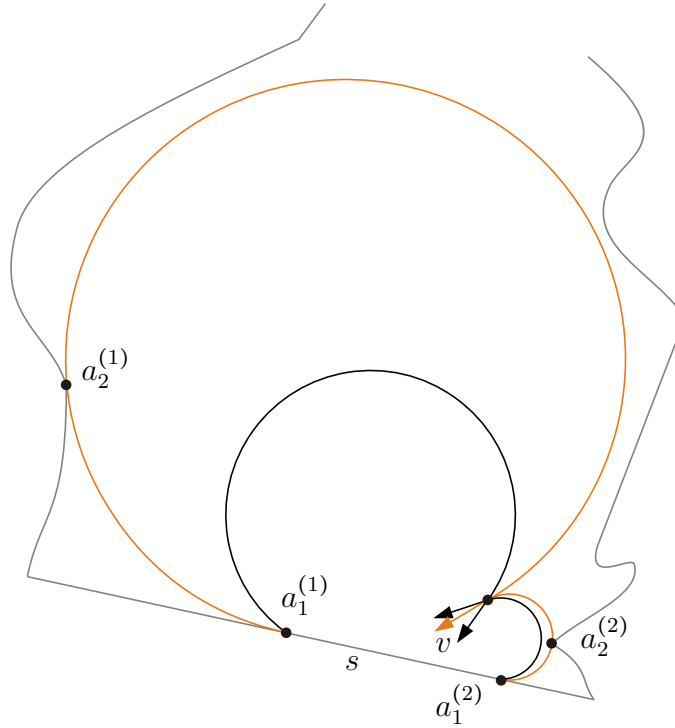


Figure 33: Non-extremal visibility arcs (orange) supplying alternating sequences $(a_1^{(i)}, a_2^{(i)})$, $i = 1, 2$ of length 2 (see Remark 3.3.10). The corresponding exiting direction is neither left nor right extremal as indicated by the two black arcs and their tangent unit vectors.

3.3.12 Proposition. *Let $a \in V_K(\sigma) \setminus \text{tr}(s)$ and let $T_K(\sigma, a) \neq \mathbb{S}^1$. Then $T_K(\sigma, a)$ contains exactly one left and one right extremal direction.*

Proof. Obviously, $T_K(\sigma, a)$ is not empty. It is sufficient to show the existence and uniqueness of a left extremal direction. We prove the existence by contradiction. For this purpose, let us assume that for every $v \in T_K(\sigma, a)$ and every neighborhood U of v in \mathbb{S}^1 the intersection $U \cap T_K(\sigma, a)$ is not empty. Since $T_K(\sigma, a)$ is closed (cf. Lemma 3.3.4) and locally connected (cf. Lemma 3.3.6), we get the contradiction that it equals \mathbb{S}^1 .

For the proof of the uniqueness let v_1 and v_2 be two left extremal directions. Then by Theorem 3.3.9 we can choose visibility arcs $\gamma_i \in \mathfrak{S}_K(\sigma, a, v_i)$ and alternating sequences $(a_1^{(i)}, a_2^{(i)})$ of length 2 with right restriction points $a_2^{(i)}$ for $i = 1, 2$. W.l.o.g $a_1^{(1)}$ and $a_1^{(2)}$ are no pseudo restriction points. Then we have $a_1^{(i)} \neq a_2^{(i)}$ for $i = 1, 2$. If $a_1^{(i)} \neq S(\gamma_i)$ for some $i = 1, 2$, we get $\text{card}(\text{tr}(\gamma_1) \cap \text{tr}(\gamma_2)) \geq 3$ and we are done. Otherwise, let w.l.o.g. $a_1^1 = S(\gamma_1)$. Since $T_K(\sigma, a) \neq \mathbb{S}^1$, the sets $\sigma_K(a, w)$ are connected for all $w \in T_K(\sigma, a)$. Again, it is not hard to show that γ_1 and γ_2 have at least three points in common, which means that they are equal. Altogether, we obtain $v_1 = v_2$ in any case. \square

3.3.13 Corollary. *The feasible direction set $T_K(\sigma, a)$ is connected for every $a \in V_K(\sigma)$.*

Proof. Follows immediately from Propositions 3.3.12 and 3.3.6. \square

Obviously, an exiting direction $v \in T_K(\sigma, a)$ is left and right extremal if and only if it is an isolated point of $T_K(\sigma, a)$. Hence by the Corollary above we obtain:

3.3.14 Corollary. *A direction $v \in T_K(\sigma, a)$ is left and right extremal if and only if $T_K(\sigma, a) = \{v\}$.*

3.3.15 Lemma. *Let $a \in V_K(\sigma)$ and $v \in T_K(\sigma, a)$ s.t. $\sigma_K(a, v)$ is connected. For every $\gamma \in \mathfrak{S}_K(\sigma, a, v)$ the following properties are equivalent:*

- 1) $v \in \partial T_K(\sigma, a)$,
- 2) *There exists an alternating sequence (a_1, a_2) of γ with length 2.*

Addendum: *In the case of $\text{card}(\sigma(a, v)) = \infty$, this is equivalent to $\sigma_K(a, v)$ being a singleton.*

An illustration can be found in Figure 31.

Proof. (1) \Rightarrow (2) follows from Theorem 3.3.9 and the implication (2) \Rightarrow (1) from Lemma 3.3.11. From the Inclusion-Lemma 3.2.7 we can easily deduce the equivalence of (2) and that $\sigma_K(a, v)$ is a singleton. \square

3.3.16 Corollary. *Let $a \in V_K(\sigma)$ and $v \in T_K(\sigma, a)^\circ$ s.t. $\sigma_K(a, v)$ is connected. Then there exists a visibility arc $\gamma \in \mathfrak{S}_K(\sigma, a, v)$ having neither a left nor a right restriction.*

Proof. Let us first suppose that $\text{card}(\sigma(a, v)) = \infty$. Since v is not an extremal direction and $\sigma_K(a, v)$ is connected, we obtain $\text{card}(\sigma_K(a, v)) = \infty$ by Lemma 3.3.15. Hence the Inclusion-Lemma 3.2.7 yields the existence of a visibility arc $\gamma \in \mathfrak{S}_K(\sigma, a, v)$ having neither a left nor a right restriction. If $\sigma(a, v)$ is a singleton, there exist a visibility arc γ with $\{\gamma\} = \mathfrak{S}_K(\sigma, a, v)$ which has a pseudo restriction at $S(\gamma)$. Hence we obtain the assertion directly by Lemma 3.3.15. \square

3.4 Characterization of the Visibility Set $V_K(\sigma)$

With the aid of the two instruments *alternating sequences* and *feasible directions cones* we are able to characterize the set $V_K(\sigma)$. Some of the results we present in this section have already been published ([22, 54]). But they were only treated in the context of visibility problems within simple polygons as starting channels.

In the previous sections we have seen that we can choose visibility arcs γ with $\mathcal{A}(\gamma) \geq 1$ for a fixed endpoint $a \in V_K(\sigma)$ and exiting direction $v \in T_K(\sigma, a)$. If v is extremal, we can even require an alternating number of at least two as two of the three degrees of freedom have been driven to an extremal position. Visibility arcs ending in a point of the boundary of $V_K(\sigma)$ with respect to the relative topology on $\overline{I_K}$ are called *blocking arcs*. We prove in Lemma 3.4.1 that blocking arcs have at least three alternating restrictions as already indicated in Figure 17 in Section 3.1. This allows us to describe them in an efficient manner and to enable a constructive approach in view of developing an algorithm. Again, we can see the correlation of the degrees of freedom and the alternating number. Blocking arcs exhaust all degrees and therefore they have an alternating sequence of length 3.

A proof of the claim made in Theorem 3.4.7 in a restricted case¹ can also be found in [22]. But the appearance of pseudo restrictions is missing there. Therefore, some of the main results of Chou et al. are not correct in full generality.

Since $V_K(\sigma)$ is (path-)connected and compact, it is sufficient to describe all the blocking arcs in order to characterize the whole circular visibility set. Hence the characterization of the blocking arcs by alternating sequences is one of the main results of this section. An example is given in Figure 34. In case of a destination channel, we will focus on one special blocking arc, namely that one which is ‘nearest’ to the destination segment d . But before we can present Theorem 3.4.7, we need some auxiliary propositions in advance.

3.4.1 Lemma. *Let $a \in V_K(\sigma)$, $v \in T_K(\sigma, a)$ and $\gamma \in \mathfrak{S}_K(\sigma, a, v)$ be a corresponding visibility arc with $\text{tr}(\gamma) \cap K \subset \{a\}$. Then γ touches K in a or $v \in T_K(\sigma, a)^\circ$.*

Proof. Suppose that γ doesn’t touch K in a . Since $\text{tr}(\gamma) \cap K \subset \{a\}$, we have $\mathcal{A}(\gamma) \leq 1$. Thus, by Theorem 3.3.9 v is not a boundary direction, and we obtain $v \in T_K(\sigma, a)^\circ$. \square

¹The claim there is limited to a polygonal starting channel (K, s, σ) with s supposed to be a line and not a generalized arc.

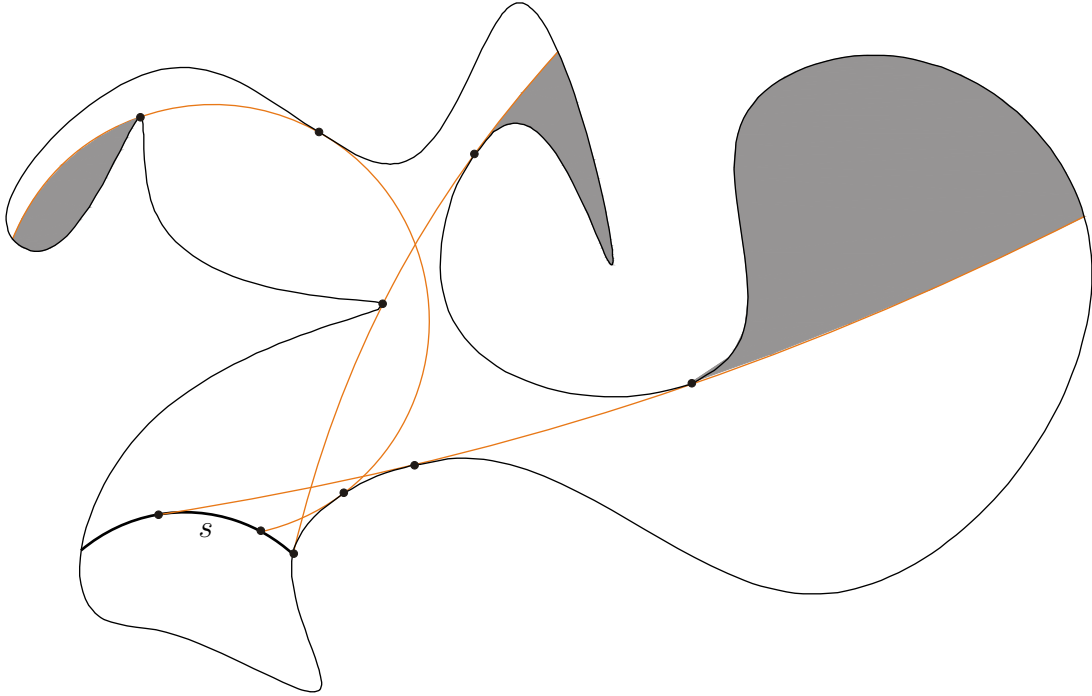


Figure 34: Example of a circular visibility set (white portion) with respect to a starting channel. The corresponding blocking arcs (orange) have an alternating number of at least three.

3.4.2 Lemma. *For $a \in V_K(\sigma)$ with $\text{card}(T_K(\sigma, a)) = 1$ we have $\text{card}(\mathfrak{S}_K(\sigma, a)) = 1$.*

Proof. Let $T_K(\sigma, a) = \{v\}$ for some $v \in \mathbb{S}^1$. Since $\sigma_K(a, v)$ has at most two connected components (cf. Proposition 3.2.10), we have $N := \text{card}(\mathfrak{S}_K(\sigma, a)) \in \{1, 2, \infty\}$. If we assume $N = \infty$, there would be a visibility arc $\gamma \in \mathfrak{S}_K(\sigma, a, v)$ without any restriction. In particular, γ wouldn't touch K and Lemma 3.4.1 would yield a contradiction. If $N = 2$, we would obtain $T_K(\sigma, a) = \mathbb{S}^1$, which is also a contradiction. Hence we get $N = 1$. \square

3.4.3 Theorem. *Let $a \in V_K(\sigma) \setminus K$ with $T_K(\sigma, a) = \{v\}$. Then there exists exactly one $\gamma \in \mathfrak{S}_K(\sigma, a)$ and we have $\mathcal{A}(\gamma) \geq 3$.*

Proof. Since $a \notin K$, the set $\mathfrak{S}_K(\sigma, a, v) = \mathfrak{S}_K(\sigma, a)$ is a singleton (cf. Lemma 3.4.2). The unique corresponding visibility arc γ is left and right extremal because v is left and right extremal. Hence we have alternating sequences (a_1, a_2) and (a_3, a_4) of γ of length 2, where a_2 is a right restriction and a_4 is a left restriction point, and we obtain an alternating sequence $(a_{i_1}, a_{i_2}, a_{i_3})$ of length 3 with $i_j \in \{1, \dots, 4\}$, i.e. $\mathcal{A}(\gamma) \geq 3$. \square

3.4.4 Theorem. *For every $a \in \partial V_K(\sigma) \setminus K$ the corresponding direction set $T_K(\sigma, a)$ is a singleton, where $\partial V_K(\sigma)$ is built with respect to the topology on \mathbb{R}^2 .*

Proof. Trivially, $T_K(\sigma, a)$ is not empty, i.e. it contains at least one feasible direction. Let us assume to the contrary that $\text{card}(T_K(\sigma, a)) > 1$. Since $T_K(\sigma, a)$ is connected (cf. Corollary 3.3.13), we can choose a direction v from the interior of $T_K(\sigma, a)$. But then there is a $\gamma \in \mathfrak{S}_K(\sigma, a, v)$ having neither a right nor a left restriction (cf. Corollary 3.3.16) since $\sigma_K(a, v)$ is connected (cf. Remark 3.3.10). For continuity reasons we obtain a whole neighborhood U that is visible, i.e. $U \subset V_K(\sigma)$, a contradiction to a being on the boundary of $V_K(\sigma)$. \square

3.4.5 Definition. A visibility arc $\gamma \in \mathfrak{S}_K(\sigma)$ is called **right-blocking** if there exists a point $a \in \text{tr}(\gamma) \cap I_K$ and a neighborhood U of a with $(U^r \setminus \text{tr}(\gamma)) \cap V_K(\sigma) = \emptyset$ and **left-blocking** respectively if $(U^l \setminus \text{tr}(\gamma)) \cap V_K(\sigma) = \emptyset$, where $U^l := U \cap \overline{\mathcal{L}_\gamma}$ and $U^r := U \cap \overline{\mathcal{R}_\gamma}$. We simply call γ **blocking** if it is left- or right-blocking.

An illustration can be found in Figure 38.

Obviously, the blocking arcs are exactly the visibility arcs γ containing boundary points $a \in \partial V_K(\sigma) \setminus K$. We will show that these arcs are exactly the arcs supplying alternating sequences of length 3 and examine how the terms right- and left-blocking relate to specific alternating sequences.

3.4.6 Remark. Let $\gamma \in \mathfrak{S}_K(\sigma, a, v)$ for some $a \in V_K(\sigma)$, $v \in T_K(\sigma, a)$ and (a_1, a_2, a_3) be an alternating sequence of γ of length 3. Obviously, $\sigma_K(a, v)$ has only one connected component (cf. Cutting-Lemma 3.2.27).

3.4.7 Theorem.

Let $a \in V_K(\sigma) \setminus K$ and γ a visibility arc with $\gamma \in \mathfrak{S}_K(\sigma, a)$. Then γ is right-blocking [left-blocking] if and only if there exists an alternating sequence of (a_1, a_2, a_3) of γ of length 3 with a right [left] restriction point a_3 .

Proof. Let γ be right-blocking. Then there exists a point $x_0 \in \text{tr}(\gamma) \cap I_K$ having a neighborhood U with $(U^r \setminus \text{tr}(\gamma)) \cap V_K(\sigma) = \emptyset$. Obviously, x_0 is a boundary point of $V_K(\sigma)$. And we can choose an alternating sequence (a_1, a_2, a_3) of γ $|_{[S(\gamma), x_0]}$ of length 3 (cf. Theorems 3.4.3 and 3.4.4), which is of course also an alternating sequence of γ . If there exists a right restriction point $a_4 \succeq_\gamma a_3$, we are done. Therefore, let us assume to the contrary that a_2 is the maximum of all right restriction points with respect to \prec_γ . Then we are able to construct a visibility arc γ_0 with an exiting direction $\tau_{\gamma_0}(x_s)$ that is

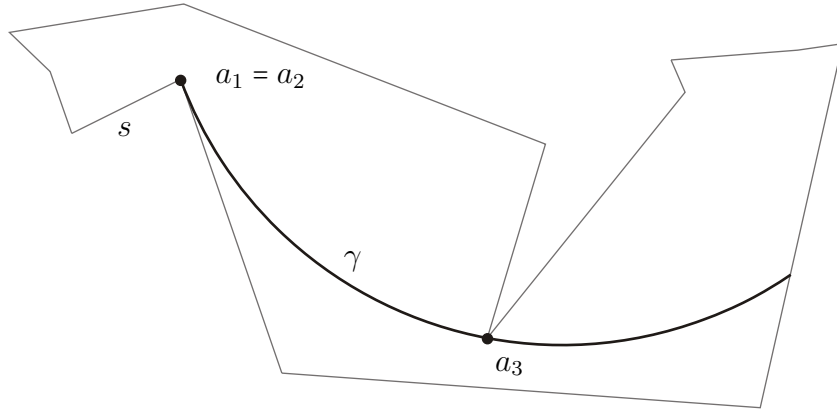


Figure 35: Blocking arc γ with $\mathcal{A}(\gamma) = 3$, but only one right restriction point a_2 and one left restriction point a_3 . Additionally, $a_1 = a_2$ is a pseudo restriction point.

at the right to the left extremal direction $\tau_\gamma(x_s) \in T_K(\sigma, x_s)$ for some $x_s \in [a_2, a_3]$ ending in a point $x \in U_r$, a contradiction.

In order to show the other implication let (a_1, a_2, a_3) be an alternating sequence of γ of length 3 with a right restriction point a_3 . If we denote the connected component of $I_K \setminus [a_2, a_3]_\gamma$ not containing $\text{tr}(s)$ by C , we can choose a point $x_0 \in]a_3, E(\gamma)[\cap C$ and a neighborhood U of x_0 included in C . By construction every visibility arc γ_x of a point $x \in U$ has to cross $[a_2, a_3]_\gamma$ at some $s_1(x)$. According to Lemma 3.3.11, $\tau_\gamma(s_1(x)) \in T_K(\sigma, s_1(x))$ is right-extremal. Hence γ_x is locally left to γ in $s_1(x)$. Supposing $x \in U_r$, γ_x is locally right to γ in x and there must be an intersection $s_2(x) \in]a_3, E(\gamma)]_\gamma \cap \text{tr}(\gamma_x)$ with $\tau_{\gamma_x}(s_2(x))$ right to $\tau_\gamma(s_2(x))$. But again by Lemma 3.3.11 $\tau_\gamma(s_2(x)) \in T_K(\sigma, s_2(x))$ is right-extremal, a contradiction. \square

Since blocking arcs are characterized by alternating sequences of length 3, they can be described in an efficient manner. Although the notation differs from our terminology and s is supposed to be a line segment and not a generalized arc within a polygon, results similar to the following corollary can be found in [22]. Note that the treatment of pseudo restrictions is missing there. Therefore, the results in [22] are not correct in full generality: Chou et al. claim that a blocking arc always has three distinct ‘supports’ which are in particular alternating left and right restrictions but not a pseudo restriction. However, Figure 35 illustrates an example with a blocking arc γ that has only one right restriction $a_1 = a_2$ and one left restriction point a_3 . Nevertheless, we have $\mathcal{A}(\gamma) = 3$ since a_1 is also a pseudo restriction point.

3.4.8 Corollary.

For $a \in V_K(\sigma) \setminus K$ and $\gamma \in \mathfrak{S}_K(\sigma, a)$
the following is equivalent:

- 1) $a \in \partial V_K(\sigma)$,
- 2) $T_K(\sigma, a)$ is a singleton,
- 3) $\mathfrak{S}_K(\sigma, a) = \{\gamma\}$ and $\mathcal{A}(\gamma) \geq 3$,
- 4) γ is a blocking arc.

Proof. The implication ‘1) \Rightarrow 2)’ is shown in Theorem 3.4.4 and ‘2) \Rightarrow 3)’ in Theorem 3.4.3. From Theorem 3.4.7 the implication ‘3) \Rightarrow 4)’ can be deduced and ‘4) \Rightarrow 1)’ follows directly from the definition of a blocking arc. \square

The terms ‘right-blocking’ and ‘left-blocking’ are not mutually exclusive. There are examples of blocking arcs which are left- and right-blocking (cf. Figure 38). By Theorem 3.4.7 these arcs can be characterized as follows:

3.4.9 Corollary. *A visibility arc γ is left- and right-blocking if and only if $\mathcal{A}(\gamma) \geq 4$.*

Proof. Follows immediately from Theorem 3.4.7 and Corollary 3.4.8. \square

Furthermore, we can easily deduce:

3.4.10 Corollary. *Let C be a connected component of $I_K \setminus V_K(\sigma)$. Up to set inclusion in $\overline{I_K}$ there exists exactly one blocking arc γ with $\overline{C} \cap V_K(\sigma) \subset \text{tr}(\gamma)$.*

Proof. Let γ be a blocking arc with $\text{tr}(\gamma) \cap \overline{C} \neq \emptyset$ whose trace is maximal with respect to inclusion in $\overline{I_K}$. Let (a_1, a_2, a_3) be an $E(\gamma)$ -adapted sequence of γ . Since $M := \overline{C} \cap V_K(\sigma)$ is connected, we can deduce from Corollary 3.4.8 that $M \subset [a_3, E(\gamma)]_\gamma$. \square

As a consequence, we obtain:

3.4.11 Corollary. *There exist arcs $\gamma_1, \dots, \gamma_m \in \mathfrak{S}_K(\sigma)$ with $\partial V_K(\sigma) \setminus K \subset \bigcup_{i=1}^m \text{tr}(\gamma_i)$.*

Proof. Corollary 3.4.10 yields that every connected component of $\partial V_K(\sigma) \setminus K$ is a subset of $\text{tr}(\gamma)$ for some $\gamma \in \mathfrak{S}_K(\sigma)$. Since $\partial V_K(\sigma) \setminus K$ is a bounded semi-analytic set, the number of its connected components is finite (cf. [13], Corollary 2.7). \square

In particular, $V_K(\sigma)$ is bounded by an arc spline if K is the trace of an arc spline. In order to deal with these blocking arcs $\gamma_1, \dots, \gamma_m$, the following definition is useful:

3.4.12 Definition. *Let us assume the situation given in Corollary 3.4.10. For an arbitrary subset $M \subset C$, we denote the unique blocking arc γ with $\overline{C} \cap V_K(\sigma) \subset \text{tr}(\gamma)$ which is maximally extended in $\overline{I_K}$ by $\gamma^{(M)}$. We say $\gamma^{(M)}$ **is associated with** M . The restriction $\omega^{(M)} := \gamma^{(M)}|_{\overline{C} \cap V_K(\sigma)}$ is called the **window of** M . If $M := \{a\}$ is a singleton, we use the abbreviations $\gamma^{(a)}$ and $\omega^{(a)}$ instead of $\gamma^{\{a\}}$ and $\omega^{\{a\}}$.*

Note that for all $x \in C$ the corresponding blocking arcs $\gamma^{(x)}$ equal each other (see Figure 36 and 38).

We now introduce another useful definition concerning maximal alternating sequences (cf. Definition 3.2.19).

3.4.13 Definition. *Let $a \in \overline{I_K} \setminus V_K(\sigma)$. An alternating sequence (a_1, a_2, a_3) of $\gamma^{(a)}$ of length 3 is called **a -adapted** if it is maximal with respect to a_3 and $a_3 = S(\omega^{(a)})$ (cf. Definition 3.2.19).*

By this definition (a_1, a_2, a_3) is uniquely determined. An illustration can be found in Figure 36.

3.4.14 Definition. *Let $a \in \overline{I_K} \setminus V_K(\sigma)$ and let (a_1, a_2, a_3) be the corresponding a -adapted sequence. Then we define the subset*

$$V_K^a(\sigma) := \{x \in V_K(\sigma) \setminus \text{tr}(s) \mid \forall \gamma \in \mathfrak{S}_K(\sigma, x) : \text{tr}(\gamma) \cap [a_2, a_3]_{\gamma^{(a)}} \neq \emptyset\}.$$

of $V_K(\sigma)$ (see Figure 36).

3.4.15 Remark. *If $a \in \overline{I_K} \setminus V_K(\sigma)$ and $\mathcal{A}(\gamma^{(a)}) = 3$, the set $V_K^a(\sigma)$ is the connected component D of $V_K(\sigma) \setminus [a_2, E(\gamma^{(a)})]_{\gamma^{(a)}}$ which doesn't contain $\text{tr}(s)$. In any case, the set $\sigma_K(x, v)$ is connected for all $x \in V_K^a(\sigma)$ and $v \in T_K(\sigma, x)$ by the Cutting-Lemma 3.2.27. Furthermore, it is not hard to prove that $V_K^a(\sigma)$ is compact if and only if $a_2 \notin \text{tr}(s)$. This might only appear if a_1 is a pseudo restriction point. An example is depicted in Figure 37.*

In the case of start-destination channels, the blocking arcs that correspond to the destination d are denoted by an extra notion according to the definitions in [73, 4, 54]:

3.4.16 Definition. *Let $\mathfrak{D} := (K, s, \sigma, d)$ be a start-destination channel and let d not be circularly visible, i.e. $\mathfrak{S}_K(\sigma, a) = \emptyset$ for all $a \in \text{tr}(d)$. Then we set $\gamma_{\mathfrak{D}} := \gamma^{(\text{tr}(d))}$ and $\omega_{\mathfrak{D}} := \omega^{(\text{tr}(d))}$. The blocking arc $\gamma_{\mathfrak{D}}$ is said to be **associated with** $\omega_{\mathfrak{D}}$ and $\omega_{\mathfrak{D}}$ is called the **window of** \mathfrak{D} (cf. Figure 38).*

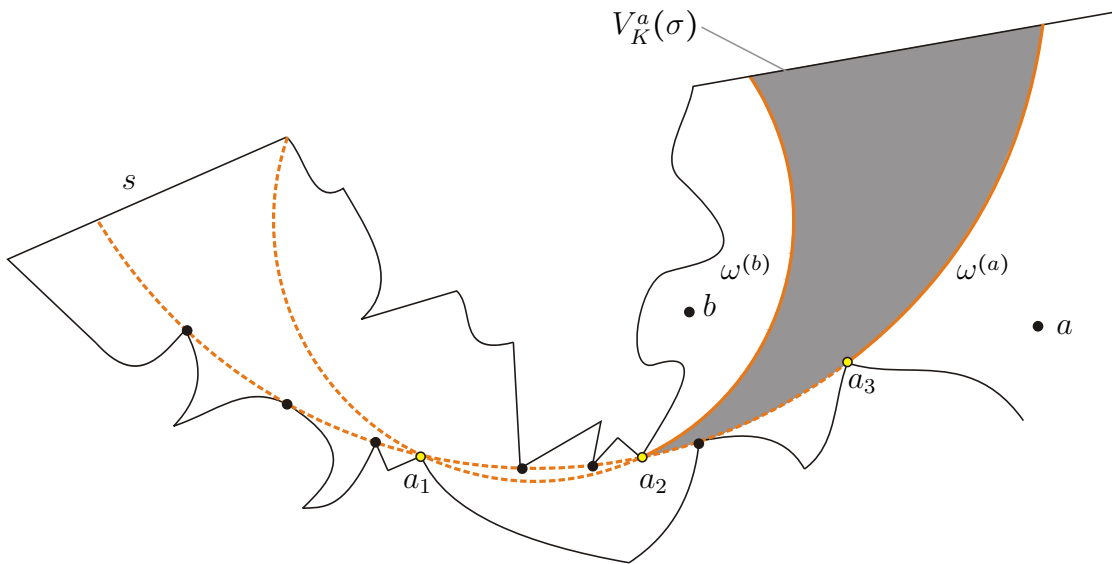


Figure 36: Illustration of the a -adapted alternating sequence $a_1 < a_2 < a_3$. The subset $V_K^a(\sigma) = V_K^b(\sigma)$ of $V_K(\sigma)$ is indicated by the shaded portion.

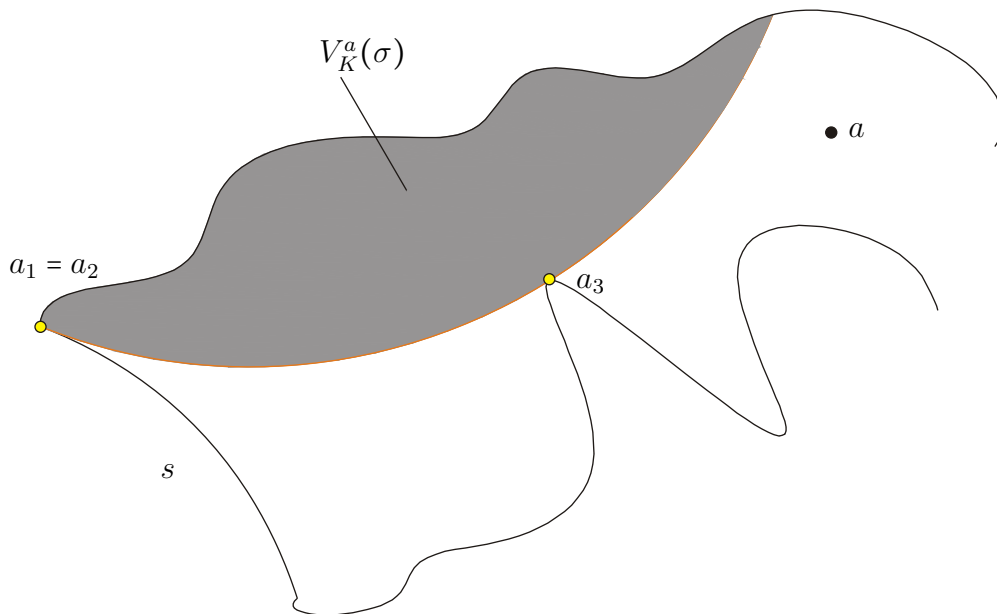


Figure 37: Illustration of the a -adapted alternating sequence $a_1 = a_2 < a_3$ in case of a degenerate continuation channel. The subset $V_K^a(\sigma) \subset V_K(\sigma)$ is indicated by the shaded portion. In this example we have $a_1 = a_2 \in \text{tr}(s)$.

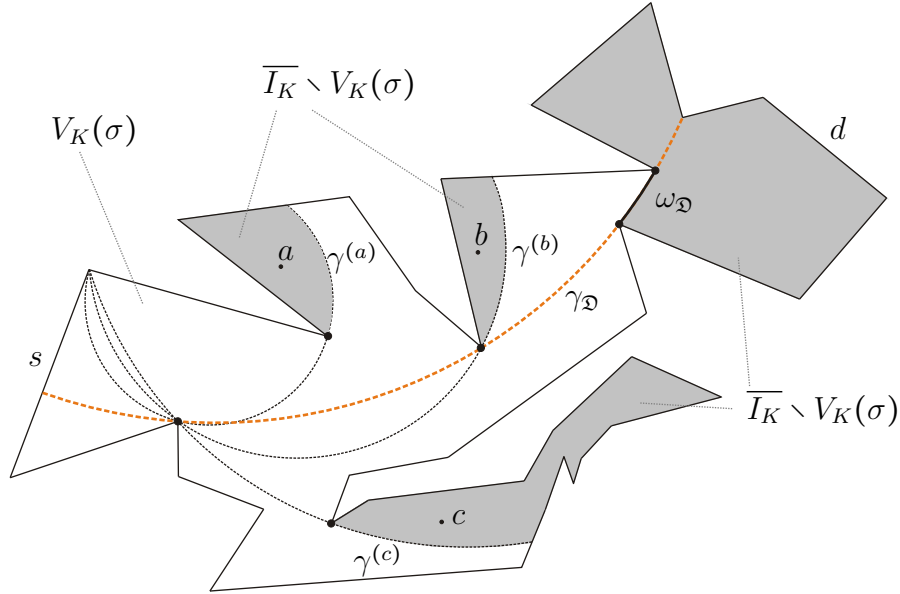


Figure 38: Illustration of a visibility set in a start-destination channel $\mathfrak{D} := (K, s, \sigma, d)$. The set of points which is not circularly visible with respect to \mathfrak{D} is shaded. The dashed arcs are the blocking arcs associated with a, b, c and the destination d respectively. They supply alternating sequences of length 3 (cf. Theorem 3.4.7). The arcs $\gamma^{(a)}, \gamma^{(b)}$ and $\gamma^{(c)}$ are all left-blocking. The solid part of $\gamma_{\mathfrak{D}}$ (orange arc) illustrates the window $\omega_{\mathfrak{D}}$. The corresponding associated arc $\gamma_{\mathfrak{D}}$ is left- and right-blocking.

We now present some further definitions and results regarding a start-destination channel $\mathfrak{D} := (K, s, \sigma, d)$. For our algorithmic approach the following terms are useful:

3.4.17 Definition. Let w_l and w_r be the arc length parametrization of K_l and K_r , with starting points in $\text{tr}(s)$. For every $x \in K_l$ we set $l_K(x) := \text{len}(w_l|_{[S(w_l), x]})$ and analogously for $x \in K_r$ $r_K(x) := \text{len}(w_r|_{[S(w_r), x]})$.

By abuse of notation, we then define the **maximal left length** and **maximal right length** of a visibility arc $\gamma \in \mathfrak{S}_K(\sigma)$ as follows:

$$l_K(\gamma) := \max \{l_K(x) \in \mathbb{R} \mid x \in \text{tr}(\gamma) \cap K_l\} \quad \text{and} \quad r_K(\gamma) := \max \{r_K(x) \in \mathbb{R} \mid x \in \text{tr}(\gamma) \cap K_r\},$$

where $\max \emptyset$ is set to 0.

Since we assumed $\text{tr}(d)$ to be disjoint from $V_K(\sigma)$, the maximal left and right length of each visibility arc in $V_K(\sigma)$ is strongly bounded by the length of K_l and K_r . Every blocking arc has at least three alternating restrictions and passes through the two points corresponding to its maximal left and right length. The window is associated with the visibility arc that goes ‘furthest’:

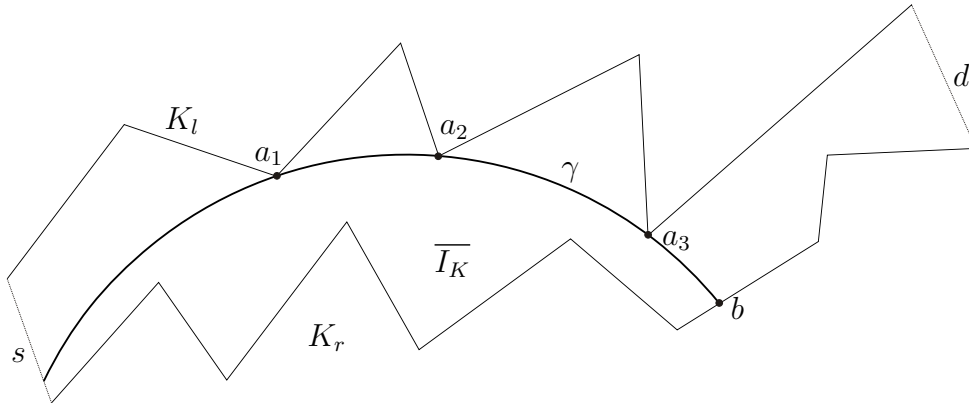


Figure 39: Illustration of a left and right sub-curve of a start-destination channel (K, s, σ, d) given by a polygon. For the visibility arc γ the equations $l_K(\gamma) = l_K(a_3)$ and $r_K(\gamma) = r_K(b)$ hold.

3.4.18 Theorem (Window characterization I). *For the blocking arc $\gamma_{\mathfrak{D}}$ we obtain: $l_K(\gamma_{\mathfrak{D}}) = \max \{l_K(\gamma) \in \mathbb{R} \mid \gamma \in \mathfrak{S}_K(\sigma)\}$ and $r_K(\gamma_{\mathfrak{D}}) = \max \{r_K(\gamma) \in \mathbb{R} \mid \gamma \in \mathfrak{S}_K(\sigma)\}$.*

Proof. Denoting the connected component of $\overline{I_K} \setminus V_K(\sigma)$ which contains $\text{tr}(d)$ by C , we have

$$\begin{aligned} \max \{l_K(\gamma) \in \mathbb{R} \mid \gamma \in \mathfrak{S}_K(\sigma)\} &= \text{len} \left(w_l \mid_{[s(w_l), \min(\overline{C} \cap K_l)]} \right) \text{ and} \\ \max \{r_K(\gamma) \in \mathbb{R} \mid \gamma \in \mathfrak{S}_K(\sigma)\} &= \text{len} \left(w_r \mid_{[s(w_r), \min(\overline{C} \cap K_r)]} \right). \end{aligned}$$

However, $V_K(\sigma) \cap \overline{C}$ is trivially a subset of $\text{tr}(\omega_{\mathfrak{D}})$. \square

We now give a more efficient characterization of the window relating to our algorithmic approach. The local property ‘left’ and ‘right’ in the definition of alternating sequences can be replaced by a global one in the case of the window. The alternating restrictions defining the window are described due to the left and right channel K_l and K_r . We can even show:

3.4.19 Theorem (Window characterization II).

There are points $a_1, a_2, a_3, a_4 := E(\omega_{\mathfrak{D}})$ of $\text{tr}(\gamma_{\mathfrak{D}})$ s.t. $(a_i)_{1 \leq i \leq 3}$ is an alternating sequence of length 3 of $\gamma_{\mathfrak{D}}$ and

- i) either $a_2, a_4 \in K_l$ and $a_3 \in K_r$*
- ii) or $a_2, a_4 \in K_r$ and $a_3 \in K_l$.*

In case i) $\gamma_{\mathfrak{D}}$ is right-blocking and in case ii) left-blocking.

Addendum: *$\gamma_{\mathfrak{D}}$ is uniquely determined by the conditions above.*

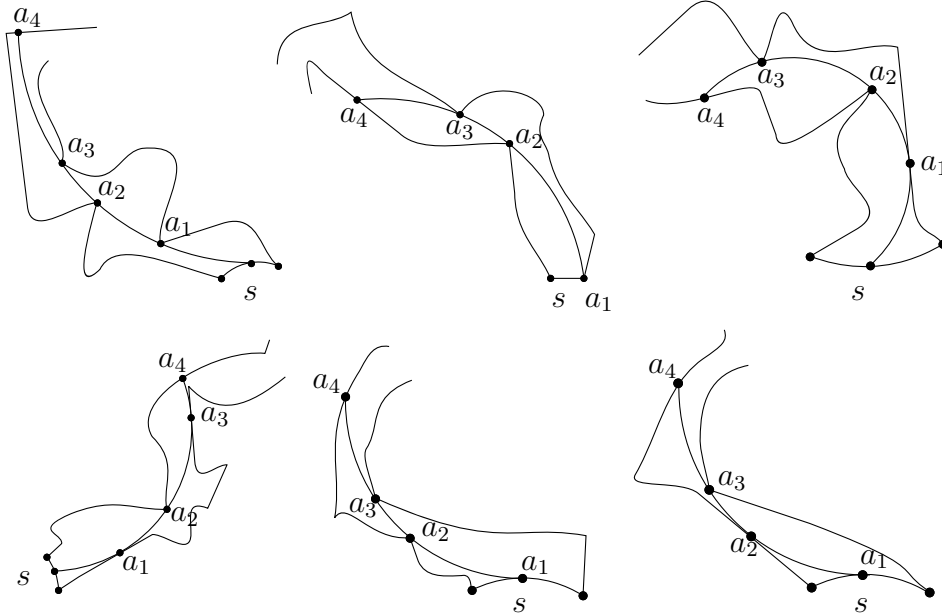


Figure 40: Illustration of Theorem 3.4.19. All configurations of alternating sequences representing the right-blocking case are illustrated. The local and global terms ‘left’ and ‘right’ equal as formulated in the theorem.

Proof. W.l.o.g. let $\gamma_{\mathfrak{D}}$ be right-blocking. By definition we can choose an alternating sequence a_1, a_2, a_3 with $a_3 \in K_r$ and $a_4 := E(\omega_{\mathfrak{D}}) \in K_l$. Hence we have $L(\gamma_{\mathfrak{D}}) \subset K_l$ and $R(\gamma_{\mathfrak{D}}) \subset K_r$ and therefore $a_2 \in K_l$.

On the one hand, only the connected component C containing $\text{tr}(d)$ satisfies $K_l \cap C \neq \emptyset \neq K_r \cap C$. On the other hand, we have $\overline{C} \cap V_K(\sigma) \subset \text{tr}(\gamma_{\mathfrak{D}})$. Thus, also the addendum follows. \square

We have discussed the properties of $V_K(\sigma)$ on the assumption that $\text{tr}(d)$ is not circularly visible. The development of the blocking arcs and the window are crucial for this purpose. If we consider $\text{tr}(d)$ and $V_K(\sigma)$ not to be disjoint, the term ‘window’ is not generally well-defined any longer. However, we have the following property:

3.4.20 Lemma. *Let $V_K(\sigma) \cap \text{tr}(d)$ be non-empty. Then there exist a visibility arc $\gamma \in \mathfrak{S}_K(\sigma, d)$ and points a_1, a_2, a_3 of $\text{tr}(\gamma)$ s.t. one of the following conditions holds:*

- 1) (a_1, a_2, a_3) is an alternating sequence of length 3.
- 2) (a_1, a_2) is an alternating sequence of length 2 and $a_3 = E(\gamma)$ with $a_3 \in \text{Ext}(d)$.

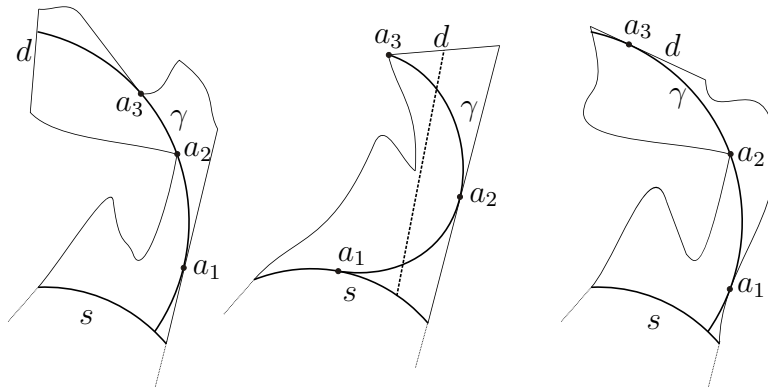


Figure 41: Illustration of Lemma 3.4.20. In the left and the right case γ has an alternating sequence of length 3, while a_3 on the right can only be chosen to be an element of $\text{tr}(d)$. In the middle a_3 can only be chosen to be the endpoint of γ with $a_3 \in \text{Ext}(d)$. In this example d is even linearly visible.

Proof. If $\text{Ext}(d) \cap V_K(\sigma) \neq \emptyset$, we have $\mathfrak{S}_K(\sigma, a, v) \neq \emptyset$ for some $a \in \text{Ext}(d) \cap V_K(\sigma)$ and $v \in \partial T_K(\sigma, a)$ since $T_K(\sigma, a) \subset (-T_{\overline{I}_K}(a)) \cap \mathbb{S}^1 \neq \mathbb{S}^1$. Hence by Theorem 3.3.9 we can choose a visibility arc $\gamma \in \mathfrak{S}_K(\sigma, a, v)$ with $\mathcal{A}(\gamma) \geq 2$. If $\text{Ext}(d) \cap V_K(\sigma)$ is empty, $V_K(\sigma) \cap \text{tr}(d)$ is a generalized arc and certainly there is a point $a \in \text{Ext}(V_K(\sigma) \cap \text{tr}(d))$. But then the arc $\gamma \in \mathfrak{S}_K(\sigma, a)$ has to be a blocking arc. Therefore, we obtain by Theorem 3.4.8: $\mathcal{A}(\gamma) \geq 3$. \square

In general, the visibility arc γ in the lemma above is not unique. Different situations of such an oriented arc γ are illustrated in Figure 41.

3.5 Continuity Properties of $T_K(\sigma, -)$

Throughout this section let (K, s, σ) be an arbitrary tolerance channel. In order to be able to characterize the n -visibility set $V_K^n(\sigma)$ with $n > 1$, we first have to work out the behavior of the feasible direction sets, when the corresponding points are varied. The continuity properties of $T_K(\sigma, a)$ are crucial for examining the $V_K^n(\sigma)$ (see Section 3.6). Our idea will be to use the continuity properties of the feasible direction sets and the intermediate value theorem in order to give an equivalent condition when an oriented arc can be joined with a predecessor visibility spline. It will turn out that this leads to a continuation channel. Hence we can use the results of Section 3.4 iteratively.

The following notion is useful in order to examine the continuity properties of the feasible direction sets:

3.5.1 Definition. *By abuse of notation we define the mapping*

$$T_K(\sigma, -) : V_K(\sigma) \setminus \text{tr}(s) \rightarrow \mathfrak{K}(\mathbb{S}^1), \quad a \mapsto T_K(\sigma, a)$$

that assigns its feasible direction set to every circularly visible point.

$T_K(\sigma, a)$ is not empty for all $a \in V_K(\sigma) \setminus \text{tr}(s)$ and compact by Lemma 3.3.4. Thus, $T_K(\sigma, -)$ is well-defined. Let us now establish the continuity properties of $a \mapsto T_K(\sigma, a)$. First we show the upper semi-continuity, which is relatively easy to prove. We will see later on that $T_K(\sigma, -)$ is not lower semi-continuous on $V_K(\sigma)$ but only on a subset. For the verification of the lower semi-continuity we will need more technical effort. However, we first show:

3.5.2 Lemma.

$T_K(\sigma, -)$ is upper semi-continuous.

Proof. Since $V_K(\sigma) \times \mathbb{S}^1$ is compact and $V_K(\sigma) \setminus \text{tr}(s)$ is locally compact, it is sufficient to show that for every compact subset $M \subset V_K(\sigma) \setminus \text{tr}(s)$ the set $\text{graph}(T_K(\sigma, -)|_M) := \{(a, v) \in M \times \mathbb{S}^1 \mid v \in T_K(\sigma, a)\}$ is closed (cf. Lemma 2.2.5). Let $(a_n, v_n)_{n \in \mathbb{N}}$ be a sequence in $\text{graph}(T_K(\sigma, -)|_M)$ converging to a pair (a, v) . Since M is compact, a is included in M . For all $n \in \mathbb{N}$ we can choose a visibility arc $\gamma_n \in \mathfrak{S}_K(\sigma, a_n, v_n)$. Furthermore, we have a subsequence of $(\text{tr}(\gamma_n))_{n \in \mathbb{N}}$ which converges to a compact set of $\overline{I_K}$. Since $\text{dist}(a, \text{tr}(s)) > 0$, by Lemma 2.5.26, we can assume the limit point given by $\text{tr}(\gamma)$ for

some $\gamma \in \mathfrak{S}_K(\sigma, a)$, and we have $\tau_\gamma(a) = \pm v$. Therefore, we even get $\tau_\gamma(a) = v$ because of the convergence of $(\text{tr}(\gamma_n))_{n \in \mathbb{N}}$. But this means $\gamma \in \mathfrak{S}_K(\sigma, a, v)$, and hence we have $(a, v) \in \text{graph}(T_K(\sigma, -)|_M)$, which concludes the proof. \square

Since we need the lower semi-continuity just for a subset of $V_K(\sigma)$, we focus on the set of all circularly visible points a where $\sigma_K(a, v)$ has only one connected component for all $v \in T_K(\sigma, a)$. Dealing with the whole set of circularly visible points would be somewhat clumsy.

3.5.3 Definition. *Let us denote the subset of all circularly visible points $a \in V_K(\sigma) \setminus \text{tr}(s)$ where $\sigma_K(a, v)$ is connected for all $v \in T_K(\sigma, a)$ by $V_K^{\text{con}}(\sigma)$.*

By Remark 3.4.15 we can deduce the following set inclusion:

$$\bigcup_{a \in \overline{I_K} \setminus V_K(\sigma)} \overline{V_K^a(\sigma)} \subset V_K^{\text{con}}(\sigma) \cup \text{tr}(s)$$

since $\overline{V_K^a(\sigma)} \subset V_K^a(\sigma) \cup \text{tr}(s)$.

Note: If (K, s, σ) is a degenerate starting channel, we obviously get the set equation $V_K^{\text{con}}(\sigma) = V_K(\sigma) \setminus \text{tr}(s)$ (cf. Figure 38).

We now show that the mapping $T_K(\sigma, -)$ is lower semi-continuous at all points of $V_K^{\text{con}}(\sigma)$ except for the vertices of K . For this purpose, we distinguish between three cases: First we focus on points $a \in V_K^{\text{con}}(\sigma) \setminus K$ and interior directions $v \in T_K(\sigma, a)^\circ$. Next, we take smooth points on the boundary $K \cap V_K^{\text{con}}(\sigma)$ and interior directions into account. Eventually, the enhancement to boundary directions can be deduced by a 'diagonal trick'.

3.5.4 Lemma. *For every $a \in V_K^{\text{con}}(\sigma) \setminus K$ and $v \in T_K(\sigma, a)^\circ$ we obtain:*

$$\forall \varepsilon > 0 \exists \delta > 0 \forall x \in B_\delta(a) \cap V_K(\sigma) \exists w \in T_K(\sigma, x) : \|v - w\| < \varepsilon.$$

Proof. Since $\sigma_K(a, v)$ has only one connected component and v is not an extremal direction, by Corollary 3.3.16 there exists a visibility arc $\gamma_0 \in \mathfrak{S}_K(\sigma, a, v)$ having neither a left nor a right restriction. Thus, by Lemma 3.2.26 there exists a $\delta > 0$ providing that $\mathfrak{S}_K(\sigma, x, v) \neq \emptyset$ and hence $v \in T_K(\sigma, x)$ for all $x \in B_\delta(a)$. In particular, the claimed is satisfied. \square

Before we can address smooth points on K , we need some elementary geometric propositions in advance.

3.5.5 Proposition. *Let $r \in]\frac{1}{2}, \infty[$ and $x := (\xi_1, \xi_2)^T \in \mathbb{R} \times (\mathbb{R} \setminus \{0\})$ with $\|x\| = r$ and $\|x - re_1\| = 1$, where $e_1 := (1, 0)^T \in \mathbb{R}^2$. Then the equation*

$$\|re_1 + \operatorname{sgn}(\xi_2) \cdot e_2 - x\|^2 = 2 - \sqrt{4 - r^{-2}}$$

holds, where $e_2 := (0, 1)^T \in \mathbb{R}^2$.

An illustration can be found in Figure 42 on the left.

Proof. Since $\xi_1^2 + \xi_2^2 = r^2$ and $(\xi_1 - r)^2 + \xi_2^2 = 1$, we obtain $-2\xi_1 r + 2r^2 = 1$, i.e. $2r(r - \xi_1) = 1$ and $\xi_2^2 = 1 - \frac{1}{4r^2} = \frac{1}{4}(4 - r^{-2})$. Therefore, the equation

$$\|re_1 + \operatorname{sgn}(\xi_2) \cdot e_2 - x\|^2 = (\xi_1 - r)^2 + (\xi_2 - \operatorname{sgn}(\xi_2))^2 = 1 - 2 \cdot \xi_2 \cdot \operatorname{sgn}(\xi_2) + 1 = 2 - \sqrt{4 - r^{-2}}$$

holds. □

We introduce some useful notions before we formulate the next auxiliary proposition.

3.5.6 Definition. *For each point $a := (\xi_1, \xi_2)^T \in \mathbb{R}^2 \setminus \{0\}$ we introduce the unit vector $a^\perp := \|a\|^{-1} \cdot (-\xi_2, \xi_1)^T$ which is orthogonal to a with $\det(a, a^\perp) > 0$. Assuming an arbitrary vector $w \in \mathbb{R}^2$, we set $a^{(w)} := \operatorname{sgn}\langle w | a^\perp \rangle \cdot a^\perp$.*

Furthermore, we set for any $a \in \mathbb{R}^2$ and $r > 0$: $S_r(a) := \{x \in \mathbb{R}^2 \mid \|x - a\| = r\}$.

3.5.7 Proposition. *If $r > \frac{1}{2}$ and $a \in \mathbb{R}^2$ with $\|a\| = r$, then we obtain for all $w \in S_r(a)$ with $\|w\| \leq 1$:*

$$\|w - \|w\| a^{(w)}\|^2 = \left(2 - \sqrt{4 - \|w\|^2 r^{-2}}\right) \|w\|^2.$$

An illustration can be found in Figure 42 on the right.

Proof. The assertion is trivial if w vanishes, so let $w \neq 0$. Setting $r_w := \frac{r}{\|w\|}$ and $u := \frac{w}{\|w\|}$, we have $u \in \mathbb{S}^1$ and $\frac{a}{\|w\|} \in S_{r_w}(0)$. After possible rotation we can assume w.l.o.g. that $\frac{a}{\|a\|} = -e_1$. We then get $a^\perp = -e_2$ and $a^{(w)} = \operatorname{sgn}(w_2) \cdot e_2$, where w_2 denotes the second coordinate of w . Furthermore, we have $-\frac{a}{\|w\|} = \frac{\|a\|}{\|w\|} e_1 = r_w e_1$. Setting $x := u - \frac{a}{\|w\|}$, we obtain

$$\|x\| = \left\| u - \frac{a}{\|w\|} \right\| = \frac{1}{\|w\|} \|w - a\| = \frac{r}{\|w\|},$$

i.e. $x \in S_{r_w}(0)$. Consequently, we have $\|x - r_w e_1\| = \|u\| = 1$. Denoting the second coordinate of x by x_2 , we can deduce from Proposition 3.5.5:

$$\begin{aligned} \|u - a^{(w)}\|^2 &= \|x - r_w e_1 - \operatorname{sgn}(w_2) \cdot e_2\|^2 = \|x - r_w e_1 - \operatorname{sgn}(x_2) \cdot e_2\|^2 = \\ &= 2 - \sqrt{4 - r_w^{-2}} = 2 - \sqrt{4 - \|w\|^2 r^{-2}}. \end{aligned}$$

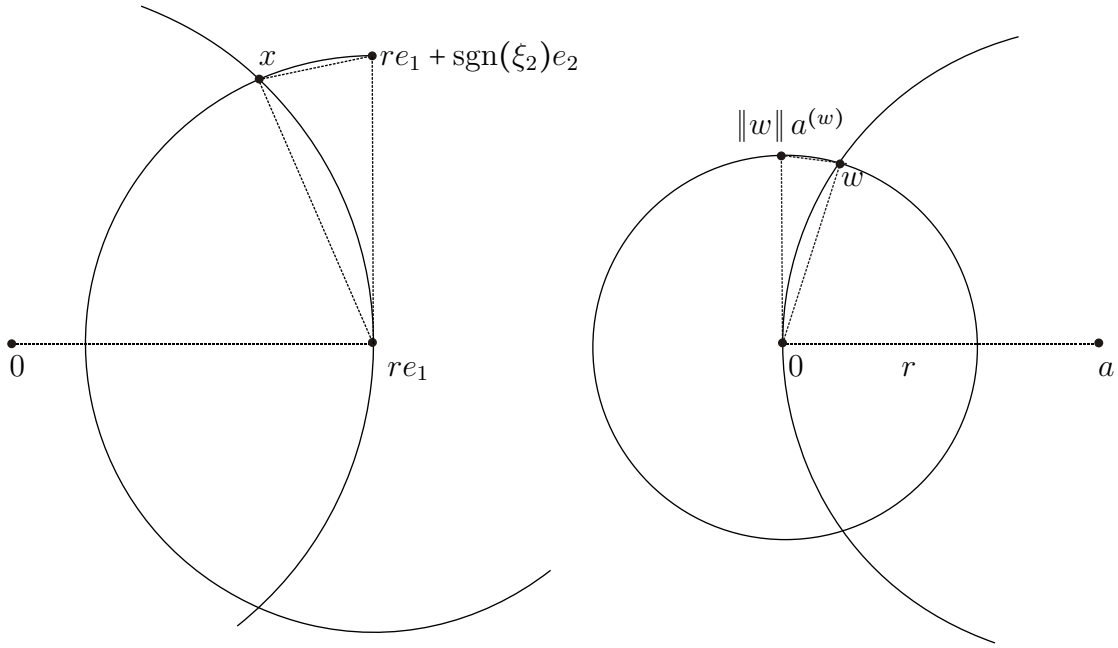


Figure 42: Illustration of Proposition 3.5.5 (left) and 3.5.7 (right).

Therefore, we have $\|w - \|w\| a^{(w)}\|^2 = \|u - a^{(w)}\|^2 \|w\|^2 = \left(2 - \sqrt{4 - \|w\|^2 r^{-2}}\right) \|w\|^2$. \square

From this proposition we conclude:

3.5.8 Proposition. *Let $r_0 > 0$, C be an open cone in \mathbb{R}^2 and $v \in C \cap \mathbb{S}^1$. Given a compact subset K of C , there exists a $\delta > 0$ satisfying the following condition: If γ is an oriented arc with $\kappa(\gamma) < \frac{1}{r_0}$ ending in $0 \in \mathbb{R}^2$ with exiting direction $v \in K \cap \mathbb{S}^1$, we have $\text{tr}(\gamma) \cap B_\delta(0) \subset -C \cup \{0\}$.*

Proof. We set $d := \text{dist}(K, \mathbb{R}^2 \setminus C)$. Since $\lim_{\varepsilon \rightarrow 0} \sqrt{1 - \frac{\varepsilon^2}{4r_0^2}} = 1$, there exist a $\delta > 0$ and an oriented arc γ s.t.

- i) $\langle x|v \rangle < 0$ for all $x \in \text{tr}(\gamma) \cap B_\delta(0)$
- ii) $\frac{r_0}{\delta} > \frac{1}{2}$
- iii) $1 - \sqrt{1 - \frac{\varepsilon^2}{4r_0^2}} < \frac{d^2}{2}$ for all $0 < \varepsilon < \delta$

W.l.o.g. we can assume that $\kappa(\gamma) \neq 0$, and we have $r := \frac{1}{|\kappa(\gamma)|} \geq r_0$. Setting $a := r \cdot \text{sgn}(\kappa(\gamma)) \cdot v^\perp$, we obtain $C(\gamma) = S_r(a)$ and $a^{(x)} = -v$ for all $x \in \text{tr}(\gamma) \setminus \{0\}$. Hence we get by Proposition 3.5.7:

$$\|x + \|x\| v\|^2 = 2 \left(1 - \sqrt{1 - \frac{\|x\|^2}{4r^2}}\right) \|x\|^2 < d^2 \|x\|^2$$

for all $x \in (\text{tr}(\gamma) \cap B_\delta(0)) \setminus \{0\}$. Therefore, we have $\left\| \frac{x}{\|x\|} - (-v) \right\| < d$. Since $-v \in K$ and $d = \text{dist}(-K, \mathbb{R}^2 \setminus (-C))$, we obtain $\frac{x}{\|x\|} \in -C$. Thus, x is included in $-C$. \square

We are now able to formulate and prove the proposition needed for examining the lower semi-continuity on smooth points $a \in K \cap V_K^{\text{con}}(\sigma)$:

3.5.9 Proposition. *Let $\kappa \in]0, \infty[$, C be an open cone in \mathbb{R}^2 and $v \in \mathbb{S}^1$ with $d := \text{dist}(-v, \mathbb{R}^2 \setminus C) > 0$. Then there exists a $\delta > 0$ s.t. for all $w \in (-C) \cap \mathbb{S}^1$ with $\|v - w\| < \frac{d}{2}$ and arcs $\gamma \in \mathfrak{S}$ ending in $x \in \mathbb{R}^2$ with exiting direction w and $|\kappa(\gamma)| < \kappa$ we have $\text{tr}(\gamma) \cap B_\delta(x) \subset x + C$.*

Proof. Follows immediately from Proposition 3.5.8. \square

In order to prove the lower semi-continuity at smooth points $a \in K \cap V_K^{\text{con}}(\sigma)$, we slightly extend the given channel (K, s, σ) s.t. a is an interior point of the extended channel (cf. Lemma 3.1.13). Combining Lemma 3.5.4 and Proposition 3.5.9, we are able to show:

3.5.10 Proposition. *Let $a \in (V_K^{\text{con}}(\sigma) \cap K)$ be a smooth point and $v \in T_K(\sigma, a)^\circ$ an interior direction. Then for all $\varepsilon > 0$ there exists a neighborhood U of a s.t. for all $x \in U$ there is a direction $v_x \in T_K(\sigma, x)$ with $\text{dist}(v, v_x) < \varepsilon$.*

Proof. Let $\varepsilon > 0$. We have $0 < d := \text{dist}\left(v, \overline{\mathbb{R}^2 \setminus T_K(\sigma, a)}\right) \leq \text{dist}\left(-v, \overline{\mathbb{R}^2 \setminus T_{I_K}(a)}\right)$ and set $\rho := \text{dist}(a, \text{tr}(s)) > 0$. First we claim the existence of some $\delta > 0$ satisfying

- 1) $-v \in C := \bigcap_{x \in B_\delta(a) \cap V_K(\sigma)} T_{I_K}(x)$.
- 2) The canonical extension (\tilde{K}, s, σ) of (K, s, σ) given by $I_{\tilde{K}} = I_K \cup B_\delta(a)$ is a tolerance channel.
- 3) For all $x \in B_\delta(a)$ and $w \in \mathbb{S}^1$ with $\|v - w\| < \frac{d}{2}$ and for all $\gamma \in \mathfrak{S}(\sigma, a, w)$ we have $\text{tr}(\gamma) \cap B_\delta(a) \subset x + C$.

Since a is a smooth point, the mapping $x \mapsto T_{I_K}(x)$ is continuous on $B_\delta(a) \cap K$ for sufficiently small δ . Thus, after possible diminution of δ we have

$$\text{dist}(T_{I_K}(x) \cap \mathbb{S}^1, T_{I_K}(a) \cap \mathbb{S}^1) < \frac{d}{2}$$

and therefore $\text{dist}\left(-v, \overline{\mathbb{R}^2 \setminus T_{I_K}(x)}\right) < \frac{d}{2}$. Hence we obtain 1). Property 2) can be satisfied because (K, s, σ) is a tolerance channel (cf. Lemma 3.1.13). Part 3) of the

claim follows directly from Proposition 3.5.9, when choosing $\delta < \rho$, since v is contained in the open cone C° and

$$\forall x \in B_\delta(a) \cap V_K(\sigma) \forall \gamma \in \mathfrak{S}(\sigma, x) : |\kappa(\gamma)| \leq \frac{2}{\rho - \delta}.$$

Then it is easy to see that $a \in V_{\tilde{K}}(\sigma)$ since $V_K(\sigma) \subset V_{\tilde{K}}(\sigma)$. Furthermore, we have $V_{\tilde{K}}(\sigma) \setminus B_\delta(a) \subset V_K(\sigma)$ and $T_K(\sigma, x) \subset T_{\tilde{K}}(\sigma, x)$ for all $x \in V_K(\sigma)$. Since a is an interior point of $V_{\tilde{K}}(\sigma)$, we obtain using Lemma 3.5.4 with respect to the tolerance channel (\tilde{K}, s, σ) : There exists a neighborhood \tilde{U} of a in $V_{\tilde{K}}(\sigma)$ s.t. for all $x \in \tilde{U}$ there exists a direction $v_x \in T_{\tilde{K}}(\sigma, x)$ with

$$\|v - v_x\| < \min\left(\varepsilon, \frac{d}{2}\right).$$

Now it remains to show that for all $x \in U := \tilde{U} \cap V_K(\sigma)$ the direction v_x is contained in $T_K(\sigma, x)$. For this purpose, let $x \in U$ and $\gamma \in \mathfrak{S}_{\tilde{K}}(\sigma, x, v_x)$. In particular, we have $\gamma \in \mathfrak{S}(\sigma, x)$ and therefore $|\kappa(\gamma)| < \frac{2}{\rho - \delta}$. Hence by 3) $\text{tr}(\gamma) \cap B_\delta(x) \cap B_\delta(a)$ is included in $(x + C) \cap B_\delta(a)$, which is obviously a subset of $\overline{I_K}$. Otherwise, we have $I_{\tilde{K}} \setminus B_\delta(a) = I_K \setminus B_\delta(a)$ and $\text{tr}(\gamma) \setminus (B_\delta(x) \cap B_\delta(a)) \subset \overline{I_K}$. Therefore, $\text{tr}(\gamma) \subset \overline{I_K}$ and so we have $v_x \in T_K(\sigma, x)$ and $\|v - v_x\| < \varepsilon$ by construction, thus completing the proof. \square

Summarizing the particular results, we are able to show that $T_K(\sigma, -)$ is lower semi-continuous on $V_K(\sigma) \cap I_K$ and at smooth points of K :

3.5.11 Lemma.

$T_K(\sigma, -)$ is lower semi-continuous on $V_K^{\text{con}}(\sigma) \setminus K$
and at all smooth points of $V_K^{\text{con}}(\sigma) \cap K$.

Proof. Let $a \in V_K^{\text{con}}(\sigma)$ be not a vertex of K and $v \in T_K(\sigma, a)$. Let $(a_n)_{n \in \mathbb{N}}$ be a sequence in $V_K(\sigma)$ convergent to a and $\varepsilon > 0$. Since $T_K(\sigma, a)$ is connected, either its interior is not empty or $T_K(\sigma, a)$ is a singleton. If $v \in T_K(\sigma, a)^\circ$, we obtain by Lemma 3.5.4 and Proposition 3.5.10:

$$\exists N \in \mathbb{N} \forall n > N \exists v_n \in T_K(\sigma, a_n) : \|v - v_n\| < \varepsilon.$$

Let us now focus on a boundary direction $v \in \partial T_K(\sigma, a)$. Since $T_K(\sigma, a)$ has no isolated points (cf. Corollary 3.3.13), we can deduce:

$$\forall m \in \mathbb{N} \setminus \{0\} \exists v_m \in (T_K(\sigma, a))^\circ \text{ with } \|v - v_m\| < \frac{1}{m}.$$

Assuming an arbitrary sequence $(a_n)_{n \in \mathbb{N}}$ converging to a and an integer $m \in \mathbb{N} \setminus \{0\}$, likewise we obtain a sequence $(v_{n,m})_{n \in \mathbb{N}}$ with $v_{n,m} \in T_K(\sigma, a_n)$ which is convergent to v_m because v_m is an interior direction. Apart from that, we have $\lim_{m \rightarrow \infty} v_m = v$. Therefore, we obtain the convergence of $(v_{n,n})_{n \in \mathbb{N}}$ to v with $v_{n,n} \in T_K(\sigma, a_n)$, which concludes the proof in the case of a point a with $\text{card}(T_K(\sigma, a)) > 1$.

Let $T_K(\sigma, a)$ now be a singleton, for instance $T_K(\sigma, a) := \{v\}$. Considering an arbitrary $\varepsilon > 0$ and a sequence $(a_n)_{n \in \mathbb{N}}$ in $V_K(\sigma)$ convergent to a , there exists a bound $N \in \mathbb{N}$ s.t. $T_K(\sigma, a_n) \subset B_\varepsilon(T_K(\sigma, a)) = B_\varepsilon(v)$ for all $n \geq N$ because $T_K(\sigma, -)$ is upper semi-continuous at a (cf. Lemma 3.5.2). In particular, we can choose a $v_n \in T_K(\sigma, a_n)$ with $\|v - v_n\| < \varepsilon$ for all $n \geq N$. Hence we obtain a sequence $(v_n)_{n \in \mathbb{N}}$ converging to v and we have shown the lower semi-continuity in points whose direction set is a singleton as well. \square

Altogether, we obtain directly:

3.5.12 Corollary.

$T_K(\sigma, -)$ is continuous on $V_K^{\text{con}}(\sigma)$ except for the vertices of K .

Proof. By Lemma 3.5.2 $T_K(\sigma, -)$ is upper semi-continuous on $V_K^{\text{con}}(\sigma)$. Furthermore, it is lower semi-continuous on $V_K^{\text{con}}(\sigma) \setminus K$ and at all smooth points of $V_K^{\text{con}}(\sigma) \cap K$ by Lemma 3.5.11. \square

3.5.13 Example. In Figure 43 the direction sets of some circularly visible points are depicted to outline the continuity attitudes of the mapping $T_K(\sigma, -)$.

Note that the direction set at a vertex can abruptly increase but not abruptly shrink when approaching the vertex since $T_K(\sigma, -)$ is at least upper semi-continuous. Furthermore, it is illustrated that $T_K(\sigma, x)$ is steadily getting smaller when approaching the boundary of $V_K(\sigma)$ and on $\partial V_K(\sigma)$ it is just a singleton (cf. Theorem 3.4.4).

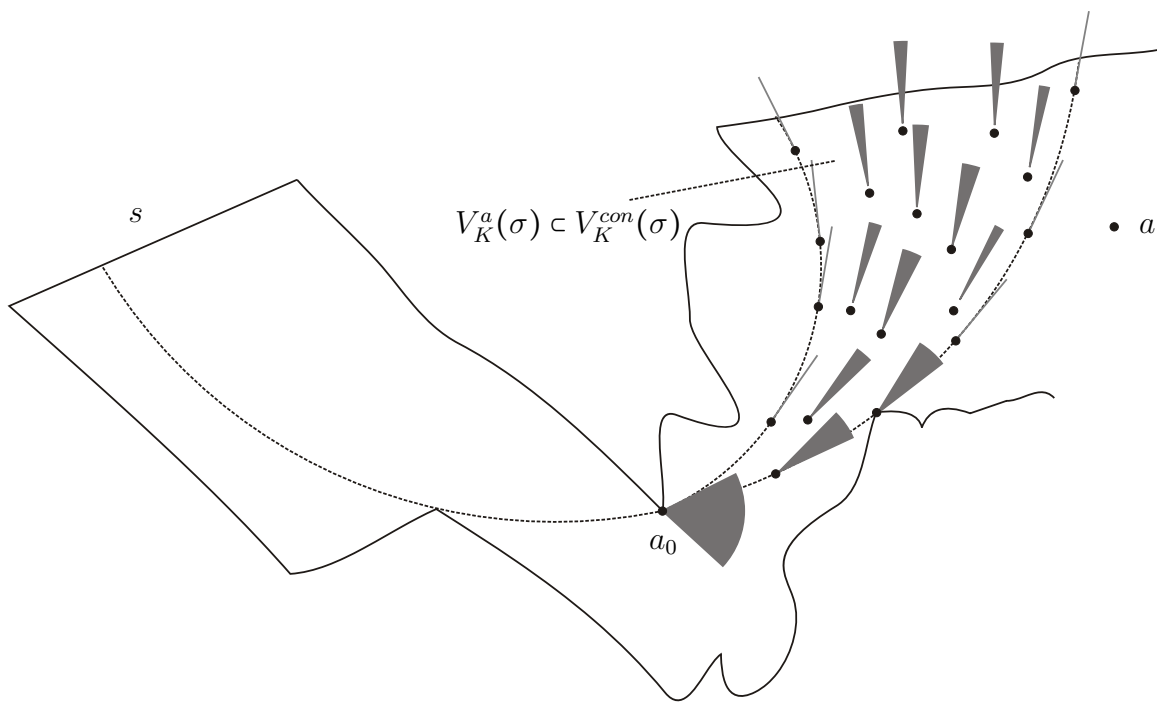


Figure 43: The continuity attitude of the mapping $T_K(\sigma, -)$ is indicated by the small 'pie slices' that shall visualize the sets $T_K(\sigma, x)$ in the points $x \in V_K^{con}(\sigma)$. At the vertex a_0 one can see a point of discontinuity.

3.6 Characterization of the n -Visibility Set $V_K^n(\sigma)$

Throughout this section let $\mathfrak{E} := (K, s, \sigma)$ be an arbitrary tolerance channel.

We give a characterization of the n -visibility set $V_K^n(\sigma)$. As already indicated, $V_K^n(\sigma)$ contains the set of all points that can be reached by a smooth arc spline with n segments, $n > 1$. We will see that $V_K^2(\sigma) \supset \{a \in \overline{I_K} \mid \mathfrak{S}_K^2(\sigma, a) \neq \emptyset\}$, but in general these sets are not equal (cf. Figure 53). The introduction of tolerance channels enables us to focus on the case $n = 2$ and to argue by induction subsequently. Unfortunately, the set $V_K^2(\sigma) \setminus V_K(\sigma)$ is not simply the set of all end points $a \in \overline{I_K}$ of visibility splines with two segments of which the first segment is a restriction of the corresponding blocking arc $\gamma^{(a)}$ (cf. Definition 3.4.12), i.e.

$$V_K^2(\sigma) \neq \{a \in \overline{I_K} \mid \exists \gamma_1 \gamma_2 \in \mathfrak{S}_K^2(\sigma, a) \text{ s.t. } C(\gamma_1) = C(\gamma^{(a)})\}.$$

A counterexample is depicted in Figure 44:

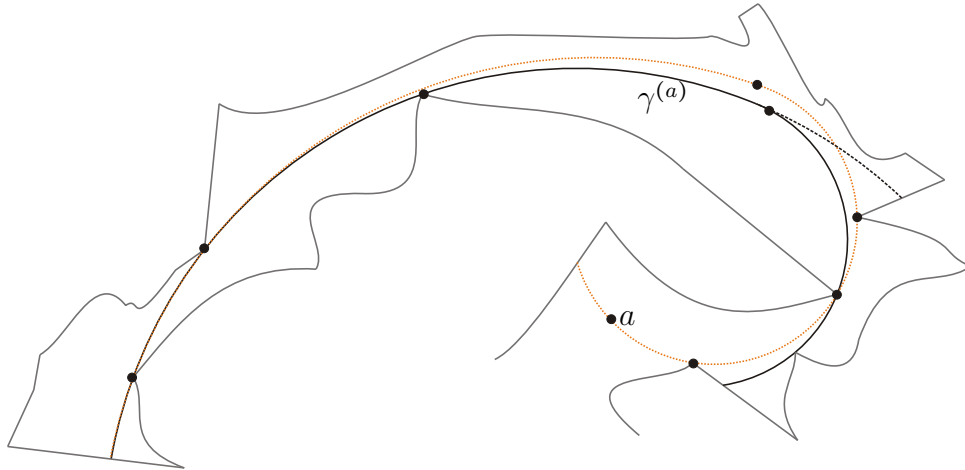


Figure 44: Visibility splines of $V_K^2(\sigma)$. The solid visibility spline is composed of a blocking arc $\gamma^{(a)}$ and another arc. There is no arc that can be joined smoothly to $\gamma^{(a)}$ reaching the point a , but the dashed arc spline (orange) is a visibility spline of a , i.e. $a \in V_K^2(\sigma)$.

In order to characterize the set $V_K^2(\sigma)$, we examine conditions in which an arbitrary arc can be smoothly joined to a visibility arc. The properties of the mapping $T_K(\sigma, -)$ worked out previously are used for this purpose. It will turn out that $V_K^2(\sigma)$ can be computed by examining certain continuation channels which can be defined by blocking arcs $\gamma^{(a)}$ for points $a \in \overline{I_K} \setminus V_K(\sigma)$. Then we will be able to proceed inductively and again define certain continuation channels to characterize the 3-, 4-, ..., n -visibility set.

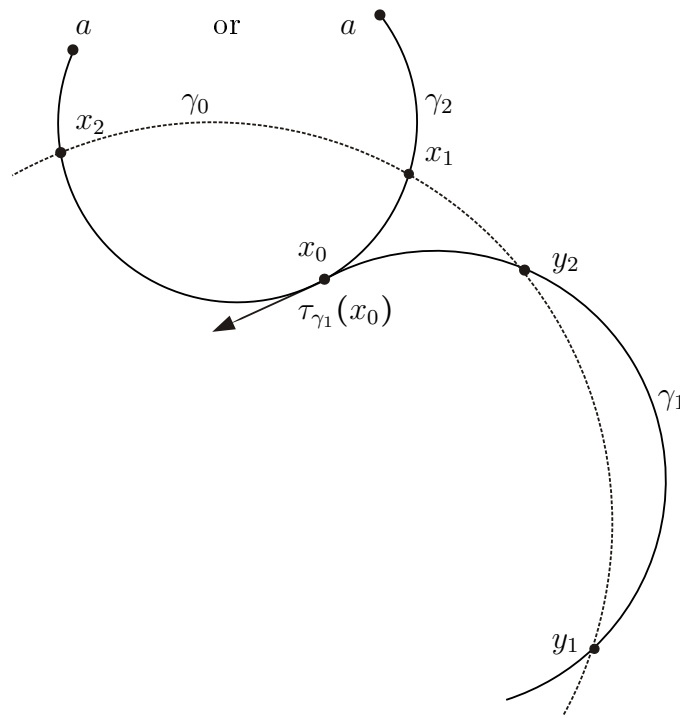


Figure 45: Illustration of the Homotopy-Lemma 3.6.1.

First we state a lemma proved with homotopy techniques. By combining this lemma with the continuity properties of the feasible direction sets, we give an equivalent condition when an oriented arc γ within $\overline{I_K}$ can be smoothly joined to a visibility arc of (K, s, σ) . The idea is stated as follows: Considering two points x_1 and x_2 of $\text{tr}(\gamma)$ where the tangent unit vector $\tau_\gamma(x_1)$ is ‘left’ of $T_K(\sigma, x_1)$ and $\tau_\gamma(x_2)$ is ‘right’ of $T_K(\sigma, x_2)$, there must be a point $x \in [x_1, x_2]_\gamma \cap \text{tr}(\gamma)$ with $\tau_\gamma(x) \in T_K(\sigma, x)$ by the intermediate value theorem. Hence there exists a visibility arc smoothly joined to γ . In particular, $E(\gamma) \in V_K^2(\sigma)$.

3.6.1 Lemma (Homotopy).

Let $\gamma_2 \in \mathfrak{S}$ end in $a \in \overline{I_K} \setminus V_K(\sigma)$, and suppose that $\gamma_1 \in \mathfrak{S}_K(\sigma, x_0)$ for a point $x_0 \in \text{tr}(\gamma_2)$ with $\tau_{\gamma_1}(x_0) = \pm \tau_{\gamma_2}(x_0)$. Let $x_1, x_2 \in \text{tr}(\gamma_0) \cap \text{tr}(\gamma_2)$ with $x_1 <_{\gamma_0} x_2$ and $\gamma_0 \in \mathfrak{S}$ s.t. $\text{tr}(\gamma^{(a)}) \subset \text{tr}(\gamma_0)$. Furthermore, suppose $y_1, y_2 \in \text{tr}(\gamma_1) \cap \text{tr}(\gamma^{(a)})$ with

i) $y_1 <_{\gamma_0} y_2$ and $y_1 <_{\gamma_1} y_2$ or

ii) $y_1 = y_2$ and $\tau_{\gamma_1}(y_1) = \tau_{\gamma_0}(y_1)$.

Then we have: $\tau_{\gamma_1}(x_0) = \tau_{\gamma_2}(x_0) \Leftrightarrow x_1 <_{\gamma_2} x_2$.

The situation is visualized in Figure 45.

Proof. Let $w : [0, 1] \rightarrow \mathbb{R}^2$ be a parametrization of $\text{tr}([x_2, x_0]_{\gamma_2})$ or $\text{tr}([x_0, x_2]_{\gamma_2})$ depending on whether $x_0 <_{\gamma_2} x_2$ or $x_2 <_{\gamma_2} x_0$ with $\|w'(t)\|$ constant, $w(0) = x_2$ and $w(1) = x_0$. Then for every $\lambda \in [0, 1]$ we define an oriented arc $\gamma^{(\lambda)} \in \mathfrak{S}$ s.t.

- i) $S(\gamma^{(\lambda)}) = y_1$ and $E(\gamma^{(\lambda)}) = w(\lambda)$
- ii) $y_2 \in \text{tr}(\gamma^{(\lambda)})$ or $\tau_{\gamma^{(\lambda)}}(y_1) = \tau_{\gamma_0}(y_1)$ if $y_1 = y_2$.

Setting $C_\lambda := C(\gamma^{(\lambda)})$ and $X(\lambda) := \text{tr}(\gamma^{(\lambda)}) \cap \text{tr}(\gamma_2)$, we claim the following:

- 1) $C_0 = C(\gamma_0)$ and $C_1 = C(\gamma_1)$,
- 2) The mapping $[0, 1] \rightarrow \mathfrak{R}(\mathbb{R}^2)$, $\lambda \mapsto \text{tr}(\gamma^{(\lambda)})$ is continuous.
- 3) $\text{card}(X(\lambda)) = 2$ for every $\lambda < 1$ and $\text{card}(X(1)) = 1$.

It is easy to verify the assertions (1) and (2). The case $\lambda = 1$ in (3) being obvious, let us suppose $\lambda < 1$. Then $C_\lambda \cap C(\gamma_2)$ has exactly two intersections. By construction of $\gamma^{(\lambda)}$, we have $E(\gamma^{(\lambda)}) \in X(\lambda) \subset C_\lambda \cap C(\gamma_2)$. Assuming $z \in C_\lambda \cap \text{tr}(\gamma_2)$ with $z \notin \text{tr}(\gamma^{(\lambda)})$, we get a contradiction to (2).

For every $\lambda \in [0, 1[$ we use the abbreviation $x_2^{(\lambda)} := E(\gamma^{(\lambda)})$ and $x_1^{(\lambda)}$ is the uniquely defined (cf. 3)) point included in $X(\lambda)$ with $x_1^{(\lambda)} \neq x_2^{(\lambda)}$. By construction, we can deduce that the mapping

$$[0, 1] \rightarrow \mathbb{R}^2, \lambda \mapsto \begin{cases} x_i^{(\lambda)}, & \lambda < 1 \\ x_0, & \lambda = 1 \end{cases}$$

is continuous for $i = 1, 2$. Furthermore, we set $G := \text{tr}([x_1, x_2]_{\gamma_2})$ or $G := \text{tr}[x_2, x_1]_{\gamma_2}$ respectively. Let $\tilde{w} : [0, 1] \rightarrow \mathbb{R}^2$ be a parametrization of G s.t. $\|\tilde{w}'(t)\|$ is constant, $\tilde{w}(0) = x_1$ and $\tilde{w}(1) = x_2$. Therefore, the orientation of \tilde{w} coincides with the orientation of G which is ed by γ_0 . Then parametrizations w_λ of $\gamma^{(\lambda)}$, $\lambda \in [0, 1]$ can be chosen s.t. $[0, 1]^2 \rightarrow \mathbb{R}^2$, $(\lambda, t) \mapsto w_\lambda(t)$ is continuously differentiable and $w'_\lambda(t)$ is constant.

Consequently, for every $\lambda \in [0, 1[$ and $i \in \{1, 2\}$ there exist uniquely determined parameters $t_i^{(\lambda)}, s_i^{(\lambda)} \in [0, 1]$ with $w_\lambda(t_i^{(\lambda)}) = x_i^{(\lambda)}$ and $\tilde{w}(s_i^{(\lambda)}) = x_i^{(\lambda)}$. Obviously, we can conclude: $t_1^{(\lambda)} < t_2^{(\lambda)} = 1$ and $s_1^{(\lambda)} < s_2^{(\lambda)}$. Therefore, the mappings

$$\tau_1 : [0, 1] \rightarrow [0, 1], \lambda \mapsto \begin{cases} t_1^{(\lambda)} + \frac{1}{2} \cdot (t_2^{(\lambda)} - t_1^{(\lambda)}), & 0 \leq \lambda < 1 \\ t_0, & \lambda = 1 \end{cases}$$

and

$$\tau_2 : [0, 1] \rightarrow [0, 1], \lambda \mapsto \begin{cases} s_1^{(\lambda)} + \frac{1}{2} \cdot (s_2^{(\lambda)} - s_1^{(\lambda)}), & 0 \leq \lambda < 1 \\ t_0, & \lambda = 1 \end{cases}$$

are continuous. Since the parametrizations w_λ and \tilde{w} are regular, the mappings

$$f_1 : [0, 1] \rightarrow \mathbb{R}^2, f_1(\lambda) := \frac{\frac{d}{dt}w_\lambda(\tau_1(\lambda))}{\left\| \frac{d}{dt}w_\lambda(\tau_1(\lambda)) \right\|} \text{ and}$$

$$f_2 : [0, 1] \rightarrow \mathbb{R}^2, f_2(\lambda) := \frac{\frac{d}{dt}\tilde{w}(\tau_2(\lambda))}{\left\| \frac{d}{dt}\tilde{w}(\tau_2(\lambda)) \right\|}.$$

are well-defined. Furthermore, the mapping $\lambda \mapsto \frac{d}{dt}w_\lambda(t)$ is continuous for every $t \in [0, 1]$ since w_λ and \tilde{w} are continuously differentiable. Hence f_1 and f_2 are continuous as well.

We now show that f_1 equals f_2 . Definitely, we have by Proposition 2.5.33:

$$f_1(\lambda) = \frac{x_2^{(\lambda)} - x_1^{(\lambda)}}{\left\| x_2^{(\lambda)} - x_1^{(\lambda)} \right\|} = f_2(\lambda)$$

for all $\lambda < 1$. Thus, f_1 and f_2 are equal on the dense subset $[0, 1[\subset [0, 1]$ and therefore, we get $f_1 = f_2$ since they are continuous. In particular, we obtain:

$$\tau_{\gamma_1}(x_0) = f_1(1) = f_2(1) = \frac{d}{dt}\tilde{w}(t_0).$$

Altogether, these results yield the following: The orientation of $\text{tr}(\tilde{w})$ induced by $\tau_{\gamma_1}(x_0)$ equals the orientation on \tilde{w} and therefore it is equal to the orientation of γ_0 as well. I.e. we have $x_1 < x_2$ with respect to $\tau_{\gamma_1}(x_0)$. From this we can easily deduce both implications of the assertion. \square

By means of the Homotopy-Lemma we obtain that oriented arcs which end in a point $a \in \overline{I_K} \setminus V_K(\sigma)$ and can be joined to a visibility arc satisfy the *continuation condition* (CC) (cf. Definition 3.1.5). This enables an inductive approach for the examination of $V_K^n(\sigma)$ for all $n > 1$, as we will see later on.

3.6.2 Corollary. *Let $a \in \overline{I_K} \setminus V_K(\sigma)$ and $\gamma_1 \gamma_2 \in \mathfrak{S}_K^2(\sigma, a)$ with $C(\gamma_1) \neq C(\gamma^{(a)})$. Then there exist $x_1, x_2 \in C(\gamma_2) \cap \text{tr}(\gamma^{(a)})$ satisfying $x_1 <_{\gamma_2} x_2$, $x_1 <_{\gamma^{(a)}} x_2$ and $[x_1, x_2]_{\gamma_2} \subset \overline{I_K}$.*

Remark: *The property $x_1 <_{\gamma_2} x_2$ is well-defined because $x_i \neq a$, $i = 1, 2$.*

Proof. Because $C(\gamma_1)$ does not equal $C(\gamma^{(a)})$, we have two distinct points x_1 and x_2 with $\{x_1, x_2\} = C(\gamma_1) \cap C(\gamma^{(a)})$. Let $\gamma_0 \in \mathfrak{S}$ be the arc with $C(\gamma_0) = C(\gamma^{(a)})$ starting

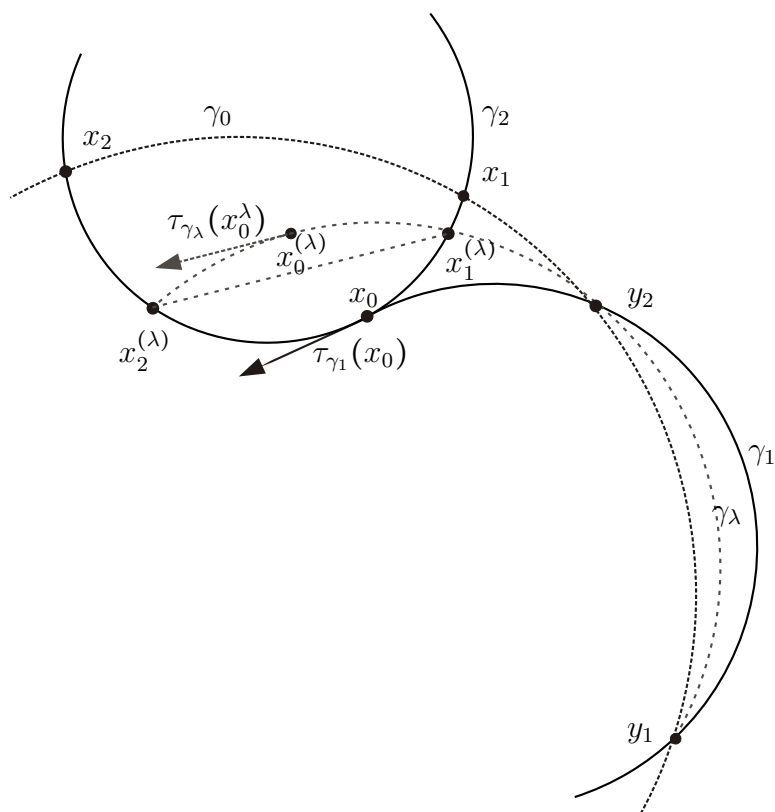


Figure 46: Illustration of the proof of the Homotopy-Lemma 3.6.1.

in $S(\gamma^{(a)})$, containing x_1 and x_2 and ending in one of these points. Likewise, we define $\tilde{\gamma}_2 \in \mathfrak{S}$ as the arc containing $\text{tr}(\gamma_2)$, x_1 and x_2 , ending in $E(\gamma_2)$ and starting in x_1 or x_2 . W.l.o.g. we can assume $x_1 <_{\gamma_0} x_2$. Let \tilde{x}_1 and \tilde{x}_2 be the points satisfying $\{\tilde{x}_1, \tilde{x}_2\} = \{x_1, x_2\}$ and $\tilde{x}_1 <_{\tilde{\gamma}_2} \tilde{x}_2$.

Claim 1: $x_1 = \tilde{x}_1$ and $x_2 = \tilde{x}_2$.

Because of the alternating properties of $\gamma^{(a)}$, we can choose an a -adapted alternating sequence (a_1, a_2, a_3) of length 3 of $\gamma^{(a)}$ s.t.

- i) $[a_1, a_2] \cap \text{tr}(\gamma_1 \gamma_2)$ is not empty, but $\tilde{x}_2 \notin [a_1, a_2]_{\gamma^{(a)}}$ (because $a \notin V_K(\sigma)$), and
- ii) $[a_2, a_3] \cap \text{tr}(\gamma_1 \gamma_2)$ is not empty as well.

If $\tilde{x}_2 \in [a_2, a_3]$, we can set $a_3 = \tilde{x}_2$. From *i*) we can easily deduce by curvature reasons that $[a_1, a_2] \cap \text{tr}(\gamma_1)$ is not empty. Because of *ii*), we now have to distinguish between two cases. If, on the one hand, we assume that γ_1 does not intersect $[a_2, a_3]$, we get $\text{card}([a_2, a_3] \cap \text{tr}(\gamma_2)) = 2$ since a is not circularly visible. Therefore, we have $[a_2, a_3] \cap \text{tr}(\gamma_2) = \{x_1, x_2\}$ and because of $\tilde{x}_2 = a_3$; consequently, $\tilde{x}_1 <_{\gamma_0} \tilde{x}_2$, which proves Claim 1. Assuming on the other hand $[a_2, a_3] \cap \text{tr}(\gamma_1)$ not to be empty, yields the following: Since $[a_1, a_2] \cap \text{tr}(\gamma_1) \neq \emptyset$ and $1 \leq \text{card}([a_2, a_3] \cap \text{tr}(\gamma_1)) \leq 2$, there exist exactly one $y_1 \in [a_1, a_2] \cap \text{tr}(\gamma_1)$ and exactly one $y_2 \in [a_2, a_3] \cap \text{tr}(\gamma_1)$ satisfying either $y_1 <_{\gamma_1} y_2$ or $y_1 = y_2$ and $\tau_{\gamma_1}(y_1) = \tau_{\gamma^{(a)}}(y_1)$. Hence the Homotopy-Lemma 3.6.1 yields Claim 1 for the second case as well.

Since x_2 is included in $\text{tr}(\gamma^{(a)})$, we also have $x_1 \in \text{tr}(\gamma^{(a)})$ and we merely have to show:

Claim 2: $[x_1, x_2]_{\tilde{\gamma}_2} \subset \overline{I_K}$

We prove this claim by contradiction. Let us assume $y \in E_K \cap \text{tr}(\tilde{\gamma}_2)$ with $x_1 < y < x_2$. By precondition, $[x_0, x_2]_{\tilde{\gamma}_2}$ is included in $\text{tr}(\gamma_1 \gamma_2) \subset \overline{I_K}$. Thus: $x_1 <_{\tilde{\gamma}_2} y <_{\tilde{\gamma}_2} x_2$. But now we can construct a Jordan curve ω in $\overline{I_K}$ with

$$\text{tr}(\omega) = [y_2, x_0]_{\gamma_1} \cup [x_0, x_2]_{\gamma_2} \cup [x_2, y_2]_{\tilde{\gamma}},$$

where $\tilde{\gamma}$ is the inverse path of $\gamma^{(a)}$. By construction, y is contained in the closure of interior of ω . Since $\overline{I_K}$ is simply connected, the loop ω is contractible, which contradicts the assumption that $y \in E_K$ and proves Claim 2.

Altogether, we have shown the desired properties claimed in this proposition. \square

We will show that, under certain conditions, the other implication is also correct, but first we need a rather technical lemma exploiting the continuity attitudes of the feasible direction sets and the determinant function:

3.6.3 Lemma. *Let (X, d) be a metric space, $x_0 \in X$ and $\sigma \in \{\pm 1\}$. Furthermore, let $f: X \rightarrow \mathbb{S}^1$ be continuous at x_0 and $g: X \rightarrow \mathfrak{K}(\mathbb{S}^1)$ be upper semi-continuous at x_0 . For every $v \in g(x_0)$ we assume $\sigma \cdot \det(f(x_0), v) > 0$. Then we claim:*

$$\exists \delta > 0 \forall x \in B_\delta(x_0) \forall v \in g(x) : \sigma \det(f(x), v) > 0.$$

Proof. Since the determinant mapping is continuous regarding the matrix entries and f is continuous at x_0 , the following is valid:

$$\exists \varepsilon > 0 \forall x \in B_\varepsilon(x_0) \forall v_0 \in B_\varepsilon(g(x_0)) : \sigma \det(f(x), v_0) > 0.$$

Because of the upper semi-continuity of g at x_0 , there exists a $0 < \delta < \varepsilon$ s.t. for every $x \in B_\delta(x_0)$ $g(x)$ is a subset of $B_\varepsilon(g(x_0))$. In particular, we have $x \in B_\varepsilon(x_0)$ for every $x \in B_\delta(x_0)$ and obviously, $v \in B_\varepsilon(g(x_0))$ for every $v \in g(x_0)$. Altogether, we obtain $\sigma \det(f(x), v) > 0$ for every $v \in g(x_0)$. \square

Oriented arcs in $\overline{I_K}$ satisfying the CC can be smoothly joined to a visibility arc. In this case we can even choose an arc that is extremal, i.e. supplying an alternating sequence of length 2, which is fundamental for a constructive approach and hence for the algorithmic design. Informally speaking, we choose a breakpoint supplying a joining tangent direction which is extremal:

3.6.4 Proposition. *Given $\gamma_2 \in \mathfrak{S}$ ending in $a \in \overline{I_K} \setminus V_K(\sigma)$ with $\text{tr}(\gamma_2) \subset \overline{I_K}$, let $x_1, x_2 \in \text{tr}(\gamma_2)$ with $x_1 <_{\gamma_2} x_2$ and $\text{tr}([x_1, x_2]_{\gamma_2}) \subset V_K^{\text{con}}(\sigma)$ s.t.*

i) $\det(\tau_{\gamma_2}(x_1), v) > 0$ and $\det(\tau_{\gamma_2}(x_2), w) < 0$ for all $v \in T_K(\sigma, x_1)$, $w \in T_K(\sigma, x_2)$

ii) $T_K(\sigma, x) \neq \mathbb{S}^1$ for all $x \in [x_1, x_2]_{\gamma_2}$

Then there exists a point $x_0 \in [x_1, x_2]_{\gamma_2}$ s.t.

1) $\pm \tau_{\gamma_2}(x_0) \in T_K(\sigma, x_0)$ and

2) x_0 is a vertex of K or $\det(\tau_{\gamma_2}(x_0), v) = 0$ for some extremal direction $v \in \partial T_K(\sigma, x_0)$.

Proof. Let us denote the subset of all vertices in $\text{tr}([x_1, x_2]_{\gamma_2}) \cap V_K(\sigma)$ by X . Then X contains all vertices which are passed through by γ_2 in $V_K^{\text{con}}(\sigma)$. If there is a point $x_0 \in X$ and a feasible direction $v \in T_K(\sigma, x_0)$ with $\det(\tau_{\gamma_2}(x_0), v) = 0$, we are done. Therefore, let $\det(\tau_{\gamma_2}(x), v) \neq 0$ for all $x \in X$ and $v \in T_K(\sigma, x)$. Because of property *ii)* and Lemma 3.6.3, the minimum of $\{x \in X \mid \det(\tau_{\gamma_2}(x), T_K(\sigma, x_2)) < 0\}$ with respect to ' $<_{\gamma_2}$ ' exists if X is not empty. In either case, we have points \tilde{x}_1 and \tilde{x}_2 with $x_1 < \tilde{x}_1 \leq \tilde{x}_2 < x_2$

s.t. $[\tilde{x}_1, \tilde{x}_2]_{\gamma_2} \subset V_K^{\text{con}}(\sigma)$ does not contain any non-smooth point of K , and which satisfy the inequalities

$$\det(\tau_{\gamma_2}(\tilde{x}_1), v) > 0 \text{ and } \det(\tau_{\gamma_2}(\tilde{x}_1), w) < 0 \text{ for all } v \in T_K(\sigma, \tilde{x}_1) \text{ and } w \in T_K(\sigma, \tilde{x}_2)$$

since $T_K(\sigma, -)$ is upper semi-continuous (cf. Corollary 3.5.12). Let $w : [0, 1] \rightarrow \mathbb{R}^2$ be a parametrization of $[\tilde{x}_1, \tilde{x}_2]_{\gamma_2}$. Then the mapping $f : [0, 1] \rightarrow \mathbb{R}^2$, $t \mapsto l(w(t))$ is a continuous selection of $T_K(\sigma, -)|_{[\tilde{x}_1, \tilde{x}_2]_{\gamma_2}}$, where $l(w(t))$ denotes the left extremal direction of $T_K(\sigma, w(t))$. Since the two inequalities $\det(w(0), f(0)) > 0$ and $\det(w(1), f(1)) < 0$ hold, we obtain by continuity reasons (see Corollary 3.5.12) from the intermediate value theorem the existence of a parameter $t_0 \in [0, 1[$ with $\det(w(t_0), f(t_0)) = 0$, which concludes the proof. \square

As already indicated, every blocking arc $\gamma^{(a)}$ corresponding to a point $a \in \overline{I_K} \setminus V_K(\sigma)$ generates a (degenerate) continuation channel, which will be essential for our inductive approach. In fact, we can interpret this channel as shrinking of \mathfrak{E} , where the starting segment is given by $\gamma^{(a)}$ instead of s . A precise formulation is given in the following definition:

3.6.5 Definition. *Let $a \in \overline{I_K} \setminus V_K(\sigma)$ and let C be the connected component of $\overline{I_K} \setminus V_K(\sigma)$ containing a . Furthermore, let (a_1, a_2, a_3) be the a -adapted sequence of $\gamma := \gamma^{(a)}$. Then γ induces a continuation channel $\mathfrak{E}_a := (K_a, s_a, \sigma_a)$ in the following way:*

1) *If $\mathcal{A}(\gamma|_{[s(\gamma), x]}) \geq 3$ for some $x \in [a_2, a_3[$, γ is left and right blocking, and we obtain a degenerate continuation channel with*

i) $K_a = \partial C$

ii) $s_a := \omega^{(a)}$

iii) σ_a is the degenerate unidirectional restriction of s_a (cf. Definition 3.1.4).

2) *Otherwise, we can define the non-degenerate channel \mathfrak{E}_a with*

i) K_a defined by $\overline{I_{K_a}} = \overline{V_K^a(\sigma) \cup C}$

ii) $s_a := [a_2, E(\omega^{(a)})]_{\gamma}$

iii) σ_a is the unidirectional restriction of s_a (cf. Definition 3.1.5).

We use the abbreviation $\sigma_{K_a} := (\sigma_a)_{K_a}$.

An illustration of Definition 3.6.5 can be found in Figure 47, where both cases 1) and 2) are exemplified. In particular, we can see that $E(s_a)$ doesn't need to be equal to $E(\gamma^{(a)})$, considering the channel defined by b .

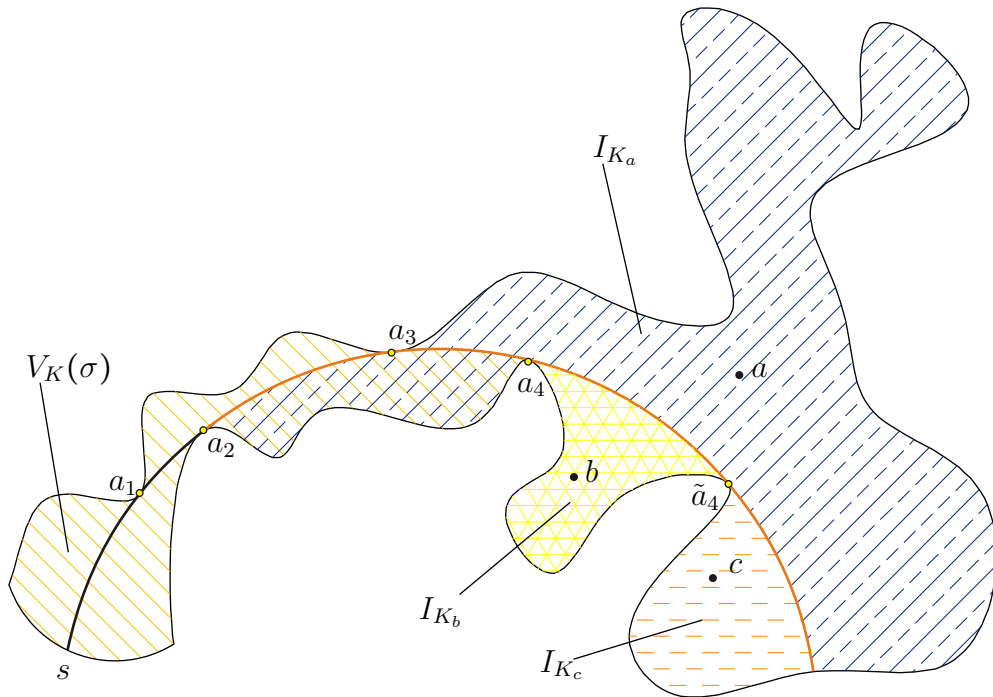


Figure 47: Illustration of the continuation channel (K_a, s_a, σ_a) . The alternating sequence (a_1, a_2, a_3) of $\gamma^{(a)} = \gamma^{(b)} = \gamma^{(c)}$ is a -adapted; (a_2, a_3, a_4) is b -adapted and (a_2, a_3, \tilde{a}_4) is c -adapted. The diverse hachures depict the corresponding interiors of the continuation channels defined by a , b and c respectively. Note: $E(\gamma^{(a)}) = E(s_a) = E(s_c)$, but $E(s_b) = \tilde{a}_4 \neq E(\gamma^{(b)})$.

3.6.6 Remark. Let us assume the second case of Definition 3.6.5. Then $\overline{I_{K_a}} \cap V_K(\sigma)$ is not a subset of $V_K^{con}(\sigma)$ if and only if $a_2 \in \text{tr}(s)$, which is disjoint to $V_K^{con}(\sigma)$, and therefore $T_K(\sigma, a_2)$ is empty. We have already seen an example indicated in Figure 37. However, $V_K^a(\sigma) \setminus \{a_2\} = \overline{I_{K_a}} \setminus \{a_2\}$ is still a subset of $V_K^{con}(\sigma)$.

The idea for characterizing $V_K^2(\sigma)$ is simply to examine the properties of the set $V_{K_a}(\sigma_a)$ for certain points $a \in \overline{I_K} \setminus V_K(\sigma)$. Since $V_{K_a}(\sigma_a)$ is a tolerance channel, the results of Section 3.4 can be applied. We will now see that an oriented arc ending in a can be joined smoothly to a visibility arc if and only if it satisfies the continuation condition (CC) with respect to the blocking arc $\gamma^{(a)}$:

3.6.7 Remark. For an arbitrary arc $\gamma \in \mathfrak{S}$ in $\overline{I_K}$ ending in $a \in V_K^2(\sigma) \setminus V_K(\sigma)$ with non-empty intersection $\text{tr}(\gamma) \cap V_K(\sigma)$, the following two properties are equivalent by definition:

- 1) There exists an arc $\tilde{\gamma} \in \mathfrak{S}_{K_a}(\sigma_a, a, v)$ with $C(\gamma) = C(\tilde{\gamma})$.
- 2) Either there exist two intersection points $x_1, x_2 \in \text{tr}(\gamma^{(a)}) \cap C(\gamma)$ with $x_1 <_\gamma x_2$, $x_1 <_{\gamma^{(a)}} x_2$ and $[x_1, x_2]_\gamma \subset V_K^{con}(\sigma)$ or we have $\gamma_1 \gamma_2 \in \mathfrak{S}_K^2(\sigma, a)$ for some γ_1, γ_2 with $C(\gamma_1) = C(\gamma^{(a)})$ and $C(\gamma_2) = C(\gamma)$.

Note that property 2 above is the CC with respect to $\gamma^{(a)}$.

The following two theorems are the key part of the examination of $V_K^2(\sigma)$:

3.6.8 Theorem (Connection).

Let $\gamma_2 \in \mathfrak{S}$ with $\text{tr}(\gamma_2) \subset \overline{I_K}$ ending in $a \in \overline{I_K} \setminus V_K(\sigma)$ and being maximally extended in $\overline{I_K}$. Then the following two properties are equivalent:

- 1) *There exist a breakpoint $x_0 \in V_K(\sigma) \cap C(\gamma_2)$ and a visibility arc*

$\gamma_1 \in \mathfrak{S}_K(\sigma, x_0)$ s.t. $\gamma_1 \tilde{\gamma} \in \mathfrak{S}_K^2(\sigma, a)$, where $\tilde{\gamma} = \gamma_2|_{[x_0, a]}$.

- 2) *There exists an arc $\tilde{\gamma}_2 \in \mathfrak{S}_{K_a}(\sigma_a, a)$ with $S(\tilde{\gamma}_2) \not\subset \text{tr}(s)$ and $C(\gamma_2) = C(\tilde{\gamma}_2)$.*

Addendum: *We can choose γ_1 in (1) extremal, i.e. $\mathcal{A}(\gamma_1) \geq 2$ or $E(\gamma_1)$ is a vertex and $\mathcal{A}(\gamma_1) \geq 1$.*

An illustration can be found in Figure 48.

Proof. In any case, we necessarily have $\text{tr}(\gamma_2) \cap V_K(\sigma) \neq \emptyset$.

(1) \Rightarrow (2): Let us assume that property (1) is valid. If $C(\gamma_1)$ equals $C(\gamma^{(a)})$, property (2) follows immediately. If this is not the case, by Corollary 3.6.2 there exist points

$x_1, x_2 \in \text{tr}(\gamma_2) \cap \text{tr}(\gamma^{(a)})$ with $x_1 \prec_{\gamma_2} x_2$, $x_1 \prec_{\gamma^{(a)}} x_2$ and $[x_1, x_2]_{\gamma_2} \subset \overline{I_K}$. Assuming to the contrary there would be a point $y \in \text{tr}(\gamma_2)$ with $x_1 \prec_{\gamma_2} y \prec_{\gamma_2} x_2$ and $y \notin V_K(\sigma)$, this point would clearly be 2-circularly visible. Obviously, we have $x_0 \prec_{\gamma_2} y$ and therefore $\gamma_1 \gamma_2 \upharpoonright_{[x_0, y]} \in \mathfrak{S}_K^2(\sigma, y)$. But then the orientations induced by $\gamma^{(y)}$ and γ_2 on the two intersection points $\tilde{x}_1, \tilde{x}_2 \in \text{tr}(\gamma^{(y)}) \cap \text{tr}(\gamma_2)$ would not be identical, which is contradictory to the Homotopy-Lemma 3.6.1. Altogether, we obtain (2).

(2) \Rightarrow (1): By Remark 3.6.7 we can assume points $x_1, x_2 \in \text{tr}(\gamma^{(a)}) \cap C(\gamma_2)$ with $x_1 \prec_{\gamma_2} x_2$, $x_1 \prec_{\gamma^{(a)}} x_2$ and $[x_1, x_2]_{\gamma_2} \subset V_K(\sigma)$ since the case $x_1 = x_2$ is obvious. Because of these orientation properties, we have w.l.o.g.

$$\det(\tau_{\gamma_2}(x_1), \tau_{\gamma^{(a)}}(x_1)) > 0 \quad \text{and} \quad \det(\tau_{\gamma_2}(x_2), \tau_{\gamma^{(a)}}(x_2)) < 0.$$

We now have to distinguish between two cases:

First Case: $\det(\tau_{\gamma_2}(x_1), v) > 0$ for all $v \in T_K(\sigma, x_1)$.

Since $T_K(\sigma, x_2) = \{\tau_{\gamma^{(a)}}(x_2)\}$, we obtain by the Proposition 3.6.4 the existence of a point $x_0 \in \text{tr}(\gamma_2)$ with $x_1 \prec_{\gamma_2} x_0 \prec_{\gamma_2} x_2$ and $\tau_{\gamma_2}(x_0) \in T_K(\sigma, x_0)$ s.t. x_0 is a vertex of K or $\tau_{\gamma_2}(x_0) \in \partial T_K(\sigma, x_0)$. In particular, property (1) and the addendum follow.

Second Case: There are directions $v \in T_K(\sigma, x_1)$ with $\det(\tau_{\gamma_2}(x_1), v) \leq 0$.

Since $T_K(\sigma, x_1)$ is connected, there exists a $v \in T_K(\sigma, x_1)$ with $\det(\tau_{\gamma_2}(x_1), v) = 0$, i.e. $\tau_{\gamma_2}(x_1) = \pm v$. By the Homotopy-Lemma we have $\tau_{\gamma_2}(x_1) \in T_K(\sigma, x_1)$. If x_1 equals a_2 within the a -adapted sequence (a_1, a_2, a_3) of $\gamma^{(a)}$, the claimed is shown. Hence we can focus on the case ' $x_1 \succ_{\gamma^{(a)}} a_2$ '. In the same manner as in the proof of the Proposition 3.6.4, we can assume the set of all vertices in $K \cap \text{tr}(\gamma_2)$ to be empty. In any case $v_1 := \tau_{\gamma^{(a)}}(x_1)$ is right or left extremal because $x_1 \succ_{\gamma^{(a)}} a_2$. W.l.o.g. let v_1 be right extremal. Now the mapping

$$r : [x_1, x_2]_{\gamma_2} \rightarrow \mathbb{S}^1, \quad x \mapsto r(T_K(\sigma, x)),$$

where $r(T_K(\sigma, x))$ denotes the uniquely determined right extremal direction of $T_K(\sigma, x)$, is well-defined. Obviously, r is a continuous selection of the set-valued mapping

$$[x_1, x_2]_{\gamma_2} \rightarrow \mathfrak{K}(\mathbb{S}^1), \quad x \mapsto T_K(\sigma, x).$$

Because of $r(x_1) = v_1$ and $r(x_2) = v_2 := \tau_{\gamma^{(a)}}(x_2)$ and the continuity of

$$f : [x_1, x_2]_{\gamma_2} \rightarrow \mathbb{R}, \quad x \mapsto \det(\tau_{\gamma_2}(x), r(x)),$$

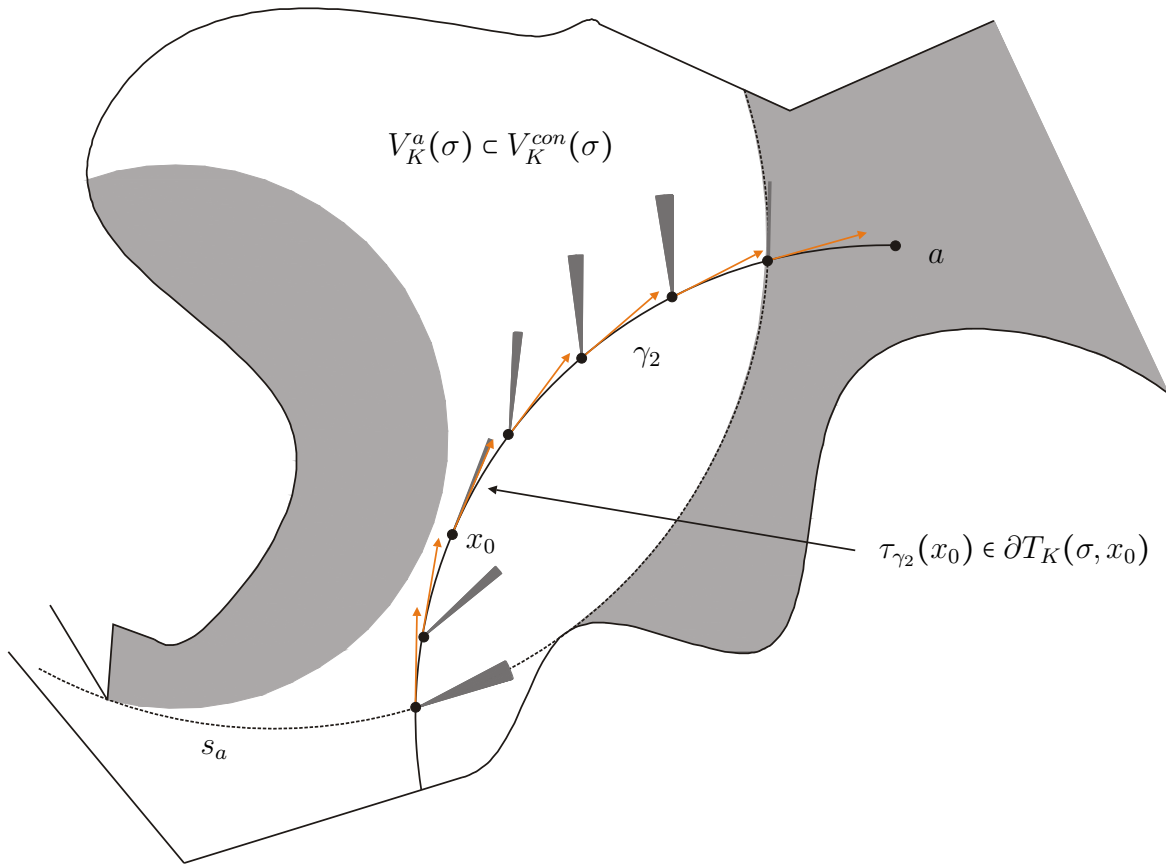


Figure 48: Illustration of Theorem 3.6.8. The shaded portion is the part of $\overline{I_K}$ that is not circularly visible. The arc γ_2 can be joined smoothly to a visibility arc γ_1 having an extremal direction at x_0 . Hence γ_1 can be chosen supplying an alternating sequence of length 2.

we obtain a point x_0 with $x_1 <_{\gamma_2} x_0 <_{\gamma_2} x_2$ and $f(x_0) = 0$, by the intermediate value theorem, since $f(x_1) < 0$ and $f(x_2) > 0$. Thus, again the Homotopy-Lemma 3.6.1 yields: $\tau_{\gamma_2}(x_0) = r(x_0) \in \partial T_K(\sigma, x_0)$. Altogether, we have shown 1) and the addendum. \square

3.6.9 Theorem (Connection II).

Let $a \in \overline{I_K} \setminus V_K(\sigma)$. Then we get $\overline{\mathfrak{S}_K^2}(\sigma, a) \neq \emptyset \Leftrightarrow \mathfrak{S}_{K_a}(\sigma_a, a) \neq \emptyset$.

Proof. Let $\gamma \in \overline{\mathfrak{S}_K^2}(\sigma, a)$. If, on the one hand, $|\gamma| = 1$, we obviously have $\gamma_2 \in \mathfrak{S}_{K_a}(\sigma_a, a)$. If $|\gamma| = 2$, on the other hand, then $\gamma =: \gamma_1 \gamma_2 \in \overline{\mathfrak{S}_K^2}(\sigma)$ and $\text{tr}(\gamma_2) \cap \text{tr}(s)$ is empty. Hence Theorem 3.6.8 yields the desired.

In order to show the other implication, let $\gamma_2 \in \mathfrak{S}_{K_a}(\sigma_a, a)$. Again, by Theorem 3.6.8 we can assume $\gamma = \gamma_2$ and $S(\gamma) \in \text{tr}(s)$. Therefore, we get $\gamma \in \overline{\mathfrak{S}_K^2}(\sigma, a)$. \square

We easily deduce from the theorem above:

3.6.10 Corollary. *We have the set equality*

$$\overline{\mathfrak{S}_K^2}(\sigma) = \mathfrak{S}_K^2(\sigma) \cup \bigcup_{a \in \overline{I_K} \setminus V_K^2(\sigma)} \mathfrak{S}_{K_a}(\sigma_a).$$

We are able to use the Connection-Theorems inductively and exploit the properties of the sets $V_K^n(\sigma)$ this way. For this purpose, we introduce some notions that are only used to simplify the claims subsequently. We denote the set of these points which can be iteratively constructed by building continuation channels as defined in Definition 3.6.5 by $W_K^n(\sigma)$:

3.6.11 Definition. *We define recursively: $W_K^1(\sigma) := V_K(\sigma)$ and for $n \geq 2$*

$$W_K^n(\sigma) := \{x \in W_K^{n-1}(\sigma) \cup V_{K_a^{n-1}}(\sigma_a^{n-1}) \mid a \in V_K^n(\sigma) \setminus V_K^{n-1}(\sigma)\}$$

where σ_a^n , s_a^n and K_a^n are defined as follows: Let $a \in \overline{I_K} \setminus V_K(\sigma)$, then

- i) $\sigma_a^1 := \sigma_a$, $s_a^1 := s_a$ and $K_a^1 := K_a$ are defined as in Definition 3.6.5 and
- ii) $K_a^n := (K_a^{n-1})_a$, $\sigma_a^n := (\sigma_a^{n-1})_a$, $s_a^n := (s_a^{n-1})_a$, for $n \geq 2$ and $a \in \overline{I_K} \setminus V_{K_a^{n-1}}(\sigma_a^{n-1})$.

Due to the notion \mathfrak{E}_a introduced in Definition 3.6.5, for $n \geq 1$ we use the abbreviation $\mathfrak{E}_a^n := (K_a^n, s_a^n, \sigma_a^n)$.

Figure 49 shows an example with a starting channel given by a polygon.

Assuming a point $a \in V_K^{n+1}(\sigma) \setminus V_K^n(\sigma)$, it is easy to verify that $a \notin V_{K_a^{n-1}}(\sigma_a^{n-1})$. Hence σ_a^n , s_a^n and K_a^n ; consequently, $W_K^{n+1}(\sigma)$ are well-defined. Using the Connection-Theorems 3.6.8 and 3.6.9, we will show that the sets $W_K^n(\sigma)$ and $V_K^n(\sigma)$ are equal. However, this means that all n -circularly visible points can be obtained by a constructive approach, which is crucial for developing an algorithm. For this purpose, it is necessary to show that the corresponding direction sets (see definition below) are equal, too.

3.6.12 Definition. *Let $a \in V_K^n(\sigma) \setminus V_K^{n-1}(\sigma)$. Then we set*

$$T_K^n(\sigma, a) = \{v \in \mathbb{S}^1 \mid \exists \gamma \in \overline{\mathfrak{S}_K^n}(\sigma, a) \text{ s.t. } \tau_\gamma(a) = v\}$$

and call it the **feasible direction set (of order n) in a** .

Assuming a point $a \in W_K^n(\sigma) \setminus W_K^{n-1}(\sigma)$, then we have $a \in V_{K_a^{n-1}}(\sigma_a^{n-1})$. By abuse of notation we also call $T_{K_a^{n-1}}(\sigma_a^{n-1}, a)$ **feasible direction set (of order n) in a** .

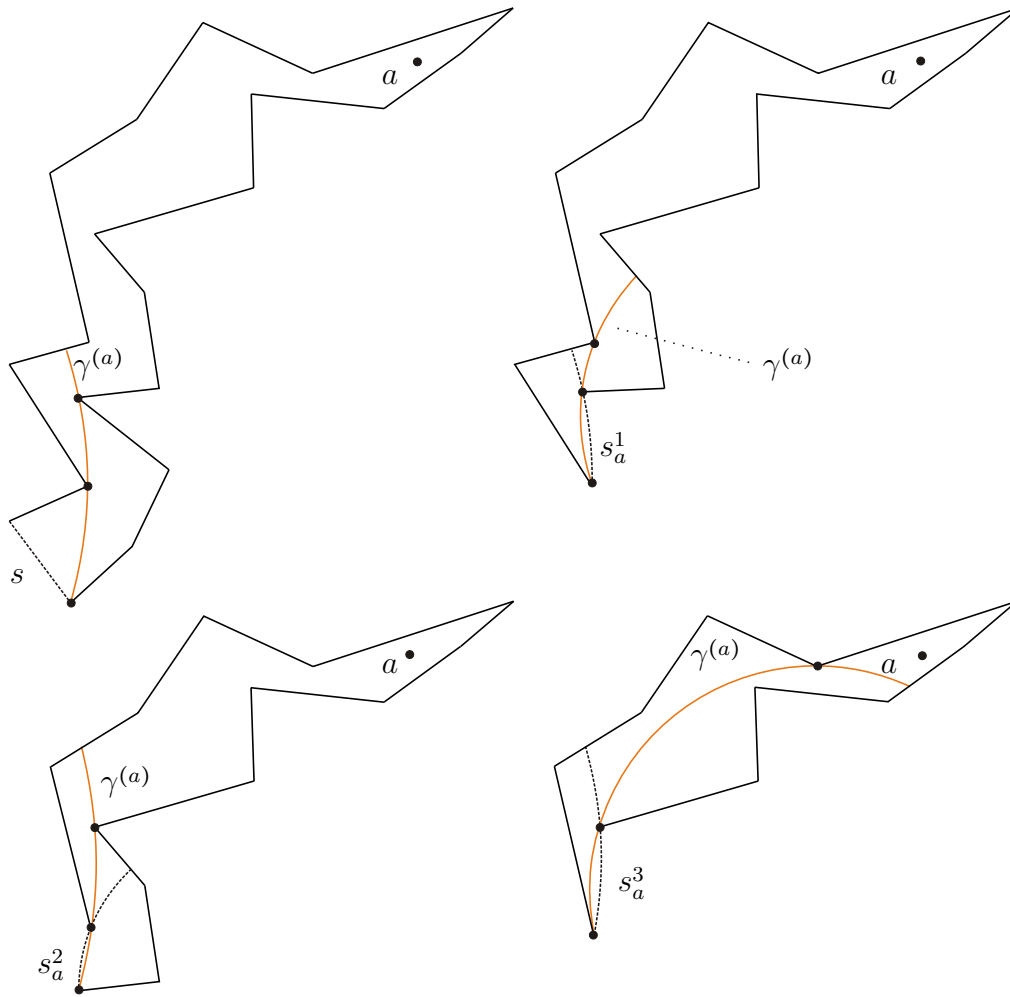


Figure 49: Illustration of the Definition 3.6.11.

Among other things, we particularly show that the definition of the feasible direction set of a point $a \in V_K^n(\sigma)$ or $a \in W_K^n(\sigma)$ yields no ambiguities. First and foremost we prove the equality of $W_K^n(\sigma)$ and $V_K^n(\sigma)$ for all $n \geq 1$.

3.6.13 Theorem.

$W_K^n(\sigma) = V_K^n(\sigma)$ and the corresponding feasible direction sets are equal for all $n \geq 1$.

Proof. We prove the claim by induction. The case $n = 1$ is trivial. First let us show the inclusion $W_K^n(\sigma) \subset V_K^n(\sigma)$. For the induction step $n \rightarrow n + 1$ let $a \in W_K^{n+1}(\sigma)$ and $v \in \mathbb{S}^1$ an arbitrary feasible direction of a . W.l.o.g. we can assume $a \notin W_K^n(\sigma)$. Obviously, we get $a \in V_{K_a^n}(\sigma_a^n)$ and $a \notin \text{tr}(s_a^n)$. Hence $\mathfrak{S}_{K_a^n}(\sigma_a^n, a, v)$ is not empty; consequently, a is

contained in $V_{K_a^{n-1}}^2(\sigma_a^{n-1})$ (cf. Theorem 3.6.9). Therefore, there exists a biarc

$$\tilde{\gamma}_n \tilde{\gamma}_{n+1} \in \overline{\mathfrak{S}_{K_a^{n-1}}^2}(\sigma_a^{n-1}, a, v)$$

with breakpoint $x_n \in V_{K_a^{n-1}}(\sigma_a^{n-1}) \subset W_K^n(\sigma)$. But then the induction hypothesis yields the existence of a generalized visibility spline $\gamma_1 \cdots \gamma_{n+1} \in \overline{\mathfrak{S}_K^n}(\sigma)$ for an arc γ_n with $C(\gamma_{n+1}) = C(\tilde{\gamma}_{n+1})$, i.e. $a \in V_K^{n+1}(\sigma)$ and $\tau_{\gamma_{n+1}}(a) = v$.

In order to show the other implication, let us assume a point $a \in V_K^{n+1}(\sigma)$ and an arbitrary feasible direction $v \in \mathbb{S}^1$ for the induction step $n \rightarrow n+1$. If a is contained in $V_K^n(\sigma)$, the induction hypothesis yields the desired, and we can suppose $a \in V_K^{n+1}(\sigma) \setminus V_K^n(\sigma)$. By definition, there exists a generalized visibility spline $\gamma := \gamma_1 \cdots \gamma_m \in \overline{\mathfrak{S}_K^{n+1}}(\sigma, a, v)$ with $m + \text{card}(V(\gamma)) = n+1$. Denoting the breakpoint of $\gamma_{m-1}\gamma_m$ by x , we surely have $x \in V_K^n(\sigma)$ because otherwise $\gamma_1 \cdots \gamma_{m-1}$ would be a generalized visibility spline of a point x contained in the deficiency set $\overline{I_K} \setminus V_K^n(\sigma)$, and the equality $n = m-1 + \text{card}(V(\gamma_1 \cdots \gamma_{m-1}))$ would yield a contradiction. Now we have to distinguish between two cases:

First Case: $x \in V_K^{n-1}(\sigma)$.

Then we get $\text{tr}(\gamma_m) \cap \text{tr}(s_a^{n-1}) \neq \emptyset$ since by induction hypothesis we have $V_{K_a^{n-1}}^2(\sigma_a^{n-1}) = W_{K_a^{n-1}}^2(\sigma_a^{n-1})$. But then there exists a generalized arc spline $\tilde{\gamma}_m \in \overline{\mathfrak{S}_{K_a^{n-1}}^2}(\sigma_a^{n-1}, a)$ with $C(\tilde{\gamma}_m) = C(\gamma_m)$ consisting of only one segment.

Second Case: $x \in V_K^n(\sigma) \setminus V_K^{n-1}(\sigma)$.

In this case x is a smooth breakpoint and by induction hypothesis we can choose $\gamma_1, \dots, \gamma_{m-1}$ s.t. for some $\tilde{\gamma}_{m-1} \in \mathfrak{S}$ with $\text{tr}(\tilde{\gamma}_{m-1}) \subset \overline{I_K}$ and $C(\tilde{\gamma}_{m-1}) = C(\gamma_{m-1})$ we get $\tilde{\gamma}_{m-1} \in \mathfrak{S}_{K_a^{n-1}}(\sigma_a^{n-1})$ and $\gamma_1 \cdots \gamma_{m-1} \tilde{\gamma}_m \in \mathfrak{S}_K^{n+1}(\sigma, a)$.

In both cases we get $a \in V_{K_a^{n-1}}^2(\sigma_a^{n-1})$. But then the Connection-Theorem II (3.6.9) yields $a \in V_{K_a^n}(\sigma_a^n) \subset W_K^{n+1}(\sigma)$. By construction, we additionally have $v \in T_K(\sigma_a^n, a)$. \square

As we are especially interested in examining the difference sets $V_K^n(\sigma) \setminus V_K^{n-1}(\sigma)$ or rather their closures, the following abbreviations are useful:

3.6.14 Definition. For $n \geq 1$ we set $D_K^n(\sigma) := \overline{V_K^n(\sigma) \setminus V_K^{n-1}(\sigma)}$, and $D_K^0(\sigma) := \text{tr}(s)$.

An illustration can be found in Figure 50. Note that the sets $D_K^i(\sigma)$ are not pairwise disjoint. In particular, we have

$$D_K^i(\sigma) \cap D_K^{i+1}(\sigma) = \bigcup_{a \in \overline{I_K} \setminus V_K^i(\sigma)} \text{tr}(s_a^{i+1})$$

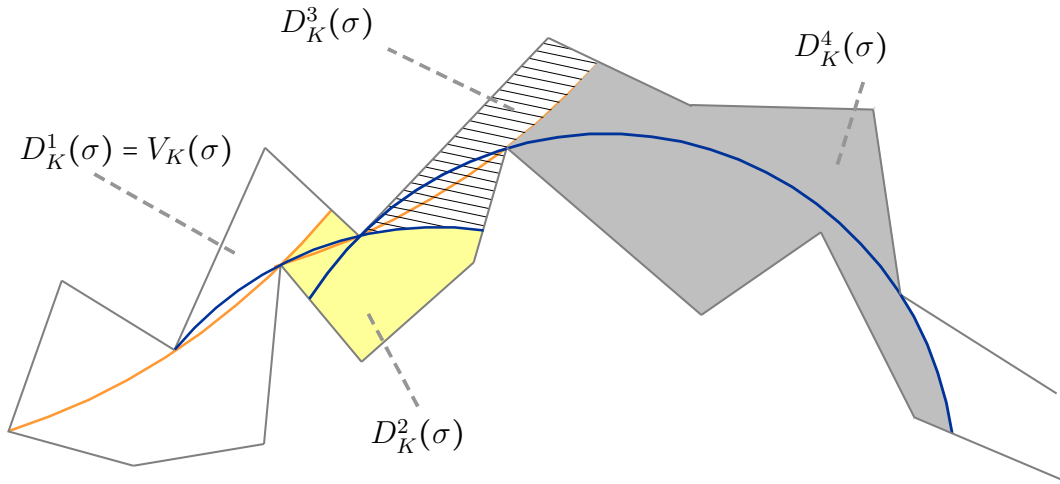


Figure 50: Illustration of Definition 3.6.14.

but $D_K^i(\sigma) \cap D_K^j(\sigma) = \emptyset$ if $|i - j| > 1$. Since $W_K^n(\sigma) = V_K^n(\sigma)$ for all $n \geq 1$, we can easily deduce:

3.6.15 Remark. For all $n \geq 1$, $a \in \overline{I_K} \setminus V_K^n(\sigma)$ and $i \leq n$ we get the following set inclusions almost directly by Theorem 3.6.13:

- 1) $V_{K_a^{i-1}}^a(\sigma_a^{i-1}) \cap V_{K_a^i}^a(\sigma_a^i) \subset \text{tr}(s_a^i)$,
- 2) $V_{K_a^{i-1}}^a(\sigma_a^{i-1}) \subset D_K^i(\sigma)$.

For our constructive method we need the existence of generalized visibility arcs having their i -th breakpoint in $D_K^i(\sigma)$, and therefore we are interested in those having a somewhat unified distribution of their breakpoints:

3.6.16 Corollary (Distribution of breakpoints). *Let $n \geq 2$ and $a \in V_K^n(\sigma) \setminus V_K^{n-2}(\sigma)$.*

Then there exists a generalized visibility spline $\gamma_1 \cdots \gamma_n \in \overline{\mathfrak{S}}_K^n(\sigma, a)$ with breakpoints $x_1 \leq \cdots \leq x_{n-1}$ s.t. $x_i \in D_K^i(\sigma)$ for all $i = 1, \dots, n - 1$.

Proof. From Theorem 3.6.13 we can deduce the existence of a generalized visibility spline $\gamma_1 \cdots \gamma_n$ with breakpoints $x_i \in V_{K_a^{i-1}}^a(\sigma_a^{i-1})$, $i = 1, \dots, n - 1$. Then Remark 3.6.15 concludes the proof. \square

3.6.17 Remark. Attention: Not all $\gamma_1 \cdots \gamma_n \in \mathfrak{S}_K^n(\sigma, a)$ for some $a \in V_K^n(\sigma) \setminus V_K^{n-1}(\sigma)$ with $n \geq 2$ satisfy the uniform distribution of breakpoints as in Lemma 3.6.16.

A counterexample is illustrated in Figure 51. However, it is easy to see that, if $\mathfrak{S}_K^n(\sigma)$ and $\overline{\mathfrak{S}}_K^n(\sigma)$ are not equal, there is a generalized visibility spline having a non-smooth breakpoint that is a left or right restriction point of a corresponding segment.

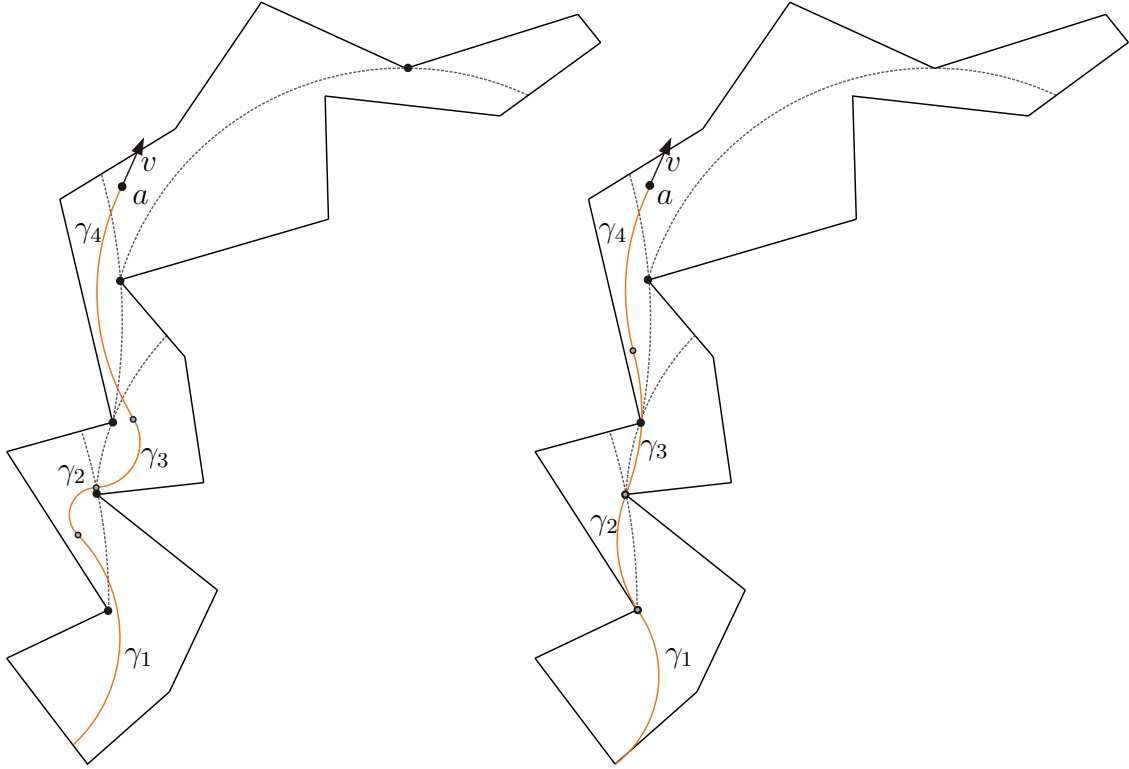


Figure 51: Uniform distribution of the breakpoints. On the left a visibility spline $\gamma_1 \dots \gamma_4$ of a point $a \in V_K^4(\sigma) \setminus V_K^3(\sigma)$, whose breakpoints are not uniformly distributed, is depicted whereas the visibility spline on the right satisfies the propositions of Corollary 3.6.16.

For the remaining part of this chapter we will always use a representation $\gamma = \gamma_1 \dots \gamma_m$ satisfying the unified distribution of the breakpoints in minimal representation whenever we consider a generalized visibility spline $\gamma \in \overline{\mathfrak{S}}_K^n(\sigma)$.

We can define *alternating numbers* for arcs splines with more than one segment and even for generalized visibility splines $\gamma \in \overline{\mathfrak{S}}_K^n(\sigma)$:

3.6.18 Definition. Let $\gamma = \gamma_1 \dots \gamma_m \in \overline{\mathfrak{S}}_K^n(\sigma)$ be a generalized visibility spline. We set $N_m := 0$ and for all $i = 1, \dots, m-1$ we define N_i to be 1 if the i -th breakpoint a_i with $\{a_i\} := \text{tr}(\gamma_i) \cap \text{tr}(\gamma_{i+1})$ is a left or right restriction point of γ_{i+1} . Otherwise, N_i shall vanish. Then we define the **alternating number of γ** as follows:

$$\mathcal{A}(\gamma) = \sum_{i=1}^m (\mathcal{A}(\gamma_i) + N_i),$$

where $\mathcal{A}(\gamma_i)$ is understood with respect to the tolerance channels \mathfrak{E}_a^i .

An example is illustrated in Figure 52.

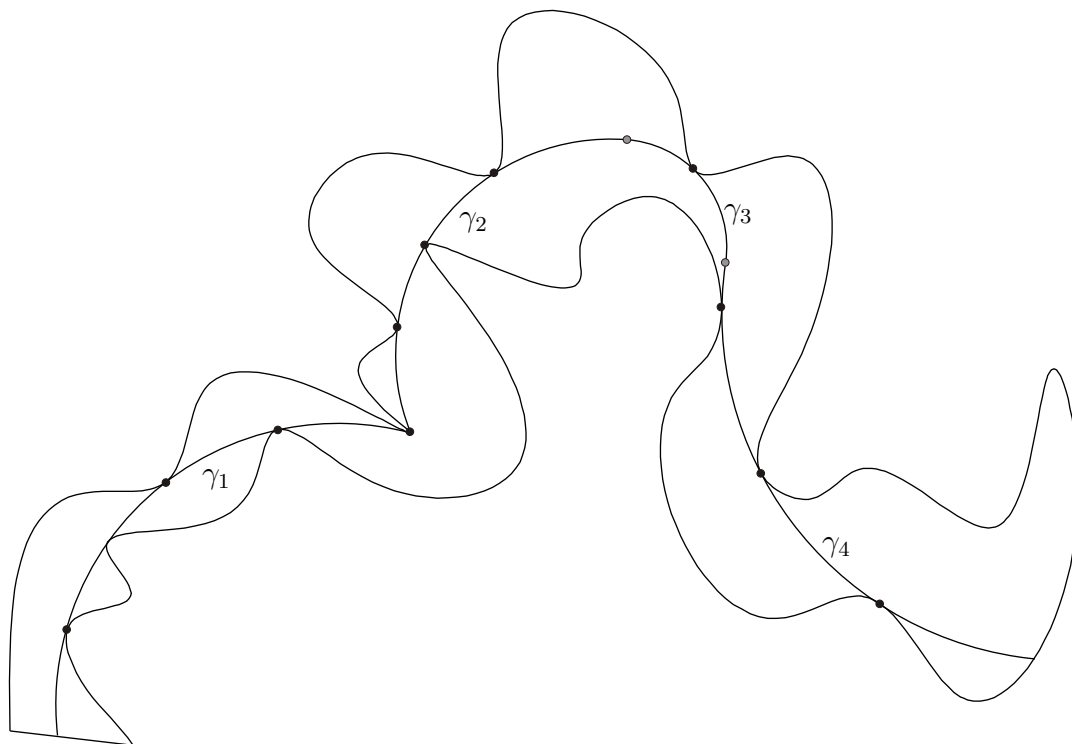


Figure 52: Alternating number of a generalized visibility spline $\gamma := \gamma_1 \cdots \gamma_4$. Since the first breakpoint is a left restriction point of γ_1 and γ_2 , we have $\mathcal{A}(\gamma) = \sum_{i=1}^4 \mathcal{A}(\gamma_i) + 1 = (3 + 3 + 1 + 3) + 1 = 11$.

3.6.19 Remark. The alternating number defined above is well-defined (cf. Theorem 3.6.13) and does not lead to any ambiguities regarding Definition 3.2.16. We can always choose a generalized visibility spline $\gamma \in \mathfrak{S}^n(\sigma, a)$ with $|\gamma| + \text{card}(V(\gamma)) = n$ if $a \in D_K^n(\sigma)$. Since non-smooth breakpoints of generalized visibility splines in uniform and minimal representation only appear as left or right restrictions, we count an additional alternation point: Supposing, for instance, an element $\gamma_1 \gamma_2 \in \overline{\mathfrak{S}_K^3}(\sigma)$ with a non-smooth breakpoint, then we get $\mathcal{A}(\gamma_1 \gamma_2) = 1 + \mathcal{A}(\gamma_1) + \mathcal{A}(\gamma_2)$ (cf. Figure 53). Since the segment number $|\gamma|$ and the number of vertices $V(\gamma)$ are unique, this yields no ambiguities.

The following theorem enables a constructive approach for examining the visibility set $V_K^n(\sigma)$ for every $n \geq 1$, which will be an essential factor for the algorithmic design. Every point $a \in V_K^n(\sigma) \setminus V_K^{n-1}(\sigma)$ can be reached by a generalized visibility spline which supplies a certain number of alternating restrictions s.t. the particular segments are uniquely determined by three conditions.

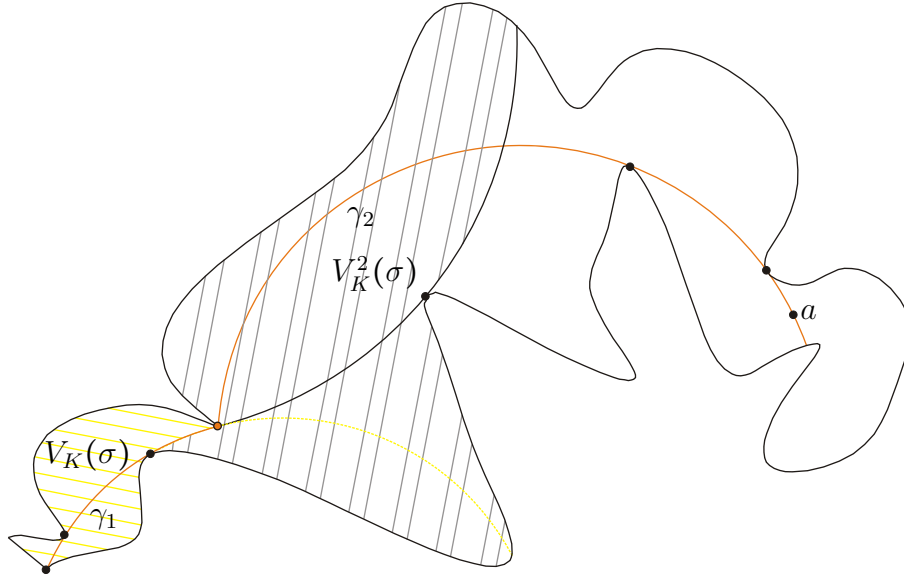


Figure 53: Accumulation of breakpoints and alternating numbers. $\gamma_1\gamma_2 \in \overline{\mathfrak{S}_K^3(\sigma)}$ with a non-smooth breakpoint. $\mathcal{A}(\gamma_1\gamma_2) = 1 + \mathcal{A}(\gamma_1) + \mathcal{A}(\gamma_2) = 1 + 3 + 3 = 7 = 2 \cdot 3 + 1$. Note: $\mathfrak{S}_K^3(\sigma, a) = \emptyset$. Hence we have $V_K^3(\sigma) \neq \{a \in \overline{I_K} \mid \mathfrak{S}_K^3(\sigma, a) \neq \emptyset\}$.

3.6.20 Theorem.

Let (K, s, σ) be a tolerance channel. For every $a \in D_K^n(\sigma)$ and feasible direction $v \in \mathbb{S}^1$ there is a generalized visibility spline $\gamma := \gamma_1 \cdots \gamma_l \in \overline{\mathfrak{S}_K^n(\sigma, a, v)}$ s.t. $\gamma_1 \cdots \gamma_{l-1} \in \overline{\mathfrak{S}_K^{n-1}(\sigma)}$

- 1) is a blocking spline and $\mathcal{A}(\gamma_l) \geq m$ or
 - 2) has an extremal exiting direction and $\mathcal{A}(\gamma_l) \geq m + 1$ or
 - 3) has an endpoint a_{l-1} that is a left or right restriction point of γ_l and $\mathcal{A}(\gamma_l) \geq m + 1$,
- where $|\gamma| = l$ and

$$m = \begin{cases} 3, & a \in \partial V_K^n(\sigma) \setminus K \\ 2, & a \in V_K^n(\sigma), v \in \partial T_K^n(\sigma, a) \\ 1, & \text{otherwise.} \end{cases}$$

Consequence: We can choose γ satisfying $\mathcal{A}(\gamma) \geq 2(n-1) + m$.

Proof. Since $V_K^n(\sigma) = W_K^n(\sigma)$, we have $V_K^n(\sigma) \setminus V_K^{n-1}(\sigma) = W_K^n(\sigma) \setminus W_K^{n-1}(\sigma)$. Hence $a \in V_{K_a^{n-1}}(\sigma_a^{n-1})$ and therefore we can choose γ_l with $\mathcal{A}(\gamma_l) \geq m$.

Again, we can argue by induction. In the case $n = 1$, clearly there exists a visibility arc $\gamma_1 \in \mathfrak{S}_K(\sigma, a, v)$ with

$$\mathcal{A}(\gamma_1) \geq m = 2 \cdot (1 - 1) + m.$$

Using the induction hypothesis and the Connection-Theorem 3.6.8, we can choose oriented arcs $\gamma_1, \dots, \gamma_l$ s.t.

$$\mathcal{A}(\gamma_1 \cdots \gamma_l) \geq \mathcal{A}(\gamma_1 \cdots \gamma_{l-1}) + m \geq 2(n-2) + 2 + m = 2n - 4 + 2 + m = 2(n-1) + m,$$

thus concluding the proof. \square

3.6.21 Corollary. *For every $a \in \partial V_K^n(\sigma)$ with $\mathfrak{S}_K^n(\sigma, a) \neq \emptyset$ there exists a visibility spline $\gamma_1 \cdots \gamma_n \in \mathfrak{S}_K^n(\sigma, a)$ with $\mathcal{A}(\tilde{\gamma}_i) \geq 2$ for all $i = 1, \dots, n$ and $\mathcal{A}(\tilde{\gamma}_{i_0}) \geq 3$ for some $i_0 \in \{1, \dots, n\}$, where $\tilde{\gamma}_i$ are generalized arcs with $C(\tilde{\gamma}_i) = C(\gamma_i)$.*

Proof. See Theorem 3.6.20. \square

3.6.22 Corollary.

Let (K, s, σ, d) be a start-destination channel and let $n \in \mathbb{N}$ be the minimal number s.t. $V_K^n(\sigma) \cap \text{tr}(d) \neq \emptyset$ for some $n \in \mathbb{N} \setminus \{0\}$. Then there exists a generalized visibility spline $\gamma \in \overline{\mathfrak{S}_K^n(\sigma, \text{tr}(d))}$ with $\mathcal{A}(\gamma) \geq 2n + 1$ or $(\mathcal{A}(\gamma) \geq 2n$ and $E(\gamma) \in \text{Ext}(d)$).

Proof. Follows immediately from Theorem 3.6.20 and Lemma 3.4.20. \square

3.7 (Smooth) Minimum Arc Paths

Let (K, s, σ) be an arbitrary tolerance channel and $n \geq 1$. We set

$$U_K^n(\sigma) := \{a \in \overline{I_K} \mid \mathfrak{S}_K^n(\sigma, a) \neq \emptyset\}.$$

As the closure bar over \mathfrak{S}_K^n is omitted in this definition, in general $U_K^n(\sigma)$ and $V_K^n(\sigma)$ are not equal, which we have already seen in Figure 53.

Furthermore, the direction sets $\{\tau_\gamma(a) \in \mathbb{S}^1 \mid \gamma \in \mathfrak{S}_K^n(\sigma, a)\}$ for points $a \in U_K^n(\sigma) \setminus U_K^{n-1}(\sigma)$ generally would not be compact.

However, recalling the problem formulated in 3.1.16, we are interested in a *smooth* minimum arc path. Thus, in particular, our solution spline should be smooth at the breakpoints. Considering a point $a \in D_K^n(\sigma)$, there exists a minimal possible number $m \in \mathbb{N}$ with $a \in U_K^{n+m}(\sigma)$.

3.7.1 Remark. Let us consider a point $a \in D_K^n(\sigma)$ and a feasible direction $v \in T_K^n(\sigma)$. Then there exists a generalized visibility spline $\gamma := \gamma_1 \cdots \gamma_l \in \overline{\mathfrak{S}_K^n}(\sigma, a, v)$ with breakpoints $x_1 \leq \cdots \leq x_{n-1}$ with $x_i = x_{i+1}$ if and only if x_i is not smooth and $x_i \in V_{K_a^{i-1}}(\sigma_a^{i-1}) \subset D_K^i(\sigma)$. Assuming $\gamma \notin \mathfrak{S}_K^n(\sigma, a, v)$, we are interested in the integer m defined above. Setting $x_0 := S(\gamma)$ and $x_n := E(\gamma)$, w.l.o.g. there is exactly one $i \in \{0, \dots, n-2\}$ with $x_i = x_{i+1}$. We now have to distinguish between two cases:

First Case: $\mathcal{A}(\gamma_{i+1}) \geq 3$.

We obviously get $m > 0$ and by Corollary 3.4.8 we have $x_{i+2} \in \partial V_K^{i+1}(\sigma)$. Thus, $m = 1$ since there exists a biarc $\tilde{\gamma}_1 \tilde{\gamma}_2 \in \mathfrak{S}^2$ s.t. $\gamma_1 \cdots \tilde{\gamma}_1 \tilde{\gamma}_2 \cdots \gamma_n \in \mathfrak{S}_K^{n+1}(\sigma, a, v)$, where γ_{i+1} has been replaced by $\tilde{\gamma}_1 \tilde{\gamma}_2$ (cf. [33, 65]). An illustration can be found in Figure 54.

Second Case: $\mathcal{A}(\gamma_{i+1}) < 3$.

This means γ_{i+1} is not extremal. Consequently, there exist a breakpoint $\tilde{x}_{i+1} \in C(\gamma_{i+1})$ and an arc $\tilde{\gamma}_{i+1} \in \mathfrak{S}_{K_a^i}(\sigma_a^i, \tilde{x}_{i+1}, \tau_{\gamma_{i+1}}(\tilde{x}_{i+1}))$. Hence $m = 0$. An example is illustrated in Figure 55.

We now introduce further useful notation for start-destination channels and corresponding smooth minimum arc paths.

3.7.2 Definition. Given a start-destination channel (K, s, σ, d) , the number

$$n(d) := \min_{\gamma \in \mathfrak{S}_K^\infty(\sigma, d)} |\gamma| \in \mathbb{N}$$

is the segment number of a smooth minimum arc path (cf. p. 57).

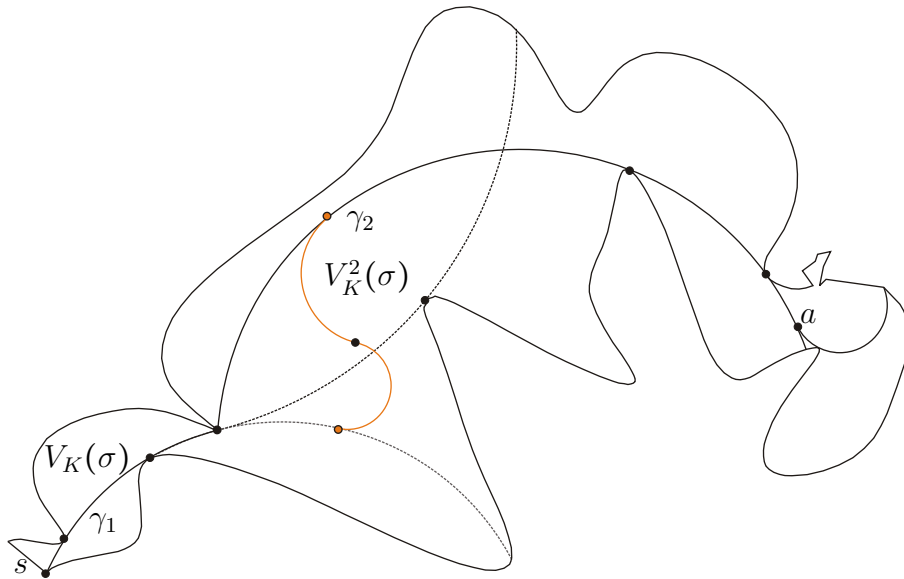


Figure 54: Smoothing generalized visibility splines. The generalized visibility spline $\gamma_1\gamma_2$ can be converted to a smooth visibility spline with four segments. Note that this conversion is not unique, as indicated by the orange biarcs.

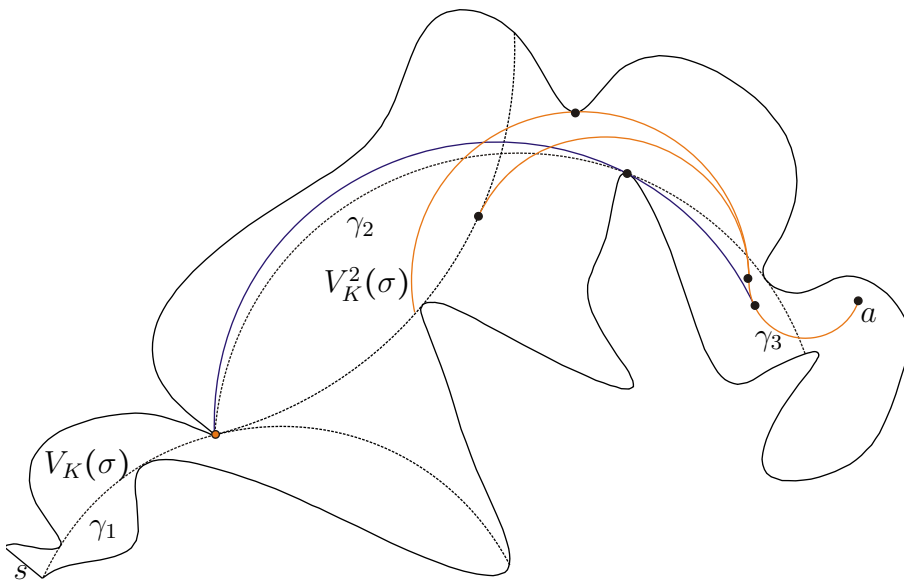


Figure 55: Smoothing generalized visibility splines. The generalized visibility spline $\gamma_1\gamma_2\gamma_3$ can be converted to a smooth visibility spline with four segments. As in Figure 54 this conversion is not unique.

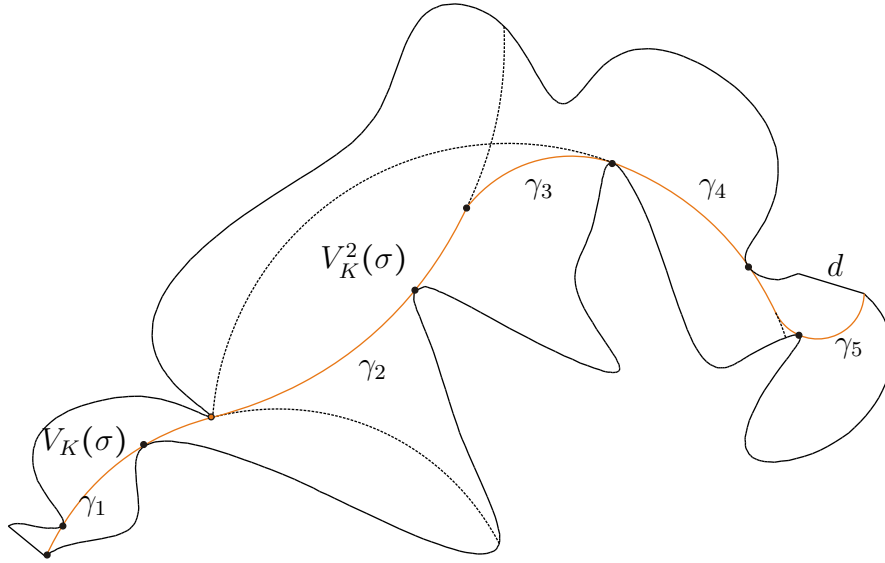


Figure 56: Smoothing minimum arc path $\gamma_1 \cdots \gamma_5$ with $n(d) = 5$ although $\text{tr}(d) \cap V_K^4(\sigma) \neq \emptyset$.

3.7.3 Definition. Let $\mathfrak{D} := (K, s, \sigma, d)$ be a start-destination channel, $a \in \text{tr}(d)$ and $n \in \mathbb{N}$ s.t. $V_K^n(\sigma) \cap \text{tr}(d)$ is empty. Setting $\mathfrak{E} := \mathfrak{E}_1 := (K, s, \sigma)$, for every $i = 2, \dots, n$ we define, $\mathfrak{E}_i := \mathfrak{E}_a^{i-1}$ regarding Definition 3.6.11.

Note that the definition does not depend on the choice of $a \in \text{tr}(d)$ but only on d itself. Let us now consider a start-destination channel (K, s, σ, d) and let us assume that $\text{tr}(d)$ is n -, but not $(n - 1)$ - circularly visible. Obviously, the inequality $n \leq n(d)$ is correct. Although in applications with numerical data this is practically always an equation, there are cases where this is a strict inequality (see Figure 56). By the strategy outlined in Remark 3.7.1, every $\gamma \in \overline{\mathfrak{S}}_K^n(\sigma, d)$ can be converted into a visibility spline $\tilde{\gamma} \in \mathfrak{S}_K^{n(d)}(\sigma, d)$. Note that this conversion is not unique, as depicted in Figure 56.

Recalling that a path which is composed of generalized arcs and not necessarily smooth at breakpoints is simply called **arc spline**, we can formulate a similar problem. But first we need some notation.

3.7.4 Definition. The set of all arc splines $\gamma \in \mathfrak{T}$ starting at $\text{tr}(s)$, ending in $\text{tr}(d)$ and staying in $\overline{I_K}$ is denoted by $\mathfrak{T}_K^\infty(s, d)$. Furthermore, we set

$$m(d) := \min \{ |\gamma| \in \mathbb{N} \mid \gamma \in \mathfrak{T}_K^\infty(s, d) \}.$$

An arc spline $\gamma \in \mathfrak{T}_K^\infty(s, d)$ with $|\gamma| = m(d)$ is called (**continuous**) **minimum arc path**.

Obviously, we have $m(d) \leq n(d)$.

3.7.5 Problem. *Let (K, s, σ, d) be a start-destination channel. Then we are seeking for a continuous minimum arc path, i.e. an arc spline $\gamma \in \mathfrak{T}_K^\infty(s, d)$ with $|\gamma| = m(d)$.*

To solve this problem, all we need to do is compute the windows of certain starting channels defined successively:

3.7.6 Definition. *Let $\mathfrak{D} := (K, s, \sigma, d)$ be a start-destination channel, and let $\text{tr}(d)$ not be circularly visible. Then we can define a new starting channel by window $\omega_{\mathfrak{D}}$ (cf. Definition 3.4.16) whose interior is the connected component of $I_K \setminus \text{tr}(\omega_{\mathfrak{D}})$ containing $\text{tr}(d)$. The corresponding restriction map is given by Definition 3.1.3 with respect to the starting arc $\omega_{\mathfrak{D}}$. We denote this channel by $\mathfrak{D}_2 := (K_2, \omega_{\mathfrak{D}}, \sigma_2, d)$. If $\text{tr}(d)$ is not circularly visible with respect to \mathfrak{D}_2 , the corresponding window $\omega_{\mathfrak{D}_2}$ is well-defined, and we can recursively define $\mathfrak{D}_{i+1} := (K_{i+1}, \omega_{\mathfrak{D}_i}, \sigma_{i+1}, d) := (\mathfrak{D}_i)_2$ as long as $\text{tr}(d)$ is not circularly visible.*

In order to show that an arc spline whose segments correspond to the windows $\omega_{\mathfrak{D}_i}$ leads to a continuous minimum arc path, we have to prove the following theorem:

3.7.7 Theorem. *Let $\mathfrak{D} := (K, s, \sigma, d)$ be a start-destination channel, and let m be the minimal number s.t. $\text{tr}(d)$ is circularly visible with respect to \mathfrak{D}_m . Then every continuous minimum arc path of \mathfrak{D} has exactly m segments, i.e. $m(d) = m$.*

Proof. By definition we have $m(d) \leq m$. Let us assume to the contrary that $m(d) < m$, and let $\gamma := \gamma_1 \cdots \gamma_{m(d)} \in \mathfrak{T}_K^\infty(s, d)$. Clearly, $\text{tr}(\gamma_1) \subset V_K(\sigma)$ and by the Cutting-Lemma 3.2.27 there is an index $i \geq 2$ s.t. γ_i cuts $\omega_{\mathfrak{D}}$. Then $\text{tr}(\gamma_i) \subset V_{K_2}(\sigma) \cup V_K(\sigma)$. Using this argument iteratively and the condition $\text{tr}(d) \cap V_{K_j}(\sigma) = \emptyset$ for all $1 \leq j < m$, this is a contradiction. Hence $m = m(d)$. \square

As a consequence we obtain that a continuous minimum arc path can be constructed iteratively and each segment can be constructed by three alternating restrictions, which is crucial for our algorithmic approach (cf. Chapter 4).

Figure 57 shows a smooth and continuous minimum arc path for the same start-destination channel.

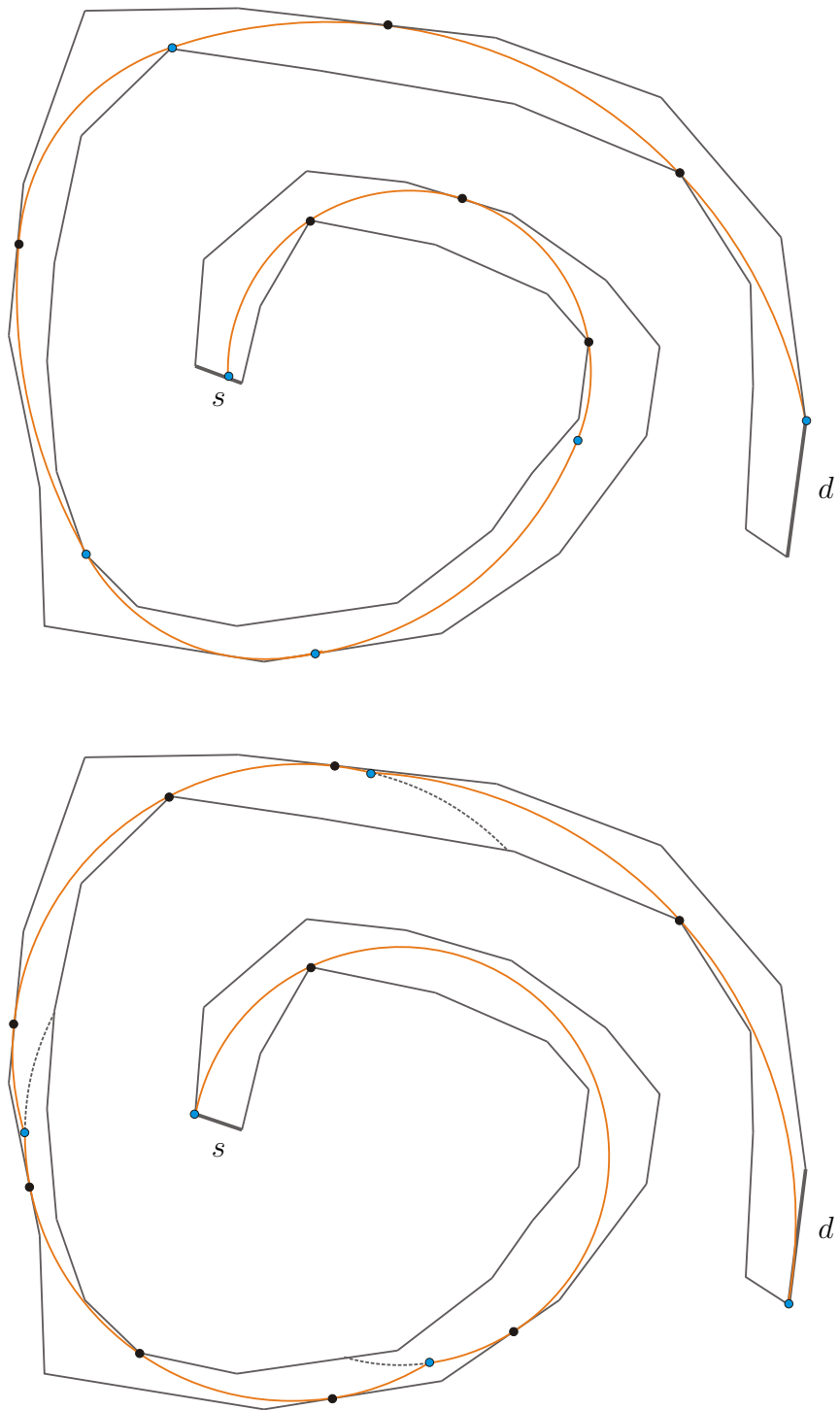


Figure 57: Comparison of a smooth (six segments) and a continuous minimum arc path (four segments). The blue circles depict the breakpoints and the black ones the alternating restrictions.

3.8 Summary and Outlook

In this section we give a summary and a short overview of our results, focusing on the four types of tolerance channels introduced: (Non-)degenerate starting / continuation channels.

Let (K, s, σ) be an arbitrary tolerance channel. We have characterized the visibility sets $V_K^n(\sigma)$, having used induction with the aid of alternating sequences and the continuity properties of the feasible direction sets. Therefore, we obtain the sets $V_K^n(\sigma)$ with $n > 1$ by computing one-circular visibility sets corresponding to tolerance channels which are defined consecutively.

Regardless of the type of (K, s, σ) , we can establish the following correspondences concerning the visibility set $V_K(\sigma)$:

- For fixed point $a \in V_K(\sigma)$ and direction $v \in T_K(\sigma, a)$ we can always choose a visibility arc $\gamma \in \mathfrak{S}_K(\sigma, a, v)$ with $\mathcal{A}(\gamma) \geq 1$ since there is one degree of freedom.
- For fixed $a \in V_K(\sigma)$ there exists a $\gamma \in \mathfrak{S}_K(\sigma, a)$ with $\mathcal{A}(\gamma) \geq 2$.
- Consequently, boundary points $\partial V_K(\sigma) \setminus K$ can be reached by a visibility arc γ with $\mathcal{A}(\gamma) \geq 3$.

Hence the degrees of freedom of visibility arcs are consistent with their alternating number.

As already indicated, the circular visibility was introduced taking the *linear visibility* into account:

3.8.1 Definition. *Let (K, s, σ) be a tolerance channel. Denoting the set of all oriented line segments by \mathfrak{L} , the set of all **visibility line segments** is defined as follows:*

$$\mathfrak{L}_K(\sigma) := \{\omega \in \mathfrak{L} \mid \text{tr}(\omega) \subset \overline{I_K}, S(\omega) \in \sigma(E(\omega), \tau_\omega(E(\omega)))\}.$$

*Likewise, $\mathfrak{L}(\sigma, a) := \{\omega \in \mathfrak{L}(\sigma) \mid E(\omega) = a\}$ and $\mathfrak{L}(\sigma, a, v) := \{\omega \in \mathfrak{L}(\sigma, a) \mid \tau_\omega(a) = v\}$ are defined. Then we obtain the **linear visibility set (with respect to (K, s, σ))**:*

$$L_K(\sigma) := \{a \in \overline{I_K} \mid \mathfrak{L}_K(\sigma, a) \neq \emptyset\}.$$

Oriented line segments are a special case of oriented arcs. Particularly, we have the set inclusion $\mathfrak{L}_K(\sigma) \subset \mathfrak{S}_K(\sigma)$. Hence alternating numbers are also well-defined for oriented line segments. Since lines have not degrees of freedom instead of three, we obtain:

- For fixed $a \in L_K(\sigma)$ and feasible exiting direction $v \in \mathbb{S}^1$ we can not guarantee the unique visibility line segment $\omega \in \mathfrak{L}_K(\sigma, a)$ supplying a non-zero alternating number.
- For fixed $a \in L_K(\sigma)$ there exists an $\omega \in \mathfrak{L}_K(\sigma, a)$ with $\mathcal{A}(\omega) \geq 1$.
- Consequently, boundary points $a \in \partial L_K(\sigma) \setminus K$ can be reached by a visibility line segment ω with $\mathcal{A}(\omega) \geq 2$.

For instance, these statements are shown in [39], but only in case of non-degenerate starting channels given by polygons or splinegons. A complete proof including the degenerate cases will not be covered here. Nevertheless, we are quite sure that the gentle reader is able to prove these statements using the techniques introduced in the previous sections.

If, additionally, a destination arc d is given s.t. $\mathfrak{D} := (K, s, \sigma, d)$ is a start-destination channel, we can define the *linear window* $\lambda_{\mathfrak{D}}$ based on Definition 3.4.16, which can be characterized analogously:

3.8.2 Proposition. *The visibility line ω which corresponds to $\lambda_{\mathfrak{D}}$ possesses an alternating sequence (a_1, a_2) with*

- i) $a_1, E(\omega) \in K_l$ and $a_2 \in K_r$ or
- ii) $a_1, E(\omega) \in K_r$ and $a_2 \in K_l$.

Addendum: ω is uniquely determined by the conditions above.

Proof. Analogous to Theorem 3.4.19 or cf. [54]. □

Iteratively computing the windows of successive starting channels always defined by the predecessor window till $\text{tr}(d)$ is linearly visible, we obtain a so called *minimum link path*:

3.8.3 Definition. *Let us denote the set of all polygonal curves staying inside $\overline{I_K}$, starting at $\text{tr}(s)$ and ending in $\text{tr}(d)$ by $\mathfrak{L}_K^\infty(s, d)$. A *minimum link path (with respect to (K, s, σ, d))* is a polygonal curve $\omega_0 \in \mathfrak{L}_K^\infty(s, d)$ with $|\omega_0| = \min \{|\omega| \in \mathbb{N} \mid \omega \in \mathfrak{L}_K^\infty(s, d)\}$.*

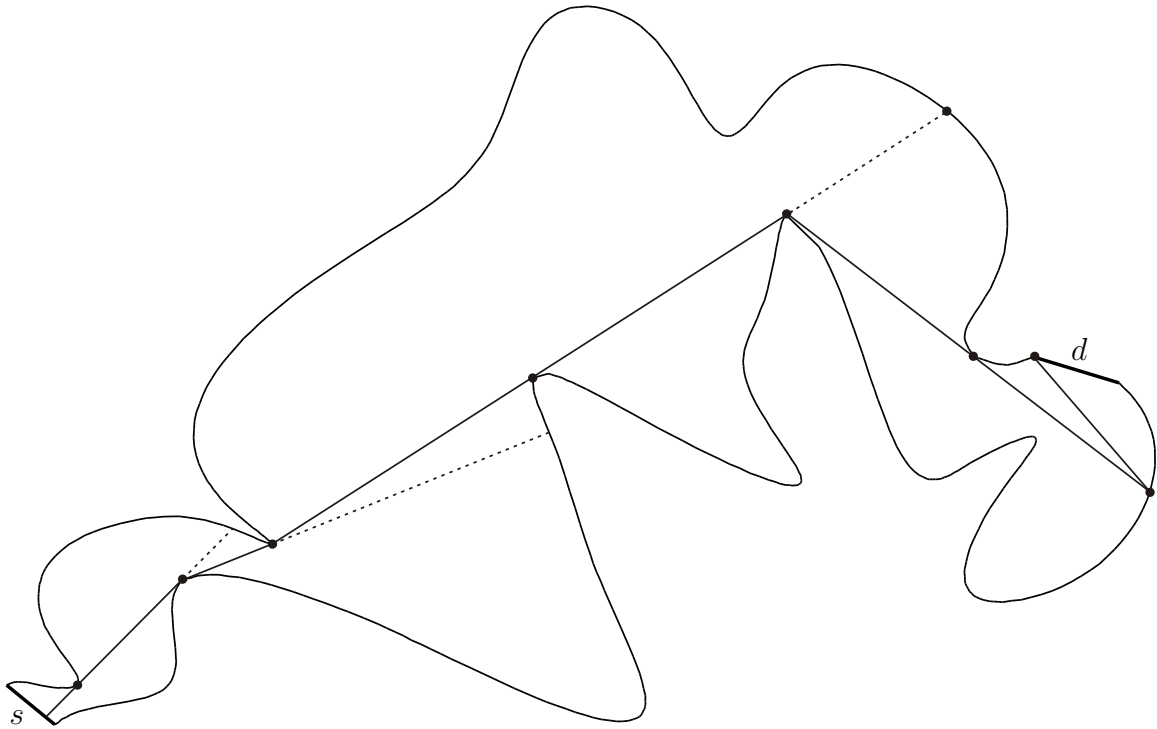


Figure 58: Minimum link path with five segments.

We are especially interested in the circularly visible points that are not linearly visible. Therefore, we introduce the following term according to [23, 22]:

3.8.4 Definition. *The connected components of the deficiency set $P_K(\sigma) := \overline{I_K} \setminus L_K(\sigma)$ are called **pockets**, and the line segments $\overline{P} \cap L_K(\sigma)$ of the pockets P are said to be **lids**. (cf. Figure 59).*

Their examination will play an important role in the algorithmic part.

The remaining part of this section is devoted to a short outlook on the so-called **cyclic case**. Frequently, a (smooth) minimum arc path is not exclusively desired within a tolerance channel but within a slightly modified version called *cyclic tolerance channel*. They appear in some applications (cf. Section 5.2), and can be defined as follows:

3.8.5 Definition. *Let ω_1 and ω_2 be two Jordan curves that are piecewise \mathcal{R}^ω and CCW oriented. Denoting the interior of ω_i by $I(\omega_i)$, we suppose $\text{tr}(\omega_2) \subset I(\omega_1)$. Let us set $K := \text{tr}(\omega_1) \cup \text{tr}(\omega_2)$ and $I_K := I(\omega_1) \setminus I(\omega_2)$. Then we call K a **cyclic tolerance channel** and use the notation $K_l := \text{tr}(\omega_1)$ and $K_r := \text{tr}(\omega_2)$.*

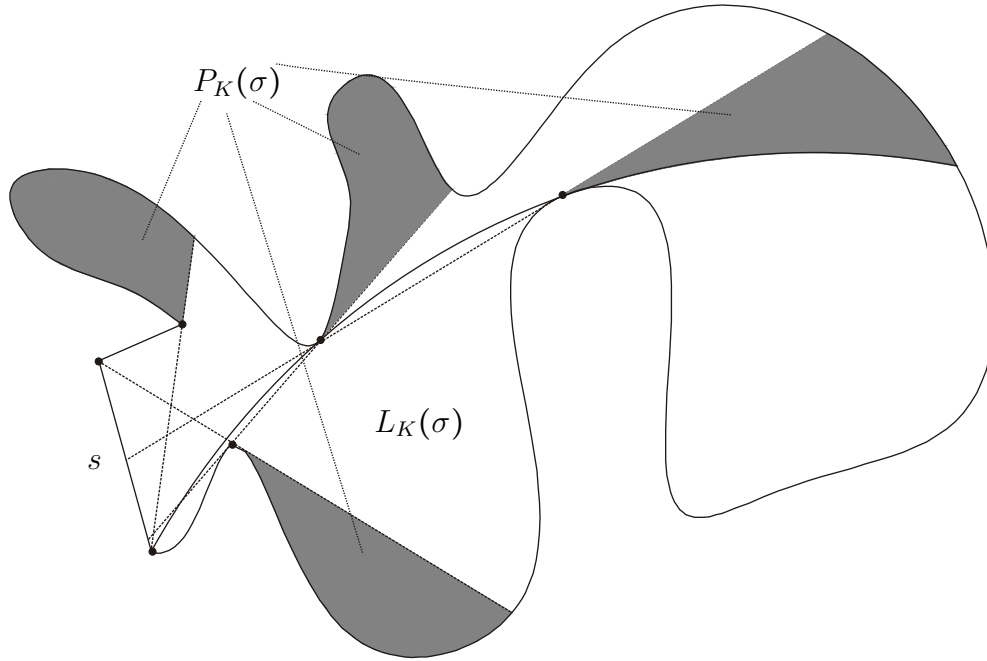


Figure 59: Illustration of Definition 3.8.4.

3.8.6 Definition. Let us denote the set of all arc splines which are Jordan curves, stay in $\overline{I_K}$ and whose winding number with respect to all points $a \in I_{K_2}$ doesn't vanish by \mathfrak{T}_K^{cycl} . Furthermore, we define the subset \mathfrak{S}_K^{cycl} of all **cyclic visibility splines** which are additionally smooth at their breakpoints.

Then we can define a (smooth) cyclic minimum arc path of a cyclic tolerance channel:

3.8.7 Definition. Let K be a cyclic tolerance channel. An arc spline $\gamma_0 \in \mathfrak{T}_K^{cycl}$ is called a **continuous cyclic minimum arc path** if

$$|\gamma_0| = \min \{ |\gamma| \in \mathbb{N} \mid \gamma \in \mathfrak{T}_K^{cycl} \}.$$

Likewise, a smooth arc spline $\gamma_0 \in \mathfrak{S}_{K,cycl}^\infty$ with

$$|\gamma_0| = \min \{ |\gamma| \in \mathbb{N} \mid \gamma \in \mathfrak{S}_K^{cycl} \}$$

is said to be a **smooth cyclic minimum arc path**.

Examples are illustrated in Figure 60.

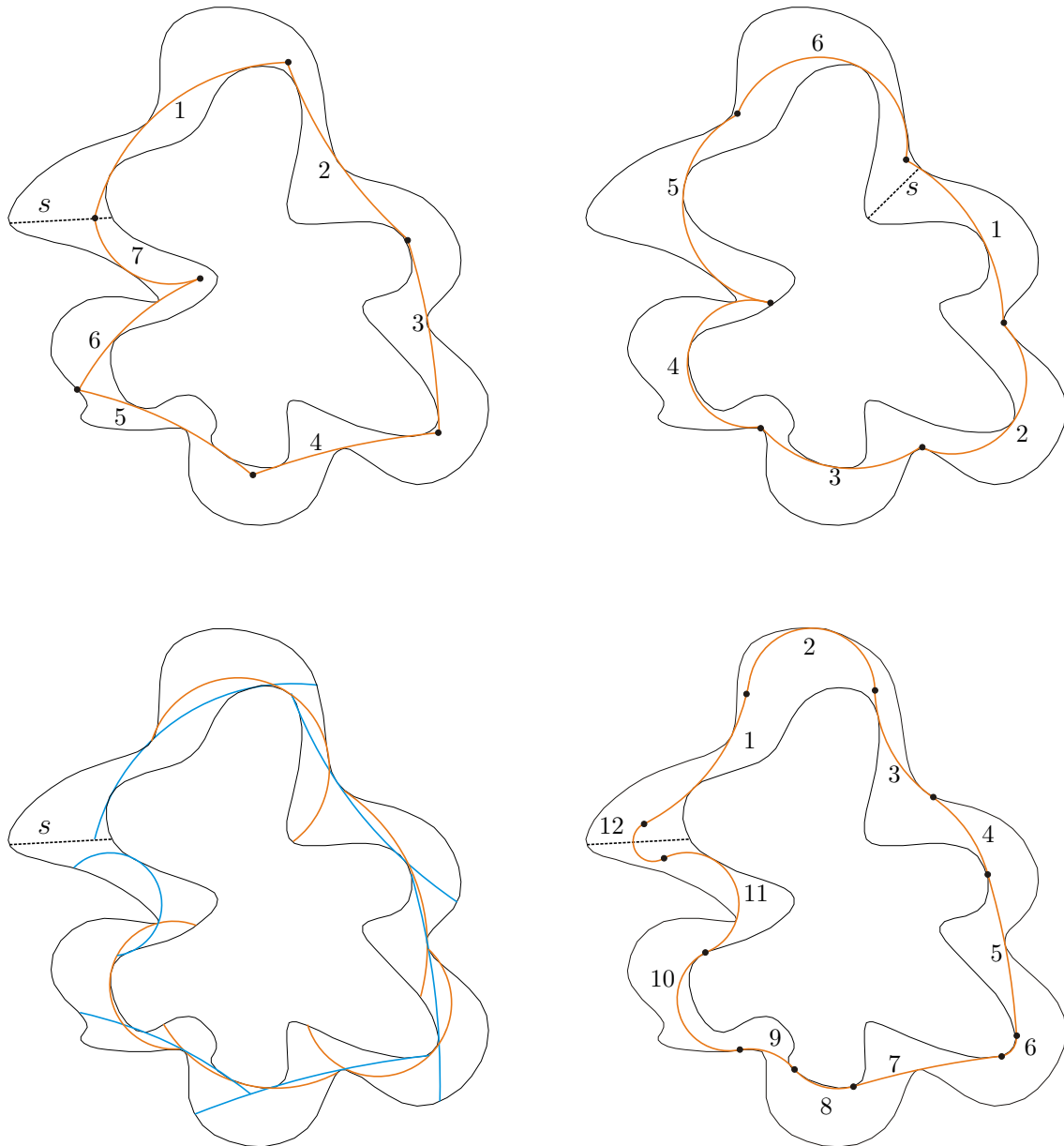


Figure 60: Cyclic smooth/continuous minimum arc path. Top: Continuous case; left: Seven segments; right: Minimum number of six segments; bottom: Smooth case; left: Blocking arcs (alternately blue and orange); right: Smooth cyclic arc splines with a not necessarily minimum number (twelve segments).

Let K be a cyclic tolerance channel and s an oriented arc with $K_l \cap \text{tr}(s) = \{S(s)\}$ and $K_r \cap \text{tr}(s) = \{E(s)\}$. Although $I_K \setminus \text{tr}(s)$ is simply connected, $K \cup \text{tr}(s)$ doesn't yield a tolerance channel since $K \cup \text{tr}(s)$ is not representable as a Jordan curve.

However, supposing the non-trivial case that every loop whose trace is a circle is contractible, we obtain: For sufficiently small $\varepsilon > 0$ we have $V_K(s) \cap M_\varepsilon = \emptyset$, where

$$M_\varepsilon := \{a \in I_K \cap \mathcal{R}_s \mid 0 < \text{dist}(a, \text{tr}(s)) \leq \varepsilon\}$$

and $V_K(s)$ denotes the set of all $a \in \overline{I_K}$ s.t. there exists a $\gamma \in \mathfrak{S}$ ending in a with $S(\gamma) \in \text{tr}(s)$, $\text{tr}(\gamma) \subset \overline{I_K}$ and $\det(\tau_\gamma(S(\gamma)), \tau_s(S(\gamma))) > 0$.

Thus, we can assume a start-destination channel $(\tilde{K}, s, \sigma, d)$ which is in fact induced by $\overline{I_K} \setminus M_\varepsilon$ and the requirements given above, which control the feasible starting directions of the valid visibility arcs. Then $V_K(s)$ is the circular visibility set of (\tilde{K}, s, σ) , i.e. $V_K(s) = V_{\tilde{K}}(\sigma)$. Let γ_1 be the blocking arc that is associated to the corresponding window. We can now define the second tolerance channel that appears when computing a cyclic minimum arc path. The starting segment and the restriction map are set due to Definition 3.6.5 or 3.7.6 respectively. How to choose the corresponding bounding curve ω_K , is indicated in Figure 61. In fact, we choose a subset of $\text{tr}(\tilde{\gamma}_1)$ as destination segment, where $\tilde{\gamma}_1$ is the maximal extension with respect to inclusion in $\overline{I_K}$.

The subsequent steps (if needed) work exactly in the same way as in the non-cyclic case: We repeat the procedure while $\text{tr}(\tilde{\gamma}_1)$ is not circularly visible.

Thus, we can guarantee the minimal possible number of segments needed for a continuous cyclic minimum arc path up to one segment. Whether we really achieve the minimal number or not depends on the choice of $\text{tr}(s)$ (cf. Figure 60 top).

In case of searching for a smooth cyclic minimum arc path, additionally the last and the first segment have to be joined smoothly. Hence we can only guarantee the minimal possible number of segments up to two segments.

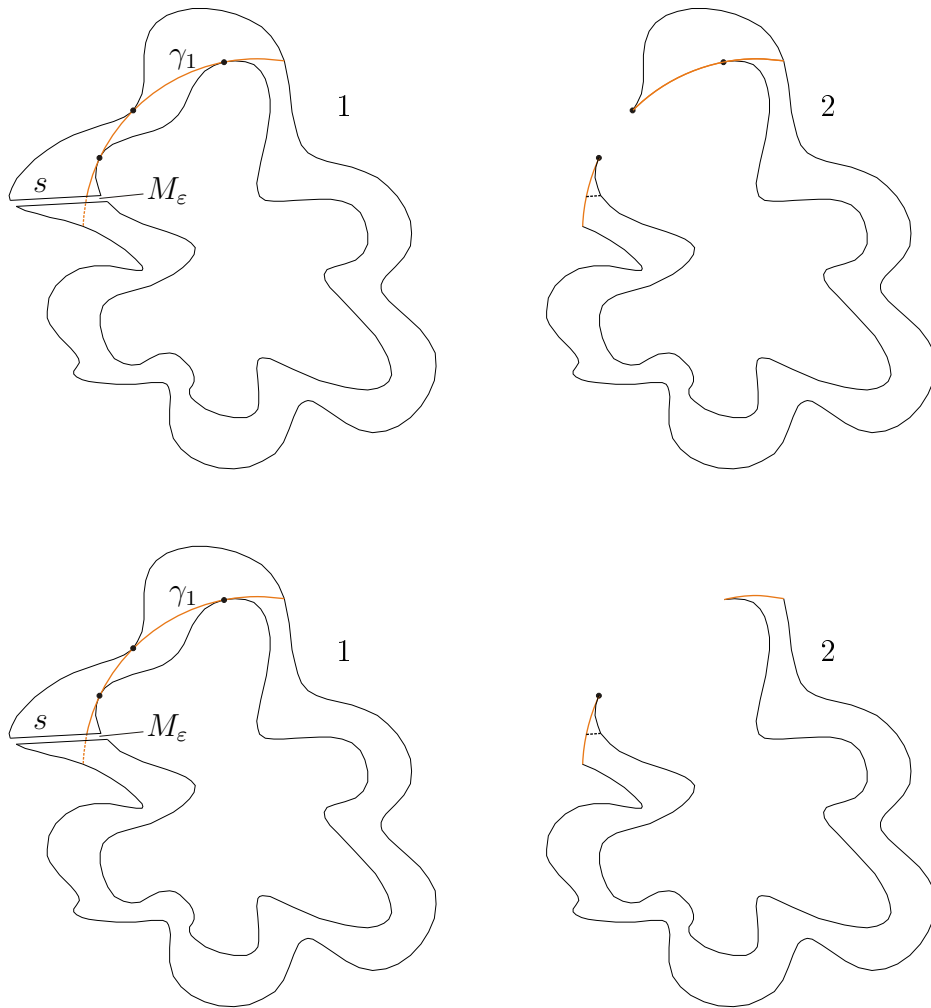
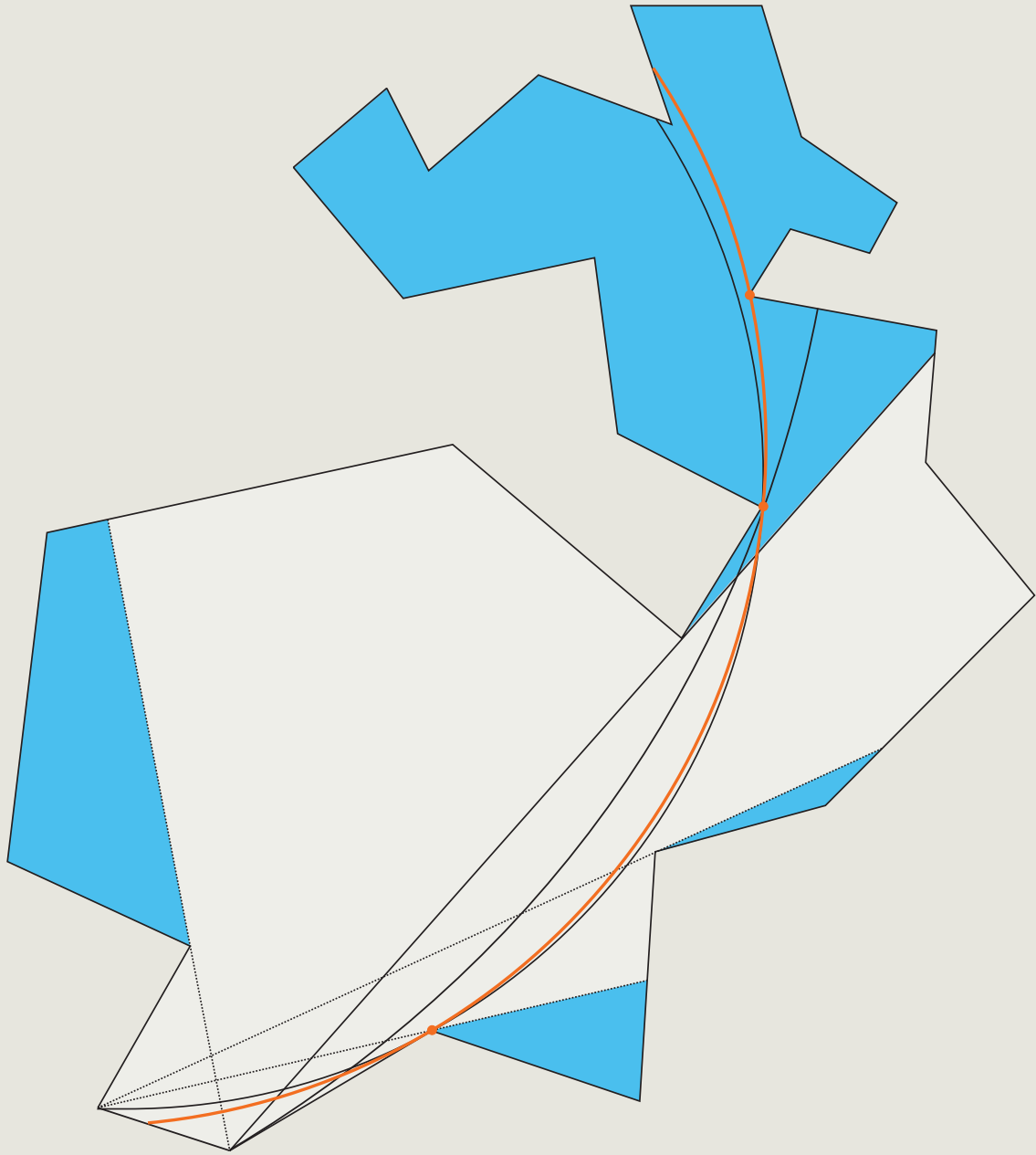


Figure 61: First and second tolerance channels given by a cyclic tolerance channel. Top: Smooth case; bottom: Continuous case.



4

THE ALGORITHMIC APPROACH

In this chapter we are dealing with an algorithmic realization of computing circular visibility sets and (smooth) minimum arc paths of an arbitrary tolerance channel. The theoretical results of Chapter 3 are used for the design of efficient algorithms.

The characterization of blocking arcs by alternating sequences is essential for a constructive approach. Due to the results of Chapter 3, we are able to develop greedy algorithms in order to compute the circular visibility sets $V_K^n(\sigma)$ and a (smooth) minimum arc path. The computation of a smooth minimum arc path requires two main steps: The ‘forward’ step constructs the windows of certain tolerance channels and the last segment of our solution. In contrast, the ‘backward’ step establishes the remaining segments. If the calculated solution is a generalized visibility spline but not a smooth arc spline, we convert it into a smooth arc spline by adding additional segments without losing the minimal possible number of segments.

In the first section of this chapter, we give a macrostructure of our proposed algorithms. Examining various configurations of alternating left and right restrictions yields alternating sequences that can be used for determining the blocking arcs of a circular visibility

*‘Man verliert die meiste Zeit damit,
dass man Zeit gewinnen will.’*

(John Steinbeck, American writer)

set and hence the whole set. Besides, we outline an iterative approach to compute the sets $V_K^n(\sigma)$ and a (smooth) minimum arc path.

Algorithmic details and runtime improvements in case of a polygon P are presented in the following sections. Chou and Woo have shown that the subset of $\overline{I_K}$ circularly visible from a point inside P can be determined by computing its Circular Visibility Diagram (CVD) in $O(n)$ time, where n is the number of the vertices of P . Therefore, a short introduction to CVDs is given in Section 4.2.

In Section 4.3, we discuss the determination of the circular visibility set $V_K(\sigma)$ of a starting channel (K, s, σ) by iteratively constructing CVDs. If $\text{tr}(s)$ is a point, we only need to compute the CVD with base point $\text{tr}(s)$. In case of a line segment, we use the strategy proposed in [22] and give some improvements.

If $\text{tr}(s)$ is an arc, we propose a method that is based on the case in which $\text{tr}(s)$ is a line segment (see Section 4.4).

Section 4.5 concerns the algorithmic adaptation to continuation channels, which can be done likewise.

In Section 4.6, we combine all the details of the previous sections in order to improve the runtime of the particular steps of the algorithms presented in the first section. Thus, we can develop an efficient algorithm for computing a smooth and a continuous minimum arc path of a polygonal start-destination channel which is therefore also based on CVDs. At the end of every particular section we show the runtime complexities of the various algorithms.

The chapter is completed by a short overview. We briefly summarize our algorithmic approaches for computing a (smooth) minimum arc path and test the implementation of the algorithms experimentally regarding the runtime and the number of CVDs needed. For this purpose, we concentrate on both real and synthetic data. However, we address the performance of our algorithms in real applications not until Chapter 5.

4.1 Greedy Proceeding and Alternating Sequences

Let (K, s, σ) be an arbitrary tolerance channel. Since $V_K(\sigma)$ is connected and compact (cf. Lemma 3.1.19), it suffices to compute the boundary $\partial V_K(\sigma)$ (with respect to \mathbb{R}^2) in order to characterize $V_K(\sigma)$. Therefore, we determine all blocking arcs and merge them with K . This way we obtain $\partial V_K(\sigma)$.

The characterization of blocking arcs by alternating sequences enables a constructive approach: Given an alternating sequence of length 3, there exists exactly one arc which is maximal with respect to inclusion in $\overline{I_K}$ corresponding to it. If we want to compute the circular n -visibility set $V_K^n(\sigma)$ ($n > 1$) or a (smooth) minimum arc path, we can proceed iteratively. The theoretical results of Chapter 3 lead us to a greedy approach.

For the examination of our algorithmic approach, we make a general assumption in order to make this chapter more easy to read: We restrict ourselves to starting channels with a starting segment given by an oriented arc s.t. there don't appear any pseudo restrictions. For this purpose, we only have to make sure that our starting segment s is contained in K and has convex vertices, i.e. there exist neighborhoods U and V of $S(s)$ and $E(s)$ s.t. $U \cap \overline{I_K}$ and $V \cap \overline{I_K}$ are convex (cf. Section 3.2).

First we want to focus on an algorithm for the computation of $V_K(\sigma)$.

4.1.1 Computation of $V_K(\sigma)$

As indicated above, we have to examine potential alternating sequences of length 3 and compute the corresponding arcs that are maximally extended in $\overline{I_K}$.

In fact, the mathematical results of Chapter 3 establish the fundamentals of an algorithm for computing the circular visibility set with respect to any tolerance channel. Specifically, the macro structure of the algorithm doesn't depend on the type of the bounding curve, but the constructive approach for searching visibility arcs with an alternating number of at least 3 depends, of course, on the class of the channel curve. We now sketch how to identify the blocking arcs in case of a polygonal channel and a channel given by an arc spline.

Let us consider, for instance, a starting channel (K, s, σ) given by an arc spline ω that is not necessarily smooth with minimal representation $\omega_1 \cdots \omega_n$, i.e. $|\omega| = n$. Using the abbreviations $K := \text{tr}(\omega)$ and $s := \omega_1$, all possible configurations of left and right restrictions are given as follows: The corresponding arc

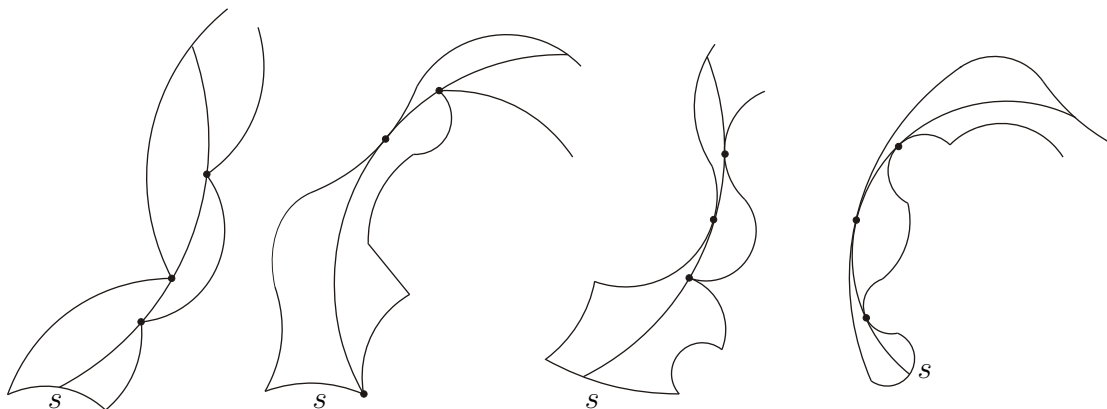


Figure 62: Examples of blocking arcs in case of an arc spline as bounding curve. In addition, the corresponding alternating sequences of length 3 are depicted. They are given by three vertices, two vertices and touching one arc, one vertex and touching two arcs, and touching three arcs respectively.

- passes through three vertices,
- passes through two vertices and touches¹ an arc of K ,
- passes through one vertex and touches two arcs of K or
- is at tangent to three arcs.

Figure 62 shows examples for each of the four configurations in case of a starting channel given by an arc spline.

Given the corresponding generalized circles of the ω_i , in a brute force approach, we could compute the circle C satisfying one of the requirements formulated above (cf. Table 2.1 on page 19 or [69] respectively). If $\text{tr}(s) \cap C \neq \emptyset$, we can determine the starting point x of a possible visibility arc γ and a corresponding alternating sequence (a_1, a_2, a_3) . If x satisfies the starting condition σ , the inclusion $[x, a_3]_\gamma \subset \overline{I_K}$ holds and if $\mathcal{A}(\gamma) \geq 3$, we have found a blocking arc.

Of course, this approach needs finitely many steps since the number of oriented arcs ω_i is finite. Nevertheless, this proceeding is not very efficient. Examining the potential alternating sequence needs $O(n^3)$ time and the check if the corresponding arc stays inside $\overline{I_K}$ can be done in linear time. The additional checks needed can be implemented in constant time. Overall, this proceeding results in an $O(n^4)$ -algorithm. How to im-

¹There exists an $i \in \{1, \dots, n\}$ and $x \in \text{tr}(\gamma) \cap \text{tr}(\omega_i)$ with $\tau_\gamma(x) = \pm\tau_{\omega_i}(x)$.

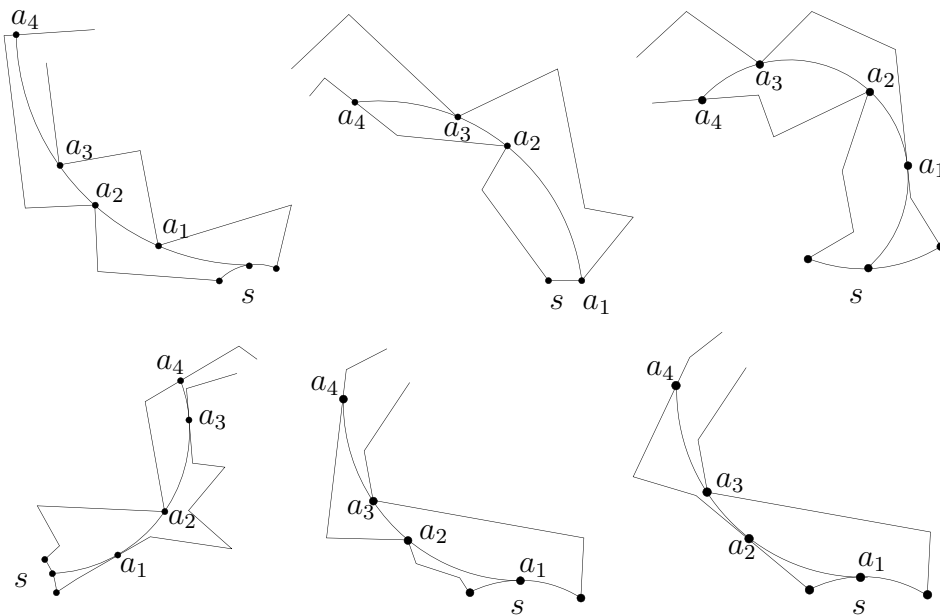


Figure 63: Illustration of blocking arcs in case of a polygon. All configurations of alternating sequences representing the right-blocking case are depicted.

prove the strategy in case of polygons, which is certainly most important for practical applications, will be discussed later on.

If $\omega_1 \cdots \omega_n \in \mathcal{L}^n$ is a polygonal curve, the blocking arcs can be determined by

- three vertices,
- two vertices and one edge or
- one vertex and two edges.

An illustration can be found in Figure 63.

Hence we obtain all blocking arcs by investigating degenerate tolerance channels (K, s_i, σ_i) with vertices $\{v_i\} := \text{tr}(s_i)$ of K and corresponding degenerate starting maps σ_i . Each set $V_K(\sigma_i)$ is briefly called *circular visibility set of* v_i .

Visibility problems are well-studied within the scope of polygons. We have already mentioned that they can be determined in linear time by constructing a *Circular Visibility Diagram (CVD)*. An efficient strategy using CVDs is presented in Sections 4.2 - 4.5.

For other types of bounding curves, individual strategies have to be developed. However, in principle they work the same way. The only question is, how to search efficiently for alternating sequences in order to construct all blocking arcs.

Before we discuss our improvements within the scope of polygons, we first sketch our algorithmic procedure for computing $V_K^n(\sigma)$, $n > 1$ and a (smooth) minimum arc path.

4.1.2 Computation of $V_K^n(\sigma)$ and Minimum Arc Paths

In the previous subsection we outlined how to compute the blocking arcs of $V_K(\sigma)$. Next, we want to determine the continuation channels given by the blocking arcs computed beforehand and compute again the blocking arcs of each continuation channel, and so on. Hence we pursue an iterative approach. As the approach for every connected component of $\overline{I_K} \setminus V_K^i(\sigma)$ is the same, we focus on the computation of a smooth/continuous minimum arc path in a start-destination channel $\mathfrak{D} := (K, s, \sigma, d)$, and we use the abbreviation $\mathfrak{E} := (K, s, \sigma)$.

In this case, the windows of the iteratively determined continuation channels are computed (cf. Section 3.7). If the blocking arc γ associated with the window with respect to \mathfrak{E}_i and d has an alternating number $\mathcal{A}(\gamma) > 3$, \mathfrak{E}_{i+1} is a degenerate continuation channel, as explained in Definition 3.7.3 and 3.6.5 respectively. The procedure is stopped when $\text{tr}(d)$ is circularly visible, and a visibility arc satisfying the conditions of Lemma 3.4.20 is computed. This arc represents the last segment of our solution spline. The predecessor segments can be computed by touching their successor and by a left and a right restriction (cf. Theorem 3.6.8). Recall that in case of a (smooth) minimum arc path only left restrictions from K_l and right restrictions from K_r have to be taken into account (cf. Theorem 3.4.19).

If necessary, the calculated solution $\gamma \in \overline{\mathfrak{S}}_K^n(\sigma)$ is smoothed by using a biarc-strategy, as proposed in Section 3.7. The whole approach is summarized in Algorithm 1.

By means of a small example, we illuminate the several steps of Algorithm 1 in order to give a better understanding of our constructive approach for computing a smooth minimum arc path. We explain and visualize the whole forward and backward step by this example.

Algorithm 1 Smooth Minimum Arc Path**Input:** Start-destination channel (K, s, σ, d) **Output:** List L of circular arcs defining a smooth minimum arc path

```

1: // Forward step
2:  $i \leftarrow 1$ 
3:  $\mathfrak{E}_i \leftarrow (K, s, \sigma)$ 
4: while  $\text{tr}(d) \cap V_K(\sigma) = \emptyset$  do
5:   Compute blocking arc  $\gamma^{(\text{tr}(d))}$  in  $\mathfrak{E}_i$  by examining
   (global) alternating sequences of length 3
6:    $\omega_i \leftarrow \omega^{(\text{tr}(d))}$ 
7:    $i \leftarrow i + 1$ 
8:   Compute and store  $\mathfrak{E}_i$  // cf. Definition 3.7.3
9:    $(K, s, \sigma) \leftarrow \mathfrak{E}_i$ 
10: end while
11: // Current value of  $i$  is the minimal number with  $V_K^i(\sigma) \cap \text{tr}(d) \neq \emptyset$ 
12:  $\gamma_i \leftarrow$  visibility arc of  $\mathfrak{E}_i$  ending in  $\text{tr}(d)$ 
13: Insert  $\gamma_i$  into  $L$ 
14: // Backward step
15: for  $j = i - 1$  to 1 do
16:    $(K, s, \sigma) \leftarrow \mathfrak{E}_j$ 
17:    $\gamma_j \leftarrow$  visibility arc of  $\mathfrak{S}_K(\sigma)$  joining  $\gamma_{j+1}$ 
18:   Insert  $\gamma_j$  into  $L$ 
19: end for
20: // Possibly: Smoothing Step
21: if  $\gamma := \gamma_1 \cdots \gamma_i$  is not smooth then
22:   Smooth  $\gamma$  and insert the  $n(d) - i$  additional segments into  $L$ 
23: end if
24: return  $L$ 

```

Example. Figure 64 and 65 show the *forward step* and *backward step* for computing a smooth minimum arc path in an arbitrary polygonal start-destination channel:

In order to compute the first window, we have to examine all visibility arcs with an alternating number of at least 3 (cf. Theorem 3.4.19), until the blocking arc γ_1 which corresponds to the window is found. We then obtain a continuation channel with a window whose corresponding blocking arc γ_2 has an alternating number of 4. The subsequent tolerance channel being degenerate, we can construct the according blocking arc γ_3 regarding the unidirectional starting restriction given by γ_2 . The construction of the remaining windows works in a complete analogy, the corresponding continuation channels and blocking arcs are also illustrated in Figure 64. The last segment of our solution spline is determined up to set inclusion in the last step of the whole forward step. In the backward step, its predecessor segments are constructed by two alternating restrictions and the requirement of smoothly joining its successor as illustrated in Figure 65. Altogether, we get a smooth minimum arc path with six segments.

If we want to compute a continuous minimum arc path, which means that the desired arc spline doesn't need to be smooth, we consider in every step starting channels as presented in Section 3.8. An algorithmic description can be found in Algorithm 2.

We want to illustrate the algorithm for the computation of a continuous minimum arc path by an example as well:

Example. For the continuous case, we consider the same start-destination channel as in the previous example in order to discuss our algorithmic approach summarized in Algorithm 2.

The very first step does not differ from the smooth case, and therefore we yield the same window and blocking arc γ_1 . Next, we clip the polygon at the first window and get a new start-destination channel. Due to Algorithm 2, this process is continued until we reach $\text{tr}(d)$ and consequently a continuous minimum arc path having a segment number of 4 is constructed. Figure 66 shows the respective necessary steps.

Since, in this section, we only gave a general overview of the whole procedure, we will discuss the particular steps in detail in the following sections, where we focus on polygons. We will present an efficient approach to compute the blocking arcs by using CVDs.

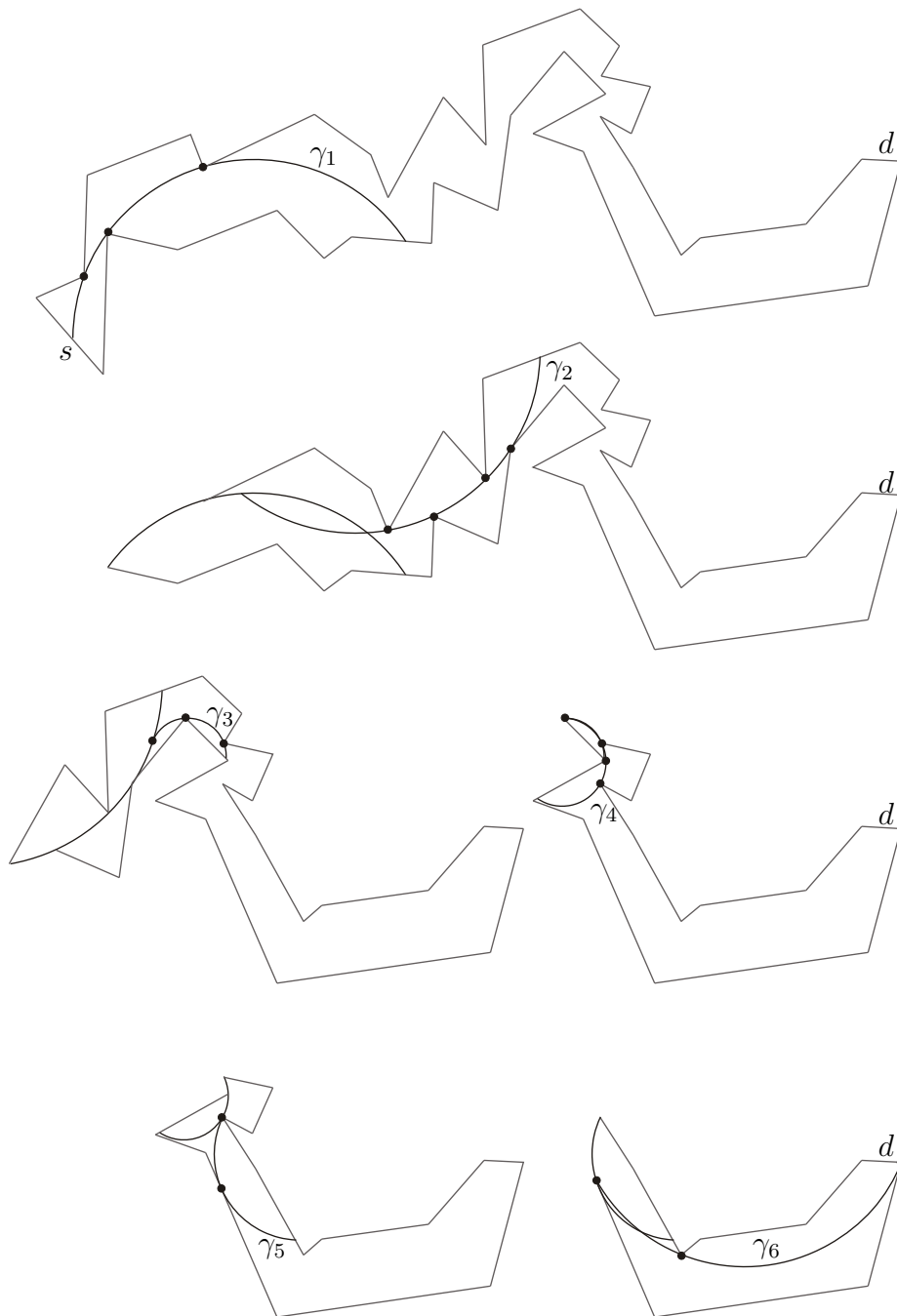


Figure 64: 'Forward step'. The several continuation channels and corresponding blocking arcs are depicted. In particular, we have $\mathcal{A}(\gamma_1) = \mathcal{A}(\gamma_3) = \mathcal{A}(\gamma_5) = \mathcal{A}(\gamma_6) = 3$ and $\mathcal{A}(\gamma_2) = \mathcal{A}(\gamma_4) = 4$. Therefore, in the third and fifth step we have to consider degenerate channels.

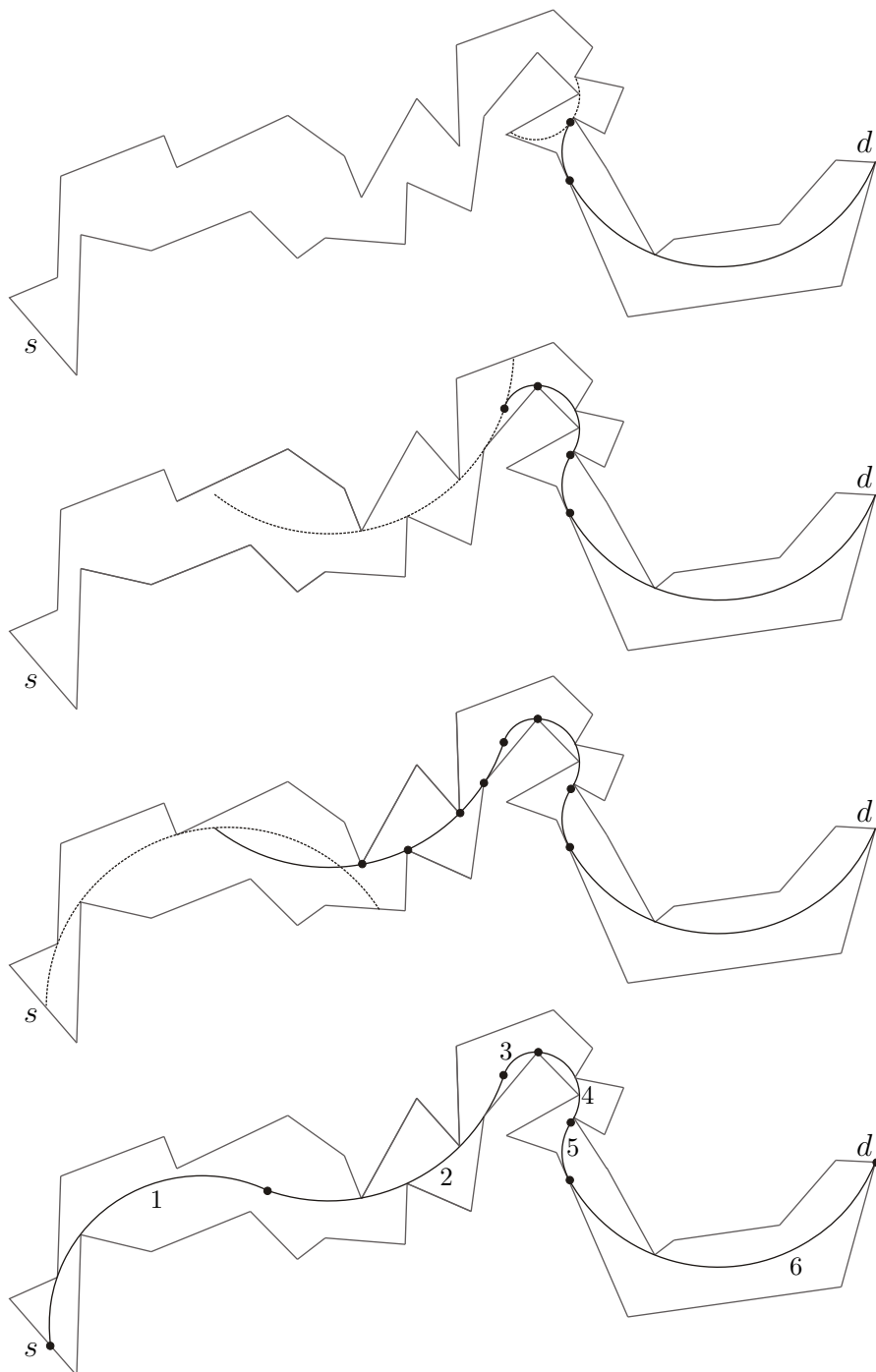


Figure 65: 'Backward step'. The construction of the particular segments is illustrated. On the bottom, we can see the smooth minimum arc path with six segments due to Algorithm 1.

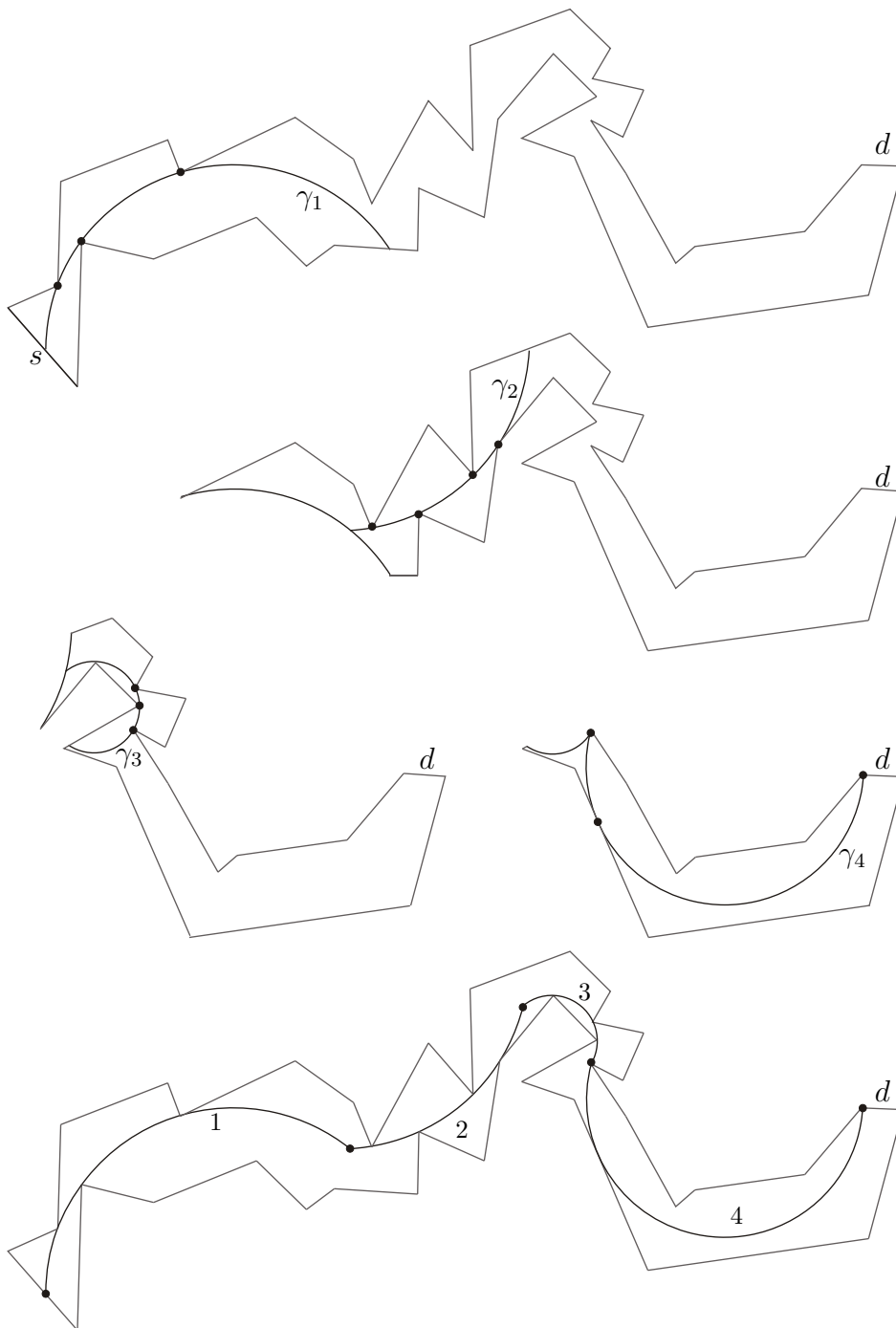


Figure 66: The particular steps of Algorithm 2, which yields a continuous minimum arc path with four segments, are illustrated.

Algorithm 2 Continuous Minimum Arc Path

Input: Start-destination channel (K, s, σ, d)

Output: List L of circular arcs defining a minimum arc path

- 1: $i \leftarrow 1$
 - 2: $\mathfrak{D}_i \leftarrow (K, s, \sigma, d)$
 - 3: **while** $\text{tr}(d) \cap V_K(\sigma) = \emptyset$ **do**
 - 4: Compute $\gamma_{\mathfrak{D}_i}$ by examining (global) alternating sequences of length 3
 - 5: $\omega_i \leftarrow \omega_{\mathfrak{D}_i}, \gamma_i \leftarrow \gamma_{\mathfrak{D}_i}$ // cf. Definition 3.7.6
 - 6: Insert γ_i into L
 - 7: $i \leftarrow i + 1$
 - 8: Compute and store \mathfrak{D}_i
 - 9: $(K, s, \sigma, d) \leftarrow \mathfrak{D}_i$
 - 10: **end while**
 - 11: $\gamma_i \leftarrow$ visibility arc starting at $\text{tr}(\omega_{i-1})$ and ending in $\text{tr}(d)$
 - 12: Insert γ_i into L
 - 13: **return** L
-

4.2 Circular Visibility Diagrams (CVD)

In this section we give a short overview of Circular Visibility Diagrams (CVDs), which were introduced by Chou and Woo (cf. [23]).

Let (K, s, σ) be a degenerate starting channel with a simple polygon K and $\{x\} := \text{tr}(s) \subset K$. We use the notations: $\omega_K := \omega_1 \cdots \omega_n$ with line segments $e_i := \text{tr}(\omega_i)$, which are maximal with respect to inclusion. We call them *edges of K* . The following abbreviations are subsequently used: $V_K(x) := V_K(\sigma)$, $\mathfrak{S}_K(x) = \mathfrak{S}_K(\sigma)$.

The main idea of the development of CVDs is the representation of visibility arcs starting from x by the centers of the corresponding circles. Whereas only one line segment connects two distinct points, there is an infinite number of circular arcs connecting them. However, considering a fixed orientation (CW or CCW), the circles passing through x can be uniquely represented by their corresponding centers. This way the visibility arcs $\gamma \in \mathfrak{S}_K(x)$ can be classified. They can be grouped with respect to the positions of their centers according to the edges they hit when exiting K (see Figure 67). Such a classification can be made for each orientation, and they are called *CW-CVD* and *CCW-CVD* respectively. We will see that the real plane is divided into different regions, which belong to exactly one edge of the polygon or represent the circles staying in $\overline{I_K}$ or starting into E_K .

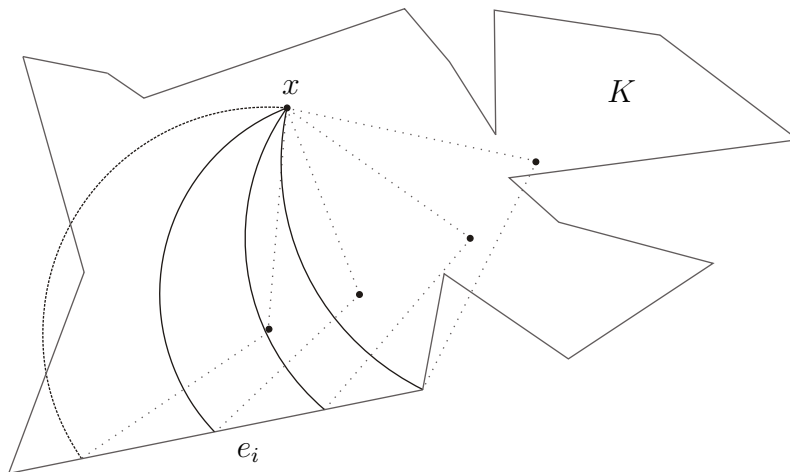


Figure 67: CCW visibility arcs emanating from x , which correspond to the edge e_i of K , represented by their centers.

4.2.1 Preliminary Definitions and Comments

Definition. Let ϵ be an arbitrary orientation (CW or CCW). Given a center $c \in \mathbb{R}^2 \setminus \{x\}$, we denote the unique arc, if it exists, that is maximal with respect to inclusion in $\overline{I_K}$ with center c and orientation ϵ , starting at x , by $\mu(c, \epsilon)$. For every $i \in \{1, \dots, n\}$, we then set:

$$R_i(\epsilon) := \{c \in \mathbb{R}^2 \mid x \neq E(\mu(c, \epsilon)) \in e_i\}.$$

Analogously, we can define the set of centers whose corresponding circles stay inside $\overline{I_K}$

$$R_\emptyset(\epsilon) := \{c \in \mathbb{R}^2 \mid E(\mu(c, \epsilon)) = x\}$$

and the region $R_E(\epsilon)$ representing the arcs starting at x into the direction of the exterior of K with orientation ϵ . The set $\{R_\emptyset(\epsilon), R_E(\epsilon), R_1(\epsilon), \dots, R_n(\epsilon)\}$ is called ϵ -CVD of K with respect to x , and x is said to be the **base point (of the CVD)**.

If there are no ambiguities, we use the abbreviations R_i, R_E and R_\emptyset .

For an illustration, please have a look at Figure 69.

Note that R_E is empty if and only if $x \notin K$. By definition, every region R_i belongs exactly to one edge e_i in the following way: A circular arc starting from x with corresponding center in R_i first crosses e_i when leaving $\overline{I_K}$, which is equivalent to $E(\mu(c, \epsilon)) \in e_i$. We get $\mathbb{R}^2 = R_\emptyset \cup R_E \cup \bigcup_{1 \leq i \leq n} R_i$ and the open sets $\overset{\circ}{R}_i, \overset{\circ}{R}_\emptyset$ are pairwise disjoint.

Nevertheless, these regions are bounded by so-called *partitioning curves* that are composed of half-lines, line segments and parabolic curve segments and are on the border of at least two regions. In fact, these curves are built by *Voronoi-diagrams* (see [23]):

Definition. Let e be an edge of K . The set of all equidistant points between x and e , $V(x, e) := \{c \in \mathbb{R}^2 \mid \text{dist}(c, e) = \|c - x\|\}$, is called **Voronoi-diagram of x and e** . The corresponding curves are referred to as **bisectors**.

A partitioning line or ray respectively given by $V(x, e)$ is a subset of the perpendicular bisector between x and a vertex of e . Hence a visibility arc with its center based on such a line segment hits a vertex of e , whereas a parabolic curve represents the loci of the centers that provide a visibility arc which is tangent to e .

Definition. The points joining two or more partitioning curves of a CVD are called **nodes (of the CVD)**.

Remark. Consider a circular arc γ whose center c is a node that is joined by exactly two partitioning curves. Then Chou and Woo proved that γ satisfies one of the following alternatives

- γ passes through two vertices of K .
- γ passes through a vertex and is tangent to an edge of K .
- γ is tangent to two edges of K .

Obviously, the corresponding points are left or right restriction points of γ if they do not coincide with its end point. Figure 69 also depicts this correspondence.

In this manner, the visibility arcs γ with $\mathcal{A}(\gamma) \geq 3$ and the window with respect to x can be identified by examining the nodes of the CCW-CVD and CW-CVD: Let N be a node, ϵ an orientation and $e_i \neq e_j$ be two corresponding edges of N . Using the abbreviation $\gamma := \mu(c, \epsilon)$, we have to examine the intersection points $a_1 < a_2$ of $\text{tr}(\gamma)$ with e_i and e_j respectively. If (a_1, a_2) is an alternating sequence of length 2, we get $\mathcal{A}(\gamma) \geq 3$ since $x \leq a_1$ is a pseudo restriction point by definition. Thus, γ is a blocking arc by Theorem 3.4.7. Blocking arcs with $\mathcal{A}(\gamma) > 3$ correspond to nodes that are generated by more than two partitioning curves. Again, by Theorem 3.4.7, we can be sure of obtaining all blocking arcs when examining all nodes of the CCW-CVD and CW-CVD.

4.2.2 Sketch of the Overall Algorithm

The data structure of the CVD is similar to the dual space data structure used by Chazelle and Guibas (cf. [20]) for solving a variety of linear visibility problems. In that paper, a line $ax + by + 1 = 0$ is represented by a point $(a, b) \in \mathbb{R}^2$. These points are then grouped into regions according to the edge their corresponding visibility rays hit. This classification results in a planar partition.

In linear visibility, a partial order in which visibility rays hit the edges of a polygon is crucial for the construction. However, in circular visibility, visibility arcs emanating from a point can hit two edges in either order, as shown in Figure 68.

To overcome the apparent lack of a partial order, a polygon is decomposed into its linear visibility polygon $L_K(\sigma)$ and the set of pockets P_1, \dots, P_m (cf. Definition 3.8.4), each of which exhibits a partial order. The boundary $\partial L_K(\sigma)$ is a polygon. According to Chou

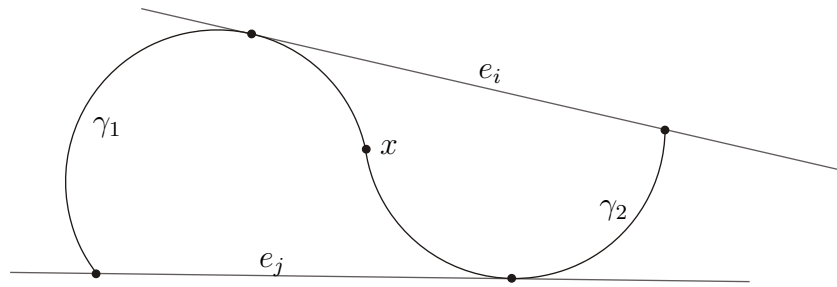


Figure 68: Possible hitting order of two edges e_i , e_j ; two arcs γ_1 and γ_2 emanating from x . γ_1 first touches e_i before leaving K at e_j ; γ_2 first touches e_j before leaving at e_i .

and Woo, we call it the *star-shaped polygon (of K)* and denote it by K^* . The CVD of a simple polygon can be obtained by constructing the CVDs for the star-shaped polygon and then for every pocket. An overview of the CVD construction procedure is outlined in Algorithm 3.

Algorithm 3 CVD Simple Polygon

Input: Simple polygon K , base point x , orientation ϵ

Output: $\text{CVD}(K, x, \epsilon)$

- 1: Compute the decomposition $\overline{I_K} = L_K(\sigma) \cup P_1 \cup \dots \cup P_m$
 - 2: Construct $\text{CVD}(L_K(\sigma), x, \epsilon)$
 - 3: **for** $i = 1$ to m **do**
 - 4: Construct $\text{CVD}(P_i, x, \epsilon)$
 - 5: **end for**
 - 6: **return** $\text{CVD}(K, x, \epsilon)$
-

The collinearity of x with the lids (cf. Definition 3.8.4) exhibits an essential property, which ensures the development of a partial order on the pockets (cf. [23]).

As already indicated, Algorithm 3 can be used for computing the circular visibility set $V_K(\sigma)$ in case of a degenerate starting channel (see Algorithm 4). In particular, the window can be examined this way if a destination segment is given additionally.

4.2.3 The Time Complexity

Algorithm 3 first computes the linear visibility set $L_K(x)$ and K^* , which can be done in linear time regarding the number of vertices n . Since a partial order in which an arc hits

Algorithm 4 Computation of $V_K(\sigma)$ in case of a degenerate starting channel.

Input: (K, s, σ) degenerate starting channel with polygon K and $\{x\} := \text{tr}(s)$

Output: Boundary of $V_K(\sigma)$

```

1:  $i \leftarrow 0$ 
2: List  $L$ ,  $L \leftarrow \text{NIL}$ 
3: Construct CVD( $K, x, \text{CW}$ )
4: Construct CVD( $K, x, \text{CCW}$ )
5: for all nodes  $N$  of the two CVDs do
6:   Compute the arc  $\gamma(N)$  corresponding to  $N$ 
7:   if  $\mathcal{A}(\gamma(N)) \geq 3$  then
8:     Insert  $\gamma(N)$  into  $L$ 
9:   end if
10: end for
11: Compute the boundary of  $V_K(\sigma)$  using  $K$  and  $L$ 

```

the edges of K^* is established, the corresponding part of the CVD can be constructed in $O(n)$ time. To compute the part generated by all the pockets with respect to x needs extra effort, but the time required is bounded by the total number of vertices in K . The time complexity for constructing the $\text{CVD}(K, x, \epsilon)$ is the sum of the time complexity for the two individual processes, which are all bounded by $O(n)$. By construction, the number of nodes and the number of partitioning curves are in the same order as the vertices of K . Hence a CVD can be computed in linear time¹.

The boundary $\partial V_K(\sigma)$ with respect to the topology on \mathbb{R}^2 consists of subsets of K and subarcs of the blocking arcs. The identification of the blocking arcs requires $O(n)$ time. With all these arcs identified, K and the blocking arcs of $V_K(\sigma)$ can be traversed in order to compute the parts contributing to $\partial V_K(\sigma)$. This can be trivially achieved in linear time. Hence the total time complexity of Algorithm 4 is $O(n)$ as well.

Note that by Lemma 3.4.19 an efficient stopping criterion is given when computing the window of a degenerate start-destination channel (K, s, σ, d) . This criterion can be directly read off the CVD. Nevertheless, the computation of the CW- and CCW-CVD cannot be avoided, which results in a linear time algorithm as well.

¹A detailed calculation of the time complexity for the computation of a CVD can be found in [23].

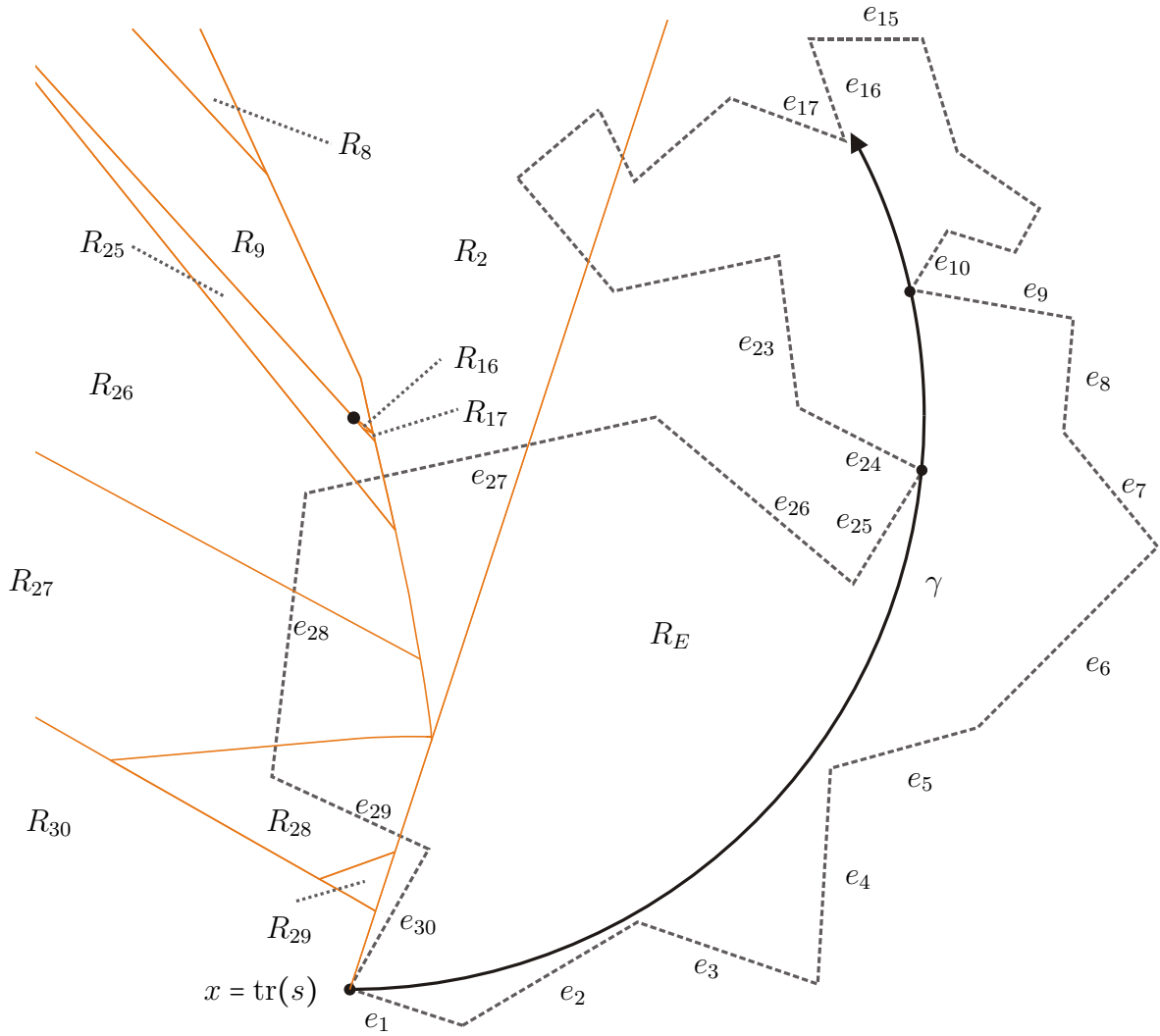


Figure 69: Illustration of a polygon K (dashed) and the CCW-CVD (solid) with base point x . A visibility arc γ starting from x with a left and a right restriction is depicted as well. Its center is located on the node generated by the regions belonging to edges e_{25} , e_9 and e_{16} . Note that γ is a blocking arc with respect to (K, s, σ) .

4.3 Circular Visibility of an Edge

Let (K, s, σ) be a starting channel with a polygon K and an oriented line segment s . W.l.o.g. we can assume $\text{tr}(s)$ to be an edge of K . Substantially, we give a brief sketch of the method presented in [22] and outline our modifications and improvements.

In case of starting channels, pseudo restrictions only appear at boundary points of s and can therefore be identified by examining the circular visibility of these boundary points. Therefore, as already mentioned in Section 4.1, we don't deal with the case where s has extroverted vertices, i.e. we don't have to concern pseudo restrictions.

4.3.1 Sketch of the Overall Algorithm

By Theorem 3.4.7, the circular visibility set $V_K(\sigma)$ is defined by visibility arcs supplying alternating sequences of length 3, namely the blocking arcs. In case of a polygon, at least one of these restriction points must be clearly given by a vertex of K as an arc cannot be touched by an edge from the interior of the corresponding circle. Figure 63 illustrates the different configurations. Hence these arcs and particularly the window in case of a start-destination channel can be found by computing CVDs of some vertices and examining the corresponding nodes as described in the previous section.

The strategy suggested by Chou et al. ([22]) attempts to constantly reduce the domain in which blocking arcs are identified: First they construct the linear visibility set $L_K(\sigma)$, which can be done in linear time. Then every pocket is examined to find the blocking arcs entering the corresponding pocket one after the other. Since blocking visibility lines defining lids have alternating sequences of length 2, either CW or CCW arcs can reach a pocket but not both. Thus, for each point, only its CVD with respect to one orientation needs to be computed. A pocket is said to be a *CW-pocket* if only CW oriented visibility arcs can reach the interior of the pocket, and *CCW-pocket* if only CCW arcs can enter it.

Next, for each pocket two initial arcs are constructed. Then two alternating restrictions of the visibility arc computed in the previous step stay fixed. One of these so-called *hinges* acts as the base point for a new CVD. From this, further visibility arcs which provide an alternating number of at least 3 can be computed, as we could see in the previous section. The first two hinges are given by the lid of the current pocket that is examined. The algorithm reduces the problem of examining the region between two

visibility arcs iteratively (see Figure 70). By propagating such supports and ‘sweeping’ visibility arcs through them, the left- and right-blocking arcs in the region between two such arcs can be efficiently constructed.¹

Algorithm 5 Edge visibility

Input: (K, s, σ) starting channel with polygon K , $\text{tr}(s)$ edge of K

Output: Boundary of $V_K(\sigma)$

- 1: Compute $L_K(\sigma)$ and the corresponding pockets P_1, \dots, P_m
 - 2: **for** $i = 1$ to m **do**
 - 3: Compute the blocking arcs $\gamma_{i1}, \dots, \gamma_{il_i}$ corresponding to P_i
 - 4: Insert $\gamma_{i1}, \dots, \gamma_{il_i}$ in List L
 - 5: **end for**
 - 6: Compute the boundary of $V_K(\sigma)$ using K and L
-

Next, we concern ourselves with an arbitrary start-destination channel \mathfrak{D} and the computation of the window $\omega_{\mathfrak{D}}$. In this case, we give a deeper insight in the algorithmic approach, as we can suggest some modifications and improvements.

4.3.2 Improvements for Start-Destination Channels

Let us assume an additional designated segment d s.t. $\mathfrak{D} := (K, s, \sigma, d)$ is a start-destination channel. We then only consider the pocket which contains the window $\omega_{\mathfrak{D}}$.

Definition. If $\text{tr}(d) \cap L_K(\sigma) = \emptyset$, we call the pocket P with $\text{tr}(d) \subset P$, **main pocket**.

As seen above, we first compute the linear window $\lambda_{\mathfrak{D}}$. Due to Proposition 3.8.2, $\lambda_{\mathfrak{D}}$ corresponds to a visibility line γ_0 having an alternating sequence (a_1, a_2) of length 2. W.l.o.g. we can assume that a_1 is a right and a_2 is a left restriction point. If $S(\gamma_0)$ is the left endpoint of s , γ_0 has an alternating sequence of length 3 and γ_0 is associated with $\omega_{\mathfrak{D}}$ (i.e. $\gamma_0 = \gamma_{\mathfrak{D}}$) and we are done. Otherwise, the main pocket exists and is a CCW-pocket. Next, the successor segment γ_1 of γ_0 is computed as follows: Since $S(\gamma_0)$ is not the left endpoint of s , we have to distinguish between two cases: Either $S(\gamma_0)$ is the right end point b of s or $S(\gamma_0) \in \text{tr}(s)^{ri}$. In the latter case, we set $\gamma_1 := \gamma_0$. Otherwise, γ_1 is the

¹For a more detailed presentation, please have a look at [22].

blocking arc associated with the window with respect to b , which can be computed by constructing the CCW-CVD of b . If γ_1 isn't associated with $\omega_{\mathfrak{D}}$, we compute the next segment γ_2 . For this purpose, the last two alternating restrictions of the $\text{tr}(d)$ -adapted alternating sequence of γ_1 stay fixed, and γ_2 is defined by these two so-called 'hinges' and has another one beforehand (cf. [22]). Then the so-called *deficiency set of γ_1 and γ_2* is examined iteratively as indicated above.

Examining only the main pocket reduces the costs significantly if $V_K(\sigma)$ has yet other pockets with the number of vertices in the same order as the number of vertices in the main pocket. Since the pockets with respect to the corresponding base point have to be examined successively while constructing a CVD, similar improvements can be made whenever a new CVD is computed. If the main lid $\lambda_{\mathfrak{D}}$ equals $\omega_{\mathfrak{D}}$, which can be easily checked by Theorem 3.4.19, we are done after only one step. As we are especially interested in the window and not in all blocking arcs, only pairs of *hinges* in K_l and K_r are chosen because the window is characterized by alternating sequences on the left and right bordering set (see Theorem 3.4.19). Therefore, the search area can be decisively restricted. As already indicated, an efficient criterion to terminate the algorithm is given by the unique representation in Theorem 3.4.19. This criterion can be easily checked by examining the edges belonging to the corresponding node in the CVD.

Before we estimate the time complexity needed for determining the circular visibility set $V_K(\sigma)$ and the window $\omega_{\mathfrak{D}}$, we present an example illustrating the strategy proposed.

Example. Considering the polygonal start-destination channel $\mathfrak{D} := (K, s, \sigma, d)$ depicted in Figure 70, the main pocket is a CCW-pocket. Let $a \in K_l$ and $b \in K_r$ be the end points of $\text{tr}(s)$. The strategy of Chou et al. suggests to compute first the CCW-CVD of b and to identify the arc γ_1 , which is associated with the window with respect to b . Since all alternating sequences of γ_1 have an alternating number less or equal two, $\omega_{\mathfrak{D}}$ and the window with respect to b are not equal. In the next step γ_2 , which is associated with the window regarding a , is computed. Since γ_2 has an alternating sequence of length 3, it is a blocking arc with respect to \mathfrak{D} . However, both the last restriction and the endpoint of γ_2 are points of K_l . Therefore, γ_2 is not associated with $\omega_{\mathfrak{D}}$ (cf. Theorem 3.4.19), which can be determined by examining the region between γ_1 and γ_2 , as described in [22]. As already mentioned, by Theorem 3.4.19 we have an efficient stopping criterion.

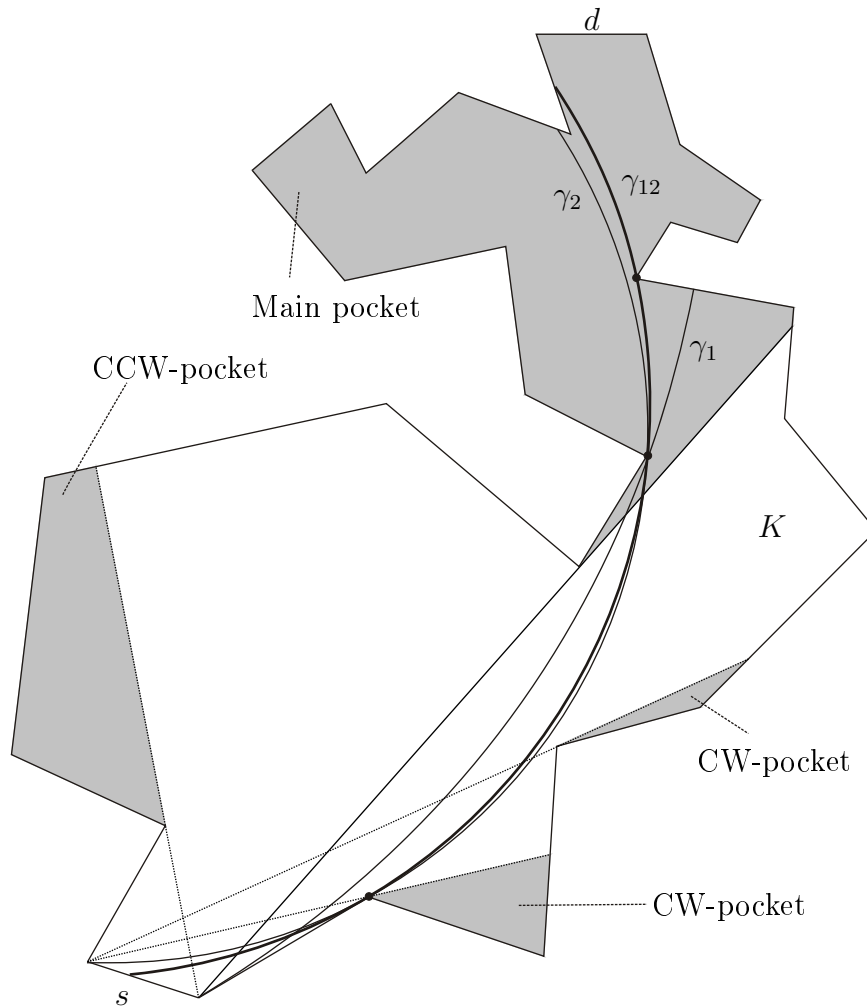


Figure 70: Polygon K and pockets (shaded) with respect to edge $\text{tr}(s)$. Additionally, the circular arcs generated by the algorithmic approach above are plotted. Note that the blocking arc γ_{12} has two alternating restrictions in common with its predecessor γ_2 . Both touch the first edge on the right and run through the 7th left vertex. The window can be constructed by examining the region between the arcs γ_1 and γ_2 computed in the first two steps.

4.3.3 The Time Complexity

Since computing the linear visibility and constructing a CVD can be done in linear time, the complexity for determining blocking arcs of $V_K(\sigma)$ and for eventually computing $\partial V_K(\sigma)$ is shown by $O(kn)$, where k is the number of CVDs required and n is the number of vertices in K .

As already outlined in the previous subsection, we have found modifications to improve the strategy and therefore the runtime of the algorithm in case of a start-destination channel. However, in the worst case, k can only be bounded by the number of vertices in $L_K(\sigma)$ and the main pocket, which is $O(n)$.

4.4 Circular Visibility of an Arc

Let (K, s, σ) be a starting channel, where K is a polygon with n vertices and s is an oriented arc. The main idea for computing $V_K(\sigma)$ for a starting segment that is an arc is to use the procedure we suggested in case of an edge, which was presented in the previous section. As our mathematical results also hold in case of a circular arc, the strategy used in this case is the same up to some modifications.

4.4.1 Sketch of the Overall Algorithm

We set $a := S(s) \in K$ and $b := E(s) \in K$. As suggested in the previous section, we first compute the linear visibility of $L_K(\sigma)$, which can be done in linear time according to [39]. Every lid λ corresponds to a visibility line γ_0 having an alternating sequence of length 2. As we proceed in a complete analogy to the case of an edge, we only present the ‘adjusting steps’, which are possibly necessary: The starting points of all visibility arcs can be determined by intersecting the corresponding circle with $\text{tr}(s)$. When computing a visibility arc γ starting at a or b , γ can be defined by examining the nodes of the CVDs in K with basepoint a and b . However, it must be checked if it intersects $\text{tr}(s)$ at only one point. If this is not the case, an adjusting step is needed, which computes the visibility arc touching s and having the same two last ‘hinges’ (cf. Fig. 71). In order to compute an arc γ touching s , at most $O(n_1)$ CVDs have to be supplied and the intersection with the bisector defined by $\text{tr}(s)$ and the respective basepoint of the CVD has to be computed, where n_1 denotes the number of vertices of $V_K(\sigma)$. The intersection with the bisector is done since every circle with its center located on the bisector given by s and a point p touches s and runs through p (cf. [22]).

In order to familiarize ourselves with the strategy proposed above, we give an example:

Example. Let us consider the situation of Figure 72 where s is the circular arc starting at a and ending in b . The visibility line γ_0 has the two restrictions b and a_2 and γ_1 is the blocking arc associated with the window with respect to b . Using the restrictions b and a_2 as hinges, we get the circular arc γ_2 touching s . Note, since γ_1 touches the first edge of K after b one restriction of γ_2 can be found along this edge. Then only the shaded region bounded between γ_1 and γ_2 needs to be examined in further steps. The next circular arc γ_3 passing through a_3 and touching s is depicted on the right. As γ_3

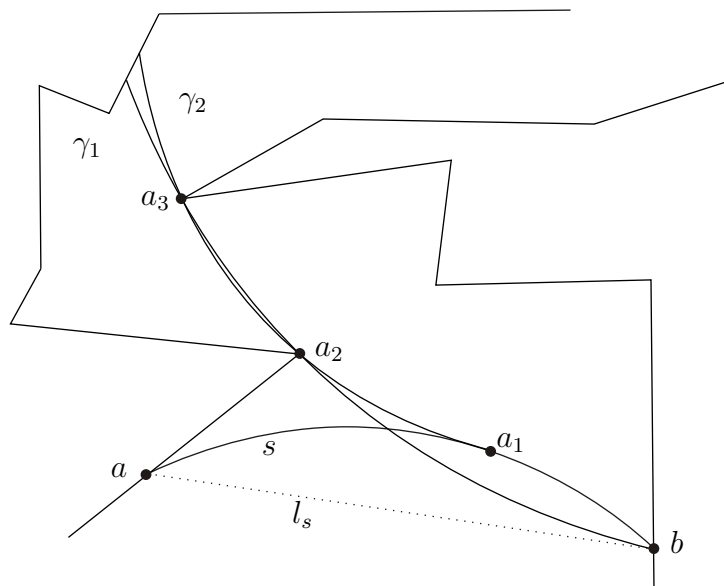


Figure 71: The arc γ_1 is a blocking arc with respect to b and l_s but is not feasible with respect to s . However, γ_2 can be computed using the restrictions a_2 and a_3 of γ_1 as hinges.

comes into contact with another right restriction a_4 , the hinges a_3 and a_4 are changed. Finally, the blocking arc γ_4 associated with the window with respect to s is constructed.

In case of a destination channel, where a destination segment d is given additionally, we can improve our method.

4.4.2 Improvements for Start-Destination Channels

Let us denote the window with respect to $a = S(s) \in K_l$ and $b = E(s) \in K_r$ by ω_a and ω_b respectively. Since almost the same argumentation can be applied in the case of d being circularly visible from s by the results of Lemma 3.4.20, we can assume $\text{tr}(d) \cap V_K(\sigma) = \emptyset$. Whether a visibility arc is the window with respect to (K, s, σ, d) or not, can be easily checked by Theorem 3.4.8 and Theorem 3.4.19 respectively. Hence we can improve the strategy. However, the worst case complexity doesn't change, and this is also true for the edge case, as we already know.

As for instance the case of a starting arc appears when constructing the second till the last segment of a continuous minimum arc path, it is reasonable to clip the polygon to a subpolygon of K which includes $\text{tr}(s)$ and $\text{tr}(d)$ and has as a minimal number of vertices. Thus, although clipping the polygon K doesn't change the time complexity needed for computing a minimum arc path, we can improve the absolute runtime since

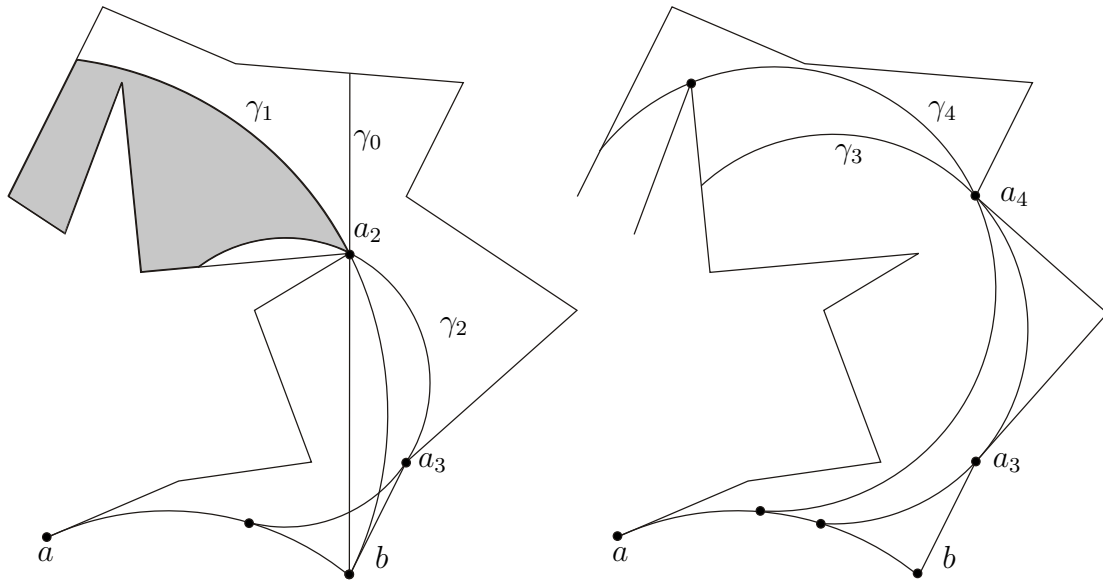


Figure 72: Illustration for the strategy used for computing the circular visibility of an arc.

the complexity of input data is reduced. For this purpose, we distinguish between two cases.

Definition. Let s' be the oriented arc with $\text{tr}(s') = \text{tr}(s)$ starting at a and ending in b . Then s is said to be *introverted* if s' is CW oriented, else it is called *extroverted*. (see Figure 73).

Let us first assume that s is introverted. Then we can consider the line segment l_s defined by a and b , which is the chord of $\text{tr}(s)$. Although this line segment does not generally stay in $\overline{I_K}$, there are points $a_0 := a, \dots, a_m := b \in \text{tr}(s)$, which are enumerated by the orientation of s , s.t. the corresponding line segments $l_i := [a_i, a_{i+1}]$ are subsets of $\overline{I_K}$. When replacing s by the vertices $\{a_i\}_{i \in \{0, \dots, m\}}$ and line segments l_i respectively, a new polygon Q can be generated. We then clearly obtain $\text{tr}(d) \subset Q$, and therefore we call Q a *sub-polygon of K* . Besides, $K \setminus Q$ is also a polygon.

Let J be the circle segment defined by $\text{tr}(s)$ and l_s , i.e. the region bounded by s and l_s , and let n_2 be the number of vertices included in the connected component of $\overline{J} \cap \overline{I_K}$ containing $\text{tr}(s)$. Denoting the number of vertices in $V_K(\sigma)$ by n_1 , we can ensure that the inequality $1 \leq m \leq \max(n_1, n_2)$ for the minimal number m holds. However, in many practical applications m is just 1 or 2 and therefore the number of vertices of Q is considerably smaller than n (cf. Fig. 73). Likewise, we are also able to construct a

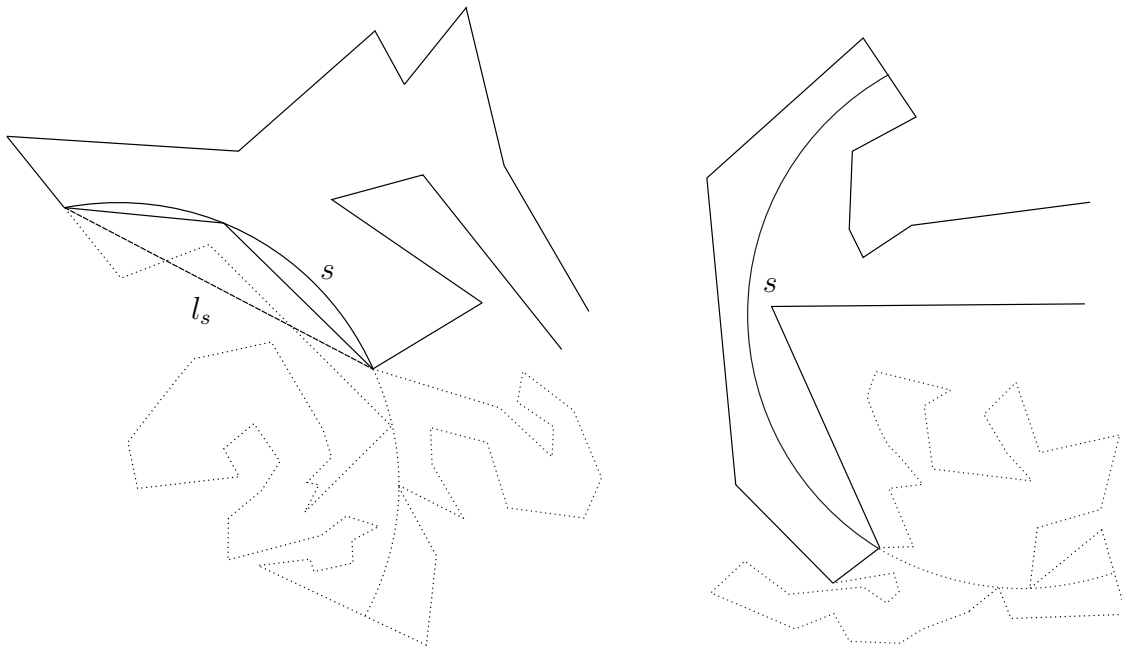


Figure 73: Illustration of introverted (left) and extroverted (right) case. In each case, we consider that s is the window of a previous step when computing a continuous minimum arc path. The subpolygon Q is depicted by the solid lines.

polygon with quite a small number of vertices in the extroverted case, as indicated in Figure 73 on the right.

4.4.3 The Time Complexity

Similar to Section 4.3, we can establish time complexity of $O(kn_1) = O(ln_1)$, where k is the number of CVDs computed and l is the number of vertices in Q . Eventually, we can only ensure quadratic runtime. When computing $\omega_{\mathfrak{D}}$ for a start-destination channel \mathfrak{D} we may make some improvements, but in the worst case the time required is still $O(ln_1) = O(n^2)$.

4.5 Continuation Channels and CVDs

Let (K, s, σ) be a continuation channel where K is a polygon with n vertices and s is an oriented arc. We then have to distinguish between two cases. In the first one (K, s, σ) is degenerate whereas in the second one it is not degenerate. In any case, we want to use an approach for examining the corresponding blocking arcs which is similar to that presented in the previous sections.

4.5.1 Sketch of the Overall Algorithm

First, let us focus on a degenerate continuation channel, where every blocking arc γ has an alternating sequence (a_1, a_2, a_3) of length 3 with a pseudo restriction point a_1 . This pseudo restriction is given by the necessity of touching s , which is induced by the degenerate unidirectional restriction map σ . In Section 4.3 and 4.4 we presented a strategy for dealing with this problem: Compute CVDs for certain vertices and merge them with the bisector of $tr(s)$ and the respective base point of the CVD.

Hence we can center on the more sophisticated case of a non-degenerate continuation channel. Although we would also be able to present an algorithm within the most general scope, we focus on a continuation channel (K, s_a, σ_a) for some $a \in \overline{I_K} \setminus V_K(\sigma)$ s.t. $V_K^2(\sigma) \cap tr(d) = \emptyset$, and we concern ourselves with the computation of the window $\omega^{(a)}$. If we have a start-destination channel $\mathfrak{D} := (K, s, \sigma, d)$ and $a \in tr(d)$, this is exactly the situation that sets in when computing a smooth minimum arc path; therefore it is most important for our interests.

Let (a_1, a_2, a_3) be the a -adapted alternating sequence of $\gamma^{(a)}$. W.l.o.g. we can assume $a_2 \in K_l$ and $a_3 \in K_r$ and define $s_1 := [a_2, a_3]_\gamma$ and $s_2 := tr(\omega^{(a)})$ (cf. Figure 74). Furthermore, we can assume windows η_1, \dots, η_m corresponding to blocking arcs reaching $V_K^a(\sigma)$. Although K_a is not a polygon, we can use the algorithms introduced in the previous sections. For this purpose, we first summarize the essential steps and illustrate the strategy by two examples later on.

Let K'_a be a subpolygon of K including K_a , which can be generated by a strategy similar to the one introduced in the previous section. We first compute the blocking arc γ_1 which is associated with the window with respect to s_1 and a in K'_a , as suggested in Section 4.3 and 4.4 respectively, depending on whether $\gamma^{(a)}$ is a line segment or not. If this arc stays inside $\overline{I_{K_a}}$, which can be checked by an intersection test with η_1, \dots, η_m , the

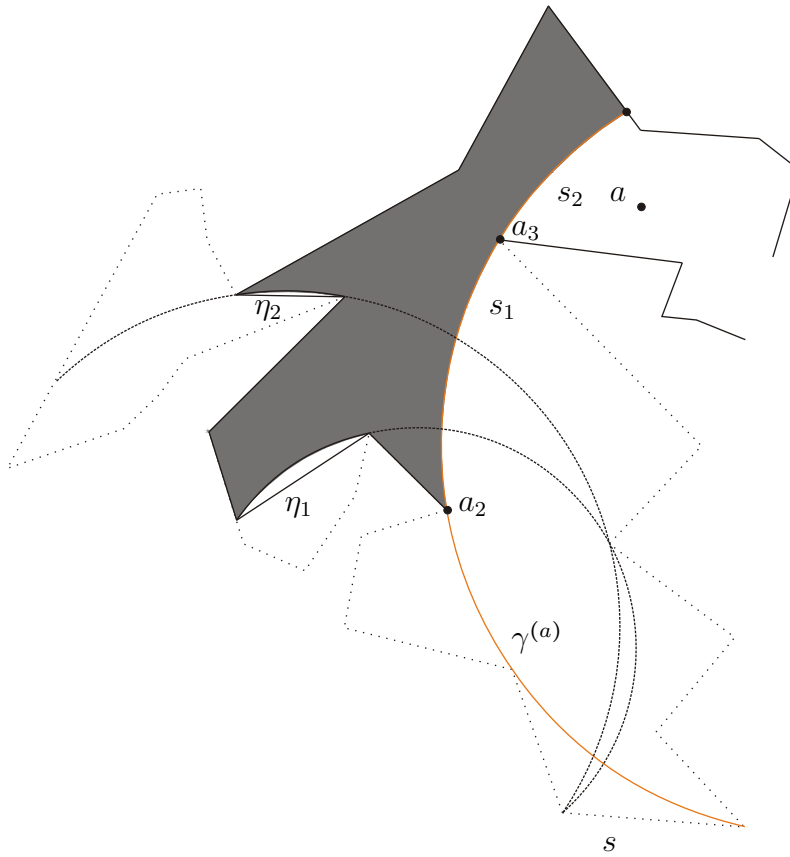


Figure 74: Continuation channel (K_a, s_a, σ_a) ; solid line: K_a ; $\gamma^{(a)}$ blocking arc of a .

starting restriction σ_a is satisfied automatically, and hence it yields the desired window. If not, we have $S(\gamma_1) = a_3$ (cf. Figure 76) or γ_1 doesn't stay in $\overline{I_{K_a}}$. In the latter case, γ_1 intersects an η_i for some $i = 1, \dots, m$, and we compute the blocking arc γ'_1 which is associated with the window of (K'_a, η_i, σ_i) , where σ_i is the degenerate unidirectional restriction map of η_i . Then we check if γ'_1 and $\gamma_{\mathfrak{E}_a}$ are equal.

It remains to consider the case $S(\gamma_1) = a_3$. In this case, we compute the blocking arc γ_2 of a regarding the channel $\mathfrak{E}'_a := (K'_a, s_2, \sigma')$, where σ' is the degenerate unidirectional restriction map of s_2 . Then the starting point $S(\gamma_2)$ is a pseudo restriction with respect to \mathfrak{E}'_a and a left/right restriction with respect to \mathfrak{E}_a . If $\mathcal{A}(\gamma_2) = 2$ with respect to \mathfrak{E}_a , we have $\gamma_2 \neq \gamma_{\mathfrak{E}_a}$. However, in this case $\gamma_{\mathfrak{E}_a}$ is located in the deficiency set of γ_2 and γ_1 or γ'_1 respectively. Thus, it can be computed with the methods introduced in the previous sections.

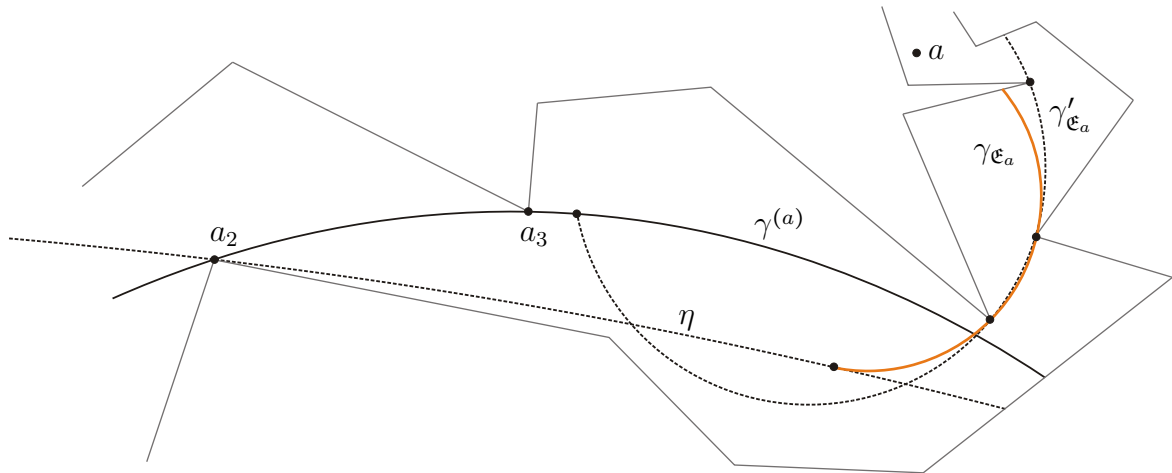


Figure 75: Algorithmic approach to a continuation channel $\mathfrak{E}_a := (K_a, s_a, \sigma_a)$. The blocking arc $\gamma_{\mathfrak{E}_a}$ can be computed by the requirement of touching the blocking arc η .

We now illustrate our algorithmic approach in case of a non-degenerate continuation channel by giving two examples:

Example. Let us assume the situation in Figure 75, where a non-degenerate continuation channel $\mathfrak{E}_a := (K_a, \sigma_a, s_a)$ with a window η reaching $V_K^a(\sigma)$ is visualized. The window with respect to (K'_a, s, σ) isn't equal to the window $\omega_{\mathfrak{E}_a}$ since the corresponding blocking arc $\gamma'_{\mathfrak{E}_a}$ has an intersection with $\text{tr}(\eta) \cap \overline{I_K \setminus V_K(\sigma)}$ and therefore it doesn't stay in $\overline{I_{K_a}}$. The window $\omega_{\mathfrak{E}_a}$ can then be obtained by the requirement of touching η .

Figure 76 shows another example of a continuation channel $\mathfrak{E}_a := (K_a, s_a, \sigma_a)$ defined by the blocking arc $\gamma^{(a)}$, which has the a -adapted alternating sequence (a_1, a_2, a_3) . As the starting point of the blocking arc γ_1 , which is associated with the window with respect to s_1 and a , is a_3 , γ_2 is computed, as suggested above. In this example, the blocking arc $\gamma_{\mathfrak{E}_a}$ is located in the deficiency set of γ_1 and γ_2 . Hence it can be found by the strategy proposed by Chou et al., which we introduced in Section 4.3 and 4.4.

The whole strategy for computing $\omega_{\mathfrak{E}_a}$ is summed up in Algorithm 6.

In order to improve the readability, we keep off a detailed algorithmic description for the computation of the circular visibility set of an arbitrary continuation channel, as already mentioned. Moreover, the procedure for an arbitrary continuation channel can be deduced from all methods introduced, and it works in a complete analogy.

Algorithm 6 Computation of the window $\omega_{\mathfrak{E}_a}$

Input: Continuation channel $\mathfrak{E} := (K, s, \sigma)$; $\gamma^{(a)}$ with a -adapted alternating sequence (a_1, a_2, a_3) ; windows ν_1, \dots, ν_m reaching $V_K^a(\sigma)$;

Output: Window $\omega_{\mathfrak{E}_a}$

- 1: Construct s_1 and s_2
- 2: $\mathfrak{E}_a \leftarrow (K_a, s_a, \sigma_a)$
- 3: **if** \mathfrak{E}_a is degenerate **then**
- 4: Compute $\omega_{\mathfrak{E}_a}$ by intersecting CVDs with the bisector defined by s_2 and the respective basepoints
- 5: **return** $\omega_{\mathfrak{E}_a}$
- 6: **end if**
- 7: Construct K'_a
- 8: Compute window ω_1 and corresponding blocking arc γ_1 w.r.t. s_1
- 9: **if** $\text{tr}(\gamma_1) \cap \text{tr}(\nu_i)$ for some $i = 1, \dots, m$ **then**
- 10: $\omega_1 \leftarrow$ window w.r.t. degenerate channel of ν_i
- 11: $\gamma_1 \leftarrow$ corresponding blocking arc
- 12: **end if**
- 13: **if** ω_1 equals $\omega_{\mathfrak{E}_a}$ **then**
- 14: **return** ω_1
- 15: **end if**
- 16: Compute the window ω_2 and the corresponding blocking arc γ_2 w.r.t. the degenerate channel given by s_2
- 17: **if** ω_2 equals $\omega_{\mathfrak{E}_a}$ **then**
- 18: **return** ω_2
- 19: **end if**
- 20: Compute $\omega_{\mathfrak{E}_a}$ using the hinges given by γ_1 and γ_2
- 21: **return** $\omega_{\mathfrak{E}_a}$

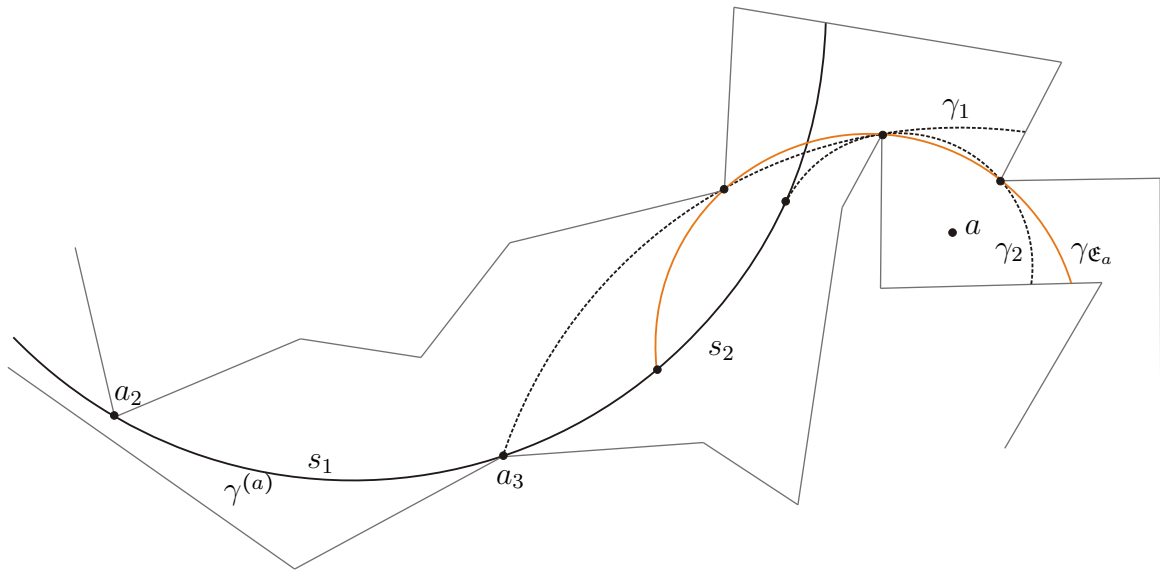


Figure 76: Algorithmic approach to a continuation channel $\mathfrak{E}_a := (K_a, s_a, \sigma_a)$. The blocking arc $\gamma_{\mathfrak{E}_a}$ is located in the deficiency set of γ_1 and γ_2 .

4.5.2 The Time Complexity

For both cases, the degenerate and the non-degenerate one, we can ensure a time complexity of $O(kn)$, where k is the number of CVDs computed. The complexity needed in the degenerate case has already been estimated in Section 4.4.

Assuming an arbitrary tolerance channel $\mathfrak{E} := (K, s, \sigma)$, a point $a \in \overline{I_K} \setminus V_K(\sigma)$ and the corresponding continuation channel $\mathfrak{E}_a = (K, s_a, \sigma_a)$, we can even give a preciser estimate than $O(kn)$. By the same argumentation as in the previous sections, we obtain: The number of all CVDs which have to be computed at most is bounded by the number of vertices l in $V_K(\sigma) \cup V_{K_a}(\sigma_a) \cup V_{K_a}(\sigma_2)$, where σ_2 is the starting restriction given by s_2 . When testing if the computed window is equal to $\omega_{\mathfrak{E}_a}$, we possibly have to check if the starting condition σ_a is satisfied, which can be done in $O(1)$, and do the intersection test with the blocking arcs η_1, \dots, η_m , which requires $O(m) = O(l)$ time. Hence the window $\omega_{\mathfrak{E}_a}$ can be computed in $O(l(n+m)) = O(ln)$ time. However, in many practical tests the number of CVDs to be computed averages just about two or three.

We can deduce similar results for an arbitrary continuation channel, which is not necessarily induced by a blocking arc computed in any previous step, but we don't explain this general case in detail here.

4.6 Minimum Arc Paths and CVDs

Let $\mathfrak{D} := (K, s, \sigma, d)$ be a start-destination channel with a polygon K , which has n vertices, and we set $\mathfrak{E} := (K, s, \sigma)$. We now summarize the several steps for computing a (smooth) minimum arc path. In the previous section we have seen how to implement the several steps of Algorithm 1 and 2 in case of a polygon efficiently by using CVDs, and we now estimate the overall complexity for this implementation. We first concern ourselves with the computation of a smooth minimum arc path.

4.6.1 The Smooth Case

Let us assume that we have already found the window with respect to the start-destination channel \mathfrak{D} . Then in every subsequent step, we have to consider the continuation channel \mathfrak{E}_i , which is of the type (K_a, s_a, σ_a) for some $a \in \text{tr}(d)$ not circularly visible in the current step. Hence the situation discussed in the previous section is given in every step since we concerned ourselves with both the degenerate and the non-degenerate case. Carrying on till $\text{tr}(d)$ is circularly visible, we characterize the whole *forward step* of Algorithm 1. We can apply the proceeding of Section 4.5 in every iterative step. Roughly speaking, the particular continuation channels, which have to be considered, don't overlap too much. Since we can always achieve a 'uniform distribution' of the breakpoints (cf. Corollary 3.6.16 and Theorem 3.6.20), we have to invest $O(nn_i)$ time in every single step, where n_i is the number of vertices in $V_K^{i+1}(\sigma) \setminus V_K^{i-1}(\sigma)$ with $V_K^0(\sigma) := \text{tr}(s)$. Thus, the time required for the forward step when computing a smooth minimum arc path is

$$\sum_{i=1}^N O(n_i n) = O(n^2),$$

where $n_0 := 0$ and N is the minimal number with $V_K^N(\sigma) \cap \text{tr}(d) \neq \emptyset$. Note that we have $N \leq n(d)$, but in general these numbers are not equal, where $n(d)$ is the number defined in Definition 3.7.2.

In the *backward step* we get all the predecessor segments by constructing an arc with two alternating restrictions and smoothly joining its successor. For this purpose, we just have to examine degenerate continuation channels given by the successor segment and check the requirements of the channels \mathfrak{E}_i with $\mathfrak{E}_1 := \mathfrak{E}$. These requirements are given by the continuation condition for the corresponding predecessor or the starting

condition σ given by s respectively. Additionally, it has to be checked whether the current segment stays inside the corresponding tolerance channel or not, which can be done by an intersection test with blocking arcs: Considering that we have already computed the i -th segment γ_i of our interim¹ minimum arc path $\gamma_1 \cdots \gamma_N$, we can construct the segment γ_{i-1} by examining the blocking arcs of the degenerate continuation channel given by γ_i and the sub-polygon including s , which satisfy the (D)CC of \mathfrak{E}_i induced by $(i-1)$ -th blocking arc or s for $i = 1$. Since $\sum_{i=1}^N n_i = O(n)$, the whole backward step needs

$$\sum_{i=1}^N O(n_i n) = O(n^2)$$

time as well.

If necessary, $\gamma_1 \cdots \gamma_N$ has to be smoothed. Considering a non-smooth breakpoint a_i , we can assume w.l.o.g. that $a_i \in K_l$. After computing the distance $\delta := \text{dist}(a_i, K_r)$, which costs $O(n)$, we can construct a biarc $\tilde{\gamma}$ smoothly joined to γ_i and γ_{i+1} with $\text{tr}(\tilde{\gamma}) \subset B_\varepsilon(x)$ for some $x \in \overline{I_K}$ and $\varepsilon < \delta/2$ s.t. $B_\varepsilon(x) \subset \overline{I_K}$. Since this procedure can be done in $O(1)$, the complexity for the complete smoothing step can be bounded by $O(Nn)$, and we have $N < n$.

Altogether, we can show a quadratic runtime complexity depending on the number of vertices n but not on the number of segments N . However, in our practical tests we discovered a sub-quadratic runtime.

In the second subsection, we discuss the algorithmic details of computing a continuous minimum arc path in a polygonal start-destination channel. Again, we estimate the time complexity needed.

4.6.2 The Continuous Case

Due to Algorithm 2, we have to compute the window of the constantly shrunk polygon with respect to the previously calculated window in every single step when constructing a continuous minimum arc path. As we have seen in Section 4.3 and 4.4, the time required for determining the window with respect to a given edge or arc s is $O(kn)$, where k is the number of CVDs computed. If $\gamma_1, \dots, \gamma_N$ is the sequence of circular arcs computed by Algorithm 2, the total time required is $O(kn)$ with $k := \sum_{i=1}^N k_i$, and k_i is

¹Possibly the resulting path is a generalized visibility spline with some non-smooth breakpoints, which means $N < n(d)$.

number of CVDs constructed in the i -th step. As k_i is limited by the number of vertices n_i in $V_{K_i}(\sigma_i) \setminus V_{K_{i-1}}(\sigma_{i-1})$ depending on the $(i-1)$ -th window $\omega_{\mathfrak{D}_{i-1}}$ (cf. Section 3.7), the worst-case total time is ($n_0 := 0$):

$$\sum_{i=1}^N O((n_i n)) = O(n^2),$$

since $O(\sum_{i=1}^N n_i) = O(n)$ holds.

Note that the overall time does not depend on the number of segments needed but only on the number of vertices. Similar to the smooth case, practical examples mostly show a sub-quadratic runtime performance.

Note that both the smooth and the continuous case yield a quadratic algorithm, although the computing of a smooth minimum arc path is much more sophisticated. As a matter of course, the absolute runtime in the smooth case is higher than the absolute runtime in the continuous case, when considering the same start-destination channel.

4.7 Summary and Experimental Results

4.7.1 Summary

In this chapter, we have thoroughly discussed the algorithmic implementation of the mathematical results presented in Chapter 3. We have described efficient algorithms to generate a continuous and smooth minimum arc path. In general, Algorithm 1 and 2 work for every start-destination channel bounded by a piecewise restricted analytic curve. Concerning a simple polygon with n vertices, we have shown that both a smooth and a continuous minimum arc path can be computed in $O(kn) = O(n^2)$ time, where k is the number of CVDs required. In many practical applications k has the same order as the number of segments N , and N is considerably smaller than n , as already mentioned. In the next subsection, we present some test results, which show this coherence.

4.7.2 Test Results

We have evaluated the performance of the presented algorithms in several scenarios and mainly focused on polygonal channels for our tests. Nevertheless, we have also implemented an algorithm that computes a smooth and continuous minimum arc path in start-destination channels given by an arc spline. However, we waived an efficient implementation in this case.

Figures 77, 78 and 79 show two examples of these test scenarios. For each polygon, we compared the number of segments and the CVDs needed regarding a minimum link, a continuous and a smooth minimum arc path. The particular numbers are listed in Table 4.1.

Scenario	Number of	min. link	continuous	smooth
Polygon 1 with 1047 vertices	segments	29	18	29
	CVDs	-	54	108
Polygon 2 with 61 vertices	segments	13	9	17
	CVDs	-	20	40

Table 4.1: Two exemplary test scenarios, which are visualized in Figure 77-79.

In Chapter 5 we present further examples and show how our algorithm can be used for approximating real data extracted from digital images or curves.

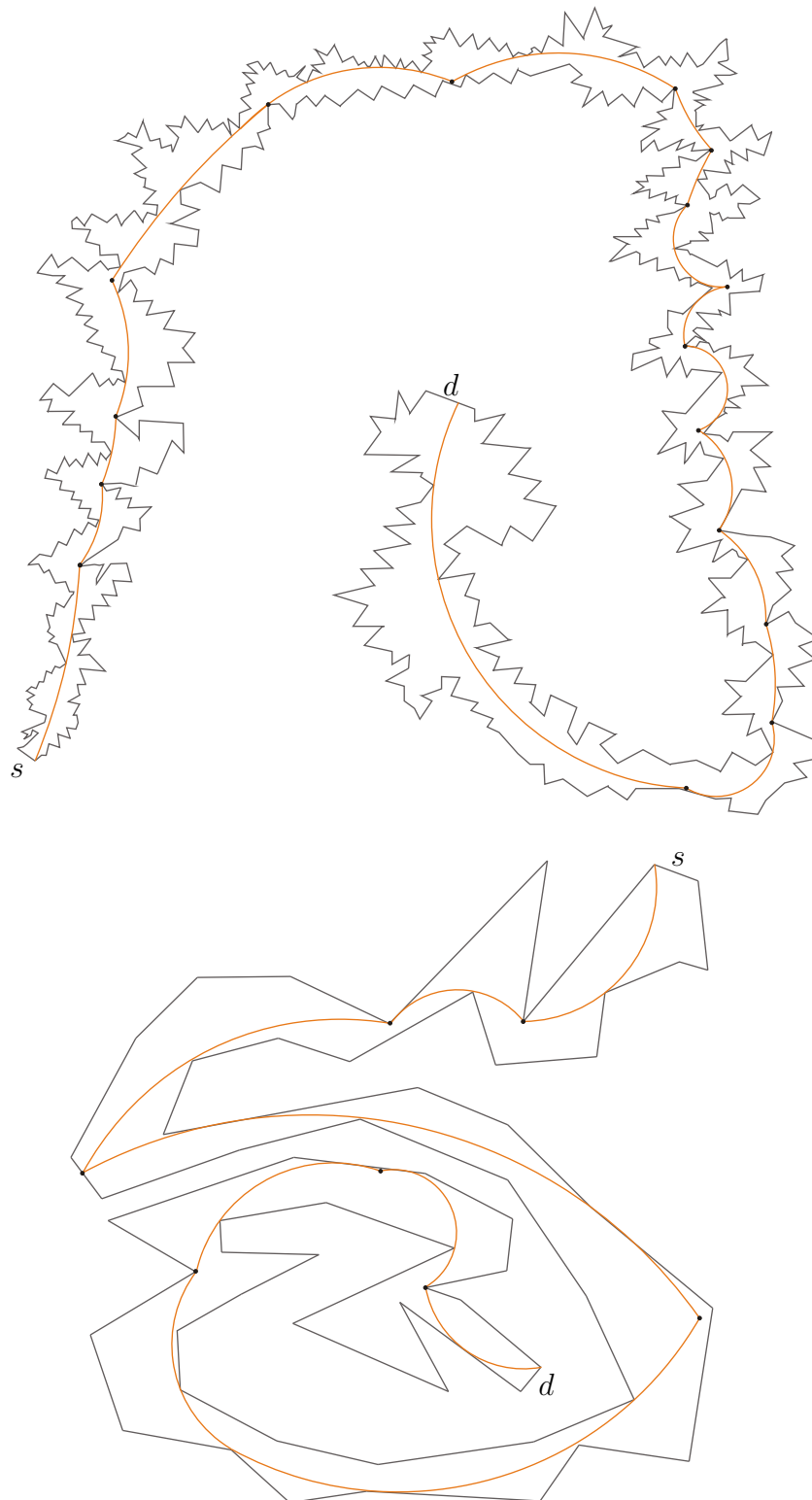


Figure 78: Example of two start-destination channels given by simple polygons and corresponding continuous minimum arc paths. Top: 1047 vertices; 18 segments; Bottom: 61 vertices; 9 segments;



Figure 79: Example of two start-destination channels given by simple polygons and corresponding continuous smooth arc paths. Top: 1047 vertices; 29 segments; Bottom: 61 vertices; 17 segments;

5

APPLICATIONS

In this chapter we thoroughly discuss various applications of minimum arc paths. We mainly sketch how the algorithms presented in the previous chapter can be used for Reverse Engineering, Object Detection and Curve Approximation. Furthermore, we point out the advantages of the usage of smooth arc splines as approximating curves within the scope of these applications.

Since we deal with contours of digital (grey scale) images in our applications, we roughly explain what contours are and how they can be represented conveniently in section 5.1. A suitable way of encoding contours yields an effective base for all the applications discussed here. As there are many well-known methods for representing contours, we introduce some of them and compare them with our approach, which suggests a description by arc splines.

In all the application examples we present, the starting situation is always the same. We consider a list of points, wherever they were extracted from, and want to approximate them by a (smooth) circular arc spline. With respect to a maximum error, we are seeking for a solution with the minimum number of segments. As we want to use the algorithms

*‘He who loves practice without theory is like the sailor
who boards ship without a rudder and compass and
never knows where he may cast.’*

(Leonardo da Vinci, Italian polymath)

presented in Chapter 4, we elucidate the design of suitable start-destination channels in Section 5.2.

Representing shapes by (smooth) circular arc splines is an efficient approach for detecting search objects in grey scale images. Hence we illuminate the field of Shape Recognition in Section 5.3. Thereby, we only amplify the coding of the search objects and don't present a complete method for detecting and classifying an object.

In Section 5.4, we address the problem of generating a masterpiece of an object by smooth circular arc splines. In contrast to the outline already given in Section 1.1, we focus on the issue of using such a masterpiece for visual quality control and vision metrology in manufacturing.

In the last section of this chapter, we describe how to use almost the same algorithmic approaches in order to approximate arbitrary curves, like polygons, NURBS or graphs of a real valued function, by smooth circular arc splines.

5.1 Edge Contours and Forms of Representation

For almost all the applications we subsequently elucidate, we consider contours or contour lists respectively that have been extracted from a camera image. However, before we start our discussion on how to approximate them by a smooth arc spline, we reason what is understood by contours in Computer Vision. For this purpose, we have to use some standard notions from Computer Vision. Since an introduction of all basic terms would go beyond the scope, we refer the readers unfamiliar with these notions to further literature (e.g. [42, 50, 66]).

We mainly devote ourselves to two questions: How to define contours and how to encode them?¹

5.1.1 What are contours?

In literature no uniform answer to this question exists, although the detection of edges is a central problem in Computer Vision and Image Processing since edges mark the borders of objects which are observed by a camera.

Algorithms for extracting bounding curves of image ‘objects’ are usually called *edge detectors*. Depending on the application, the requirements of edge detectors vary considerably, but most of them search for pixel indices with high values of the gradient norm which results from some local approximation of grey values. One of the standard methods for edge detection is the *Canny Edge Detector*² (cf. [18]). The problem of the Canny Edge Detector and most of the other methods is the choice of parameters which are required. The output of an edge detector usually consists of many pixel indices, some of them being parallel to the same edge. *Non-maximal suppression*³ is an approach which yields a representation of edges with a width of one pixel.

However, the term ‘contour’ is not defined this way. Figuratively speaking, contours are outlines or boundaries of objects in a real scene which are observed by a camera image. Since they yield steep grey-scale transitions if somewhat articulate contrast is

¹The following overview mainly follows [66] and [50].

²Canny considered the mathematical problem of deriving an optimal smoothing filter given the criteria of detection, localization and minimizing multiple responses to a single edge.

³Non-maximum suppression means that given the presmoothing filters, edge points are defined as points where the gradient magnitude assumes a local maximum in the gradient direction (cf. [18]).

given, positions of the image with absolute large gradients are examined. Obviously, the term 'gradient' is well-defined only for stepless functions. Also, the contours should not depend on any thresholds. An approach to an exact definition can be found in [66]. Using this definition in the non-discrete case, the contour points are a union of the traces of some curves. Due to the digitalization of an image, the contours are not given by continuous functions but only by so-called *contour point lists*. Due to Definition 5.2.15 in [66], it is legitimate to perceive a contour point list as a finite family $(p_i)_{1 \leq i \leq k}$ of pairwise distinct points in \mathbb{R}^2 s.t. the polygonal curve passing through these points, starting at p_1 and ending in p_k is simple or a Jordan curve. If p_1 and p_k are neighbors regarding the *Moore neighborhood* (cf. [42]), we call it **closed**.

To sum it up, edge detection results in a sequence of adjacent contour pixels. If bifurcations and crossings are omitted, the pixel positions of a single contour sequence are supposed to belong to the same curve (cf. [66]).

Now we can concern ourselves with answering the second question: How to encode contours?

5.1.2 Encoding contours

The simplest representation of a contour is using an ordered list of its edge points. This is as accurate as the location estimates for the edge points. However, a contour point list isn't a very compact representation and it is not very effective for subsequent image analysis.

A more powerful representation is fitting an appropriate curve which has some analytical description, like line segments, circular arcs or conic segments. For instance, fitting a line to a set of edge points that lie along a line, results in a considerably more compact and efficient representation for subsequent image analysis. When talking about curve fitting, we have to be more precise. Do we want to interpolate or approximate the curve? Curve interpolation methods are more appropriate when the edges have been extracted accurately. However, in practice, curve approximation methods yield better results because the edge locations can not be extracted very accurately because of e.g. digitizing effects. Using mathematical curve descriptions to approximate such a sequence of pixels results in a compact and effective representation and, therefore, it is useful for *shape representation* (cf. [12]), *data reduction* (cf. [67]) and *feature extraction* (cf. [52]). The

approximating curve can also be used for structural analysis of the sequence of pixels and is very useful for Reverse Engineering techniques.

When dealing with approximation tasks, we have to tell how the approximation error is defined, which means how to measure the error between the pixel positions $p_1, \dots, p_n \in \mathbb{R}^2$ and the approximating curve γ . For instance:

- The *mean squared error* gives an overall measure of the deviation of the curve from the edge points since it is defined by

$$\frac{1}{n} \sum_{i=1}^n \text{dist}(p_i, \text{tr}(\gamma))^2.$$

- The *normalized maximum absolute error* regards the ratio of the maximum absolute error to the length of the curve. Therefore, the error becomes independent of the length of the curve $L := \text{len}(\gamma)$. It is defined by

$$\frac{1}{L} \max \{ \text{dist}(p_i, \text{tr}(\gamma)) \mid i \in \{1, \dots, n\} \}.$$

- The *maximum absolute error*, which measures how much the points deviate from γ in the worst case, is given by

$$\max \{ \text{dist}(p_i, \text{tr}(\gamma)) \mid i \in \{1, \dots, n\} \}.$$

How to measure the error is a question of modeling and we will provide an answer to that question later on.

We also have to define which class of curves we want to take into account. To obtain compatibility with CAD-representations, the curve should consist of basic primitives such as line segments and circular arcs (cf. [79]), i.e. an arc spline. Due to [42], reasonable fitting models are polygonal curves, arc splines or conic splines.

Using line segments leads to a polygonal representation that fits the edge points with a sequence of line segments. Thus, the contour is represented as a polygon which interpolates a selected subset of edge points. In general, there are various ways to compute the polygonal approximation of a contour:¹

A representation by polygonal curves is more economical than using edge points. We can make the error as small as desired by splitting the contour into very small line segments.

¹For a detailed description have a look at e.g. [50].

Once an edge list has been approximated by line segments, subsequences of the line segments can be replaced by circular arcs. This involves fitting circular arcs through the endpoints of two or more line segments. Of course, the number of segments decreases this way, but it is still relatively large. In any case, arc splines are very suitable for representing contours since they are invariant with respect to translation, rotations and scalings (cf. Proposition 2.5.28), and their curvature functions are piecewise constant. Conic sections¹, which correspond to zero sets of second degree polynomials, allow more complex contours to be represented by fewer segments; however, the computational complexity increases.

Both the number of segments and the accuracy of an approximation are important criteria. As the approximation error diminishes if the number of segments increases, we have to tackle a multi-objective problem. Contour pixels can be extracted only with a certain accuracy. Therefore, the contour approximation problem can be formulated by specifying a tolerance and looking for the smallest number of curve segments s.t. the error of approximation does not exceed the given tolerance (cf. [81]). Hence we consider an approximation problem with respect to the maximum absolute error as defined above. In order to compute an approximation s.t. the determined arc spline is within a specified (possibly locally varying) tolerance $\varepsilon > 0$ to the pixel positions, developing a suitable start-destination channel and computing a smooth minimum arc path lends itself as a good solution. Therefore, the next section is dedicated to the development of suitable tolerance channels.

¹For instance, segments of hyperbolas, parabolas and ellipses are conic sections. An exact definition can be found in Chapter 6.

5.2 Design of Suitable Channels

We suppose a finite family of points (p_1, \dots, p_N) with $P := \{p_1, \dots, p_N\}$ s.t. the polygonal curve ω successively passing through the points p_i , starting at p_1 and ending at p_N is simple. The cyclic case, i.e. P is supposed to lead to a Jordan curve, can be done analogously. As already indicated, we address the approximation of P by a (smooth) arc spline with a minimal number of segments under the constraint of satisfying the bounding requirements of an error function. Hence we consider the optimization problem

$$\min_{\gamma \in \mathcal{G}^\infty} |\gamma| \text{ subject to } \Phi(\text{tr}(\gamma), P) < C$$

for some $C > 0$ and error function Φ . As justified beforehand, dealing with the maximum norm

$$\Phi(\text{tr}(\gamma), P) = \max_{i=1, \dots, N} \text{dist}(p_i, \text{tr}(\gamma))$$

or the Hausdorff-distance of $\text{tr}(\omega)$

$$\Phi(\text{tr}(\gamma), \text{tr}(\omega)) = \mathfrak{h}(\text{tr}(\gamma), \text{tr}(\omega)) = \max \left(\max_{x \in \text{tr}(\omega)} \text{dist}(x, \text{tr}(\gamma)), \max_{x \in \text{tr}(\gamma)} \text{dist}(x, \text{tr}(\omega)) \right)$$

would be appropriate. Choosing one of these proposed norms, it isn't sure if there exists a constructive solution to the optimization problem formulated above at all. Also it isn't clear how such an approach should look like. Hence we concern ourselves with the design of a suitable start-destination channel \mathfrak{D} and use the methods proposed in Chapter 4. However, computing a smooth minimum arc path of \mathfrak{D} is not necessarily equivalent to the problem formulated above. Nevertheless, this approach has a considerable advantage. We are able to control the behavior of the approximating curve between each two points p_i and p_{i+1} by the bounding channel. This way we also get geometric constraints, which can be locally varied in quite an easy manner and are easier to modify than constraints defined by a metric or norm.

5.2.1 Offset Channels

When computing an approximation s.t. the determined arc spline is within a specified tolerance $\varepsilon > 0$ to the p_i , the offset $\Omega_\varepsilon(\omega) = \{a \in \mathbb{R}^2 \mid \text{dist}(a, \text{tr}(\omega)) = \varepsilon\}$ of the polygonal path ω can be considered (e.g. Figure 80). In Remark 2.5.30, we have already mentioned that for sufficiently small ε , the offset curve of a polygonal is an arc spline. If we want

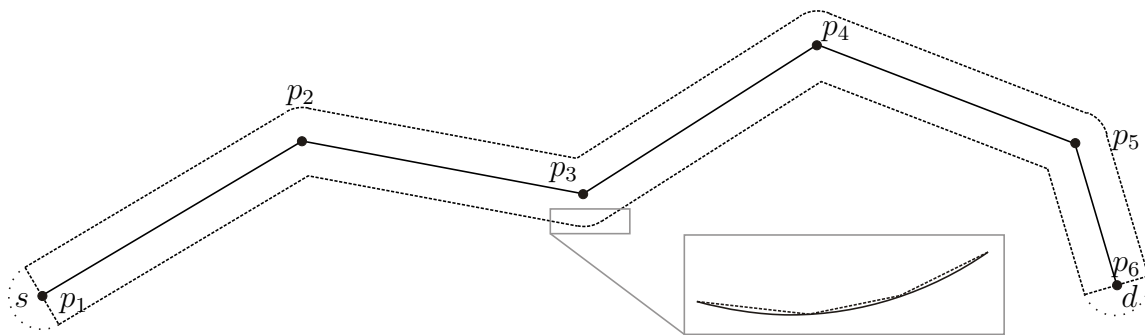


Figure 80: Polygonal path from p_1 to p_6 and offset curve (dashed arc spline) for some $\varepsilon > 0$; s and d are two line segments passing through p_1 and p_6 respectively.

to use our CVD-based approach, we can again approximate the arcs in the offset by a polygonal path (see Figure 80) in order to obtain a polygon channel, where mostly the semi-circles at p_1 and p_N are replaced by a start and a destination line segment. Generally speaking, the ε -Offset is a region formed from strips of width 2ε which are centered at the polygon edges. Thus, in a neighborhood of sharp corners this doesn't guarantee that the curve remains close to the given points. Therefore, Drysdale et al. suggest a so-called *polygonal tolerance region* in [33]. They also want their approximating curve to have distance at most $\varepsilon > 0$ from $\text{tr}(\omega)$. Figure 81 shows an example of a polygonal tolerance region, which ensures $\mathfrak{h}(\text{tr}(\gamma), \text{tr}(\omega)) \leq \varepsilon$ for every curve γ from $\text{tr}(s)$ to $\text{tr}(d)$ staying inside the closure of this region.¹ Although the channel depicted in Figure 82 might not exactly guarantee a Hausdorff distance less or equal ε , it is appropriate if P doesn't yield sharp corners. Furthermore, it can be computed straightforwardly and is sufficient for most applications with real data.

The corresponding restriction maps σ arise from the continuation channels defined by the constructive approach for computing a (smooth) minimum arc path. If we have some preliminary knowledge of some parts of the curve which should be our result, we can flexibly adapt the tolerance channel passing through this part. For instance, knowing that in a certain neighborhood there should be a line not an arc segment, we can search for the linear window in this area. Furthermore, if we want the approximation to have vertices, we choose the tolerance channel located in a corresponding neighborhood to be a starting not a continuation channel.

¹A more detailed description can be found in [33].

5.2.2 Other Channels and Preliminary Approximations

Varying the width at different points can also be taken into account if at some local parts of P there are different tolerance requirements. Held and Eibl propose *asymmetric tolerance bands*, which are important for approximations used by NC machines¹ (cf. [46]).

Furthermore, probabilistic approaches lead to a conic spline as bounding curve.

In fact, we would be able to continue this list of reasonable tolerance channels almost perpetually. However, the design of suitable channels depends considerably on specific applications. Since we have chosen the very broad class of piecewise \mathcal{R}^ω curves as valid bounding channels in our theoretical part, we can practically cover all types of curves which can be represented by computers.

In any case, it makes sense to reduce the complexity of input data by a pre-approximation. As computing a minimum link path can be done in linear time, we could consider an offset channel with width ε (radius $\varepsilon/2$) resulting in polygonal curve ω . When offsetting the curve ω again, we can define another start-destination channel having less vertices. Furthermore, the *Douglas-Peucker algorithm* reduces the number of points P (cf. [32]) and yields a subset P' of P with $\mathfrak{h}(\text{tr}(\omega'), \text{tr}(\omega)) \leq \varepsilon$, where ω' is the polygonal curve running through P' . Although there is no warranty that P' has the minimal possible number, the algorithm performs very well in practical applications.

As outliers might appear because of errors during the capturing process, it is also reasonable to pre-approximate the original points P regarding least squares, which can be done, for instance, by using a curvature estimator (cf. [66]).

Having computed a smooth minimum arc path within a possibly reduced start-destination channel, we obtain an approximation of P by a smooth arc spline γ . If desired, we can use γ as a starting solution for a non-linear optimization problem which aims at minimizing the least squares error regarding P subject to the fixed breakpoints of γ .

¹‘NC’ is an abbreviation for ‘numerically controlled’.

5.3 Shape Recognition

Whereas *distinctive points* of images yield 0-dimensional structures that are suitable for *matching*, contours can be used as 1-dimensional search-structures for the recognition of a transformed object. They are also crucial for describing a detected object.

Automatically determining the geometry of a detected object is achieved by placing it in some pre-established classification which is the preliminary knowledge. Algorithms try to compare the detected object to known ones. This classification is called *shape recognition*¹. In other words: If we have a set of prototype objects, we want to know which one the detected shape matches best. This raises at least two questions:

- What kind of properties should a shape recognition algorithm satisfy?
- What kind of representation do we take for a shape?

Due to D. Marr (cf. [56]), object recognition demands a stable (insensitive to noise) description that hardly depends on the view point. Although Marr didn't give practical algorithms for shape representation, he initiated an axiomatic approach, which is generalized in [19] as follows:

First, the distance between two objects should not depend on the way they are represented. The most important property is *invariance*. Therefore, we consider a set of feasible transformations (e.g. rotations and translations). Stability is another criterion, meaning the invariance regarding noise. Hence it seems natural to smooth the shapes. It is fairly obvious that an algorithm will be more efficient and fast if the amount of input data is small.

In shape recognition tasks the comparison of two contours is necessary. Since a comparison point by point is too complex, an encoding which supplies a fast comparison has to be found. Curvature would be suitable for that since it is invariant with respect to rotations and translations. However, it can only approximatively be determined from contour points. One possibility is, to first approximate the contour points e.g. by a smooth arc spline and then compute the curvature function. Since the corresponding curvature function is a step function, a relatively simple form of encoding is possible. This way, the axioms given above are all satisfied.

¹This summary partly follows [19].

We can approximate the contours of our prototype object by a smooth arc spline if we compute a smooth minimum arc path $\gamma := \gamma_1 \cdots \gamma_n$ of a suitable start-destination channel and compute the curvature of γ , which can be done very easily (cf. Proposition 2.5.31). We can proceed analogously if the contour we consider is cyclic. Figure 83 shows an example of window frames, which is taken from [66]. However, our algorithm does not stand up to the runtime requirements of real time applications. This isn't a problem when generating the prototype, but when approximating the curvature of an arbitrary object which is compared to the prototype, we follow the method proposed in [66]. If (y_1, \dots, y_N) is the contour of an object which is supposed to correspond to the prototype contour with the approximation γ , then we compute the *curvature characteristic of* (y_1, \dots, y_N) , which is, in fact, the curvature function of the arc length parametrization of an arc spline approximating the points y_1, \dots, y_N .

The whole method results in the comparison of two step functions κ_1 and κ_2 modeling the curvature of the prototype contour and another contour. When dealing with closed contours, we extend κ_1 and κ_2 periodically since the starting point $S(\gamma)$ and the first contour point y_1 , generally, don't correspond. In any case, Pisinger gives an efficient comparison of such two curvature functions in [66], where it is crucial that the functions consist of as few steps as possible.

Using this comparison method, a classification of search objects can be implemented efficiently. A subsequent *prototype matching*, which is based on a mutual minimization (cf. [43]), can use the result computed by the method above as initial value. The next section concerns, among others, this kind of 'alternating prototype matching'.

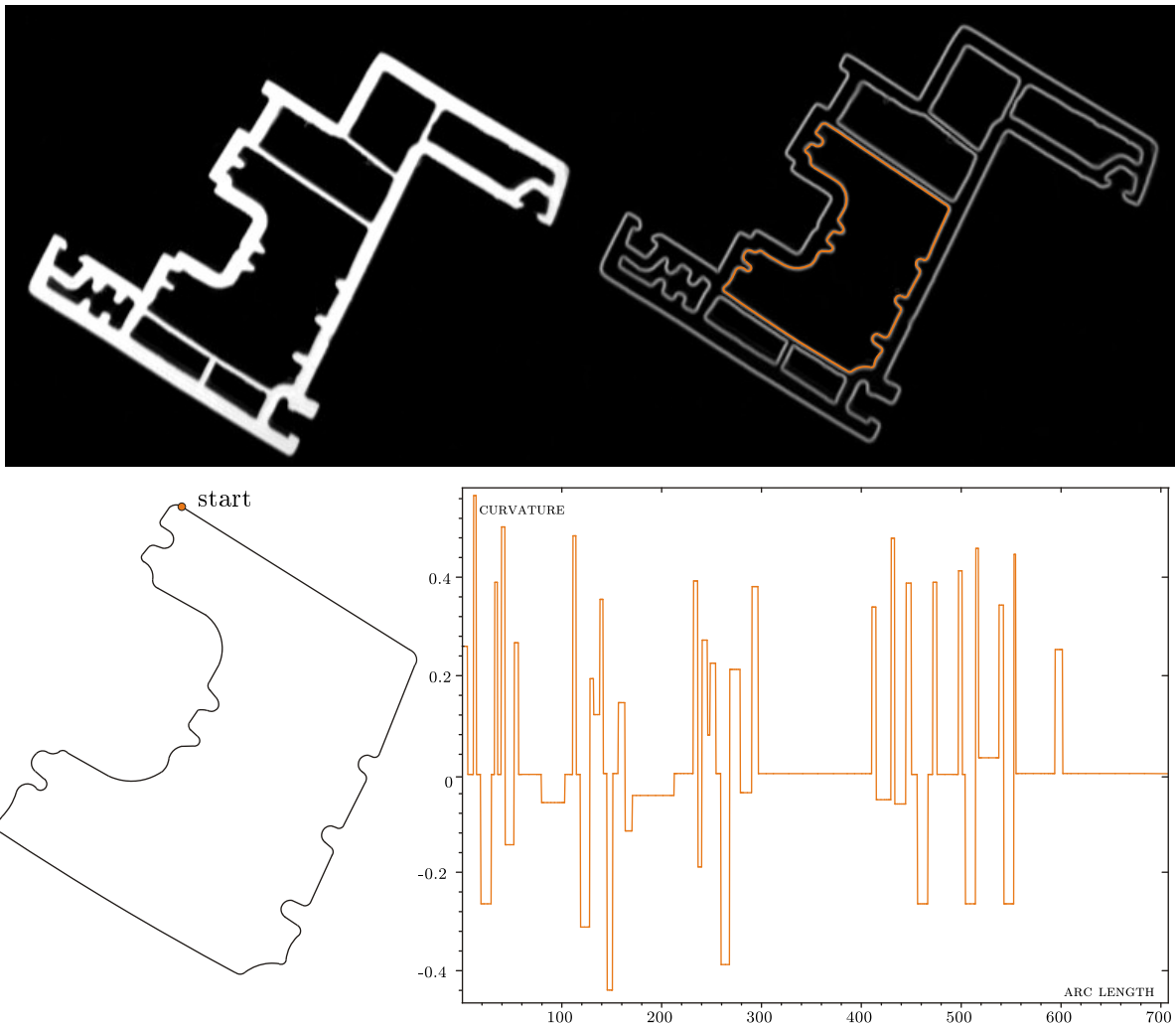


Figure 83: Approximation of the inner contour of a window frame and corresponding curvature function. Top left: Reworked image with high contrast. Top right: Extracted contours. Bottom left: Approximation of the inner contour (orange) by a smooth arc spline. Bottom right: Corresponding curvature function.

5.4 Reverse Engineering

In industrial manufacturing we often encounter the case that the produced piece doesn't fit very well to the CAD-design because of variances during the production process. Sometimes there doesn't even exist a CAD-drawing. In any case, the automatic generation of CAD-layouts of industrially manufactured workpieces is a crucial step in Reverse Engineering, especially for quality assurance purposes and for extracting the commands needed to operate CNC machines¹ for production.

We subsequently discuss an approach to generating a so-called *masterpiece*² or rather a CAD-layout of it, and we show how this serves in optical quality control and vision metrology. For instance, it can be used for target-performance comparisons of planar geometries like laminations, panes of glass and planks of shelves.

5.4.1 Generation of a Masterpiece

In fact, many approaches assume that the working pieces observed by a camera are *planar* (e.g. [48]). As already mentioned in Section 1.1, it is appropriate to code the detected contours by arc splines, since they are invariant with respect to rotation, scalings and translations and stand out due to their easy offset computation. Furthermore, arc splines are often used as the description of tool paths of CNC machines. When programming a CNC tool path, fewer arc segments can help to improve the production efficiency by reducing the number of instructions and tool motions (e.g. [62]). Hence computing a (smooth) minimum arc path is an appropriate approach.

If we want to derive (a draft of) a masterpiece with an accuracy given by a maximum error $\varepsilon > 0$, the very first step is to extract the contours of a digital image which results when capturing the masterpiece. Since we are situated in an industrial environment, we can take proper illumination and high accuracy of the detecting system as a starting point. Thus, accurate input data can be expected, possibly after a preprocessing step. Next, we design a start-destination channel sticking to the tolerance ε . Which of the approaches for developing a channel proposed in Section 5.2 should be chosen, depends

¹CNC stands for computer numerical control. Numerical control (NC) refers to the automation of machine tools that are operated by abstractly programmed commands encoded on a storage medium.

²A masterpiece is a specimen of a working piece with the exact size required. Often, the corresponding CAD-layout is also called 'masterpiece'.

on the requirements of the masterpiece and on the desired exactness. In any case, we then compute a smooth minimum arc path for every contour list and export it as a CAD-drawing. As this process can be done off-line, it needn't satisfy real time requirements. Before we elucidate how to use a masterpiece for optical quality control, we show two examples.

Example. In Figure 84 we can see the approximation of the shape of garden scissors by a minimum arc path and a minimum link path. In this example we have focused on the external contour. All the other contours can be approximated in the same way. Ten arcs are needed on the one hand and 17 line segments on the other hand. The line representation not only suffers from a higher number of segments but also yields no realistic draft of the real image. Although the number of vertices is nearly 400, only 19 CVDs have to be computed to obtain the arc spline depicted. This averages out about two CVDs per step of the algorithm.

The second example is not taken from an industrial setting, but it also shows an interesting model.

Example. The shape of a hand, which has been extracted from a camera image with a resolution of about 640x480 pixels, is approximated by a smooth arc spline with 35 segments. The maximum distance from the shape to the contour points is about 0.5 pixels, which corresponds to about 0.2 mm (cf. Figure 85). The corresponding start-destination channel has been constructed after a pre-processing step as proposed in Section 5.2. It has about 400 vertices. The following table summarizes the results at different tolerance levels. Figure 86 compares a continuous to a smooth solution.

Tolerance	Number of segments	Number of CVDs
2 px	12	39
1 px	20	67
0.5 px	35	112
0.2 px	61	207

Table 5.1: Approximation of the shape of a hand by a smooth arc spline.

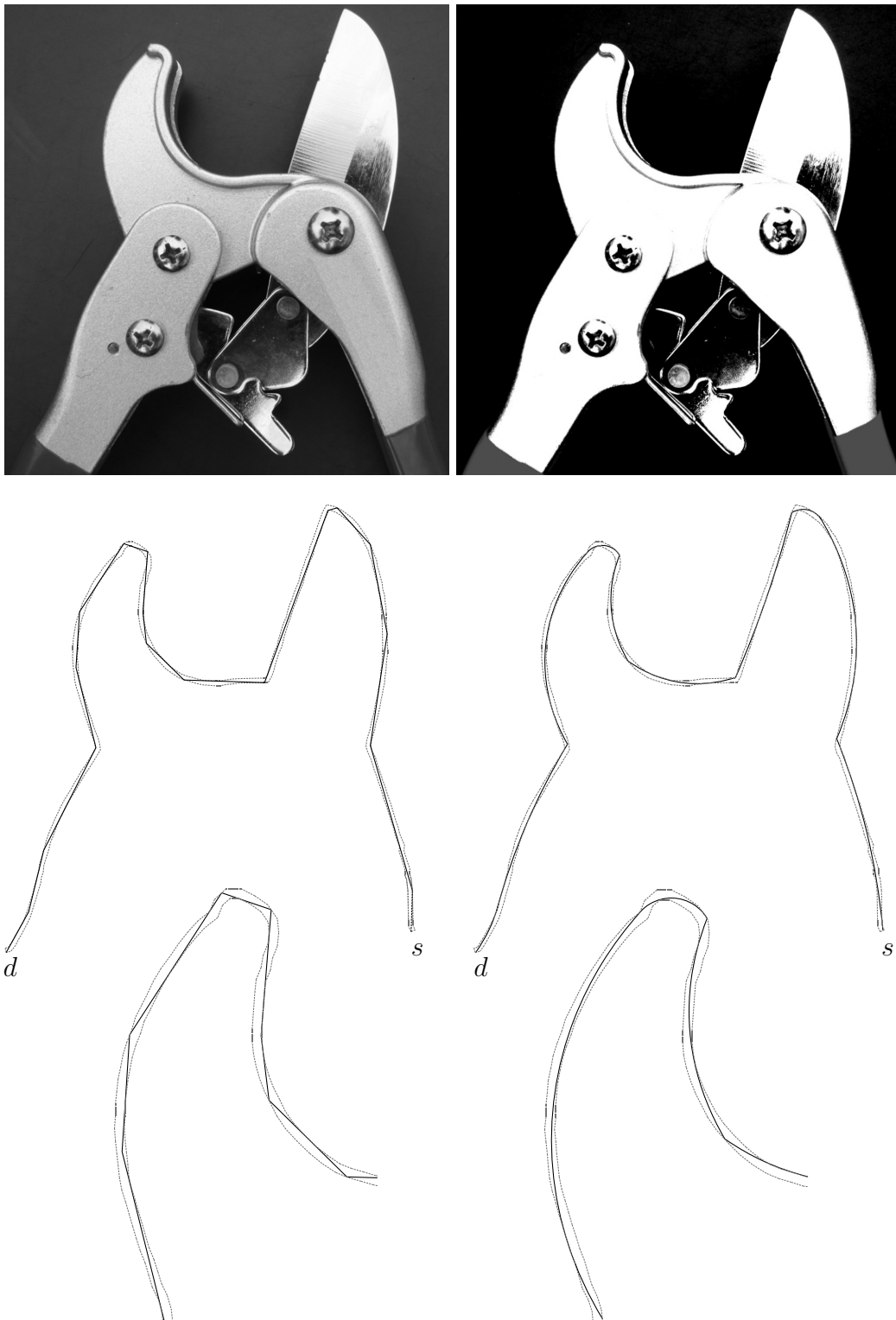


Figure 84: Approximation of a part of garden scissors. Top left: Original image. Top right: Reworked copy with higher contrast. Middle: Approximations of the external contour by lines (left) and by arcs (right) with respect to the same polygon containing the extracted contour points of the shape. Bottom: Enlarged details of the two approximations.

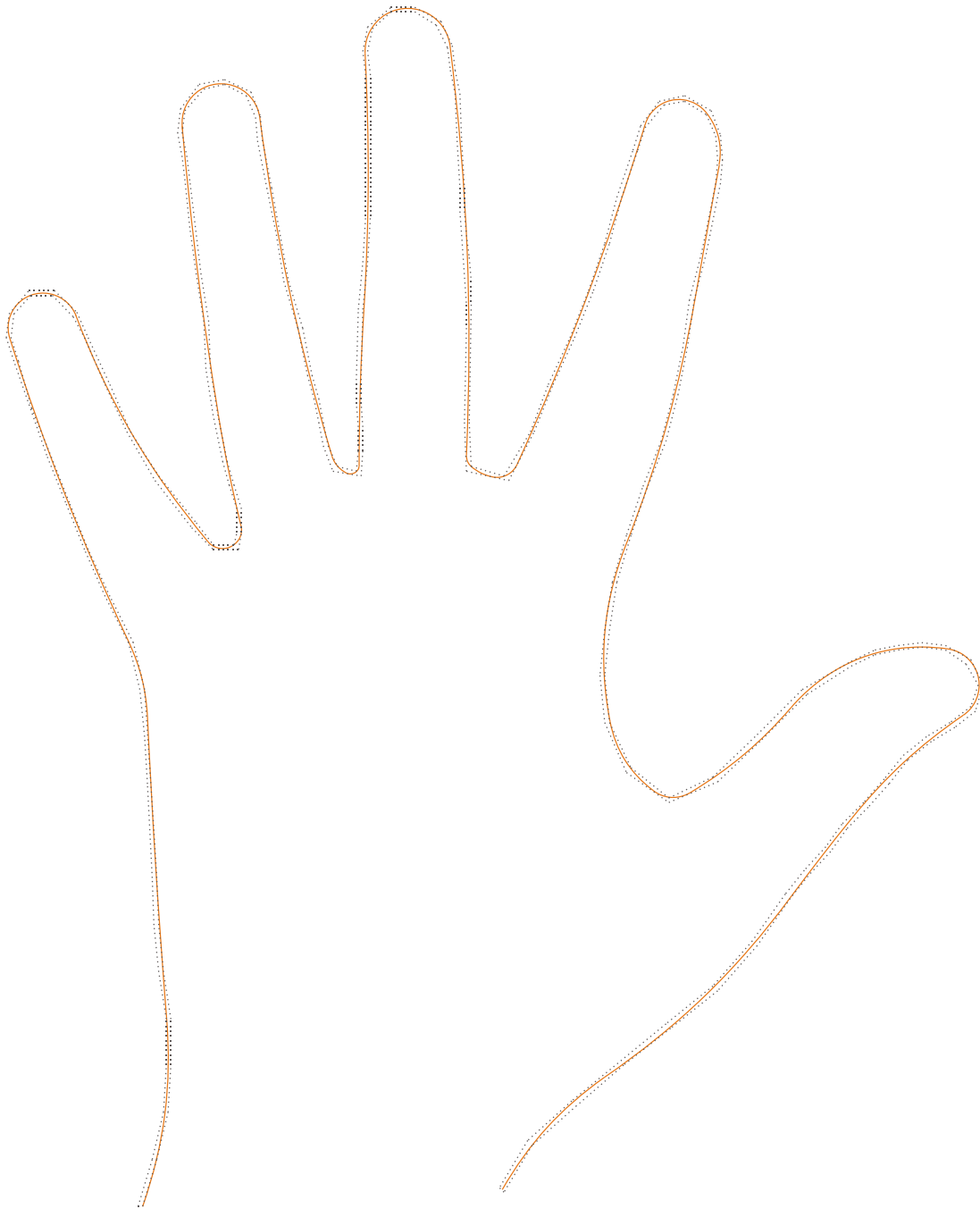


Figure 85: Approximation of the shape of a hand. Polygonal channel (dotted) approximating the ε -offset of the extracted points with $\varepsilon = 0.5$. The corresponding smooth minimum arc path (orange) needs 35 segments.

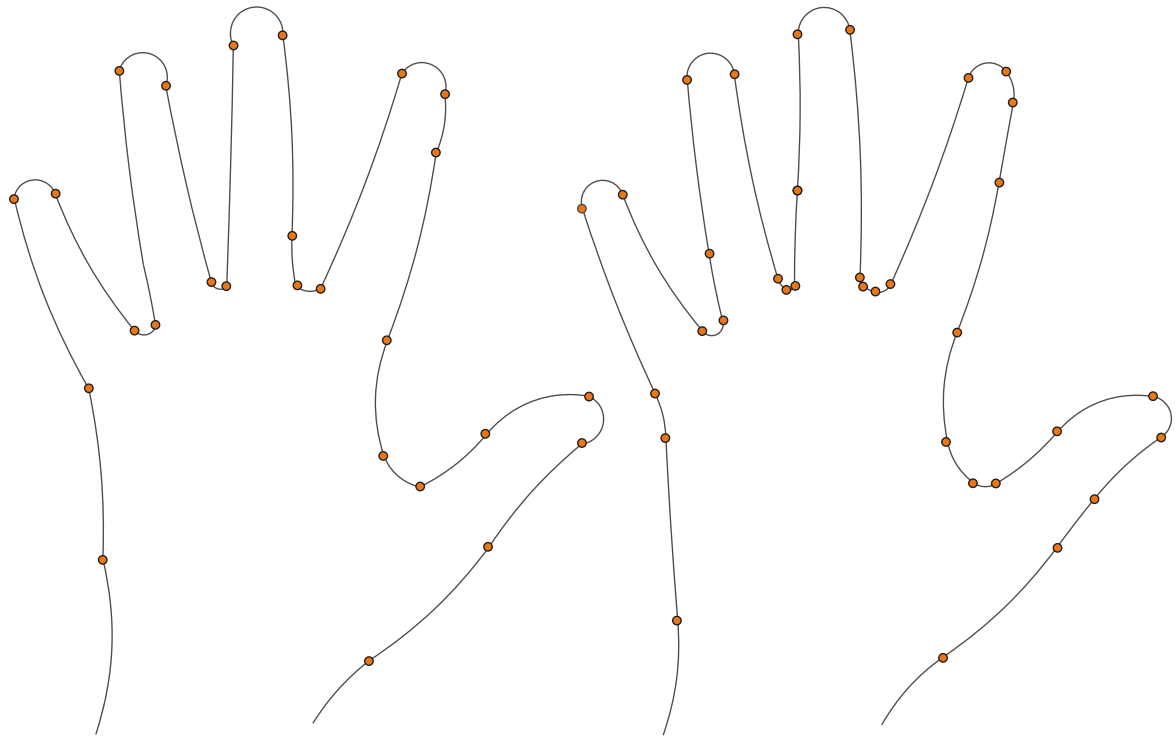


Figure 86: Comparison of continuous and smooth approximation; tolerance: 0.5 pixels. Left: Continuous arc spline with 28 segments. Right: Smooth arc spline with 35 segments.

We now concern ourselves with the usage of a masterpiece for quality assurance purposes. Therefore, an efficient approach to comparing the masterpiece with an arbitrary working piece detected on a line of a factory is needed.

5.4.2 Quality Control and Vision Metrology

When we consider an arbitrary working piece, its position is not the same as the location of the masterpiece, i.e. the observed object might be rotated, translated and even scaled. W.l.o.g. we can assume that the computed masterpiece is the trace of only one arc spline $\gamma := \gamma_1 \cdots \gamma_N$. If y_1, \dots, y_n are the contour points of an observed working piece, we search for a motion $\Phi : \mathbb{R}^2 \rightarrow \mathbb{R}^2$ minimizing the sum of squares $\sum_{i=1}^n \text{dist}(\Phi(\text{tr}(\gamma)), y_i)^2$. Naturally, the existence of such optimal motions can only be assured if we make some restrictions and assumptions on the feasible transformations. Here we focus on motions that consist of translations, isotropic scalings¹ and rotations, which are mappings of the

¹By an isotropic scaling a function $g_\alpha : \mathbb{R}^2 \rightarrow \mathbb{R}^2$, $x \mapsto \alpha x$ for some $\alpha \in \mathbb{R}$ is meant.

form

$$T : \mathbb{R}^2 \rightarrow \mathbb{R}^2, x \mapsto \lambda \cdot \begin{pmatrix} \cos(\varphi) & -\sin(\varphi) \\ \sin(\varphi) & \cos(\varphi) \end{pmatrix} \cdot x + \begin{pmatrix} \vartheta_1 \\ \vartheta_2 \end{pmatrix},$$

where $\varphi \in [0, 2\pi[$ and $\lambda, \vartheta_1, \vartheta_2 \in \mathbb{R}$. We denote the set of all these mappings by \mathcal{T} and note that these function can also be written in the form

$$T_{c,s,t} : \mathbb{R}^2 \rightarrow \mathbb{R}^2, x \mapsto A_{c,s} \cdot x + t$$

with scaled rotation

$$A_{c,s} := \begin{pmatrix} c & -s \\ s & c \end{pmatrix} \text{ for all } c, s, \in \mathbb{R}.$$

and translation $t \in \mathbb{R}^2$. Hence we search for optimal parameters $c, s \in \mathbb{R}$ and $t \in \mathbb{R}^2$.

Then, the problem formulated above can be solved very fast by an iterative approach. First, we use the method proposed in Section 5.3, which is based on curvature characteristics. We follow this strategy in order to initially check the quality of the object and obtain a good initial estimation R_0 of the rotation¹ for subsequent *prototype matching*, as already indicated in Section 5.3. A suitable initial value t_1 for the translation vector is the difference between the barycenters of the points y_i and the masterpiece

$$t_1 := \frac{1}{n} \sum_{i=1}^n y_i - \frac{1}{l} \sum_{i=1}^N s_i l_i,$$

where s_i is the barycenter of $\text{tr}(\gamma_i)$, $l_i := \text{len}(\gamma_i)$ and $l := \sum_{i=1}^N l_i$

We can now compute the best approximating points x_i of y_i with respect to the set $M := R_0 \text{tr}(\gamma) + t_1$. Since γ is an arc spline, M is also the trace of an arc spline $\gamma^{(1)} := \gamma_1^{(1)} \dots \gamma_N^{(1)}$. The correspondence between a point y_i and a segment $\gamma_j^{(1)}$ can be quickly and efficiently determined, for instance, by a (transformed) tree structure like a *quadtree decomposition*², which can be established beforehand. The best approximating point x_i of y_i to the nearest circular segment $\gamma_j^{(1)}$ can be calculated by intersecting $\text{tr}(\gamma_j^{(1)})$ with the line segment defined by y_i and the center of $C(\gamma_j^{(1)})$, and it is therefore very cheap in comparison to parametric curves, which need iterative strategies. If the nearest segment $\gamma_j^{(1)}$ is a line segment, we only have to compute the orthogonal projection of y_i on $\gamma_j^{(1)}$.

Using the abbreviation

$$\tilde{x}_i := \begin{pmatrix} 0 & -1 \\ 1 & 0 \end{pmatrix} x_i \text{ for all } i = 1, \dots, m$$

¹If the contour is not cyclic, an initial value can be found by matching the starting and endpoints.

²e.g. [26], Chapter 14: Quadtrees: pp. 291 - 306

and denoting the barycenters of x_1, \dots, x_m and y_1, \dots, y_m by

$$s_x := \frac{1}{m} \sum_{i=1}^m x_i \text{ and } s_y := \frac{1}{m} \sum_{i=1}^m y_i,$$

the optimal values $s_1, c_1 \in \mathbb{R}$ and $t_1 \in \mathbb{R}^2$, i.e.

$$\sum_{i=1}^m \|T_{c_1, s_1, t_1}(x_i) - y_i\|^2 = \min_{s, c \in \mathbb{R}, t \in \mathbb{R}^2} \sum_{i=1}^m \|T_{c, s, t}(x_i) - y_i\|^2$$

can be derived in a closed form:

$$c_1 = \frac{1}{\rho} \sum_{i=1}^m y_i (x_i - s_x)^T y_i, \quad s_1 = \frac{1}{\rho} \sum_{i=1}^m y_i (\tilde{x}_i - s_x)^T y_i,$$

where $\rho = \sum_{i=1}^m \|x_i\|^2$, and the optimal translation is given by $t_1 = s_y - A_{c_1, s_1} s_x$. The value $E := \sum_{i=1}^m \|T_{c_1, s_1, t_1}(x_i) - y_i\|^2$ indicates the fitting quality.

Again, we can compute the best approximating points $x_i^{(2)}$ of y_i with respect to

$$T_{c_1, s_1, t_1}(\text{tr}(\gamma^{(1)})) =: \text{tr}(\gamma^{(2)})$$

and solve the least squares problem as above. We carry on with this alternating procedure while E is greater than a given threshold C or the difference between the predecessor error and the current error is not too small. Assuming that the algorithm has terminated in the k -th iteration step, we can additionally check if $\text{dist}(y_i, \text{tr}(\gamma^{(k)})) > \varepsilon$ for some $i = 1, \dots, n$ and $\varepsilon > 0$ in order to guarantee a good dimension accuracy satisfying the quality of the product. If E is still larger than a given tolerance, the object doesn't ensure the quality requirements and has to be sorted out.

5.5 Curve Approximation

Fitting data by parametric curves¹ is used in Pattern Recognition, Image Processing and many other industrial applications. While most curve fitting algorithms try to construct a smooth curve passing through or near the given points of the curve which has to be approximated, in the field of Computer Aided Geometric Design it is often desirable to fit a point set by a curve, which has a convenient shape, close to the points (e.g. [83]). Furthermore, the curvature plot of the fitting curve should consist of as few as possible monotone pieces ([36]). As already seen, arc splines satisfy all these criteria.

Approximating data by curves of higher order has been investigated extensively for a couple of decades (cf. [58, 59, 60, 46, 63, 70, 84]). With the capability of representing free form curves in a unified way, NURBS have become the de facto standard in Computer Aided Design (e.g. [35]). Therefore, most of the CAD models of working pieces are designed in NURBS. In contrast to their flexibility in shape modeling, point to curve distances cannot be computed in closed form for NURBS-curves. Compared to arc splines, the computation of distances from NURBS is quite slow. Thus, dealing with NURBS in pose estimation and prototype fitting algorithms is clumsy. Therefore, it is desirable to approximate the original CAD-layout by (smooth) arc splines. One possibility for approximation with arc splines is sampling the original curve, designing an offset channel and then computing a minimum arc path.

For instance, Figure 87 depicts the point list of a s-shaped curve and approximations by a continuous minimum arc path. The curve, which is taken from [62], is enclosed in a 200px x 300px rectangle and is sampled by 612 points.

In Section 1.3 we have seen that there already exist some approaches to the approximation of curves by arc splines. The smooth arc spline interpolation problem on a closed point set was first proposed by Hoschek ([49]) in 1992. Given $n > 2$ different points with a certain order, a closed smooth arc spline is required to be built in order to connect those points in the given order. This approach has recently been improved by Chen et al. ([21]). There are numerous approaches to approximation and interpolation by smooth arc splines based on biarc techniques. We just want to mention three of them: Yang and Du ([81]) use techniques from optimization theory to approximate planar digitized curves by arc splines. A (smooth) arc spline which is bounded by a maximum approxi-

¹This overview follows [83].

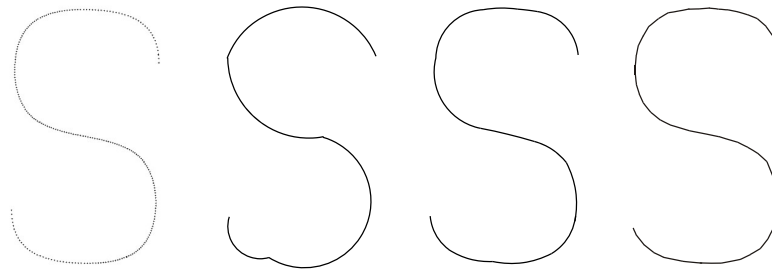


Figure 87: Input point set with 612 pixel positions and approximations with tolerance 10, 1 and 0.1 pixels.

mation error given by an arbitrary tolerance but without any control of the number of segments is constructed. In [82] Yang et al. presented an algorithm for approximating arbitrary types of smooth parametric curves, which is based on interpolation with biarcs within a given tolerance. Furthermore, Drysdale et al. [33] presented an $O(n^2 \log n)$ algorithm for approximating a polygonal curve with n vertices by an arc spline with a minimum number of circular arcs. Given a sequence of points and tangent directions, computing a smooth approximation with the minimum number of biarcs results in a runtime complexity of $O(n^2 \log^2 n)$.

However, the interpolation case as well as the approaches mentioned above force the breakpoints of their solutions to be original points. Even more, the biarc techniques need additional tangent data. This has a huge impact on the number of segments the resulting arc spline possesses. For instance, Figure 88 shows the plot of the sine-curve restricted to the interval $[0, 6]$ and approximations at four different tolerance levels computed with our method. Due to the algorithm suggested by Yang, we sampled the sine-curve and then constructed a start-destination channel providing the desired maximum tolerance error. Table 5.2 compares the results obtained by the method of Yang and by computing a smooth minimum arc path.

Number of segments	Approximation tolerance			
	10^{-1}	10^{-2}	10^{-3}	10^{-4}
Yang	-	-	23	45
Ours	2	6	12	29

Table 5.2: Approximation of the sine-curve segment defined on the interval $[0, 6]$.

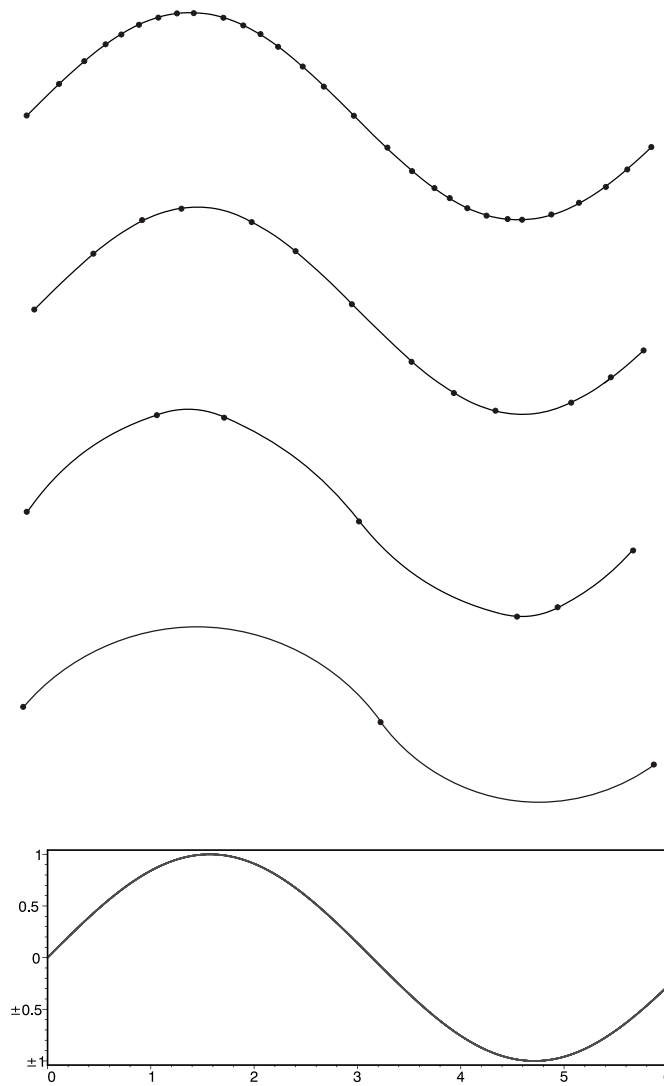
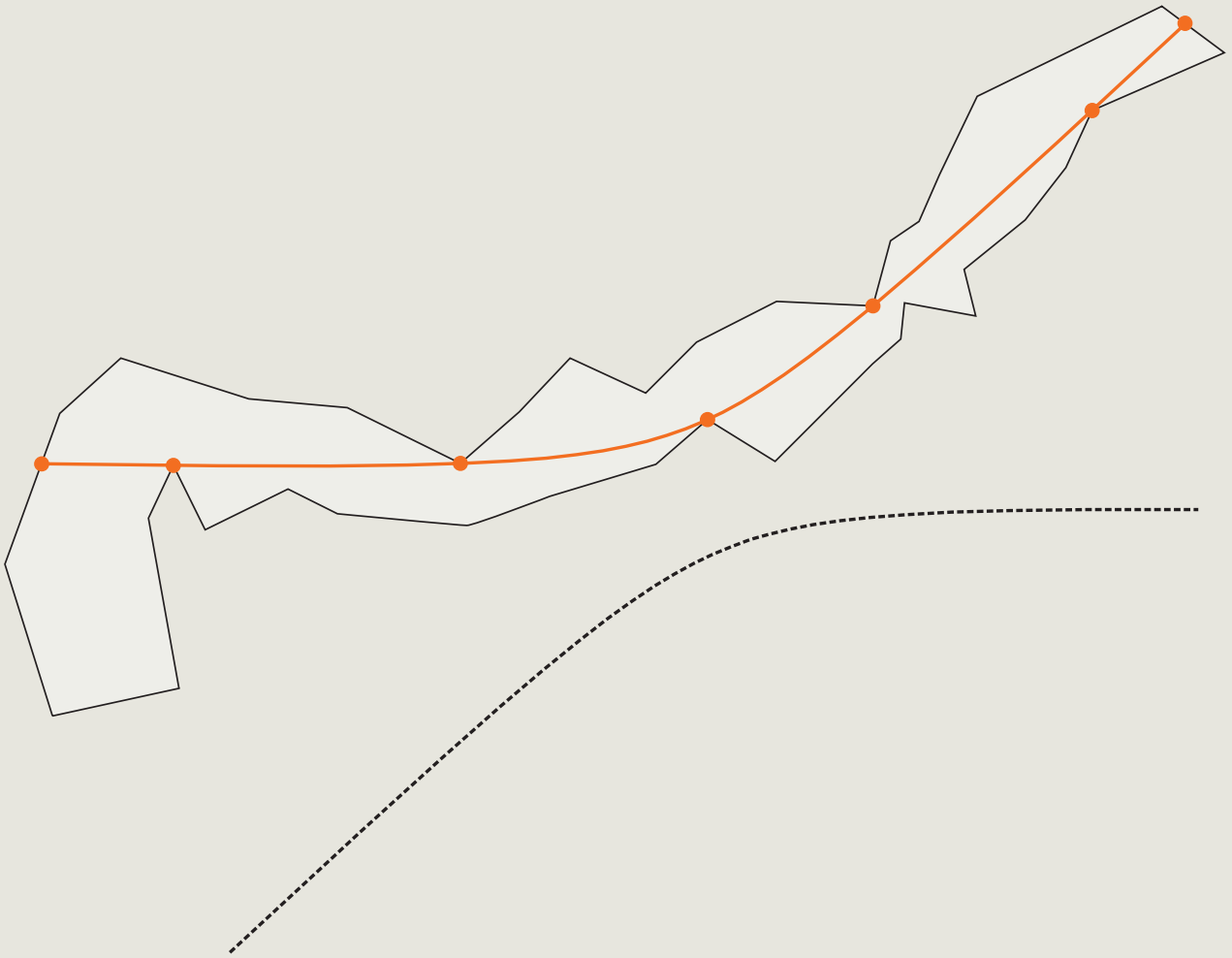


Figure 88: Plot (bottom) and approximation of the sine curve segment by smooth arc splines with maximum error 10^{-4} , 10^{-3} , 10^{-2} and 10^{-1} .



6

RÉSUMÉ AND FURTHER WORK

6.1 Overview and Main Results

In this thesis, we have developed an approach to approximating two-dimensional point data by smooth arc splines within a start-destination channel. The main aim was to supply a fundamental mathematical characterization of circular visibility and (smooth) minimum arc paths which arises as a natural generalization of minimum link paths. Similar to minimum link paths, a minimum arc path of a start-destination channel is not generally unique, but the minimum number of segments is naturally unique. We have worked out a constructive solution for computing a (smooth) minimum arc path, and we have shown that there is a minimum arc path which consists of segments having a special configuration of alternating restrictions. Alternating sequences and feasible direction cones have turned out to be the key instruments for characterizing them efficiently. For this purpose, it was essential that circular arcs have three degrees of freedom, which results in the fact that blocking arcs have an alternating sequence of length 3. The concept of feasible direction cones and their continuity properties was crucial for finding an effective condition for an arc to be joined smoothly.

*‘The outcome of any serious research can only be
to make two questions grow where only one grew before.’*

(Thorstein Veblen, Norwegian-American economist)

Our theoretical results even hold for start-destination channels given by piecewise analytically extended Jordan curves and enable the design of a greedy algorithm. However, in the presentation of our algorithmic approach we focused on polygons as bounding channels. In that case, we gave an efficient method based on the iterative use of CVDs, which led us to a quadratic algorithm. As indicated in Chapter 4 and 5, this algorithm is mostly sub-quadratic in practice.

The algorithms introduced can be used for a wide range of applications, as seen in Chapter 5. We have discussed some possibilities for the development of a suitable channel, which is important for modeling a specific application example. But in the end, the choice of suitable channels depends very much on real applications. In turn, the great advantage of our method is that it works for every tolerance channel and does not depend on any geometric details (cf. Algorithm 1). In case the bounding curve ω_K is not a polygon, a good strategy has to be developed in order to construct the blocking arcs. However, these approaches might not be as efficient as in case of a polygonal channel.

Altogether, we have solved a problem based in the field of Approximation and Computational Geometry with methods of Set-Valued Analysis and Nonlinear Approximation Theory. We have focused on applications in Computer Aided Design, Computer Vision and Graphics.

Clearly, this thesis can only be an extract of all possibilities and challenges in the context of approximation tasks with arc splines, approaches to curve approximation and Reverse Engineering tasks. Both the theoretical and the practical part could be generalized and extended, and there are still some interesting and unsolved problems. Therefore, we conclude by mentioning a few research avenues for future work which seem to be particularly important and promising.

6.2 Possible Future Work and Open Problems

Among others, a more detailed investigation of the cyclic case and algorithmic improvements in case of non-polygonal channels are interesting challenges. Furthermore, the generalization to conic splines as well as arc splines in three dimensions lends itself to a natural extension of this thesis.

Even in three dimensions, the simple but powerful class of arc splines offers a number of remarkable advantages, (cf. [71]): The offset of an arc spline in three dimensions has a simple, closed-form parameterization consisting of segments of tori and cylinders (cf. [11]). Thus, arc splines also provide a quick and non-iterative method for closest point computation in space. For a set of given points in \mathbb{R}^3 , the best approximating points on the curve can be computed by solving quadratic equations. As already seen in the planar case, for polynomial or rational spline curves, the same problem leads to non-linear optimization problems, which require iterative solution techniques. Due to Wang et al. ([77]), arc spline curves are very useful for sweep surface modeling since they provide high-quality approximations of rotation-minimizing frames.

Research on arc splines in three dimensions is currently being very active (e.g. [80, 71]). A generalization of our results regarding arc splines in space would probably make a considerable contribution to this field of research. However, certain questions are likely to arise

- How must be tolerance channels defined?
- What are the starting and continuation conditions?
- What is the analogue to left and right restriction in space in order to generalize alternating sequences for this purpose?

Such questions would have to be answered in advance.

Another important extension of arc splines are *conic splines*, which are simple or Jordan curves composed of conic segments, i.e. non-empty, connected and compact subsets of conics (cf. Section 2.1). A conic spline is called *smooth* if it has a \mathcal{C}^1 -parametrization. Each segment can be represented by both an algebraic curve segment or a rational Bézier curve (cf. [34]). As one main defect of arc splines is that their curvature function is not continuous, they can hardly be used for high quality shape modeling. In

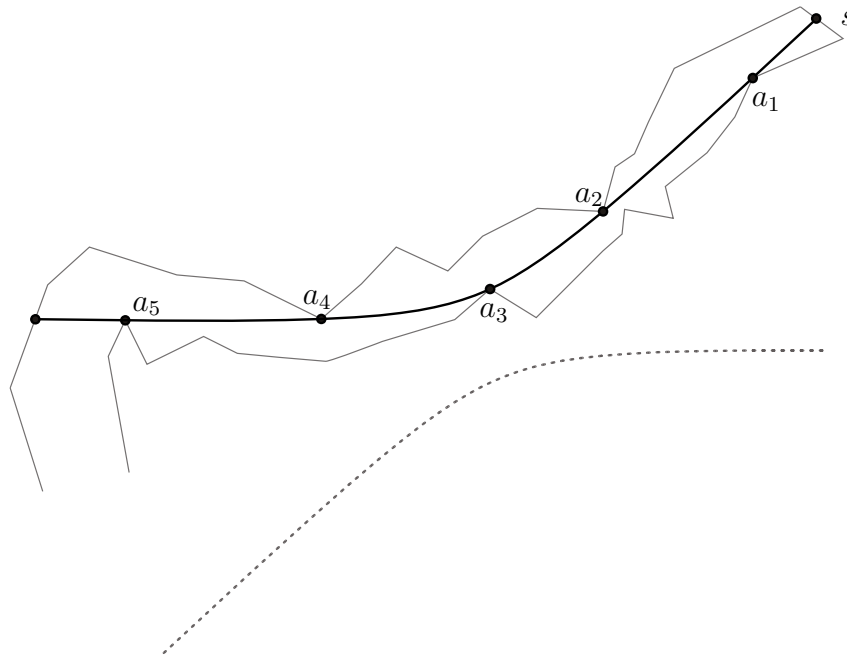


Figure 89: Hyperbola segment in polygonal channel with alternating sequence (a_1, \dots, a_5) of length 5. The dashed curve indicates the second branch of the corresponding hyperbola.

contrast, conic splines and surfaces own many elegant properties which make them a powerful tool for shape modeling ([71]). Thus, many research contributions deal with the approximation of points and curves by conic splines. Some recently published papers are [83], [5], [40] and [39].

A promising approach to approximating planar point lists and curves by (smooth) conic splines would be *(smooth) minimum conic paths*, which can be defined analogous to (smooth) arc paths. However, we cannot transfer the methods proposed in this thesis to conic visibility directly since conics are not connected in general. Nevertheless, as conics have five degrees of freedom¹, the following conjecture seems reasonable:

Blocking conic segments have an alternating sequence of length 5 (cf. Figure 89).

It is not clear at all if feasible direction cones, defined in the same way as for arc splines, are connected in terms of *conic visibility*. Besides, the necessity of examining alternating sequences of length 5 probably increases the computational complexity compared to minimum arc paths.

¹A conic segment can be uniquely determined by five distinct points or by three points and two tangent directions.

REFERENCES

- [1] AGARWAL, P. K., ET AL. Curvature-constrained shortest paths in a convex polygon. *SIAM Journal on Computing* 31, 6 (2002), 1814–1851.
- [2] AGARWAL, P. K., AND SHARIR, M. Correction to Lee’s visibility polygon algorithm. *BIT Numerical Mathematics* 27, 1 (1987), 458–473.
- [3] AGARWAL, P. K., AND SHARIR, M. Circle shooting in a simple polygon. *Journal of Algorithms* 14, 1 (1993), 69–87.
- [4] AGARWAL, P. K., AND SHARIR, M. Circular visibility of a simple polygon from a fixed point. *International Journal of Computational Geometry and Applications* 3, 1 (1993), 1–25.
- [5] AHN, Y. J. Conic approximation of planar curves. *Computer-Aided Design* 33, 12 (2001), 867 – 872.
- [6] ARKIN, E. M., MITCHELL, J. S. B., AND SURI, S. Optimal link path queries in a simple polygon. In *Proceedings 3rd ACM-SIAM Symposium. Discrete Algorithms* (1992), pp. 269–279.
- [7] ARONOV, B., ET AL. Visibility queries and maintenance in simple polygons. *Discrete and Computational Geometry* 27 (2002), 461–483.
- [8] AUBIN, J., AND FRANKOWSKA, H. *Set-Valued Analysis*. Birkhauser, 1990.

-
- [9] AVIS, D., GUM, T., AND TOUSSAINT, G. Visibility between two edges of a simple polygon. *The Visual Computer 2* (1986), 342–357.
- [10] AVIS, D., AND TOUSSAINT, G. T. An optimal algorithm for determining the visibility of a polygon from an edge. *IEEE Transactions on Computers 30*, 1 (1981), 910–914.
- [11] BAUER, U., AND POLTHIER, K. Parametric reconstruction of bent tube surfaces. *International Conference on Cyberworlds* (2007), 465–474.
- [12] BENGTTSSON, A., AND EKLUNDH, J.-O. Shape representation by multiscale contour approximation. *IEEE Transaction on Pattern Analysis and Machine Intelligence 13*, 1 (1991), 85–93.
- [13] BIERSTONE, E., AND MILMAN, P. Semianalytic and subanalytic sets. *Publications Mathématiques de L’IHÉS 67*, 1 (1988), 5–42.
- [14] BIX, R. *Conics and Cubics*. Springer, New York, 2005.
- [15] BOISSONNAT, J.-D., ET AL. An algorithm for computing a convex and simple path of bounded curvature in a simple polygon. *Algorithmica 34* (2002), 109–156.
- [16] BOYER, C. B. *A History of Mathematics*. Wiley, New York, 1968.
- [17] BRAESS, D. *Nonlinear approximation theory*. Springer Series in Computational Mathematics, Berlin, New York, 1986.
- [18] CANNY, J. A computational approach to edge detection. *IEEE Transactions on Pattern Analysis and Machine Intelligence 8*, 6 (1986), 679–698.
- [19] CAO, F. *Geometric Curve Evolution and Image Processing*. Springer, New York, 2003.
- [20] CHAZELLE, B. M., AND GUIBAS, L. T. Visibility and intersection problems in plane geometry. *Discrete and Computational Geometry 4*, 1 (1989), 551–581.
- [21] CHEN, X.-D., ET AL. Automatic \mathbf{G}^1 arc spline interpolation for closed point set. *Computer-Aided Design 36* (2004), 1205–1218.

-
- [22] CHOU, S.-Y., ET AL. Circular visibility of a simple polygon. Tech. rep., Department of Industrial and Manufacturing Systems Engineering, Iowa State University, 1992.
- [23] CHOU, S.-Y., AND WOO, T. C. A linear-time algorithm for constructing a circular visibility diagram. *Algorithmica* 14 (1995), 203–228.
- [24] CORMEN, T., ET AL. *Introduction to Algorithms*. MIT Press, Cambridge, MA, 2009.
- [25] COURANT, R., AND ROBBINS, H. *What Is Mathematics?: An Elementary Approach to Ideas and Methods*. Oxford University Press, Oxford, 1996.
- [26] DE BERG, M., ET AL. *Computational Geometry*. Springer, New York, 2000.
- [27] DIEUDONNÉ, J. *Foundations of Modern Analysis*. Academic Press, London, 1960.
- [28] DO CARMO, M. *Riemannian Geometry*. Birkhäuser, Basel, 1992.
- [29] DOBKIN, D. P., AND SOUVAINE, D. L. Computational geometry in a curved world. *Algorithmica* 5, 5 (1990), 421–457.
- [30] DONNER, K. Image interpretation based on local transform characterization. *Pattern Recognition and Image Analysis* 7, 4 (1997).
- [31] DONNER, K. Tangentialkegel. Tech. Rep. MIP-1005, Fakultät für Mathematik und Informatik, Universität Passau, 2010 (to appear).
- [32] DOUGLAS, D., AND PEUCKER, T. Algorithms for the reduction of the number of points required to represent a digitized line or its caricature. *The Canadian Cartographer* 10, 2 (1973), 112–122.
- [33] DRYSDALE, R., ET AL. Approximation of an open polygonal curve with a minimum number of circular arcs and biarcs. *Computational Geometry* 41 (2008), 31–47.
- [34] FANG, L. A rational quartic Bézier representation for conics. *Computer Aided Geometric Design* 19, 5 (2002), 297 – 312.
- [35] FARIN, G. From conics to NURBS: A tutorial and survey. *IEEE Computer Graphics and Applications* 12, 5 (1992), 78–86.

-
- [36] FARIN, G., AND SAPIDIS, N. Curvature and the fairness of curves and surfaces. *IEEE Computer Graphics and Applications* 9, 2 (1989), 52–57.
- [37] FORSTER, O. *Analysis 1: Differential- und Integralrechnung einer Veränderlichen*. Vieweg, Wiesbaden, 2008.
- [38] GALLOT, S., ET AL. *Riemannian Geometry*. Springer, Berlin, 1990.
- [39] GARCÍA-LÓPEZ, J., AND RAMOS, P. A. A unified approach to conic visibility. *Algorithmica* 28, 3 (2000), 307–322.
- [40] GHOSH, S., ET AL. Approximation by conic splines. *Mathematics in Computer Science* 1, 1 (2007), 39–69.
- [41] GHOSH, S. K. *Visibility algorithms in the plane*. Cambridge University Press, Cambridge, 2007.
- [42] GONZALEZ, R., AND WOOD, R. E. *Digital Image Processing*. Prentice Hall, Reading, Mass., 2002.
- [43] GREIPL, D. *Passung endlicher Punktmengen mit nicht-parametrisierten Kurven und Oberflächen*. Schuch, Weiden, 1992.
- [44] GUIBAS, L., ET AL. Linear-time visibility and shortest path problems inside triangulated simple polygons. *Algorithmica* 1, 2 (1987), 209–233.
- [45] HARTSHORNE, R. *Geometry: Euclid and Beyond*. Springer, New York, 2000.
- [46] HELD, M., AND EIBL, J. Biarc approximation of polygons within asymmetric tolerance bands. *Computer-Aided Design* 37, 1 (2005), 357–371.
- [47] HENRIKSON, J. Completeness and total boundedness of the Hausdorff metric. *The MIT Undergraduate Journal of Mathematics* 1, 1 (1999), 69–79.
- [48] HONG, D., ET AL. A prototype indexing approach to 2D-object description and recognition. *Pattern Recognition* 31, 6 (1998), 699–725.
- [49] HOSCHEK, J. Circular splines. *Computer-Aided Design* 24 (1992), 611–618.
- [50] JAIN, R., ET AL. *Digital Image Processing*. McGraw-Hill, New York, 1995.

-
- [51] KURATOWSKI, K. *Topology*. Academic Press, New York, 1966.
- [52] LANGRIDGE, D. J. Curve encoding and the detection of discontinuities. *Computer Graphics and Image Processing 20* (1982), 58–71.
- [53] LEE, D. T., AND PREPARATA, F. P. An optimal algorithm for finding the kernel of a polygon. *J. ACM 26*, 3 (1979), 415–421.
- [54] MAIER, G., AND PISINGER, G. Minimum arc paths in simple polygons. In *International Journal of Computational Geometry & Applications (to appear)* (2010).
- [55] MARCINIAK, K., AND PUTZ, B. Approximation of spirals by piecewise curves of fewest circular arc segments. *Computer-Aided Design 16*, 2 (1984), 87–90.
- [56] MARR, D. *Vision: A Computational Investigation into the Human Representation and Processing of Visual Information*. Freeman, New York, 1982.
- [57] MATHERON, G. *Random Sets and Integral Geometry*. John Wiley & Sons, New York, 1975.
- [58] MEEK, D. S., AND WALTON, D. J. Approximation of discrete data by \mathbf{G}^1 arc splines. *Computer-Aided Design 24*, 1 (1992), 301–306.
- [59] MEEK, D. S., AND WALTON, D. J. Approximating quadratic NURBS curves by arc splines. *Computer-Aided Design 25*, 1 (1993), 371–376.
- [60] MEEK, D. S., AND WALTON, D. J. Approximating smooth planar curves by arc splines. *Journal of Computational and Applied Mathematics 59*, 1 (1995), 221–231.
- [61] NUTBOURNE, A. W., AND MARTIN, R. R. *Differential geometry applied to curve and surface design*. Ellis Horwood, Chichester, 1988.
- [62] PARK, H. Optimal single biarc fitting and its applications. *Computer-Aided Design and Applications 1*, 1–4 (2004), 187–195.
- [63] PIEGL, L. A. Curve fitting for rough cutting. *Computer-Aided Design 18*, 1 (1986), 79–82.
- [64] PIEGL, L. A., AND TILLER, W. Biarc approximation of NURBS curves. *Computer-Aided Design 34*, 11 (2002), 807–814.

-
- [65] PIEGL, L. A., AND TILLER, W. Data approximation using biarcs. *Engineering with Computers* 18, 1 (2002), 59–65.
- [66] PISINGER, G. *Lokale Stützstrukturen zur Transformationspassung von Bildern*. Shaker, Aachen, 2003.
- [67] ROBERGE, J. A data reduction algorithm for planar curves. *Computer Vision, Graphics, and Image Processing* 29 (1985), 168–195.
- [68] ROSIN, P. L. A survey and comparison of traditional piecewise circular approximations to the ellipse. *Computer Aided Geometric Design* 16, 4 (1999), 269–286.
- [69] RÖTGEN-BURTSCHIEDT, J. Das Apollonische Berührproblem. *Seminar für Mathematik und ihre Didaktik, Universität zu Köln* (2007).
- [70] SCHOENHERR, J. Smooth biarc curves. *Computer-Aided Design* 25, 1 (1993), 365–370.
- [71] SONG, X., ET AL. Circular spline fitting using an evolution process. *Journal of Computational and Applied Mathematics* 231, 1 (2009), 423 – 433.
- [72] SU, B., AND LIU, D. *Computational Geometry: Curve and Surface Modeling*. Academic Press, San Diego, 1989.
- [73] SURI, S. A linear time algorithm for minimum link paths inside a simple polygon. *Computer Vision, Graphics, and Image Processing* 35 (1986), 99–110.
- [74] SURI, S. On some link distance problems in a simple polygon. *IEEE Trans. Robot. Autom.* 6 (1990), 108–113.
- [75] VAN DEN DRIES, L. A generalization of the tarski-seidenberg theorem, and some nondefinability results. *Bulletin of the American Mathematical Society* 15, 2 (1986), 189–193.
- [76] VAN DEN DRIES, L. *Tame topology and o-minimal structures*, vol. 248 of *London Mathematical Society Lecture Note Series*. Cambridge University Press, Cambridge, 1998.

-
- [77] WANG, W., ET AL. Computation of rotation minimizing frames. *ACM Trans. Graph.* 27, 1 (2008), 1–18.
- [78] WEISSTEIN, E. W. Apollonius' problem. <http://mathworld.wolfram.com/ApolloniusProblem.html>, 2010.
- [79] WEST, G., AND ROSIN, P. L. Techniques for segmenting image curves into meaningful descriptions. *Pattern Recognition* 24 (1991), 643–652.
- [80] YANG, L., AND WANG, W. A revisit to least squares orthogonal distance fitting of parametric curves and surfaces. In *Advances in Geometric Modeling and Processing* (2008), pp. 384–397.
- [81] YANG, S., AND DU, W. Numerical methods for approximation digitized curves by piecewise circular arcs. *Journal of Computational and Applied Mathematics* 66 (1996), 557–569.
- [82] YANG, X. Efficient circular arc interpolation based on active tolerance control. *Computer-Aided Design* 34 (2002), 1037–1046.
- [83] YANG, X. Curve fitting and fairing using conic splines. *Computer-Aided Design* 65, 5 (2004), 461–472.
- [84] YEUNG, M., AND WALTON, D. J. Curve fitting with arc splines for NC toolpath generation. *Computer-Aided Design* 26, 1 (1994), 845–849.
- [85] YONG, J.-H., ET AL. A note on approximation of discrete data by \mathbf{G}^1 arc splines. *Computer-Aided Design* 31, 4 (1999), 911–915.
- [86] YONG, J.-H., ET AL. Bisection algorithms for approximating quadratic Bezier curves by \mathbf{G}^1 arc splines. *Computer-Aided Design* 32, 4 (2000), 253–260.

LIST OF SYMBOLS

General Notation

$:=$	'is defined as'	$T_M(a)$	tangent cone to M at a
\mathbb{N}	set of natural numbers ($0 \in \mathbb{N}$)	$f _A$	restriction f on A
\mathbb{Z}	ring of integers	∇f	gradient of f
\mathbb{R}	field of real numbers	D	differential operator
\mathbb{C}	field of complex numbers	$\mathcal{P}_n(\mathbb{R}^m, \mathbb{R})$	vector space of the real valued polynomial functions on \mathbb{R}^m of degree at most n
$\Re(z)$	real part of z	Ω	set of all quadrics
$\Im(z)$	imaginary part of z	$\text{dist}(A, B)$	euclidean distance of A and B
$\arg(z)$	argument of z	\mathfrak{h}	Hausdorff metric
$A \subset B$	A is a subset of B	$\mathfrak{K}(X)$	set of all non-empty, compact subsets of X
∂A	boundary of A	$\mathfrak{C}(X)$	set of all closed subsets of X
$\overset{\circ}{A}$	interior of A	\mathcal{O}_M	cf. p.60
A^{ri}	relative interior of A	P_M	metric projection
$Ext(A)$	extremal points of A	π_M	cf. p.60
$\text{card}(A)$	cardinality of A	U^l, U^r	cf. Definition 3.3.5, p.77
$\mathfrak{P}(A)$	power set of A		
\mathbb{S}^1	unit sphere of \mathbb{R}^2		
$\langle \cdot \cdot \rangle$	standard scalar product		
$\ \cdot\ $	euclidean norm		
$B_\varepsilon(a)$	$= \{x \in \mathbb{R}^2 \mid \ x - a\ < \varepsilon\}$		
$B_\varepsilon(M)$	$\bigcup_{x \in M} B_\varepsilon(x)$		

Curves and arc splines

$\mathcal{W}(\mathbb{R}^2)$	oriented curves in \mathbb{R}^2
$<_\gamma$	order given by γ
$S(\gamma), E(\gamma)$	start, end point of γ
$\gamma_1 \cdots \gamma_n$	juxtaposition of $\gamma_1, \dots, \gamma_n$
γ^{-1}	inverse path of γ
$\text{tr}(\gamma)$	trace of γ
$\text{len}(\gamma)$	length of γ
$\mathfrak{w}(\omega, a)$	winding number of ω
$\tau_\gamma(a)$	tangent unit vector of γ at $a \in \text{tr}(\gamma)$
$\kappa(\gamma)$	curvature of γ
$[x_1, x_2]_\gamma$	cf. Definition 2.4.14, p.29
$\gamma _{[x_1, x_2]}$	cf. Definition 2.4.14, p.29
\mathfrak{S}	set of all oriented arcs
\mathfrak{S}^n	set of all smooth arc spline with n segments
$\overline{\mathfrak{S}^n}$	cf. Definition 2.5.22, p.38
\mathfrak{T}	set of all (not necessarily smooth) arc splines
$V(\gamma)$	set of vertices of γ
$\mathcal{L}_\gamma, \mathcal{R}_\gamma$	left, right region of γ
$C(\gamma)$	corresponding generalized circle of oriented arc γ
$\gamma_{x,a,v}$	oriented arc starting at x , ending in a with exiting direction v
$ \gamma $	number of segments of γ
$\mathcal{A}(\gamma)$	alternating number of γ
$\mathfrak{A}(\gamma)$	set of all alternating sequences of γ

Tolerance channels

$\mathfrak{E}, (K, s, \sigma)$	tolerance channel with starting segment s and restriction map σ
$\mathfrak{E}_i, i \geq 1$	cf. Definition 3.7.3, p.124
$\mathfrak{E}_a, (K_a, s_a, \sigma_a)$	continuation channel defined by $a \in \overline{I_K} \setminus V_K(\sigma)$
$\mathfrak{D}, (K, s, \sigma, d)$	start-destination channel with destination d
$\mathfrak{D}_i, i \geq 1$	cf. Definition 3.7.6, p.125
I_K, E_K	interior, exterior of K
ω_K	CCW oriented curve with $K = \text{tr}(\omega_K)$
σ	restriction map
σ_K	cf. Definition 3.2.8, p.65
K_l, K_r	left, right bordering set
$l_K(\gamma), r_K(\gamma)$	maximal left/right length
$L(\gamma), R(\gamma)$	left/right contour w.r.t. γ

Visibility

$V_K(\sigma)$	circular visibility set	$\overline{\mathfrak{S}^n}$	cf. Definition 2.5.22, p.38
$V_K^n(\sigma)$	circular n - visibility set	$\overline{\mathfrak{S}_K^n(\sigma)}$	set of all generalized visibility splines with n segments
$V_K^a(\sigma)$	subset of $V_K(\sigma)$, cf. Definition 3.4.14, p.88	$\mathfrak{S}_K(x)$	p.147
$V_K^{con}(\sigma)$	subset of all circularly visible points a where $\sigma_K(a, v)$ is connected	$T_K(\sigma, a)$	feasible direction set of a
$V_K(x)$	p.147	$T_K(\sigma, -)$	mapping $a \mapsto T_K(\sigma, a)$
$D_K^n(\sigma)$	$= \overline{V_K^n(\sigma) \setminus V_K^{n-1}(\sigma)}$	$\omega^{(M)}, \omega^{(a)}$	window of M, a
$W_K^n(\sigma)$	cf. Definition 3.6.11, p.114	$\gamma^{(M)}, \gamma^{(a)}$	blocking arc of M, a
$U_K^n(\sigma)$	cf. p.122	$\omega_{\mathfrak{D}}$	window w.r.t. \mathfrak{D}
$\mathfrak{S}_K(\sigma)$	set of all visibility arcs	$\gamma_{\mathfrak{D}}$	corresponding blocking arc
$\mathfrak{S}_K(\sigma, a)$	cf. Definition 3.1.8, p.53	$L_K(\sigma)$	linear visibility set
$\mathfrak{S}_K(\sigma, a, v)$	cf. Definition 3.1.8, p.53	\mathfrak{L}	set of all oriented lines
$\mathfrak{S}_K^n(\sigma)$	set of all visibility splines with n segments	$\mathfrak{L}_K(\sigma)$	set of all visibility lines
$\mathfrak{S}_K^\infty(s, d)$	p.57	$\mathfrak{L}_K^\infty(s, d)$	cf. Definition 3.8.3, p.128
		$n(d)$	cf. Definition 3.7.2, p.122
		$m(d)$	cf. Definition 3.7.4, p.124

LIST OF FIGURES

1	The particular steps from a real object to a CAD drawing.	3
2	Start-destination including contour points and smooth minimum arc path.	4
3	Various types of visibility polygons (shaded portions).	8
4	Minimum link path and minimum arc path.	9
5	Example of the three-circle problem.	20
6	Illustration of Definitions 2.4.10 and 2.4.11	28
7	Illustration of Definition 2.5.1 and 2.5.3.	33
8	Visualization of the arc $\gamma_{a,b,v}$	35
9	Illustration of all circular arcs from a to b with the same radius.	36
10	Convergent sequence in $\overline{\text{tr}(\mathfrak{S}^3)}$	38
11	Convergent sequence in $\overline{\text{tr}(\mathfrak{S}^7)}$	39
12	Visualization of Proposition 2.5.33.	42
13	Simple polygon K and circular visibility.	46
14	Illustration of a channel (K, s)	48
15	Illustration of restriction maps.	52
16	Example of $\sigma(a, v)$ having two connected components.	53
17	Illustration of (degenerate) starting /continuation channel and corresponding visibility sets.	56
18	Left K_l and right bordering set K_r	59

19	Illustration of Definition 3.2.1.	61
20	Illustration of Definition 3.2.3.	62
21	Extremal points of $\sigma(a, v) \subset \text{tr}(s)$	64
22	Counterexample.	65
23	Pseudo restrictions.	67
24	Illustration of Definition 3.2.11 in case of a starting channel.	68
25	Right restrictions at the endpoint of a visibility arc.	68
26	Illustration of Definition 3.2.11 in case of a continuation channel.	69
27	Example for the calculation of the alternating number of a visibility arc.	71
28	Illustration of alternating sequences I.	72
29	Illustration of alternating sequences II.	72
30	Restrictions given by K . In general we have $\sigma(a, v) \neq \sigma_K(a, v)$	73
31	Extremal directions of a feasible direction set $T_K(\sigma, a)$	78
32	Illustration of the proof of Theorem 3.3.9.	80
33	Visibility arcs γ_1, γ_2 with $\mathcal{A}(\gamma_i) \geq 2$ that are not extremal.	81
34	Example of a circular visibility set.	84
35	Counterexample.	86
36	Adapted alternating sequences.	89
37	Adapted alternating sequences II.	89
38	Illustration of a visibility set	90
39	Illustration of a left and right sub-curve of a start-destination channel given by a polygon.	91
40	Illustration of Theorem 3.4.19.	92
41	Illustration of Lemma 3.4.20.	93
42	Illustration of Proposition 3.5.5 (left) and 3.5.7 (right).	97
43	Continuity attitudes of the mapping $T_K(\sigma, -)$	101
44	Visibility splines of $V_K^2(\sigma)$	102
45	Illustration of the Homotopy-Lemma 3.6.1.	103
46	Illustration of the proof of the Homotopy- Lemma 3.6.1.	106
47	Illustration of the continuation channel (K_a, s_a, σ_a)	110
48	Illustration of Theorem 3.6.8.	113
49	Illustration of the Definition 3.6.11.	115
50	Illustration of Definition 3.6.14.	117

51	Uniform distribution of the breakpoints.	118
52	Alternating number of a generalized visibility spline.	119
53	Accumulation of breakpoints and alternating numbers.	120
54	Smoothing generalized visibility splines I.	123
55	Smoothing generalized visibility splines II.	123
56	Smoothing minimum arc path $\gamma_1 \cdots \gamma_5$ with $n(d) = 5$	124
57	Comparison of a smooth and a continuous minimum arc path.	126
58	Minimum link path with five segments.	129
59	Illustration of Definition 3.8.4.	130
60	Cyclic smooth/continuous minimum arc path.	131
61	First and second tolerance channels given by a cyclic tolerance channel.	133
62	Examples of blocking arcs in case of an arc spline as bounding curve.	138
63	Illustration of blocking arcs in case of a polygon.	139
64	'Forward step'.	143
65	'Backward step'.	144
66	Illustration of Algorithm 2	145
67	CCW visibility arcs emanating from x , which correspond to the edge e_i of K , represented by their centers.	147
68	Possible hitting order of two edges.	150
69	CCW-CVD of a polygon K with base point x	152
70	Illustration for computing the circular visibility of an edge.	156
71	Blocking arcs w.r.t. b and l_s	159
72	Illustration for the strategy used for computing the circular visibility of an circular arc.	160
73	Illustration of introverted and extroverted case.	161
74	Continuation channel (K_a, s_a, σ_a) ; s_1 and s_2	163
75	Algorithmic approach to a continuation channel $\mathfrak{E}_a := (K_a, s_a, \sigma_a)$ I.	164
76	Algorithmic approach to a continuation channel $\mathfrak{E}_a := (K_a, s_a, \sigma_a)$ II.	166
77	Example of two start-destination channels given by a simple polygons and corresponding minimum link paths.	171
78	Example of two start-destination channels given by a simple polygons and corresponding continuous minimum arc paths.	172

79	Example of two start-destination channels given by a simple polygons and corresponding smooth minimum arc paths.	173
80	Offset of p_1, \dots, p_6	182
81	Polygonal tolerance region suggested by Drysdale et al.	183
82	Approximation of an ε -Offset.	183
83	Approximation of the inner contour of a window frame and corresponding curvature function.	187
84	Approximation of a part of garden scissors.	190
85	Approximation of the shape of a hand.	191
86	Comparison of continuous and smooth approximation.	192
87	Input point set with 612 pixel positions and approximations with tolerance 10, 1 and 0.1 pixels.	196
88	Approximation of the sine curve segment by smooth arc splines.	197
89	Hyperbola segment in polygonal channel with alternating sequence of length 5.	202

LIST OF TABLES

2.1	The different constellations of the Apollonius' Problem	19
4.1	Two exemplary test scenarios, which are visualized in Figure 77-79. . .	170
5.1	Approximation of the shape of a hand by a smooth arc spline.	189
5.2	Approximation of the sine-curve segment defined on the interval $[0, 6]$. . .	196

LIST OF ALGORITHMS

1	Smooth Minimum Arc Path	141
2	Continuous Minimum Arc Path	146
3	CVD Simple Polygon	150
4	Computation of $V_K(\sigma)$ in case of a degenerate starting channel.	151
5	Edge visibility	154
6	Computation of the window $\omega_{\mathbf{e}_a}$	165

INDEX

A

arg 34
a-adapted 88
adapted 88
alternating number 70, 118
alternating sequence 70
 a-adapted 88
 maximal 71
 of number 70
analytic 30
 piecewise restricted 30
 restricted 30
Apollonius 18
 Circles 19
 Problem 18
approximation 179
arc 18
 generalized 18
 oriented 32

arc conglomerate 38
arc length parametrization 29
arc spline 10, 32
 circular 32
 smooth 32
argument 34
associated 88
asymmetric tolerance band 184

B

backward step 167
best approximating point 60
biarc 10, 32, 122
bisector 148
blocking 85
 left 85
 right 85
bordering set 58
 left 58

- right 58
- C**
- \mathcal{C}^1 26
- \mathcal{C}^n 26
- \mathcal{C}^ω 30
- Canny edge detector 177
- CC 50
- CCW 28
- change of parameters 26
- channel 47
- continuation 54
- offset 181
- start-destination 55
- starting 54
- tolerance 54
- circle 16
- generalized 16
- Circular Visibility Diagram 147
- clockwise oriented 28
- CNC 10, 188
- compact
- locally 23
- cone 22
- tangent 22
- conglomerate 38
- conic 16
- spline 201
- visibility 202
- continuation channel 54
- degenerate 54
- continuation condition 50
- degenerate 50
- continuity
- \mathbf{G}^1 32
- continuous 21
- contour 2, 62, 177
- left 62
- point list 2, 178
- right 62
- counterclockwise oriented 28
- curvature 30, 42
- curvature characteristic 186
- curve 26, 29
- closed 27
- Jordan 27
- length of 29
- oriented 26
- polygonal 33
- simple 27
- CVD 147
- base point of 148
- CCW- 147
- CW- 147
- node of 148
- CW 28
- D**
- DCC 50
- deficiency set 155
- degenerate continuation condition ... 50
- distinctive points 185
- Douglas-Peucker algorithm 184
- E**
- edge 147
- edge detector 177

- Canny 177
- euclidean distance 23
- exhaustive sequence 23
- exiting direction 32
- exterior 28
- extremal 77
- left extremal 77
- right extremal 77
- extremal point 62, 63
- left 63
- right 63
- extroverted 160
- F**
- feasible direction set 76
- of order n in a 114
- forward step 167
- G**
- $\gamma^{(M)}$ 88
- $\gamma^{(a)}$ 88
- graph 22
- greedy algorithm 11
- H**
- Hausdorff metric 23
- hinge 153
- I**
- interior 28
- interpolation 179
- introverted 160
- J**
- Jordan curve 27
- exterior of 28
- interior of 28
- juxtaposition 27
- L**
- LH-topology 24
- linear visibility set 127
- local Hausdorff topology 24
- loop 27
- M**
- mapping
- set-valued 21
- matching 185
- maximal left length 90
- maximal right length 90
- metric projection 60
- metrizable 23
- minimum arc path 57, 124
- continuous 124
- continuous cyclic 130
- cyclic 130
- smooth 57
- smooth cyclic 130
- minimum link path 128
- Moore neighborhood 178
- N**
- nearest point 60
- node 148
- non-maximal suppression 177
- normal 30
- NURBS 195

- O**
- offset 41, 181
- oriented arc 32
- oriented curve 26
- oriented path 26
- P**
- parallel curve 41
- parametrization 26
- arc length 29
- normal 29
- regular 29
- parametrized curve 26
- partitioning curve 148
- path 26
- inverse 27
- oriented 26
- piecewise \mathcal{C}^1 26
- piecewise restricted analytic 30
- pocket 129
- CCW 153
- CW 153
- main 154
- polygon 33
- polygonal curve 33
- polygonal tolerance region 182
- prototype matching 186, 193
- pseudo restriction 66
- point 66
- Q**
- quadric 16
- R**
- \mathcal{R}^ω 30
- piecewise 30
- region 61
- left 61
- right 61
- regular 29
- relative interior 62
- restricted analytic 30
- piecewise 30
- restriction
- left 66
- point 66
- pseudo 66
- right 66
- restriction map 48
- degenerate unidirectional restriction
- 50
- starting restriction 49
- unidirectional restriction 50
- restriction point
- left 66
- right 66
- Reverse Engineering 2, 188
- S**
- $\overline{\mathfrak{S}^n}$ 38
- σ -compact 23
- segment 33
- semi-continuous
- lower 21
- upper 21, 24
- set-valued mapping 21
- shape recognition 185
- shape representation 179

smooth 28
 start-destination channel 55
 starting channel 54
 degenerate 54
 starting restriction 49
 degenerate 49
 sub-polygon 160
 subpolygon 162

T

tangent cone 22
 tangent unit vector 28
 tolerance channel 54
 cyclic 129
 tr 38
 trace 27, 38

U

unidirectional restriction 50
 degenerate 50

V

$V(\gamma)$ 38
 vertex 28
 vertex set 38
 visibility
 line segment 127
 linear 127
 visibility arc 53
 visibility line 6
 visibility line segment 127
 visibility set
 linear 127
 visibility spline 53

 generalized 54
 visible 54
 n - 54
 circularly 54
 n - 54
 completely 6
 strongly 6
 weakly 6
 Voronoi-diagram 148

W

winding number 27
 window 88